

Method Development for the Detection and Identification of Pathophysiologically Relevant Electrophiles in Pollen

Inauguraldissertation

zur

Erlangung der Würde eines Doktors der Philosophie

vorgelegt der

Philosophisch-Naturwissenschaftlichen Fakultät

der Universität Basel

von

Jue Theresa Wang

Basel, 2021

Originaldokument gespeichert auf dem Dokumentenserver der Universität Basel
edoc.unibas.ch

Genehmigt von der Philosophisch-Naturwissenschaftlichen Fakultät
auf Antrag von

Prof. Dr. Matthias Hamburger

Prof. Dr. Daniel Ricklin

Prof. Dr. Nunziatina De Tommasi

Basel, 15.12.2020

Prof. Dr. Martin Spiess

Dekan

Come on, you know how this works. You fail and then you try something else. And you fail again and again, and you fail a thousand times, and you keep trying because maybe the 1001st idea might work. Now, I'm going to go and try to find our 1001st idea.

- *The Good Place*



IT'S JUST ALLERGIES

artwork by the author

Acknowledgements

The journey as a PhD student is exciting and curious, and at times, also challenging and tough which is why it would not be possible without the support of others.

First, I would like to give my sincerest thanks to Prof. Matthias Hamburger, my supervising professor. You took me in a month after I had just graduated with my master's degree and believed that I had what it takes for an explorative project. Thank you for pushing and challenging me, for all your advice and for giving me the opportunity to also educate myself in techniques and areas outside of my actual project scope. You gave me the freedom to explore and to learn, and my journey would have been completely different if it were not for you.

Next to my main supervisor, I would also like to say thank you to Prof. Daniel Ricklin who agreed to be my second supervisor. I am grateful for all the time you took to discuss the progress of the PhD with me, and I am also thankful for the opportunity to work in your lab for parts of the project. Your group members Dr. Christina Lamers and Clément Bechtler took good care of me during my work in your lab, and I appreciate all the discussions we had together. I have learned a lot from all of you.

Furthermore, I want to thank the group members of the Pharmaceutical Biology lab. All of you contributed to this invaluable experience and to the atmosphere in the lab. I think we can count ourselves as lucky for having the group that we have – this does not mean everything was always peaceful and harmonious, but it certainly was never boring and people in the lab did stick up for each other and supported each other when the situation called for it. There are a couple of people I want to mention by name because they directly contributed to the project.

Prof. Olivier Potterat, thank you for all the interesting discussions we had and for being a sounding board for ideas.

Dr. Mouhssin Oufir, thank you for all that you have taught me in the area of UPLC and for giving me courage during a very chaotic time period of my PhD. I do not know if I would be where I am now without you.

Dr. Andrea Treyer, thank you for all the HPLC and UPLC support you provided. Your enthusiasm is infectious, and your vision of teaching and knowledge sharing should be present in every laboratory.

I want to give my thanks to Dr. Ombeline Danton who is the resident NMR expert of our lab. As many other students before me and probably also after me, I want to acknowledge you for your expertise in the lab and your cheery attitude.

Dr. Alen Bozicevic, thank you for introducing me to the project. I know that project handovers are never easy, but in our case, it worked just fine.

I am grateful to Dr. Jakob Reinhardt for our immunology sessions, for your input in the lab and for always knowing how to really get on someone's nerves but in a funny way. It is a great thing to start your PhD at the same time as another person and I think we made some fun memories together on this journey.

Thank you, Morris Keller, for all the times you helped me with instruments in the lab, especially the preparative HPLC. I would have lost a lot of time without you.

Thank you to Orlando Fertig for all the technical support you have provided. The lab would not run nearly as smoothly without you.

It takes more than just colleagues, and four years is a long time. Therefore, I also want to thank all the friends who have been there for me and supported me behind the scenes. Among my friends, there are also some I want to give a special shoutout to.

First, I want to thank my dear friend, Kristel, for being the bedrock that will always be there for support. We have done our PhDs together. I cannot count the times we have shared our ups and downs and how many times we have lifted each other up. Every PhD student should have someone to share their journey with like you, and every person should have a friend like you. I consider myself very lucky to have a friend like you.

Thank you, Marie, for being a friend that will last for a lifetime and my professional comma setter. Thank you also for proof-reading my introduction, I know thermodynamics and kinetics are not exactly your favourite subjects so I appreciate you having battled through those chapters even more. You and Bruno were always here for me for giggles, tea, and memes.

Thank you, Vanessa, for your continuous encouragement. Your resilience has inspired me many times and I think I have not met many people who can match you in inner strength. I thank you for being an inspiration.

Thank you, Nico, for your helpful support, cheerful optimism and refreshing humour. Having had you as a lab buddy and remaining friends even though you are quite literally on the other side of the world is one of the greatest things.

I want to thank you, Jana, for being the most awesome neighbour ever and basically my PhD mentor. You have walked this road before I started walking it and your experience has helped me overcome so many struggles. For that, I am immensely grateful. Also, please adopt a dog so that I can be a dog godparent.

Liga, it is funny how friendships sometimes work and how they persist even if the timing seems to be off, me being away for one year, you being away for the other during our studies in Edinburgh. I am grateful that fate has somehow led us back into the same country and that we could support each other during our respective PhDs. I will be cheering you on when you are about to finish.

I want to thank all the friends that I have made during my time at the GCC. You guys absolutely rock. You are everything one could wish for in a team. Patrizia, Matija, Kathrin, Arka, Olga, Bram, you guys and the many, many others that were involved. We built something great together next to our studies and I think in doing so we balanced out the science that usually preoccupied our daily life.

I want to thank my 'med school girls' Maggie, Miriam and Denise for laughter, board games, and seriously nerdy medicine humour. You have been a constant in my life ever since high school. Brunch and board games together with you were the B&B I needed.

I want to thank Juliana and Toni for always providing me a safe harbour to return to. What do they say? Miles apart, but close at heart.

Furthermore, I want to thank my childhood friends Alex, Stella, Mingkang and David. We have come so far together and I do not think we will ever stop being friends. Or, if we do, it will be because we dropped 'friends' for 'family'.

Liz, with you, I will always have someone to look up to. Thank you for being the big sister I never had and for all the support and advice you have given me over the years. Words cannot express how much you mean to me as a source of constant inspiration.

And lastly, I want to thank my family. You guys made me into what I am right now, thank you for all the love and support that I have received from you ever since childhood. I quite literally would not be the same without you.

Abbreviations

Common Abbreviations

2-BME	2-Mercaptoethanol
2-PrOH	Isopropyl alcohol
6His	Hexa histidine
ASE	Accelerated solvent extraction
C6His	H ₂ N-HHHHHHC-OH
CD6His	H ₂ N-HHHHHHDC-OH
COSY	Correlation spectroscopy
CuAAC	Copper(I)-catalysed azide-alkyne cycloaddition
DCM	Dichloromethane
DIC	Diisopropylcarbodiimide
DIPEA	<i>N,N</i> -Diisopropylethylamine
DMF	Dimethylformamide
DMSO	Dimethyl sulfoxide
DTT	Dithiothreitol
Ellman's Reagent	5,5'-Dithiobis-(2-nitrobenzoic acid)
EtOH	Ethanol
FA	Formic acid
FcεRI	High-affinity immunoglobulin E receptor
FITC	Fluorescein isothiocyanate
FTH	Fluorescein thiohydantoin
GFM	Gram formula mass
GSH	Glutathione
GSSG	Glutathione disulfide
HFIP	Hexafluoroisopropyl alcohol
HMBC	Heteronuclear multiple bond correlation
HPLC	High performance liquid chromatography
HRMS	High resolution mass spectrometry
HSAB	Hard and soft acids and bases
HSQC	Heteronuclear single quantum coherence
IFN-γ	Interferon gamma
IgE	Immunoglobulin E
IL	Interleukin
LC	Liquid chromatography
MeOH	Methanol
MRM	Multiple reaction monitoring
MS	Mass spectrometry
MSMS	Tandem mass spectrometry

NAC	<i>N</i> -Acetylcysteine
NLS	Neutral loss scan
NMP	1-Methyl-2-pyrrolidinone
NMR	Nuclear magnetic resonance
PDA	Photodiode array
PI 3-kinase	Phosphatidylinositol 3-kinase
pKa	Negative logarithm of the acid dissociation constant
PLK	Polo-like kinase
PEG	Polyethylene glycol
PIS	Precursor ion scan
RT	Room temperature
rt	Retention time
SPE	Solid-phase extraction
SPPS	Solid-phase peptide synthesis
SRM	Selected reaction monitoring
TEA	Triethylamine
TFA	Trifluoroacetic acid
Th0	Naive T helper cell
Th1	T helper type 1
Th2	T helper type 2
THF	Tetrahydrofuran
TIS	Triisopropylsilane
Treg	Regulatory T cell
TRPA1	Transient Receptor Potential cation channel A1
UPLC	Ultra performance liquid chromatography
UV	Ultraviolet
Vis	Visible

Protecting Groups

Boc	<i>tert</i> -Butyloxycarbonyl protecting group
Fmoc	Fluorenylmethoxycarbonyl protecting group
OtBu	<i>tert</i> -Butyl ester protecting group
Trt	Triphenylmethyl protecting group

Amino Acid Abbreviations

A	Ala	Alanine
C	Cys	Cysteine
D	Asp	Aspartic Acid
H	His	Histidine

Summary

Pollen allergy is a complex, multicausal disease with rising prevalence across the world. Currently, pollen allergy is treated mainly by symptom management and allergen-specific immunotherapy. In order to develop new treatment options, a greater understanding of the underlying mechanism of the disease is needed. Based on disease hypotheses like the hapten theory and the danger model, electrophilic small molecules in pollen could play a part in the sensitisation process and the exacerbative nature of the disease. The research on small molecules in pollen is lagging behind in contrast to their protein counterparts, which is why the aim of this project was to develop a method to enable the detection and identification of electrophiles in pollen extracts.

Method development in this work explored i) *in situ* detection and identification methods with liquid chromatography-mass spectrometry and ii) nucleophilic labelling with an affinity tag in order to facilitate a subsequent purification step, before investigating the potential of using a solid-supported nucleophilic probe. Finally, a probe was developed, consisting of a polystyrene solid support, a hyperacid-sensitive linker and a disulfide-protected cysteine that could act as a nucleophile to capture the electrophilic target molecules upon deprotection. The advantages of the probe are the following: i) the nucleophilic cysteine could be selectively deprotected, and a method was developed to quantify the released cysteine (8.65 ± 2.65 %) and therefore the amount of reactive sites on the resin; ii) the solid nature of the probe enabled a set-up in cartridges intended for solid-phase extraction, which allowed consecutive washes and reagent additions; iii) the hyperacid sensitive linker enabled the release of formed cysteine adducts after reaction; and finally, iv) due to the design of the probe, only mono-addition of cysteine was observed, except in cases where adducts could decompose. The probe was tested on model compounds, a model extract that was spiked with model compound and lastly, on diverse pollen extracts (*Ambrosia psilostachya*, *Ambrosia artemisiifolia*, *Phleum pratense*, *Betula pendula*, *Urtica dioica*, *Corylus avellana*). Both model compound and model extract experiments were successful; adduct formation was observed and the adducts were successfully isolated and characterised by nuclear magnetic resonance. However, due to the low abundance of electrophilic compounds in the extract, it unfortunately was not possible to isolate and characterise any compounds from pollen extracts, aside from two compounds isolated from a larger pollen extract experiment with *Ambrosia*

psilostachya. The two isolated compounds were shown to be coumaroyl spermidine-like structures, however, their exact structure could not be determined.

Zusammenfassung

Pollenallergie ist eine komplexe multikausale Krankheit mit weltweit steigender Prävalenz. Derzeit wird die Pollenallergie hauptsächlich durch Symptommanagement und allergenspezifische Immuntherapie behandelt. Ein besseres Verständnis des Krankheitsmechanismus ist erforderlich, um neue Behandlungsmöglichkeiten zu entwickeln. Basierend auf Krankheitshypothesen wie der Hapten-Theorie und dem Gefahrenmodell könnten elektrophile kleine Moleküle in Pollen eine Rolle im Sensibilisierungsprozess und in Exazerbationsepisoden der Krankheit spielen. Die Forschung an solchen Molekülen ist im Gegensatz zu Proteinallergenforschung zurückgeblieben, weshalb das Ziel dieses Projekts darin bestand, eine Methode zu entwickeln, mit der solche Moleküle nachgewiesen und identifiziert werden können.

Die Methodenentwicklung in dieser Arbeit untersuchte i) *In-situ*-Nachweis- und Identifizierungsmethoden durch Flüssigchromatographie mit Massenspektrometrie-Kopplung und ii) eine Nachweismethode durch nukleophile Adduktbildung mit einer Affinitätsmarkierung, um einen nachfolgenden Reinigungsschritt zu erleichtern, bevor schlussendlich das Potenzial der Verwendung von einer feststoffgetragenen nukleophilen Sonde untersucht wurde. Eine Sonde wurde entwickelt, die aus einem festen Polystyrolträger, einem säureempfindlichen Linker und einem disulfidgeschützten Cystein besteht, das als Nukleophil mit elektrophilen Zielmolekülen reagieren kann. Die Vorteile der Sonde sind die folgenden: i) das nukleophile Cystein konnte selektiv entschützt werden, und es wurde eine Methode entwickelt, um das freigesetzte Cystein und damit die Menge an reaktiven Stellen auf dem polymären Trägermaterial zu quantifizieren ($8,65 \pm 2,65\%$); ii) der feste Aggregatzustand der Sonde ermöglichte einen Aufbau in Kartuschen, die für die Festphasenextraktion vorgesehen waren; dieser Aufbau ermöglichte aufeinanderfolgende Waschungen und Reagenzzugaben; iii) der säureempfindliche Linker ermöglichte die Freisetzung gebildeter Cysteinaddukte nach der Reaktion; und schließlich, iv) aufgrund des Designs der Sonde wurde nur Monoaddition von Cystein beobachtet, außer in Fällen, in denen sich Addukte zersetzen konnten. Die Sonde wurde an Modellverbindungen getestet, einem Modellextrakt, das mit einer Modellverbindung versetzt war, und schließlich an verschiedenen Pollenextrakten (*Ambrosia psilostachya*, *Ambrosia artemisiifolia*, *Phleum pratense*, *Betula pendula*, *Urtica dioica*, *Corylus avellana*). Sowohl die Experimente mit Modellverbindungen als auch mit dem Modellextrakt waren erfolgreich; Adduktbildung wurde beobachtet und

die Addukte wurden erfolgreich isoliert und durch Kernspinresonanzspektroskopie charakterisiert. Aufgrund der geringen Menge elektrophiler Verbindungen im Extrakt war es jedoch leider nicht möglich, abgesehen von zwei Verbindungen, die aus einem größeren Pollenextraktversuch mit *Ambrosia psilostachya* isoliert wurden, Verbindungen aus Pollenextrakten zu isolieren und zu charakterisieren. Es wurde gezeigt, dass die beiden isolierten Verbindungen Cumaroylspermidin-ähnliche Strukturen sind, ihre genaue Struktur konnte jedoch nicht bestimmt werden.

Contents

Acknowledgements	I
Abbreviations	IV
Summary	VI
Zusammenfassung	VIII
Chapter 1 Introduction	1
1.1 Pollen Allergy.....	1
1.1.1 Pathophysiology.....	2
1.1.1.1 Sensitisation	5
1.1.1.2 Early Phase	6
1.1.1.3 Late Phase	7
1.1.2 Treatment.....	7
1.1.2.1 Small Molecule Approaches in the Treatment of Allergy.....	8
1.1.2.1.1 Small Molecule Drugs with Organ-Specific Symptom Alleviation .	9
1.1.2.1.2 Small Molecule Drugs Addressing the Immune Response Chain	10
.....	10
1.1.2.2 Treatments enabled by Monoclonal Antibodies	12
1.1.2.3 Outlook on Pollen Allergy Treatment.....	14
1.1.3 Disease Hypotheses	15
1.1.3.1 Hygiene Hypothesis	15
1.1.3.2 Hapten Theory.....	17
1.1.3.3 Danger Model	18
1.1.4 Composition of Pollen	19
1.2 Identifying Reactive Compounds.....	23
1.2.1 Chemical Reactivity	23
1.2.1.1 Thermodynamics in Chemical Reactivity.....	23
1.2.1.2 Kinetics in Chemical Reactivity.....	27
1.2.2 Electrophiles and Their Chemical Reactivity.....	29
1.2.3 Methods for Detection and Identification of Electrophiles	35
1.2.3.1 Biological Methods	36
1.2.3.2 Chemical Methods.....	39
1.3 Conclusion and Project Aims.....	42
Chapter 2 Materials and Methods	44

2.1 Materials	44
2.1.1 Solvents	44
2.1.2 Reagents.....	45
2.1.3 Buffers.....	46
2.1.4 Model Compounds.....	46
2.1.5 Plant Material	47
2.2 Methods	48
2.2.1 Extract Preparation	48
2.2.2 Sample Drying.....	48
2.2.3 Liquid Chromatography (LC) Analysis	49
2.2.3.1 Analytical High Pressure Liquid Chromatography (HPLC).....	49
2.2.3.2 Semi-preparative HPLC.....	50
2.2.4 Spectrophotometric Assay	51
2.2.5 Nuclear Magnetic Resonance (NMR) Analysis	52
2.2.6 <i>In Situ</i> Detection Methods	52
2.2.6.1 GSH Experiment with Parthenolide	52
2.2.6.2 GSH Experiment with <i>Ambrosia psilostachya</i> Extract.....	53
2.2.6.3 <i>In Situ</i> Detection Using Tandem Mass Spectrometry (MSMS) Methods	53
2.2.7 Methods for the Assessment of Affinity-Tag Assisted Electrophile Detection	53
2.2.7.1 Synthesis of Nucleophilic Peptide	53
2.2.7.2 Experiments with Nucleophilic Peptide.....	54
2.2.7.2.1 Experiments with C6His and 6His.....	54
2.2.7.2.2 Experiments with CD6His	54
2.2.8 Experiments with the Solid-Supported Nucleophilic Probe.....	55
2.2.8.1 Synthesis of the Solid-Supported Nucleophilic Probe	55
2.2.8.2 Pilot Study Utilising the Solid-Supported Nucleophilic Probe	55
2.2.8.2.1 Pilot Experiment Procedure	55
2.2.8.2.2 Pilot Experiment Repeat	56
2.2.8.2.3 Adapted Method for Spectroscopic Cysteine Quantification.....	57
2.2.8.3 Method Optimisation.....	57
2.2.8.3.1 Adjustment of Cleavage Conditions.....	57
2.2.8.3.2 Wash Solvent Optimisation.....	57

2.2.8.3.3 Cysteine Quantification by Ultra Performance Liquid Chromatography (UPLC)-MSMS	58
2.2.8.4 Updated Method Utilising the Solid-Supported Nucleophilic Probe ..	60
2.2.8.5 Reactions with Model Reactions	61
2.2.8.5.1 Model Reactions with Cysteine.....	61
2.2.8.5.2 Purification of Model Compound Adducts.....	61
2.2.8.5 Adapted Method for the Processing of the Larger Batch	62
Chapter 3 Quantifying Electrophiles in Extracts	63
3.1 Introduction	63
3.2 Pollen Batches and Extract Generation.....	64
3.3 Extract Analysis by HPLC.....	67
3.4 Spectrophotometric Quantification with Ellman's Reagent.....	67
3.5 Conclusions	71
Chapter 4 <i>In situ</i> Detection of Electrophiles in Chromatography	72
4.1 Introduction	72
4.2 <i>In Situ</i> Detection by Mass Spectrometry (MS) Scan	72
4.3 <i>In Situ</i> Detection by MSMS Methods.....	78
4.4 Conclusions	81
Chapter 5 Affinity Tag-Assisted Electrophile Detection and Purification	82
5.1 Introduction.....	82
5.2 Probe Design.....	82
5.2.1 Affinity Tag	82
5.2.2 Linker	83
5.2.3 Nucleophilic Centre	84
5.2.4 Probe Structure Considerations.....	84
5.3 Nucleophilic Peptide Probe Pilot Study	86
5.4 Conclusions	90
Chapter 6 Solid-Supported Nucleophilic Probe Development and Optimisation	91
6.1 Introduction	91
6.2 Solid-Supported Nucleophilic Probe Design.....	91
6.2.1 Anchor.....	92
6.2.2 Linker	92
6.2.3 Probe	93

6.3 Solid-Supported Nucleophilic Probe Pilot Experiment.....	93
6.3.1 Solid-supported Cysteinyl Probe Synthesis	93
6.3.2 Solid-Phase Extraction (SPE) Set-Up.....	94
6.3.3 Purification of Parthenolide-Adduct.....	98
6.3.4 Spectroscopic Quantification of Cysteine.....	101
6.3.5 Learnings from the Pilot Experiment.....	102
6.4 Method Optimisation.....	103
6.4.1 Adjustment of Cleavage Conditions	103
6.4.2 Wash Solvent Optimisation	104
6.4.3 SPE Set-Up.....	108
6.4.4 Quantification of Cysteine Residues as Quality Control.....	109
6.5 Proof-Of-Concept.....	111
6.6 Conclusions	116
Chapter 7 Application of the Cysteinyl Probe	117
7.1 Introduction	117
7.1 Model Compounds.....	117
7.1.1 Model Compound Selection	117
7.1.2 Experiments with Model Compounds.....	119
7.2 Model Compound Spiked in a Test Extract	122
7.3 Testing Pollen Extracts	123
7.4 Conclusions	130
Chapter 8 Conclusions and Future Perspectives	131
Appendix	135
Methods	135
Figures.....	138
Tables.....	157
References	171

Chapter 1 Introduction

1.1 Pollen Allergy

The term 'allergy' was introduced by Clemens von Pirquet in 1906 and is used to describe an exaggerated immune response to stimuli generally considered harmless¹. Nowadays this term has been adulterated to describe a set of immunoglobulin E(IgE)-mediated allergic diseases which are often characterised by atopy. Atopy is defined as a tendency to develop an exaggerated IgE immune response². Both allergy and atopy fall under type I hypersensitivity, but while all atopic disorders are allergic, there are many allergic disorders that are not IgE-mediated and hence not atopic³.

Pollen allergy is one of the allergic diseases classified as type I hypersensitivity. Although the term *pollen allergy* is often used to describe solely seasonal allergic rhinitis, pollen can also induce asthma⁴⁻⁸, eczema⁹⁻¹⁰ and, in rare cases, anaphylaxis¹¹⁻¹². Therefore, in this thesis the term 'pollen allergy' will include all exaggerated immune responses towards pollen.

Hence, pollen allergy is the suffering from one or more of these allergic disease conditions when exposed to specific plant pollen. Plant pollen is an important aeroallergen since it is responsible for up to 40 % of respiratory allergies, which affect around 20 % of the population worldwide¹³⁻¹⁴. A more precise estimation for the incidence of pollen allergy in general is difficult, as respiratory allergy can also be caused by other allergens. In polluted regions, pollen can carry and interact with additional pollutants and irritants in the air. These agglomerates of airborne particles can have enhanced allergenicity¹⁵ which may influence the sensitisation process¹⁶. The resulting respiratory allergy is therefore not fully attributable to pollen allergy.

Interestingly, higher socioeconomic status and living in urban areas increase the prevalence of pollen allergy. In industrialised countries, the prevalence of allergic respiratory disease has been on the rise due to changes in living standards, climate change and air pollution¹⁷⁻¹⁸, and is projected to continue rising¹⁹⁻²⁰. Pollen allergy could become even more prevalent or be more aggravated due to association to pollutants that can act as irritants/exacerbators, and/or because certain substances in pollen are upregulated by abiotic stress on the pollen-producing plants, in other words, pollution could make pollen more allergenic²¹.

Chapter 1

This thesis chapter will first review the pathophysiology of allergic diseases, then discuss treatment options for the disease, followed by an overview of three disease hypotheses and lastly, discuss pollen and its composition in order to set the scene for Chapter 1.2.

1.1.1 Pathophysiology

In principle, allergy is an inappropriate immune response of the adaptive immune system to an innocuous entity, which results in inflammation. Most commonly, this inappropriate hypersensitivity is atopic and characterised by an excess production of IgE²². There are also non-atopic allergic diseases³, but the mechanisms behind these are less well-understood, which is why this thesis will focus on atopic, IgE-mediated allergy.

Depending on the site of allergen entry and the predisposition of the individual towards allergy, the affected organs and symptoms can vary (Table 1.1). Several organs can be affected and numerous symptoms can appear at the same time. Episodes of exacerbation during which symptoms break out suddenly can occur as well, e.g. an asthma attack or a breakout of eczema. If an allergen reaches the bloodstream or the body reacts in an especially violent way, the effects can be systemic and lead to allergic anaphylaxis. Allergic anaphylaxis is a severe, rapid onset systemic reaction that can be potentially life threatening. It can affect several of the aforementioned organs and the severity and rapid eruption is what makes it so dangerous if no adequate treatment is given.

Affected Organ	Response
Airways	Asthma, bronchial constriction, increased mucus production, inflammation of the airways leading to bronchial hyperreactivity
Ears	Inflammation of the external, middle and inner ear
Eyes	Allergic conjunctivitis, redness, itching
Gastrointestinal tract	Abdominal pain, bloating, vomiting, diarrhea
Nose	Allergic rhinitis, increased mucus production
Sinuses	Allergic sinusitis, increased mucus production
Skin	Allergic eczema, contact dermatitis, wheal-and-flare reaction, edema, increased vascular permeability
Systemic	Anaphylaxis, edema, increased vascular permeability

Table 1.1 Symptoms of allergic response²³.

The symptoms experienced as part of an allergic reaction are the result of inflammation. Inflammation is an orchestrated effort that involves cells of the immune system, inflammatory mediators, and structural cells. In allergic disease, it is not possible to account for the breadth of allergic disease manifestation with the malfunctioning of a single cell or mediator, as a factor that plays a key role in one disease phenotype may only have a minor role in another phenotype. An overview of the main cells and components involved in the manifestation of allergy is shown in Figure 1.1.

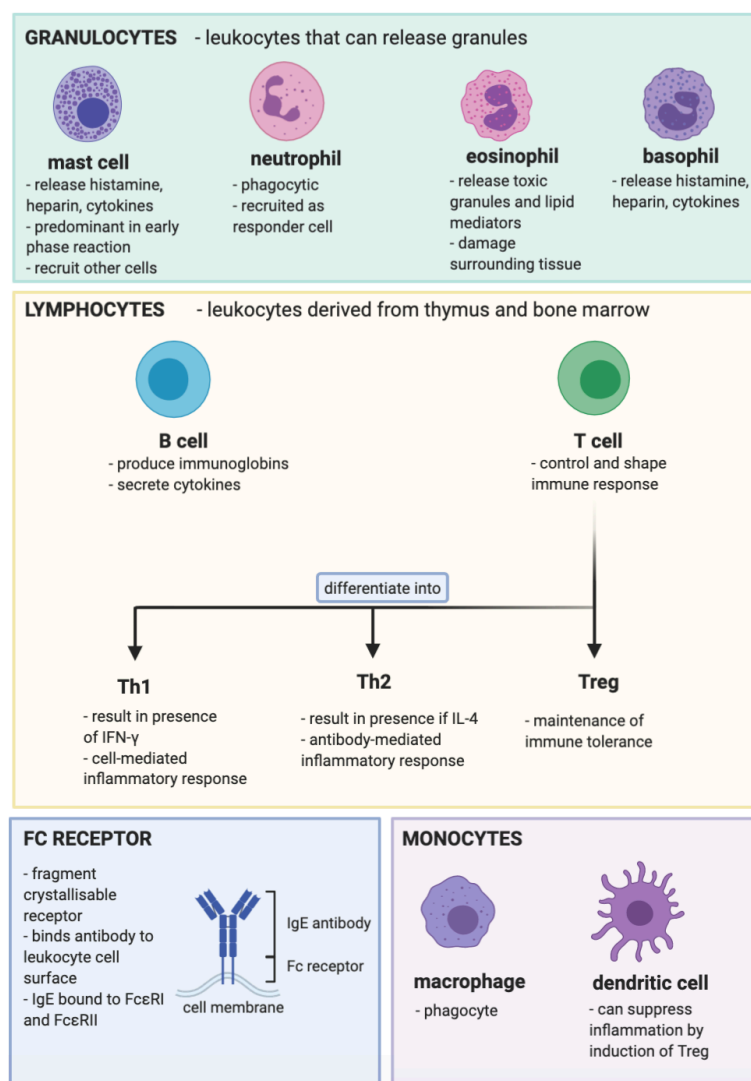


Figure 1.1 Overview of the main cells and components involved in the manifestation of allergy; granulocytes: mast cells²⁴⁻²⁵, neutrophils²⁶, eosinophils²⁷, basophils²⁸; lymphocytes included in the T helper Type 1/T helper type 2 (Th1/Th2) balance²⁹; monocytes: macrophages³⁰ and dendritic cells³¹⁻³²; IgE³³ and high-affinity IgE receptor (Fc ϵ RI)³⁴.

A characteristic across all allergic diseases, however, is the involvement of hyperactive Th2 cells, causing a tilt in the Th1/Th2 balance, which alters the nature of the immune response³⁵. T cells control and shape the immune response. A Th1-mediated response leads to cell-mediated immunity whereas a Th2-mediated response leads to antibody-mediated immunity. Both ultimately cause inflammation, though the mode in which it develops is different, and, due to the nature of the cytokines they excrete, Interferon gamma (IFN- γ) for Th1 and Interleukin(IL)-4 for Th2, these pathways mutually suppress each other. Th1 is thought to have developed for the defence against intracellular parasites, and bacterial and fungal infections,

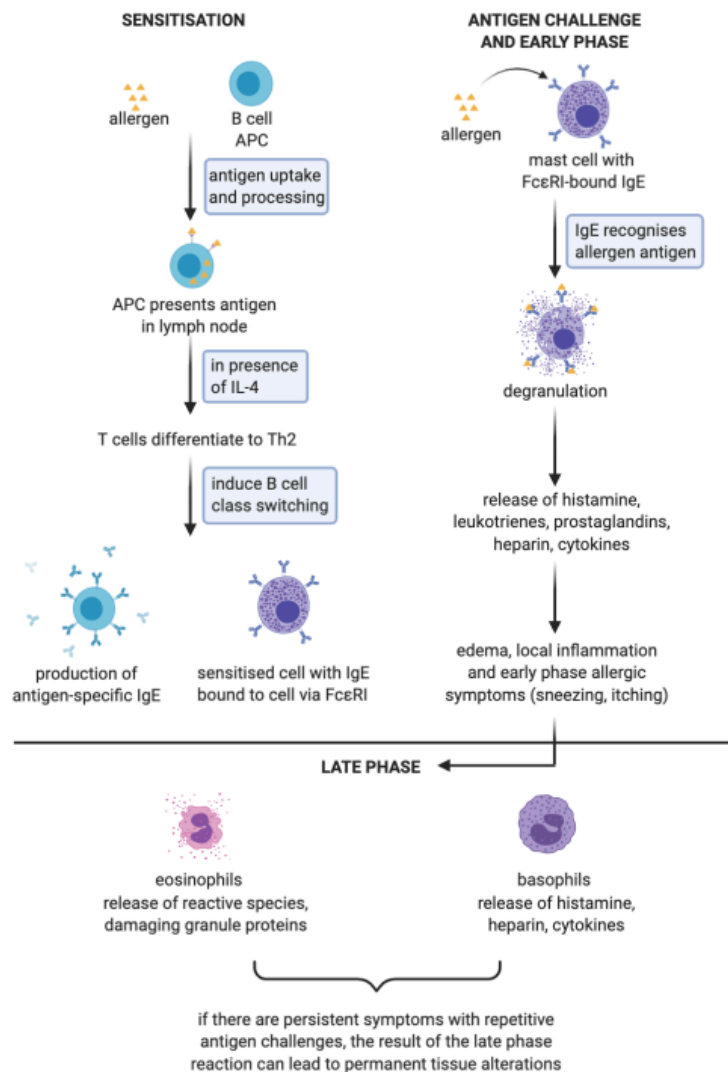


Figure 1.2 Disease progression of allergy, showing the three phases: sensitisation, antigen challenge and early phase and late phase.

whereas Th2 is thought to have evolved as another response to pathogens, particularly helminths^{29,36}. Th2 and Th1 cells both develop from naïve T helper cells (Th0). These Th0 helper cells differentiate as a response to the stimuli they receive. These stimuli include the surrounding cytokine profile, the hormones present, the nature of the antigen, the cell type presenting an antigen, and the binding of the T cell receptor with the major histocompatibility complex-antigen complex²⁹. Both mature T cell subsets promote further differentiation of their own kind with their cytokine secretion, which is why once one subset is hyperactive, it is hard to reverse the trend. Another interesting fact is that in cases where either Th1 or Th2 polarization can occur, there is a bias towards Th2²⁹. In allergy, a Th2-dominated response leads to the exaggerated production of allergen-specific IgE, which is not counter-regulated by other cells or mediators³⁷.

The progress of allergic disease can be roughly divided into three phases: i) sensitisation phase, ii) early phase reaction and iii) late phase reaction. A pictorial representation of the three phases can be found in Figure 1.2.

1.1.1.1 Sensitisation

Before an allergic reaction can be initiated by allergen binding to antigen-specific FcεRI-bound IgE on mast cells or basophiles, an individual needs to be sensitised to the allergen, i.e. antigen-specific FcεRI-bound IgE needs to be present³⁸. Sensitisation is the process in which antigen-specific IgE is formed for the first time³⁹.

First, the individual needs to be exposed to the allergen. Not all encounters with a potential allergen lead to sensitisation, even in genetically predisposed (atopic) individuals. In order to produce antigen-specific IgE, an allergen antigen has to be taken up by a cell capable of antigen presentation⁴⁰⁻⁴¹. This cell migrates to a lymph node and, in the presence of IL-4⁴², presents the processed antigen to naïve T cells that then differentiate to Th2 cells⁴³. These Th2 cells secrete IL-4 and IL-13 and thus induce B cells to undergo class switching by changing from immature immunoglobulin M production to mature, antigen-specific IgE production. This process is highly regulated and influenced by a plethora of factors as both cells and mediators influence each other⁴⁴. After class switching, IgE levels modulate the amount of FcεRI by affecting the turnover rate and in turn, the receptor dictates the intensity of the immune response⁴⁵⁻⁴⁷. How the upregulation of FcεRI is triggered in the disease progress is not precisely known; what is known, is that IgE binding to the alpha chain is a minimal requirement for induction of upregulation⁴⁸.

Chapter 1

Ultimately, class switching is regulated by Th1 and Th2 cytokine secretion. Th1 and Th2 are mutually suppressive by promoting differentiation of Th0 cell towards their own kind; cytokines IL-4, IL-5, IL-9 and IL-13 promote the development of Th2 cells whereas IFN- γ and IL-2 promote Th1 cell development. In allergy, overactive Th2 secrete IL-4, IL-5, IL-9 and IL-13 and thus further skew the balance towards Th2 cell differentiation. There seems to be a strong genetic component to this imbalance. Examples for genes that affect the Th1/Th2 balance are the GATA3 gene and the TBX21 gene, which promote Th2⁴⁹⁻⁵⁰ and Th1⁵¹ differentiation respectively. The source of the initial stimulus that first enables switching to a Th2 phenotype and thus causes sensitisation has not been identified⁴⁹.

There are pathways that can rein in the allergic response and induce tolerance. Dendritic cells that encounter allergenic antigen with their Fc ϵ RI-bound IgE induce CD4 T cells to differentiate into regulatory T cells (Treg) that suppress T cell responses and thus induce tolerance of antigens, which means not all IgE action is necessarily pro-inflammatory⁵². This mechanism of tolerance induction, however, seems to be absent in allergic individuals.

1.1.1.2 Early Phase

After sensitisation has taken place, an early-phase IgE-mediated reaction can occur within the first minute upon allergen exposure. This reaction can be either localised or systemic. Allergic reactions are triggered when allergens cross-link with IgE bound to Fc ϵ RI on various immune cells⁵³⁻⁵⁴. Aside from mast cells, IgE can also be Fc ϵ RI-bound to basophils, eosinophils, monocytes, macrophages and platelets.

The early phase response is predominantly characterised by mast cell degranulation following the crosslinking with antigen⁵⁵. Mast cell degranulation involves secretion of mediators like histamine, cytokines and chemokines, as well as the *de novo* synthesis and release prostaglandins⁵⁶, leukotrienes⁵⁶ and platelet-activating factor⁵⁷. Histamine, upon binding to histamine H1 receptors, causes an immediate increase in local blood flow and vessel permeability, in turn leading to edema and local inflammation. By triggering additional receptors like neural receptors, histamine can also cause itching and sneezing. The effects of histamine characterise the early phase⁵⁸.

The resulting effects are the symptoms that allergic individuals experience, which can vary depending on intracellular molecular events that further influence *de novo*

synthesis and release of mediators⁵⁹. This reaction is further amplified by the recruitment of other cells like eosinophils, basophils, Th2 cells and B cells. Usually this very strong reaction is reserved to combat parasitic infections, but in allergic individuals this response is dysregulated.

1.1.1.3 Late Phase

Depending on the dose of allergen and on how strong an immune reaction was triggered, a late reaction may occur. Caused by the mediators released from mast cells in the early phase reaction and by recruitment of other cells like eosinophils, basophils and neutrophils⁶⁰⁻⁶¹, the late phase reaction usually develops after 2-6 h and peaks 6-9 h after allergen exposure and usually fully resolves in 1-2 days⁶².

Eosinophils can synthesise chemical mediators, as well as release toxic granule proteins and free radicals. These can kill invading organisms but can also cause damage to the surrounding tissues. Because eosinophil activation involves damage to the host, this process is highly regulated and only few eosinophils are produced in absence of an infection. When Th2 cells are activated, however, more eosinophils are produced and released into circulation. Eosinophil degranulation releases major basic protein which leads to the degranulation of basophils and more mast cells.

Basophils are similar to eosinophils in terms of their abundance when no infection is present versus when an infection is present. They express FcεRI on their cell surface and are recruited to sites where defence against pathogens is required or where an allergic reaction is occurring.

A persistent late phase reaction can lead to permanent alterations in the tissue affected, an example being airway tissue remodelling in asthma. In this way, a single allergen exposure leads to an acute allergic reaction and cools off after 1-2 days, but persistent or repetitive challenge can lead to development of chronic allergic inflammation that comes with associated tissue alterations. An example for this phenomenon is the asthmatic lung in which the layers of the airway wall are permanently altered⁶².

1.1.2 Treatment

As allergy is a complex disease, the disease phenotype of individuals can vary vastly. An individual can be allergic by developing rhinitis, asthma, eczema or a combination of these conditions with varying severity, and sometimes also with associated comorbidities, which can also exacerbate the disease⁶³⁻⁶⁴. Additionally, the disease

phenotype and severity can change with age, an example being the atopic or allergic march, a term coined to describe the progress of allergic disease from childhood to adolescence, often initiated with atopic dermatitis and followed by allergic rhinitis and asthma⁶⁵. Pollen allergy is a very heterogeneous disease and thus treatments have to be tailored to the patient's clinical case. Current treatment strategies for allergy are allergen avoidance, desensitisation therapy and symptom management.

The long-term effects of avoiding allergens have been previously studied in the context of dust mite allergy; i) improved bronchial reactivity to histamine⁶⁶ and ii) reduced dust mite-specific IgE serum levels have been reported in patients allergic to dust mites⁶⁷⁻⁶⁸. This, however, is not a viable long-term strategy for individuals with pollen allergy since pollen is ubiquitous in the air during flowering season of its respective plant⁶⁹. Furthermore, it is not known whether the conclusions from a dust mite study can be applied to pollen allergy. All in all, allergen avoidance, although a cornerstone of treating allergic patients, finds little applicability in patients that are allergic to pollen⁷⁰.

Desensitisation therapy, also called allergen-specific immunotherapy, is a therapeutic approach during which allergen is administered to the patient subcutaneously or sublingually over an extended period of time⁷¹⁻⁷⁴. Although the mechanism is not thoroughly understood, the clinical efficacy of this therapy is well documented⁷⁵, with tolerance being sustained for at least 2-3 years after stopping the treatment⁷⁶⁻⁷⁷. A hypothesis is that immunoglobulin G induced by desensitisation therapy inhibits IgE-mediated mast cell degranulation⁷⁸. So far, desensitisation therapy is the only approach that tackles the cause of the disease and not only the symptoms.

Lastly and the most used therapeutic approach is symptom management. Symptom management with drugs ameliorates the symptoms but does not stop the disease progression. Due to the heterogeneity of the disease and different organs being affected depending on disease phenotype, many different treatment approaches have been developed. This chapter will first introduce small molecule approaches, then discuss new treatment options enabled by monoclonal antibodies and lastly give an outlook on pollen allergy treatment.

1.1.2.1 Small Molecule Approaches in the Treatment of Allergy

The treatment of allergic diseases with various chemical substances started almost a century ago. Today, small molecule drugs used in the treatment of allergy include a

variety of structures inspired by nature, as well as some completely synthetic drugs. Some of these were developed to address symptoms caused by physiological changes induced by the immune response chain, whereas others directly address the allergic cascade. Several examples of small molecules used in the treatment of allergy are shown in Table 1.2 and will be discussed in the course of this chapter. Small molecule drugs that address the physiological manifestations of the disease, i.e. do not interfere with the immune response chain and offer organ-specific alleviation of the symptoms, will be discussed first. Next, drugs that address the immune response chain directly, also termed 'drugs with systemic application', will be discussed.

Drugs with organ-specific effects	Disease Phenotype	Effect
Alpha-1 receptor agonists	Rhinitis	Vasoconstriction
Beta agonists	Asthma	Bronchodilation
Muscarinic antagonists	Asthma	Bronchodilation
Leukotriene receptor antagonists	Asthma	Mitigation of Bronchoconstriction
Lipoxygenase inhibitors	Asthma	Mitigation of Bronchoconstriction
GABAergic agonists	Skin	Mitigation of Itching Sensation
Drugs targeting the immune response chain	Mechanism	
Antihistamines	Block H1 receptors and prevent histamine	
Mast cell stabilisers	Prevent mast cell degranulation	
Cromones	Unknown/prevent mast cell degranulation	
Corticosteroids	Anti-inflammatory effects, mediator suppression	

Table 1.2 Small molecules used in the treatment of allergy.

1.1.2.1.1 Small Molecule Drugs with Organ-Specific Symptom Alleviation

Symptoms of allergic reactions can be localised in different organs and thus can be treated using organ-specific solutions. These drugs specifically address the physiological manifestation of the immune response, e.g. constriction of the airways in asthma. This chapter will highlight some examples that are used in the treatment of allergic rhinitis, asthma and eczema.

In allergic rhinitis, nasal congestion occurs through the same mechanism as rhinitis caused by the common cold, and hence can be treated with nasal decongestant usually used for the common cold. Alpha-1 receptor agonists like phenylephrine cause vasoconstriction and thus symptom relief. Anticholinergic nasal allergy sprays can also be used to achieve the same effect.

Asthma can be treated with a number of asthma-specific approaches. One of the most commonly used drug classes in asthma are beta agonists, e.g. salbutamol. Beta agonists act as bronchodilators and thus can be used to prevent bronchoconstriction

and asthma attacks⁷⁹. Another mechanism to achieve bronchodilation is by utilisation of muscarinic antagonists, like tiotropium bromide. Bencycloquidium bromide and methscopolamine are being investigated for their action as muscarinic bronchodilators⁸⁰. Another drug class used specifically for asthma are antileukotrienes, also called leukotriene receptor antagonists. Leukotrienes cause contraction of airway smooth muscle, microvascular hyperpermeability and mucus hypersecretion⁸¹. Drugs like montelukast inhibit leukotriene receptors and thus suppress the function of these inflammatory mediators⁸²⁻⁸⁶. Lipoxygenase inhibitors, like zileuton, inhibit 5-lipoxygenase which is involved in leukotriene synthesis and thus interrupt the mediator chain⁸⁷⁻⁹⁰.

GABAergic agonists are being investigated as a potential means to address the itching sensation of eczema. Recently gained understanding of the pathophysiology of acute and chronic itch shows that GABAergic agonists like ethchlorvynol could potentially be used against the histamine-induced itching sensation in allergy. This, however, is still investigatory due to the sedative side-effects⁹¹⁻⁹².

Many of these drugs are very effective in the treatment of symptoms caused by allergy without targeting the immune response chain at play in allergic disease. Especially in the treatment of asthma, where immediate symptom relief is of utmost importance, these drugs have an essential function in managing episodes of exacerbation.

1.1.2.1.2 Small Molecule Drugs Addressing the Immune Response Chain

Having looked at organ-specific treatment options, treatment options that have targets in the immune response chain of allergic disease and thus can address allergy symptoms regardless of their localisation. This subchapter will discuss these major classes of drugs: antihistamines, mast cell stabilisers, cromones and lastly, corticosteroids.

Antihistamines bind histamine H1 receptors on mast cells, effectively suppressing the effect of histamine in the allergic cascade. They are one of the oldest treatment options. First generation antihistamines were approved for medical use starting from the 1950s and include a variety of drug classes, like ethylenediamines, ethanolamines, alkylamines, piperazines and tri- and tetracyclics. Examples of drugs of each of these groups are mepyramine, clemastine, pheniramine, chlorcyclizine and promethazine. Many of these drugs have undesirable properties due to their additional systemic effect on also the central nervous system and their generally

promiscuous nature, causing e.g. anticholinergic effects. This is why they have largely been superseded by the second generation of antihistamines. Second generation antihistamines were developed to be more selective for the peripheral H1 receptor and thus have less side effects⁹³. Some examples that are in use are cetirizine and loratadine. For the treatment of allergic eczema, topical drugs such as azelastine and olopatadine were developed⁹⁴. Antihistamines find application in eye drops for the treatment of allergic rhinitis and can be used as a prophylactic drug for pollen-induced asthma during flowering season.

Mast cell stabilisers prevent mast cell degranulation and thus prevent histamine and other mediators from being released⁹⁴. Finn and Walsh⁹⁵ have compiled an overview of natural and synthetic mast cell stabilisers, which demonstrates the variety in structures that are reported to prevent degranulation. Natural mast cell stabilisers include flavonoids, coumarins, phenols, terpenoids and theanine; examples for synthetic mast cell stabilisers are midostaurin⁹⁶, hypothemycin⁹⁷ and fullerenes⁹⁸. Some, like azelastine and olopatadine, also have H1 receptor antagonism as a property⁹⁹. The precise mode of action of mast cell stabilising molecules is still unknown⁹⁴⁻⁹⁵. It seems likely that these very different structures have different mechanisms of action. As mast cell stabilisers are a very heterogeneous group, their applications in the treatment of pollen allergy are similarly varied.

Anti-allergic cromones were originally found in the 1960s, the first one being cromolyn sodium¹⁰⁰, followed by the discovery of nedocromil¹⁰¹. They are a subset of mast cell stabilisers as their mechanism of action was found to be different from other mast cell stabilisers. What is known about their mechanism of action is that tachyphylaxis is observed, and protein kinase C activation is promoted. Putative therapeutic mechanisms that would be in line with these observations are G protein-coupled receptor 35 activation, so far regarded as an orphan receptor with downstream effects on protein kinase C, and activation of an endogenous anti-inflammatory loop, the Anx-A1/FPR system¹⁰²⁻¹⁰³. The exact mechanism is still a mystery. Nedocromil is used as an inhaler for asthma and as eye drops for rhinitis, whereas cromolyn sodium is no longer used due to its short half-life.

Corticosteroids are a class of steroid hormones that includes glucocorticoids and mineralocorticoids. The reason why corticoids, or more precisely, glucocorticoids that are analogues of cortisol, are used in the treatment of allergic symptoms is due to their anti-inflammatory, immunosuppressive and vasoconstrictive effects. They

display three principal mechanisms of action: i) NF- κ B inhibition, ii) induction of anti-inflammatory protein expression by MAPK phosphatase I and I κ B kinase and iii) inhibition of 5-lipoxygenase and cyclooxygenase-2¹⁰⁴. Corticosteroids remain one of the most effective anti-inflammatory drug classes available for the treatment of allergic diseases¹⁰⁵⁻¹⁰⁸. Their side effects, however, are considerable, and include immunosuppression, hypertension, hyperglycemia, osteoporosis and changes in metabolism¹⁰⁴. In addition to the physical side effects, 20 % of patients receiving high doses of corticosteroids also develop psychiatric disorders¹⁰⁴. These symptoms reverse upon discontinuation of therapy¹⁰⁹. Therefore, although corticosteroids remain one of the most used treatments for severe cases of allergy-induced inflammation, the physiological and psychiatric side effects are not to be overlooked. Corticosteroids are used e.g. as steroidal nasal sprays in rhinitis, as inhalers in asthma and for variety of topical formulations for the treatment of eczema.

Drugs that can be used to manage different manifestations of the same disease are powerful tools in disease management. Their effects, however, come with associated side effects, thus some of the drugs discussed have dedicated formulations and administration routes in order to minimise these side effects. Nonetheless, the side effects of some of the systemically active drugs are considerable and therefore do not make those drugs an ideal choice. Often, these drugs are used in tandem with drugs discussed in Chapter 1.1.2.1.1 as a treatment regimen for both the chronic disease and episodes of exacerbations.

1.1.2.2 Treatments enabled by Monoclonal Antibodies

Monoclonal antibodies have recently opened the door to a plethora of treatment options since they enable binding modes inaccessible to small molecules¹¹⁰. Several monoclonal antibodies have been approved for medical use, e.g. omalizumab (approved 2003), dupilumab (2017) and benralizumab (2017). Omalizumab is an anti-IgE Fc region antibody, whereas dupilumab and benralizumab use the so-called anti-IL approach¹¹¹⁻¹¹². Both the anti-IgE and the anti-IL approaches will be discussed in order to give an overview of the developments in the field of treating allergic disease.

Since allergy is a disease characterised by an excess of IgE which causes the exaggerated immune response, it stands to reason that inhibiting IgE signalling would inhibit the allergic cascade and thus positively impact the clinical manifestation of the disease. Omalizumab is an anti-IgE Fc region antibody that results in a reduction of IgE available for binding to Fc ϵ RI and at the same time also reduces Fc ϵ RI on mast

cells and basophils¹¹³. Numerous monoclonal antibodies that target IgE are currently being evaluated in clinical trials, an example being ligelizumab¹¹⁰. Once approved, ligelizumab is expected to supersede the currently used treatment, omalizumab, for the indication of chronic spontaneous urticaria¹¹⁴⁻¹¹⁵. Omalizumab and ligelizumab are two examples of targeted monoclonal antibody development for therapeutic applications; however, not all of antibody approaches that target IgE signalling are successful. An example is the antibody quilizumab¹¹⁶, which targets the IgE pathway and although the treatment lowered the serum IgE levels by 30 % in patients, there were no observable changes in disease severity¹¹⁷⁻¹¹⁸.

ILs are important mediators in allergic disease: they are involved in the differentiation of Th2 cells and serve as signalling molecules in the allergic cascade. IL-inhibitors like dupilumab and benralizumab serve to inhibit effects caused by disease-associated ILs and thus alleviate symptoms by breaking part of the mediator chain. IL-4, IL-5, IL-13, IL-4R α and IL-5R α approaches are under investigation and will be discussed in turn^{112,119}.

IL-4 is an attractive target since it is involved in the class switching from immature immunoglobulin M to mature IgE producing B cells¹²⁰. Together with IL-13, IL-4 facilitates transmigration of eosinophils, T cells, monocytes and basophils. Although blocking IL-4 seems like an attractive approach, clinical trials have yet to show efficacy and benefits in patient treatment, as shown by the example of the aborted clinical trial of pascolizumab¹²¹⁻¹²².

IL-5 is a critical agent for regulating eosinophils¹²³⁻¹²⁵. When eosinophils degranulate, their granules cause damage to the surrounding tissues, therefore they play an important role in the pathogenesis and severity of the allergic disease. Inhibiting IL-5 can reduce the eosinophil count and ameliorate clinical symptoms in some patients^{111,126}. Examples for anti-IL-5 treatments are mepolizumab¹²⁷⁻¹²⁸ and reslizumab¹²⁹.

IL-13 is reported to induce cells towards the Th2 pathway¹³⁰. Lebrikizumab¹³¹⁻¹³⁴ and tralokinumab¹³⁵⁻¹³⁷ both bind to IL-13 and are both still under investigation and pending approval.

An alternative to inhibition of the signalling pathway by targeting the ILs themselves is binding to their receptors. Two receptors have been identified as successful therapeutic targets. IL-4R α and IL-5R α . Both IL-4 and IL-13 bind to the heterodimeric

combination of the IL-4R α and IL-13R α receptor, thus, blocking IL-4R α inhibits both IL-4 and IL-13 signalling. Dupilumab is an approved drug with IL-4R α as target¹³⁸. Functioning in the same manner, IL-5 signalling can also be suppressed by targeting the alpha chain of the IL-5 receptor (IL-5R α). Benralizumab binds to IL-5R α and is approved as a treatment for asthma¹³⁹.

To conclude this chapter, different targets for monoclonal antibodies and their efficacy have been discussed. Monoclonal antibodies allow for new ways to treat the disease since they can be used to address targets that are inaccessible to small molecules. They are found to be an effective addition to the assortment of treatment options for allergy. They do, however, come with one major disadvantage not addressed in this chapter, which is their cost. Furthermore, they are predominantly used for symptom management rather than treating the disease itself.

1.1.2.3 Outlook on Pollen Allergy Treatment

Pollen allergy remains a major health burden that has a substantial impact on quality of life and the economy¹⁴⁰. Patients with pollen allergy often trivialise their disease and neglect it¹⁴¹.

Currently, treatment options for pollen allergy mostly address the symptoms of the disease rather than the cause. Although a lot of progress has been made in finding genetic markers for the disease and examining environmental factors that could be relevant for the disease progression, many questions remain open as to the origin and sensitisation process of the disease and why pollen allergy seems to be clustered around specific types of pollen allergens. The treatment options are largely the same as they were 20 years ago, and new findings have not translated into new treatment options addressing the root cause of this disease¹⁴². Symptom management remains the most common approach. Monoclonal antibodies have enabled new ways of treating the disease, however, they are inaccessible to many people due to their associated cost.

To conclude, pollen allergy is a complex, heterogeneous disease and is still difficult to treat directly. Desensitisation therapy remains the only therapeutic approach to obtain long-lasting cessation of symptoms but comes at the price of having to undergo a lengthy treatment regimen. Understanding the disease pathology better will ultimately be key in treating the root cause of the disease.

1.1.3 Disease Hypotheses

Since many aspects of the disease, most importantly, the origin for its manifestation, are not clearly understood, hypotheses have been made in an attempt to explain the sudden rise in prevalence. First of all, there seems to be a nature versus nurture dichotomy; allergic diseases have a genetic component that is additionally also heavily influenced by environmental factors^{15,17,143}. The relationship can be illustrated with the analogy 'genetics loads the gun and epigenetics pulls the trigger'¹⁴⁴. It seems evident that there is a genetic component to the disease¹⁴⁵⁻¹⁴⁶, and at the same time, genetics alone cannot fully account for the sharp rise in prevalence of this disease.

There also seems to be a consensus that allergic sensitisation can start during the embryo-fetal development, and that the first three post-natal years are important in shaping the immune system and thus also the immune responses of an individual. Materno-fetal interactions during pregnancy are skewed towards the Th2 phenotype, as Th1-mediated immune responses are avoided due to the potential of IFN- γ to act as an abortifacient. IgE levels in the fetus are proportionate to maternal levels, so mothers who are atopic will expose their fetuses to higher quantities of IgE through the amniotic fluid. The human immune system is thought to have a Th2 bias¹⁴⁷⁻¹⁴⁸ and this bias gradually diminishes during the first 2 years of infancy (correlated with IL-12 productive capacity in early life). In patients that develop allergy, the Th2 response becomes increasingly stronger¹⁴⁸⁻¹⁴⁹. Furthermore, the first years determine the gut microbial flora which is also thought to play a vital role in the development of the immune system, and thus in the determination of whether an individual will be prone to allergic disease or not.

Besides these known facts and correlations, some hypotheses have also been postulated as an attempt to explain other aspects of the disease. Three of them will be discussed in the following subchapters, namely the hygiene hypothesis, the hapten theory and the danger model.

1.1.3.1 Hygiene Hypothesis

The hygiene hypothesis is a theory that traces its origins back to an article written by Strachan¹⁵⁰. He observed that prevalence of atopy is inversely correlated with household size, and concluded that infection in early childhood can prevent the development of allergic disease. This hypothesis was then named the 'hygiene hypothesis', which in a way is a misnomer, as priming the immune system is not

necessarily related to personal hygiene and can be misunderstood by laymen¹⁵¹. Renaming the hypothesis, however, was unfruitful. Thus, the now so-called hygiene hypothesis explains the rise in allergic diseases by a decline in infection during childhood, or conversely, by the reduced exposure to beneficial symbiotic bacteria or parasites¹⁵²⁻¹⁵³.

This comes from the evidence that there is a stark contrast between allergy prevalence in industrialised versus developing countries¹⁵⁴, as well as urban versus rural areas within the same country¹⁵⁵⁻¹⁵⁹. This observation is explained by the differing lifestyles, which includes dietary changes, better sanitation, and increased vaccination and usage of antibiotics. These observations tie in with the Th1 and Th2 imbalance. Less exposure to bacterial and viral infections during infancy leads to insufficient stimulation of Th1 cells, resulting in the immune system leaning towards proallergic Th2 responses. Arguably, there are two findings that contradict this theory: i) the rise in prevalence of Th1-mediated autoimmune diseases and ii) that helminth infections, to which the immune response is also Th2-mediated, are reported to be protective from allergic disease^{154,160-164}.

To elaborate on i), incidences of Th1-mediated autoimmune diseases such as type 1 diabetes have been steadily increasing. Th1-mediated autoimmune diseases and Th2-mediated allergic diseases seem to be linked at a population level, which stands in stark contrast to the Th1/Th2 imbalance hypothesis; according to the hypothesis, these two disease groups should be negatively associated as Th1 and Th2 are mutually inhibitory¹⁶⁵. The hypothesis here is that these two diseases are determined even more upstream from the Th1/Th2 imbalance, and the observed imbalance is a symptom, not a cause¹⁶⁵. This is further substantiated by the fact that both autoimmune disease and allergic disease can co-exist in the same individual¹⁶⁶.

In short, the hygiene hypothesis is too general to explain the complex group of allergic diseases and their relationship to helminth infections and autoimmune diseases^{65,167}. So far, the hypothesis is consistent with the fact that infection with certain agents is as protective against autoimmune diseases as it is against allergic disease¹⁶⁸. Evidence suggests that strategies like giving birth naturally as opposed to having a caesarean section, breast feeding, social and hence infectious exposure to other children and an appropriate diet and antibiotic use, can ensure that a proper microbiome is built up during infancy and can mitigate potential allergic diseases¹⁶⁹⁻

¹⁷⁰.

1.1.3.2 Hapten Theory

Karl Landsteiner conceived the original definition of haptens in the 1920s¹⁷¹⁻¹⁷². Haptens are small molecules that are not inherently immunogenic, but can bind to a protein and in this way become immunogenic due to their newly formed structural properties being able to interact with the immune system¹⁷³. The allergen in this case is the hapten, i.e. the chemical, but the antigen is the haptenated peptide. The definition in itself is elegant, although the reality is that unconjugated haptens can also react within the body via mechanisms that do not affect the immune system.

The evidence to date shows that hapten association has to be covalent in order to result in a bond that is strong enough to produce an antigen that can be recognised¹⁷⁴⁻¹⁷⁶. The primary targets for hapten binding are nucleophilic amino acid side chains like lysine, cysteine and histidine. Research shows that many contact allergens are hapten-originated¹⁷⁷. Oftentimes, haptens are drugs or synthetic additives, but they can also come from nature. It is also possible that haptens are endogenous in the body, as is the case in some autoimmune diseases. If the hapten derives from another compound by metabolism in the body, this compound is called a pro-hapten.

In the case of hapten research, which is usually conducted with experimental haptens¹⁷⁸, two phases are distinguished: the afferent phase, also known as sensitisation phase, and the efferent phase, also known as the elicitation phase. Usually, the sensitisation phase lasts 10-15 days in humans and the elicitation phase takes 24-72 h, and possibly even longer with weaker haptens¹⁷⁸. In allergic contact dermatitis, it was found that for strong haptens, a single contact was sufficient to induce both the afferent and the efferent phases of disease at the same time¹⁷⁹.

The hapten theory gathers special interest in two areas of allergic disease, namely in contact dermatitis, in which it presents a key theory in sensitisation¹⁸⁰⁻¹⁸¹, and in drug allergy^{174,182}, but it is also an interesting theory when looking at other allergic diseases¹⁸³. Molecules that can act as haptens are also being researched as a therapeutic tool to saturate mast-cell bound IgE prior to allergen exposure¹⁸⁴.

Interestingly, haptens can elicit allergic reactions in both airways and the skin, but the actual sensitisation process has been reported to occur through the skin¹⁸⁵. By using the example of allergic contact dermatitis, many roles of individual cell types like T cells, Langerhans cells and mast cells have been elucidated, but the treatment options

remain symptomatic and the exact link between haptens and atopy is still poorly understood^{178,186-188}.

1.1.3.3 Danger Model

A commonly used model to explain why the immune system reacts is the self-nonself model; the immune system recognises something as nonself and thus reacts. This model, however, struggles to explain some findings, like non-rejection of an embryo in a mother's womb, or the necessity of adjuvants in vaccines. This has made it necessary to adapt the model by making exceptions and building even more models on top of this model¹⁸⁹⁻¹⁹⁰. In order to better accommodate for these observations, Polly Matzinger suggested the so-called danger model in 1994¹⁹¹ (Figure 1.3). This model stands on the shoulders of the self-nonself model by adding another layer: it suggests that the body is more concerned with dangerous and potentially harmful stimuli rather than foreign stimuli, and shows a different viewpoint on how we can think about immunology. It is proposed that rather than react to nonself entities, the body will answer to 'danger signals'. In principle, that means that in absence of a danger signal, an antigenic signal will induce tolerance while in presence of a danger signal, it will lead to sensitisation¹⁹².

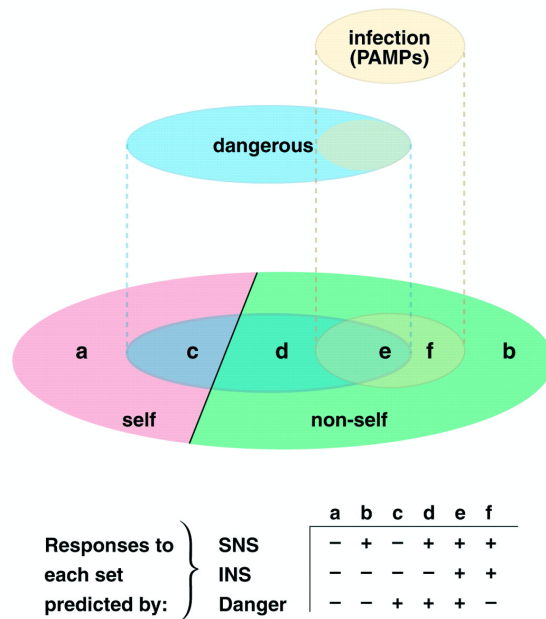


Figure 1.3 Self-nonself paradigm and the danger model. Abbreviations from in figure: PAMPs: pathogen-associated molecular patterns; SNS: self-nonself; INS: infectious-nonself. Reproduced with permission*, copyright AAAS.

* From Matzinger, P., The Danger Model: A Renewed Sense of Self, Science 296 (2002) 301-305. Reprinted with permission from AAAS.

This analogy also has some interesting aspects in the context of pollen allergy, as it is an exaggerated response to agents that are otherwise considered innocuous. It has also been suggested that this model has implications for the hapten theory, as haptens can also act as irritants and in this way trigger sensitisation, followed by exaggerated hostile immune reactions¹⁹³. So far, most of the publications involving the danger model and allergy have been in the fields of contact dermatitis¹⁹²⁻¹⁹⁴ and drug allergy¹⁹⁵, and some have also tried to address how this model can fit into what we already know about the immune system¹⁹⁶⁻¹⁹⁷.

1.1.4 Composition of Pollen

Since the origin and sensitisation process in pollen allergy are unclear (Chapter 1.1.1) and hypotheses introduced in Chapter 1.1.3 give reason to believe that small reactive molecules associated with the allergen could lead to sensitisation and thus to disease, this chapter will now take a step back and examine the cause for pollen allergy: pollen.

In pollen allergy, pollen is the trigger for the allergic cascade. Scientists have studied both the entity itself, and the proteins and small molecules it can contain. Pollens are two- or three-celled organisms¹⁹⁸ with a diameter between 15 μm and 60 μm ¹⁵. They are complex constructs of proteins and small molecules that are used by angiosperms and gymnosperms to transport genetic material for sexual reproduction¹⁹⁹. Pollen can be either wind-dispersed by being released in a vast surplus during the flowering period of the respective plant, or insect-dispersed by being carried by pollinating insects which transport and disperse pollen in the search of nectar.

The immune system recognises various pollen protein antigens from various plant species. The allergens have been catalogued on databases such as Allergome (www.allergome.org) and Allergen (www.allergen.org). Many protein allergens have been extensively studied in order to elucidate the origin of allergenicity and also in the pursuit of better understanding of the disease. It has been reported that out of 157 at least partially sequenced pollen allergens, those that can be clustered are clustered into 29 protein families (Figure 1.4)²⁰⁰. These protein families feature proteins with both known and unknown functions. Expansin²⁰¹, for example, is a protein that is involved in plant growth, and profilin is a ubiquitously present protein that is known for cross-reactivity²⁰². Other protein family clusters, like the Bet v 1-like cluster, are still under investigation as it is currently still unknown what their exact function are, but many of their effects in the human physiological system have been studied²⁰³⁻²⁰⁴. Some allergenic proteins, like beta-expansins, also have nonallergenic analogues,

the alpha-expansins, which serve a similar function but are not as allergenic as their counterpart. The question that begs to be asked is this: if function is not the key to allergenicity, what other defining feature could be?

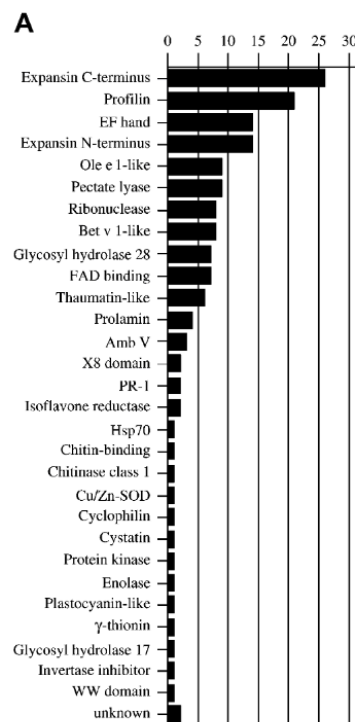


Figure 1.4 Protein family distribution of pollen allergens, showing numbers of sequences in all families in pollen. Reproduced with permission²⁰⁰, copyright Elsevier.

Whilst the cause for the triggering of the allergic cascade can be attributed to various protein components of the pollen, which serve tasks like pollen germination, pollen tube growth or protection of genetic information²⁰⁵, the possible role of small molecules in the context of pollen allergy has barely been investigated. The body, however, is exposed to these compounds at the same time as it is exposed to the allergen, so their effect on the body could play a role in allergic disease.

Pollen grains have walls made out of cellulose and sporopollenin which make them very resistant to degradation. They have been reported to be stable for over centuries under dry conditions¹⁵. The outside of the grain is also covered with proteins, saccharides and lipids that are only loosely attached to pollen. The mixture of compounds covering the outside is species-specific and relevant bioactive compounds tend to be water soluble²⁰⁶. The outside can furthermore contain flavonoid

and carotenoid pigments, lignin, and pectin. Wind-pollinated plants tend to have starchy pollen whereas insect-pollinated plants tend to have pollen rich in fat²⁰⁷.

Inside the pollen interior are mainly proteins, lipids, carbohydrates and nucleic acids²⁰⁸. Some of the aforementioned serve as precursors for plant hormones, such as dinor isoprostanes. These are the plant analogue to human prostaglandins and isoprostanes²⁰⁹⁻²¹⁰ that are thought to be involved in plant host defence and stress signalling, but their effects on the human immune system are not known²¹¹⁻²¹². Under physiological conditions, pollen grains release lipids that activate human neutrophils and eosinophils *in vitro*; furthermore, pollen can induce activation and maturation of dendritic cells *in vitro*²¹³.

Pollen grains are generally too large to penetrate the small airways where asthma occurs²¹⁴. Cytoplasmic fragments, however, are small enough⁸, thus pollen fragmentation or rupture could be why they are allergenic. It also appears that pollen as a whole structure is not the problem; the issue is what it contains. Experiments with pollen extract show that it can reach the areas relevant for asthma and also induce bronchospasm within a few minutes, which is in agreement with the sudden acute symptoms of asthma, whereas whole pollen only triggers a reaction several hours later²¹⁵.

Another hypothesis is that pollen actually acts as a carrier for small particles that are able to penetrate into the bronchial regions and be responsible for symptoms seen in this area²¹⁶. An additional interesting observation is that pollen, under humid conditions, liberates pro-inflammatory eicosanoid-like substances²¹⁷⁻²¹⁸, can activate granulocytes²¹⁹ and induce activation and maturation of dendritic cells *in vitro*²²⁰, which means that pollen grains themselves could potentially contribute to an inflammatory response, even in non-atopic individuals. This is interesting, considering that currently we only have limited understanding as to how allergic sensitisation works, and these mediators liberated from pollen could play a part in the process. It is not clear why proteins pose as allergens; there is the question of why individuals develop allergies against technically speaking a biologically inert protein in the first place, and whether this is actually induced by some sort of adjuvant which could be a small molecule component of pollen²²⁰.

In summary, although secondary metabolites of pollen have been investigated, their role in the development of allergic disease has not been thoroughly questioned as of yet. Pollen could harbour reactive secondary metabolites that, additionally to their

Chapter 1

intended function, could play a role in the pathogenesis of pollen allergy and in the sensitisation process. Examining reactive small molecules contained in pollen could potentially shed light on the origin of the disease and thus identifying such molecules of interest is the next logical step.

1.2 Identifying Reactive Compounds

Reactive compounds readily undergo chemical reactions. In the human body, such compounds can have positive effects, e.g. be used in the treatment of a disease, and can also have negative effects, e.g. side effects of medication. Reactivity can thus be desirable but also undesirable. Identifying reactive compounds is key to examining such reactivity. When discussing reactive compounds and as such, reactivity, the terms and reaction conditions need to be defined exactly, because reactivity is a relative term. Under the right circumstances, even the most inert structures, like noble gases, can display reactivity. In order to identify reactive compounds, one has to first understand the underlying principles of reactivity, then, define the type of reactivity that is relevant for the study and lastly, review how one could experimentally identify and analyse reactive compounds of interest. This chapter will address these three points in the following subchapters, starting with chemical reactivity.

1.2.1 Chemical Reactivity

In principle, chemical reactions are governed by the principles of thermodynamics and kinetics. Thermodynamics describe the energy states, i.e. heat and work involved in chemical reactions, and thus the direction of a reaction process, whereas kinetics concerns itself with the rate of chemical reactions. This section will first talk about thermodynamic aspects, followed by kinetic aspects, and then come to a conclusion on what makes a compound reactive.

1.2.1.1 Thermodynamics in Chemical Reactivity

All chemical reactions involve energy. Thermodynamics concerns itself with the energy levels of states and whether a resulting energy state from a reaction is more stable, i.e. favourable, or less stable, i.e. unfavourable, than the initial energy state. This determines whether a reaction is feasible and thus is very relevant when discussing chemical reactivity.

Thermodynamics has four fundamental laws that express empirical facts about energy. Two of these laws, the first (1) and the second (2), are relevant when it comes to examining chemical reactivity and explain why certain reactions happen and why certain molecules are reactive under physiological conditions.

Chapter 1

(1) *Energy can be neither created nor be destroyed.*

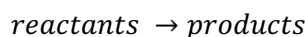
(2) *Entropy of the entire universe, as an isolated system, will always increase over time.*

The first law of thermodynamics (1) describes the law of energy conservation. In the context of chemical reactions this means that the net energy of an isolated system (neither energy nor mass can be exchanged with surroundings) does not change. Changing the make-up of a molecule, however, can result in a net energy gain or loss with respect to just the reactants and products within a thermodynamically closed system (heat and work can be exchanged with its surroundings, but not matter). This energy change in chemical reactions is thermodynamically described by the Gibbs free energy (Equation 1.1).

$$G = H - TS$$

Equation 1.1 Gibbs free energy definition. Enthalpy (H) is a thermodynamic measure of the total heat content of a system, i.e. the internal energy and the product of pressure and volume. Entropy (S) is a measure of the number of microstates in a system, often also called the degree of disorder or randomness in a system.

G is the Gibbs free energy which is used to quantify the maximum amount of non-expansion work that can be extracted from the system in question at chemical equilibrium. Since total enthalpy and entropy are hard to quantify, the equation is most often used to express the change of two states (Equation 1.2): the reactant state and the product state. This equation also shows directionality; the products and reactants can be reversed in order to examine the retro-reaction.



$$\Delta G = G_{\text{products}} - G_{\text{reactants}}$$

$$\Delta G = \Delta H - T\Delta S$$

Equation 1.2 Change in Gibbs free energy and directionality of the equation.

ΔG is the difference in maximum amount of work of the reactants and products states. A positive ΔG means that the new energetic state (products state) is outside of the maximum amount of non-expansion work that can be extracted from the preceding state (reactants state), and thus it means that this reaction is thermodynamically unfavourable or unfeasible. Conversely, a negative ΔG indicates that the new energetic state (products state) is achievable within the maximum amount of non-

expansion work that can be extracted of the preceding energetic state (reactants state). A reaction that has negative ΔG is also called a 'spontaneous' reaction, in other words, a thermodynamically feasible reaction. This means that in order for a compound to be reactive and its associated reaction to be thermodynamically feasible, the compound needs to be in a higher energy state than the prospective product, i.e. the reactive compound needs to carry an inherent thermodynamic instability. The energy difference between products and reactants as a result of this instability drives the reaction towards a more stable product. Such an instability, also quantified by potential energy, can be due to a partial positive or negative charge, as is the case with electrophiles and nucleophiles, or due to angle, torsional or steric strain.

Knowing the relationships between G , H and S , and their individual definitions, it becomes evident why negative ΔG is favourable. There is, however, one more way to explain this relationship, and this involves the not yet discussed second law of thermodynamics (2). The second law of thermodynamics can be stated as the maximum entropy principle. As stated previously in (2), entropy is maximised in an isolated system at equilibrium. The minimum energy principle is a restatement of the same law: for a closed system with fixed entropy, the total energy is minimised at equilibrium. This means that the system strives to minimise energy and form more stable bonds. This is another way to explain the relationship between ΔG , ΔH and ΔS .

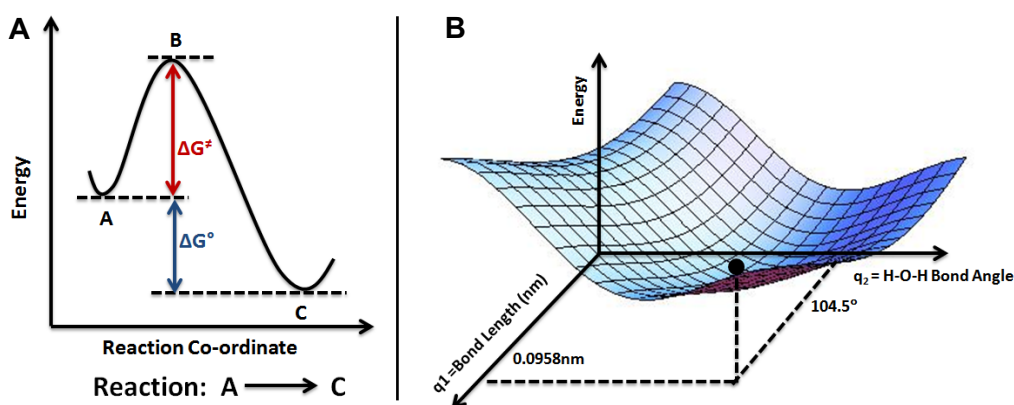


Figure 1.6 Examples for reaction diagrams. **A** shows a 2D reaction coordinate diagram; **B** shows a 3D reaction coordinate diagram, also called a potential energy surface. Reproduced with permission[†].

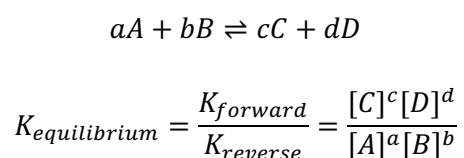
[†] CC BY-SA 3.0 license, copyright AimNature.

Chapter 1

Consolidating all the relevant principles of thermodynamics, these states can be depicted in an energy diagram, also called a reaction coordinate diagram. The diagram plots the relative energies of reactants, products, and the transition states that are involved in the process, against the reaction progress, also called the reaction coordinate. This energy profile is most commonly used as a theoretical representation of a chemical reaction and serves to illustrate kinetic and thermodynamic concepts (Figure 1.6A); there is also a branch of computational chemistry that concerns itself with calculating and modelling potential energy surfaces to examine molecules and their interactions (Figure 1.6B).

Figure 1.6A depicts a reaction where the reactants A undergo a reaction via the transition state B to form the products C. In the course of this bond breaking and making process, the intermediate state B represents the highest energy state on the reaction coordinate. The height difference between A and C is ΔG° , which can be equated to ΔG found in Equation 1.2. This height difference comes into play when discussing directionality of the reaction; the thermodynamically more stable outcome will be formed. In the example of Figure 1.6A, C would be preferentially formed over A, so the direction of the reaction is towards the formation of C. If the positions of A and C would be reversed, i.e. A would be at lower energy than C, the reaction would proceed in the reverse manner because then, thermodynamically, A would be preferentially formed over C. This example leads to the next concept to be discussed: reversibility.

The Gibbs free energy equation (Equation 1.2) describes that ΔG is the difference in maximum amount of work of the reactant and product states. This maximum can only be obtained if the process in question is a completely reversible process, with a forward and a reverse reaction. A reversible reaction may reach an equilibrium, quantified by $K_{\text{equilibrium}}$, which can be expressed by the reaction constants K_{forward} for the forward reaction and K_{reverse} for the reverse reaction at reaction conditions (Equation 1.3).



Equation 1.3 Reaction constants at equilibrium for a sample reaction of **a** stoichiometric equivalents of **A** and **b** stoichiometric equivalents of **B** to give **c** stoichiometric equivalents of **C** and **d** stoichiometric equivalents of **D**.

When an equilibrium is reached between the starting materials and the products, their relative abundance is decided by $K_{\text{equilibrium}}$ which is also related to ΔG° (Equation 1.4).

$$\Delta G^\circ = -RT \ln(K_{\text{equilibrium}})$$

Equation 1.4 Relationship between Gibbs free energy and the equilibrium constant $K_{\text{equilibrium}}$

Ultimately, the directionality and the relative abundance of starting materials and products at equilibrium is decided by the difference in Gibbs free energy ΔG° at constant reaction conditions. An equilibrium can be changed by a change of concentration, temperature, volume or pressure, upon which a new equilibrium will be established according to the changed conditions, as stated by Chatelier's principle. In principle, all reactions are reversible. In many cases, however, the equilibrium lies so much towards the product side that the reaction will continue to proceed in one direction until the starting material is effectively no longer present. Practically, such a reaction is considered to be irreversible, as it will only reverse under certain conditions.

To summarise the key points of this chapter, there is a thermodynamic driving force for reactions to happen; they can be driven by enthalpy or entropy. This directional driving force can be quantified by the Gibbs free energy difference ΔG° , which then indicates whether a reaction is feasible or not. This, however, does not mean that the reaction will actually occur. In order for a reaction to occur within a reasonable timeframe it needs to be kinetically feasible. The next chapter will examine chemical kinetics.

1.2.1.2 Kinetics in Chemical Reactivity

Kinetics is the study of reaction rates. Kinetics concerns itself with elementary steps, reaction mechanisms, and collisions between reaction partners. The prerequisite for a reaction is the collision of the reactants. This, as dictated by kinetics, needs to occur with enough energy for the reaction to happen.

In the energy diagram, whilst thermodynamics is depicted by the energetic difference between reactants and products ΔG° , kinetics of the reaction are depicted by the height of the activation energy ΔG^\ddagger . Going back to the sample reaction diagram depicted in Figure 1.6A, the height of the energy difference between starting material A and transition state B is the activation energy ΔG^\ddagger that needs to be overcome in order to form the products C. While thermodynamics indicates the direction of the

Chapter 1

reaction, i.e. whether the forward or the reverse reaction is favoured, kinetics dictates how fast this process occurs, i.e. the rate of the reaction. This is especially important in physiological systems, as we often deal with both bioavailability and affinity to the target at the same time as we deal with rate of clearance and elimination.

Thus, the smaller the activation energy ΔG^\ddagger is, the faster the reaction will occur. A reaction can be thermodynamically very favourable but have a huge kinetic barrier, e.g. the conversion of carbon from diamond to graphite which is thermodynamically very favourable, but practically will not happen at ambient conditions because the energy barrier is so high²²¹.

The activation barrier represents the energy required to reach the transition state. In this transition state, chemical bonds are partially broken and partially formed. This is a very high energy state, which is why enough energy has to be supplied in order to for the reaction to proceed to this state. Optimal orbital overlap and favourable steric interactions can lower the energy required to overcome this activation barrier. Catalysis can also considerably lower the energy barrier. Catalysts can stabilise the transition state, optimise orbital overlap and open an alternative reaction mechanism. This can lower the activation energy required and thus can speed up the reaction.

There is a transition state per elemental step and thus an activation barrier for each elemental step in a reaction mechanism. As a consequence, measuring a reaction constant for a multistep reaction is sometimes difficult. The rate law of a reaction is dependent on the reaction mechanism by which the products are formed from reactants. When reactions have more than one transition state, the highest energy transition states represent reaction bottlenecks. The rate of these elemental steps will determine the overall rate of the entire reaction. Once bottlenecks are recognised, the specific elemental steps can be optimised in order to stabilise the transition state and thus lower the energy barrier. Another way to speed up the rate of reaction is by changing the temperature, or the concentration. The more likely the reaction partners are to collide, the higher the rate constant. The rate constant essentially quantifies the frequency of collisions that result in a reaction. Increased temperature and concentration both make collision of particles more likely. Both of these factors, however, can cause unwanted side reactions if they are too high.

If a reaction can produce more than one product, the reaction outcome will depend on whether the reaction is under thermodynamic or kinetic control at given reaction

conditions. If the reaction is reversible, the thermodynamically most stable product will form. If the reaction is irreversible, then reaction is under kinetic control and the product with the lowest activation barrier will form, even if it is thermodynamically a less stable product. This explains i) why some non-equilibrium reactions have a number of side products as not only the thermodynamically most stable product is formed, and also ii) why a reaction that results in enantiomers will always give a racemic mixture under achiral conditions – there is no thermodynamic or kinetic preference for either enantiomer.

To conclude this chapter, reactivity is a relative term and thus will always depend on the reaction partner. The study of both kinetics and thermodynamics of a specific reaction can enable researchers to tweak the conditions towards a more optimised reaction outcome. Having reviewed both thermodynamic and kinetic factors, we can conclude that compounds are generally reactive because of two reasons: i) they are high energy and strive to minimise their energy and ii) the transition state towards the products is energetically feasible; in other words, the activation barrier is comparatively low. In the next chapter, these concepts will be contextualised with the reactivity that we are interested in: electrophilicity.

1.2.2 Electrophiles and Their Chemical Reactivity

Sourcing from the theories mentioned in Chapter 1.1.3, one can hypothesise that small molecules in plant pollen could play a part in the sensitisation, elicitation and/or exacerbation of the disease. They could act as haptens, chemical irritants or trigger an effector mechanism related to the allergic cascade. The latter could occur via non-covalent interactions, but the former two, hapten and irritant activity, necessitate the formation of bonds with entities in the body. In Chapter 1.2.1, it was discussed that reactivity is a relative concept and that it depends on the reaction partner in question. In this case, we are interested in compounds that would react in a physiological system. One group of compounds that are known to react in the body are electrophiles. This chapter will give an overview of concepts that are important for assessing electrophilicity, then explain why electrophiles are especially interesting in a physiological setting, and lastly discuss some examples and applications of electrophilic reactivity.

An electron-rich species is termed nucleophile, because it is attracted to a full or partial positive charge to which it can donate its excess electrons, whereas an electron-deficient species is termed electrophile. By donating electron density to the

Chapter 1

electron-deficient partner, a covalent bond is formed between the nucleophile and the electrophile, and a thermodynamically more stable product is formed. The driving force for the bond formation is the increased thermodynamic stability of the products. Molecules can have several sites of varying electron density, which means that molecules can carry several reactive sites, and sometimes even possess both nucleophilic and electrophilic moieties at the same time.

Nucleophiles are electron donors, and thus Lewis bases, and electrophiles are electron acceptors, and can also be called Lewis acids. Thus, scales of the negative logarithm of the acid dissociation constant (pKa) can be used as an approximation for relative reactivity. In general, factors that influence the pKa also influence electrophilicity; these factors are the charge on the electrophilic site, inductive effects of the surrounding atoms, resonance stability of the conjugate base, and steric accessibility of the electrophilic side. Generally speaking, the more charged, the more negative the inductive effect of the surrounding atoms, the more stable the conjugate base and the more sterically accessible, the stronger the electrophile. All these factors will influence which products will be formed if several products can be formed as a result of a reaction, which can be explained by concepts found in Chapter 1.2.1. This, however, is not the only concept to judge electrophilicity by.

Another concept that is often used to explain reactivity of Lewis acids and bases is the 'hard and soft acids and bases' (HSAB) theory, also called the Pearson acid-base concept²²²⁻²²³. It is a theory used to qualitatively explain chemical properties and reaction outcomes²²⁴. 'Hard' describes species that are small, have high charge density and thus are weakly polarisable, whereas "soft" would describes species that are big, have low charge density and are therefore highly polarisable. Hard acids react faster and form stronger bonds with hard bases, and the same holds true for soft acids and soft bases. An example for a hard and a soft electrophilic site in a single molecule is an α,β -unsaturated carbonyl group, also known as a Michael acceptor. Michael acceptors can react in two positions, the 2 position and the 4 position (Figure 1.8).

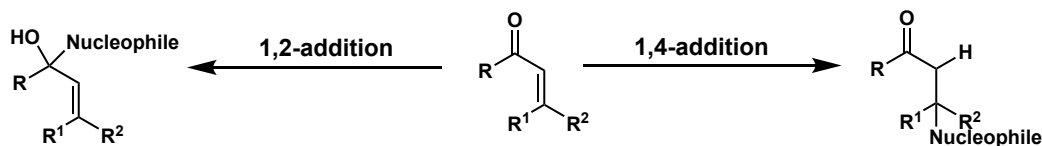


Figure 1.8 Scheme depicting the both 1,2- and 1,4-addition to a Michael acceptor.

Although in the same molecule, these two positions have different characteristics according to the HSAB theory. The 2 position is considered a hard electrophilic site due to the strong negative inductive effect exerted by carbonyl oxygen, which results in a low degree of polarisation, whereas the 4 position is considered to be soft, as the electrons in the double bond are more loosely held and more polarisable. Depending on the nucleophile, either the product of 1,2- or of 1,4-addition can be preferentially formed. Hard nucleophiles add quickly to the 2 position. Since these nucleophiles are often strong bases, this process is irreversible and the 1,2-product, the kinetic product, is formed. Examples for hard nucleophiles are metal hydrides, Grignard reagents and strong bases like organolithium compounds. If the nucleophile is soft and thus a weak base, the 1,2-addition is reversible which then means that the reaction is under thermodynamic control, and the 1,4-addition is preferred, as the thermodynamically stable double bond of the carbonyl group is retained. Examples for such soft nucleophiles are alcohols, thiols and amines.

Since the reactivity of electrophiles, as well as the degree of electrophilic behaviour, is highly dependent on the reaction partner, it is important to know what sort of reactivity can be expected in a physiological setting. Proteins and nucleic acids make up the majority of biological matter and these tend to contain nucleophilic centres like cysteine, lysine, serine and threonine²²⁵. In terms of HSAB, these nucleophiles are rather soft. Thus, soft electrophiles can bind to these sites and interfere with biological functions²²⁶⁻²²⁷. Such electrophiles could potentially also react as haptens or act as danger signals, as described in Chapter 1.1.3.

Having established that the body has potential nucleophiles that electrophiles could react with, examples and applications of electrophilic reactivity will now be discussed. First, electrophilic natural products in general will be discussed, followed by examples of uses of electrophiles in the industry, and lastly, some examples of natural product electrophiles will be highlighted.

Electrophilic natural products and their biological targets have been extensively reviewed by Gersch *et al*²²⁵. They have categorised electrophiles into three major groups: Michael acceptor systems, ring-strained scaffolds and other compounds (Figure 1.9).

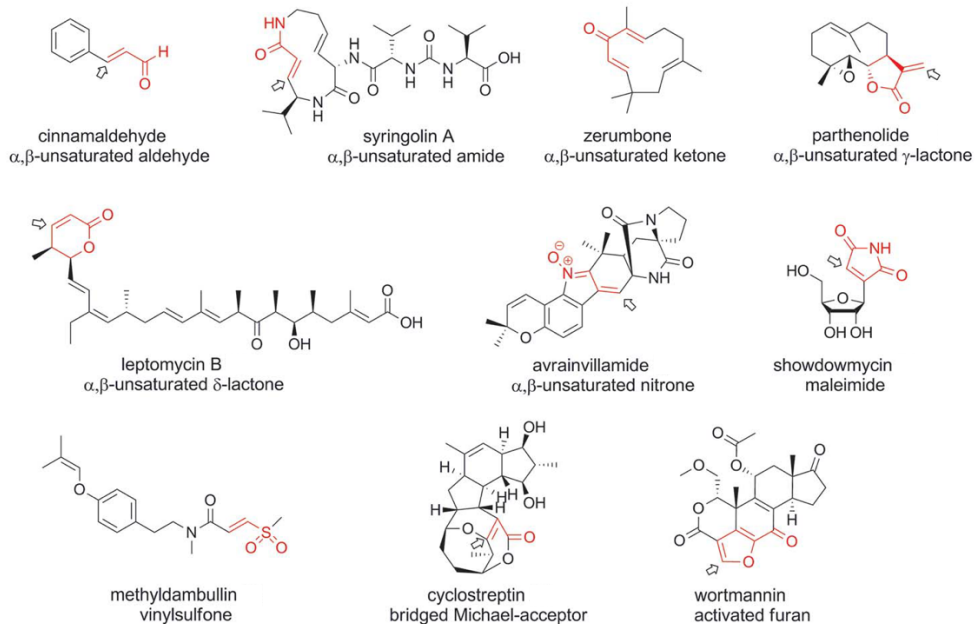
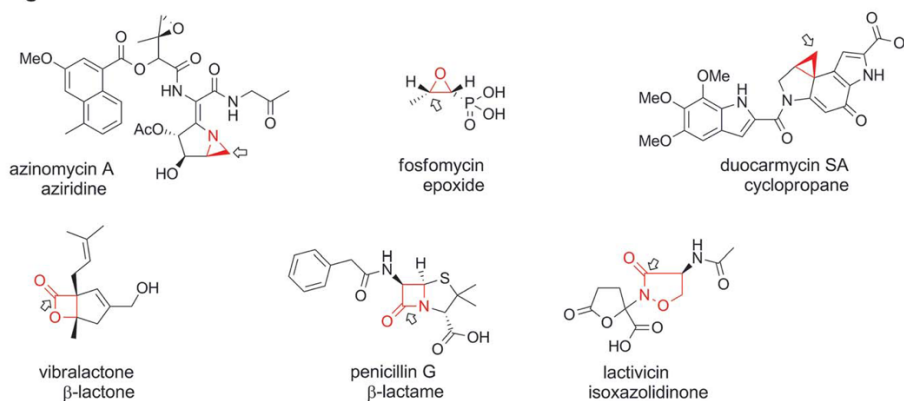
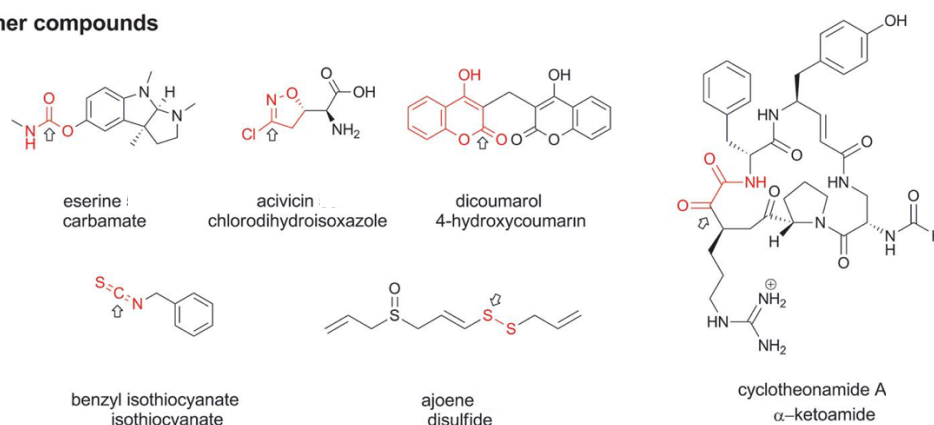
A Michael acceptor systems**B Ring-strained scaffolds****C Other compounds**

Figure 1.9 Electrophilic moieties grouped into three categories, **A** Michael acceptor systems, **B** ring-strained scaffolds and **C** other compounds. Adapted with permission²²⁵, copyright The Royal Society of Chemistry.

As can be seen in Figure 1.9, electrophilic natural products make up a diverse group of structures with different electrophilic moieties. Natural products, just like enzymes, have evolved as a result of selective pressure since they give organisms a selective advantage²²⁸. In the words of Ho *et al*, they are made by proteins to interact with other proteins²²⁹. In order to provide a selective advantage, they have to be tailored for a specific use, e.g. to inhibit microbes, deter predators or attract potential mates. Thus, it stands to reason that they also cover a wide variety of biological functions. Some natural products can also interact with multiple targets and hence be multifunctional. This phenomenon in which multiple targets are addressed by the same compound by design is called polypharmacology²²⁹. Another phenomenon that is similar to polypharmacology is reactive promiscuity, in which compounds serendipitously or inconveniently react with unintended targets. Electrophiles found in plant pollen could also express such reactive promiscuity and interact with proteins in the human body.

As natural products have evolved to bind with other proteins, they find two main uses in the industry: their potential as leads in drug discovery and as model compounds for the study of biological targets. These two uses will be discussed in the following paragraphs.

To this date, natural products and their derivatives are important as leads for drug discovery in the pharmaceutical industry²³⁰. Natural product electrophiles, however, have an ambivalent position in drug discovery. Electrophiles are often associated with toxicity or carcinogenicity²³¹⁻²³². Electrophiles can cause toxicity via irreversible adduct formation at regulatory cysteine thiolate residues of functionally important proteins²³³⁻²³⁴. Cysteine is a thiol-containing amino acid and a highly reactive soft nucleophile. It is a privileged structure due to this property: it can serve as a catalytic nucleophile in enzymes, is crucial to protein folding due to its ability to form disulfide bridges and used as a redox scavenger and switch due to its oxidation potential²³⁵⁻²³⁷. Due to the inherent reactivity as a potential nucleophile and as a redox participant, there seems to be an evolutionary selection against the use of cysteine²³⁸⁻²³⁹. Mutations of cysteine, next to tryptophan, have the highest probability of causing disease²⁴⁰⁻²⁴¹. Covalent binding to such cysteine residues can be equally detrimental. Thus, as reactivity at off-target cysteine is a high risk, electrophiles are often ruled out as potential drug leads.

On the other hand, electrophiles can be selectively employed for their specific reactivity. They can be used in modern drug development as chaperones to deliver

targeted therapy, e.g. as warheads for targeted covalent inhibitors²⁴²⁻²⁴³. These inhibitors need to be carefully designed in order to prevent irreversible reaction with off-target thiols. Long *et al* propose to target kinetically privileged cysteines in the body for selective drug development²⁴⁴. Another example for the potential for electrophiles in drug development is the covalent inhibition of the Transient Receptor Potential cation channel A1 (TRPA1) by electrophiles²⁴⁵. Inhibition of TRPA1 is found to induce phase-2-enzymes that protect against carcinogenesis. Furthermore, some of the most important drugs to be ever discovered are electrophiles: electrophilic antibiotics like penicillin have been in use ever since their discovery²⁴⁶. Therefore, even though the reactive potential of electrophiles can be a detriment, it can also be precisely what makes a drug selective and effective.

Another practical use for reactive electrophiles is in research. As electrophiles form covalent bonds, the study of natural product electrophiles has enabled researchers to identify their biological targets and find out more about their function^{227,247}. Many electrophiles found in Figure 1.9 are used as model compounds for the study of biological functions. Parthenolide, wortmannin and lactivicin (shown in Figure 1.9), will now be discussed in detail as examples for electrophilic natural products with applications in research and in drug development.

Parthenolide is a sesquiterpene lactone produced by plants of the Asteraceae and Magnoliaceae family. It is reported to have anti-inflammatory and anti-tumour properties, and novel targets continue to be reported due to its polypharmacology²⁴⁸. The two electrophilic moieties of parthenolide are the α -*exo*-methylene γ -butyrolactone (Michael acceptor type reactivity) and the epoxide (ring strain reactivity), both of which have been reported to be involved in the compound's bioactivity²⁴⁹. Parthenolide is investigated as a potential lead in drug discovery and used as a model compound for research²⁵⁰.

Wortmannin is an example for an activated furan, which falls into the Michael acceptor type electrophile group. It was isolated from *Penicillium wortmannii* and it possesses antifungal and antiproliferative activity. Wortmannin inhibits the lipid kinase phosphatidylinositol 3-kinase (PI 3-kinase) and the Polo-like kinase (PLK)²⁵¹⁻²⁵². Its mechanism of action involves nucleophilic addition of lysine residue 802, which results in ring opening of the furan and formation of a β -amino α,β -unsaturated ester (Figure 1.10). Wortmannin continues to be used as a model compound for the study of PI 3-kinase and PLK²⁵³⁻²⁵⁵.

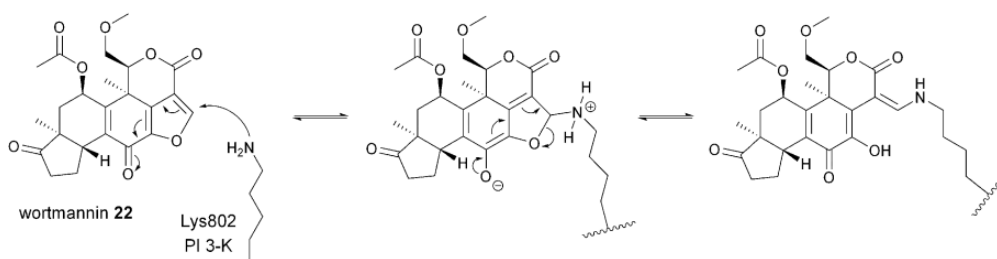


Figure 1.10 Mechanism of the reaction of wortmannin with the active site of PI 3-kinase. Reproduced with permission²²⁵, copyright The Royal Society of Chemistry.

Lactivicin is a non-beta-lactam antibiotic that was discovered in a screen for new inhibitors of bacterial cell wall biosynthesis²⁵⁶. It inhibits penicillin binding proteins and β -lactamases. Serine in the catalytic site attacks the cycloserine of lactivicin and opens the adjacent γ -lactone (Figure 1.11)²⁵⁷. This reaction mechanism may make this structure a useful lead for making even better penicillin binding protein and β -lactamase inhibitors²⁵⁸.

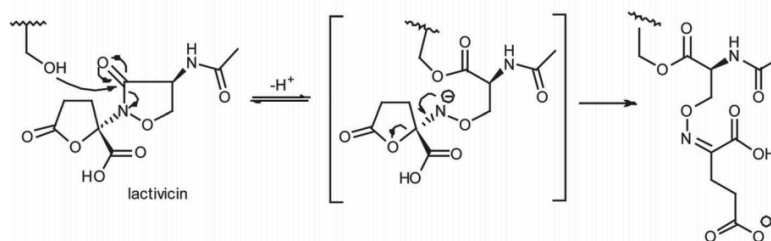


Figure 1.11 Mechanism of lactivicin with the active serine residue of penicillin binding protein. Reproduced with permission²²⁵, copyright The Royal Society of Chemistry.

In this chapter, the reactivity of electrophiles, electrophiles in physiological systems and examples for electrophiles in use in both research and drug development have been discussed. It was shown that highly reactive compounds can be both shunned for their reactivity and exploited for their reactivity. The next chapter will discuss methods for the detection and identification of electrophiles.

1.2.3 Methods for Detection and Identification of Electrophiles

This chapter will give an overview of methods for the detection and identification of electrophiles. Although electrophiles are clearly compounds of interest in a biological context, a lot of research with electrophiles actually involves using electrophiles to identify new protein targets, rather than using proteins and other compounds to identify new electrophiles^{227,259}. There are, however, two research fields in particular that have invested interest in the detection and identification of reactive electrophiles,

namely the study of environmental pollutants as cause for chronic diseases, and drug development. A variety of methods have been developed, which can be classified as biological methods and purely chemical methods. Examples for both will be discussed in the subsequent subchapters.

1.2.3.1 Biological Methods

The methods presented in this chapter are a selection of methods that employ cells or enzymes, and in general are intended for the use on biological samples. Depending on what the context of the interest in electrophiles is, there are different approaches to detecting and identifying them. This chapter will first discuss the methods addressing environmental pollutants, followed by the methods used in drug development.

Electrophiles have garnered a specific interest in the field of environmental causes for chronic diseases because of their associated toxicity. Adductomics, the study of DNA and protein adducts, utilises a variety of MS analysis methods of gas chromatography-MS and LC-MS, including (MSMS) scan modes like product ion scan (PIS), neutral loss scan (NLS), selected reaction monitoring (SRM) and multiple reaction monitoring (MRM) (Figure 1.12)²⁶⁰⁻²⁶¹.

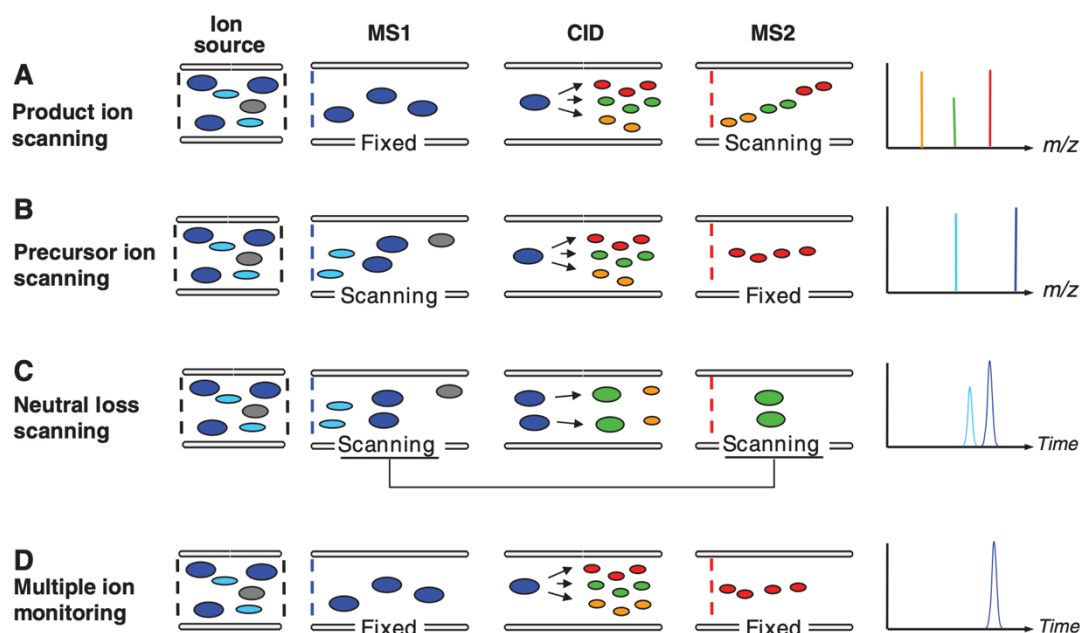


Figure 1.12 MSMS scan modes on a triple quadrupole. Abbreviations in figure: MS1: mass analyser 1; CID: collision-induced dissociation; MS2: mass analyser 2; **A** Product ion scan: a precursor ion is selected in the first mass analyser quadrupole and the second one scans for all its product ions; **B** PIS: a product ion is selected by the second mass analyser quadrupole and the precursor masses of this

product are scanned for in the first mass analyser quadrupole; **C** NLS: the two mass analysers are synchronised and scan for a mass difference; **D** MRM: also called multiple ion monitoring, a fixed mass transition is scanned for by scanning for a fixed ion mass in the first quadrupole mass analyser and then for a specific fragment of that ion in the second quadrupole mass analyser. Reproduced with permission[‡], copyright AAAS.

High resolution mass spectrometry (HRMS) is also used to obtain high accuracy mass measurements in order to be able to resolve isotopic peaks of ions. The aim is to measure adducts in tissue samples specific to chronic diseases. Glutathione (GSH) and DNA adductomes include metals, thiols and electrophilic species. A commonly used method for measuring protein adducts is the analysis of adducts with haemoglobin and human serum albumin²⁶². In this way, exogenous reactive electrophiles²⁶³ and also endogenous electrophiles²⁶⁴ can be analysed. One of the approaches is the so-called FIRE procedure. The acronym describes the procedure: fluorescein isothiocyanate (**FITC**) is used for measurement of adducts (**R**) formed with electrophiles using a modified **E**dman procedure²⁶⁵. *N*-alkylated valine adducts are detached from the haemoglobin structure by cyclisation with FITC to give a product that can be selectively enriched by SPE (Figure 1.13). These adducts are then analysed using LC-MSMS.

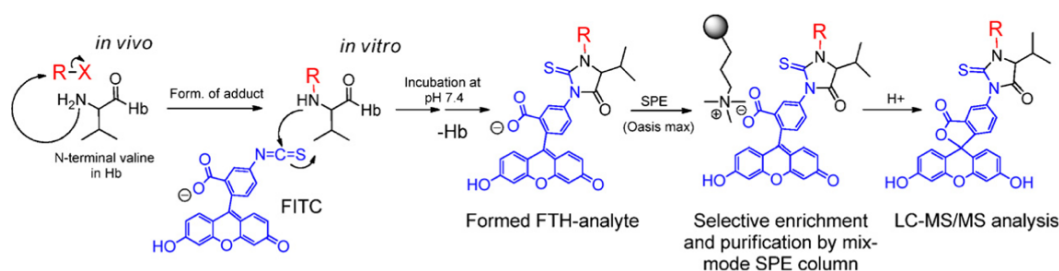


Figure 1.13 Reaction mechanism of the FIRE procedure. Abbreviation in figure: FTH (fluorescein thiohydantoin). Reproduced with permission²⁶⁵, copyright Elsevier.

This modified Edman procedure allowed the identification and quantification of acrylamide, glycidamide and ethylene oxide in blood samples from non-smokers²⁶⁵, and was further used to investigate adduct differences in between smokers and non-smokers²⁶⁶. In general, these studies are aimed towards low molecular weight electrophiles as they are often volatile environmental pollutants.

[‡] Reprinted from Domon, B., Aebersold, R., Mass spectrometry and protein analysis, Science 312 (2006) 212-217. Reprinted with permission from AAAS.

The second category of biological methods to be discussed are the ones employed for drug development. In drug development, the identification of reactive metabolites is paramount in order to assess the safety of drug leads and to be able to discard problematic drug leads early on²⁶⁷.

In the analysis of reactive electrophilic metabolites, human or rat liver microsomes are often used with a nucleophilic trapping agent, since reactive metabolites tend to be short-lived due to their reactivity. Examples of trapping reagents include GSH, *N*-acetylcysteine (NAC), amines (like semicarbazide and methoxylamine), or cyanide anion²⁶⁷⁻²⁷⁰. While GSH and NAC are soft nucleophiles, semicarbazide, methoxylamine and cyanide are hard nucleophiles.

GSH is the body's endogenous electrophile scavenger and thus is one of the most commonly used trapping reagents. GSH can be detected using MSMS in the NLS and PIS mode: NLS due to a fragment neutral loss of 129 Da from GSH or loss of a whole GSH molecule, which would result in a neutral loss of 307 Da; PIS by detection of a parent ion of *m/z* (Figure 1.14). This was demonstrated on a variety of known compounds²⁷¹⁻²⁷².

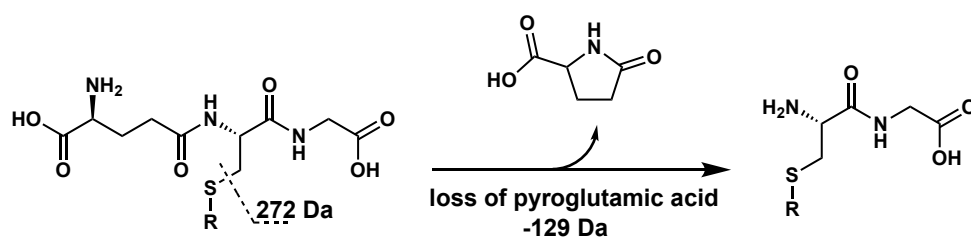


Figure 1.14 Fragments of GSH for NLS and PIS.

Gan *et al* utilised derivatised GSH with a dansyl group in order to be able to quantify reactive metabolites *in vitro*²⁷². The incorporation of the dansyl group allowed LC analysis with a fluorescence detector additionally to MS. Dansylated GSH was found to be as reactive as GSH, although it did not serve as a substrate for glutathione-S-transferase and thus could not make use of this conjugation mechanism.

Another example for electrophile screening was published by Nikolic *et al*²⁷³. The aim was to identify xenobiotic electrophilic cytochrome P450 metabolites of potential drug leads by using ultrafiltration-MS. Rat liver microsomes were trapped by an ultrafiltration membrane in a flow-through chamber, and samples were flow-injected through this chamber and directly led into an on-line electrospray mass spectrometer for analysis. Trapping of reactive xenobiotic metabolites was achieved by using GSH.

In contrast to the methods used for the identification of biologically relevant environmental pollutants, the methods for drug development are generally aimed at compounds that are in the size range of secondary metabolites, which is more similar to what we are interested in examining.

1.2.3.2 Chemical Methods

This subchapter will address methods that are chemistry-based and do not involve cells or enzymes. Many of the presented methods will approach the detection and identification of electrophiles from a more general and theoretical angle, examining reactivity of a sample itself as opposed to reactive metabolites formed by enzymatic digest. This chapter will first briefly discuss *in silico* methods before moving on to *in vitro* methods.

There is the possibility to use *in silico* calculations and modelling to predict reactivity. This, however, requires advance knowledge of the structures to be assessed. It is more of a tool to assess relative reactivity rather than to discover new reactive natural products. An example is the paper published by Mulliner *et al*, who modelled reactivity using GSH as a model nucleophile²⁷⁴. *In silico* assessment and bioinformatics can be a powerful tool to be used in tandem with wet lab methods to narrow down potential leads.

Several research groups have explored different experimental approaches for identification, and sometimes also isolation, of reactive electrophiles. These methods range from *in situ* methods, sometimes followed up with tag-assisted purification, and purification facilitated with a solid support²⁷⁵⁻²⁸¹.

In *in situ* methods, the nucleophile is added directly to the sample. Electrophiles in the sample form covalent adducts with the nucleophile, which, when analysed via LC-MS, will manifest as a shift in retention time (rt), mass, and potentially will also add some other spectroscopically detectable property.

Caprioglio *et al* have developed an NMR assay which leverages the reactivity of thia-Michael reactivity of cysteamine²⁷⁵. The thia-Michael reaction is known for its possible reversibility and its potential to undergo redox reaction which makes it difficult to assess the reactivity of thia-Michael acceptors. In order to characterise the reactivity of different thia-Michael acceptors, the cysteamine assay records NMR spectra *in situ*, thus enabling the characterisation of the formed products and, if present, the reaction equilibrium²⁸².

As an example, Castro-Falcón *et al* have successfully used two different tags with phenyl halide moieties that served both as an MS and ultraviolet (UV) tag (Figure 1.15)²⁷⁶. Their phenyl bromide probe was found to be more reactive with beta-lactam and beta-lactone-based electrophiles, while their phenyl chloride probe was found to be more reactive with epoxides. Testing these probes in bacterial extracts resulted in successful tagging and identification of electrophilic compounds in the mixture, e.g. salinosporamide A via reaction with its beta-lactone, and cyclomarin A and salinamide A via epoxide ring opening.

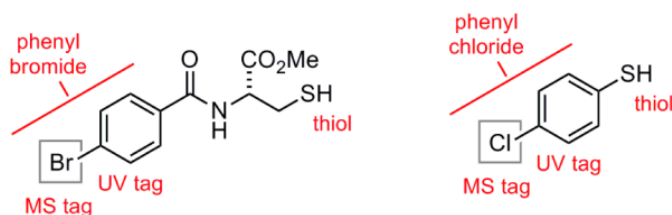


Figure 1.15 Pharmacophore probes. Reproduced with permission[§], copyright American Chemical Society.

Detecting and identifying compounds *in situ* by LC-MS has the advantage of not having to isolate and purify the compounds prior. This, however, only works with known compounds. When previously unknown compounds are detected, isolation and purification are an unavoidable necessity in order to accurately elucidate their structures. This is the reason why, although many methods are technically *in situ*, when faced with new compounds researchers still have to undergo the lengthy process of isolation and purification. Cox *et al* used a combination of bioinformatics and nucleophilic labelling of dehydrated amino acids with dithiothreitol (DTT) to investigate natural products containing dehydrated amino acid moieties. After LC purification and comparison to analogous structures, they discovered a new structure, cyclothiazomycin C²⁷⁷.

Since purification and isolation are unavoidable, another approach can be used to link the purification and isolation to detection. An immobilised probe on a solid support was used by Jeon *et al* to isolate natural products with terminal alkyne moieties²⁸¹. An azide probe was designed that would form a fluorescent probe upon successful copper(I)-catalysed azide-alkyne cycloaddition (CuAAC) (Figure 1.16). The

[§] Reproduced with permission from Castro-Perez, J., Plumb, R., Liang, L., Yang, E., A high-throughput liquid chromatography/tandem mass spectrometry method for screening GSH conjugates using exact mass neutral loss acquisition, *Rapid Commun. Mass Spectrom.* 19 (2005) 798-804. Copyright (2016) American Chemical Society.

fluorescent moiety was used to identify extracts in which adduct formation had occurred.

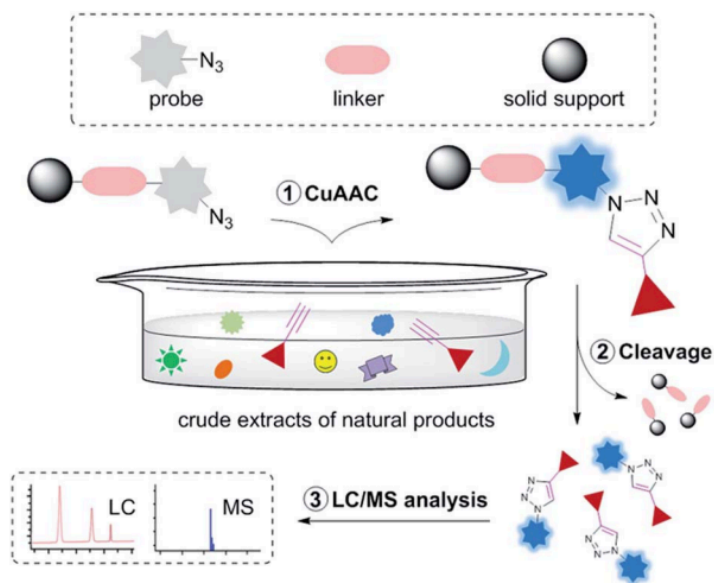


Figure 1.16 Concept for the procedure employed by Jeon *et al* for the analysis of natural products with terminal alkyne moieties from natural product extracts²⁸¹. Reproduced with permission**, copyright The Royal Society of Chemistry.

After cycloaddition and removal of unreacted extracts, they cleaved the formed adducts from the bead. Their linker was a (2-phenyl-2-trimethylsilyl)ethyl-linker which they cleaved with a solution of tetra-*n*-butylammonium fluoride in water²⁸³. Adducts were analysed by LC-MS and UV/visible (Vis) spectroscopy; the triazole formed by CuAAC additionally served as a UV tag for detection.

** Jeon, H., Lim, C., Lee, J. M., Kim, S., Chemical assay-guided natural product isolation via solid-supported chemodosimetric fluorescent probe, *Chem. Sci.* 6 (2015) 2806-2811. - Published by The Royal Society of Chemistry

1.3 Conclusion and Project Aims

This thesis, titled 'the method development for the detection and identification of pathophysiologically relevant electrophiles', touches on several topics that needed to be addressed to set the scene for an investigation. This chapter will consolidate all the conclusions from Chapter 1.1 and 1.2 relevant for this dissertation and present the rationale and aims of this project.

In Chapter 1.1, pollen allergy was introduced as a complex, multicausal disease with rising prevalence across the world. Currently, this disease is mainly treated by symptom management rather than by addressing the disease at its roots. The only true disease treatment that exists to this date is allergen-specific immunotherapy, which is a lengthy and cumbersome treatment and often does not offer permanent cessation of allergic symptoms. Even though allergen-specific immunotherapy is used to achieve desensitisation, ultimately, our understanding for why this process works is just as limited as it is for why sensitisation occurs in the first place. Since sensitisation and desensitisation are inextricably linked, understanding one will potentially lead to a deeper understanding of the other.

Many disease hypotheses have been formulated in an attempt to explain the rising prevalence and the origins of the disease. The introduction reviewed three of them: the hygiene hypothesis, the hapten theory and the danger model. The latter two could lead to believe that reactive molecules associated with pollen allergens could be involved in the sensitisation process. Furthermore, reactive molecules could have a role in the exacerbative episodes of the disease. Both of these arguments make a solid case that studying reactive molecules in pollen could lead to new learnings about the disease.

How one could go about identifying reactive compounds is explored in Chapter 1.2. As reactivity is a relative term, Chapter 1.2.1 introduced thermodynamic and kinetic concepts, which lay the foundation for a discussion about reactivity in subsequent method chapters of this dissertation. Chapter 1.2.2 presented electrophiles as our main compound class of interest, explained their biological relevance and highlighted some examples and uses in industry and research. Chapter 1.2.3 reviewed published methods that detect and identify electrophiles, which showed what had already been done. Further, the efforts of these research groups and their strategies could serve as an inspiration for our method development efforts.

Having reviewed the introductory chapters, Chapter 1.1 and 1.2, this finally leads us to the rationale and extended working hypothesis of this project.

Reactive small molecules in pollen represent an underresearched area, especially in comparison to protein allergens. Electrophiles in pollen have the potential to react as haptens and danger signals, therefore could play a crucial role in both the sensitisation and exacerbation phase via immunological mechanisms. The extended working hypothesis is that small molecules could also exacerbate allergic disease by eliciting a purely physiological reaction in the human body that adds to the immunological response. Small molecules present in pollen can stimulate body tissue via traditional drug-receptor interactions, causing for instance contraction of the airway smooth muscle, as found in asthma attacks.

Thus, the aim of this project was to develop a method that can detect and identify pathophysiologically relevant electrophiles in pollen extracts. This could serve as a starting point to discover molecules previously undiscovered or deemed uninteresting, and their study could lead to new learnings in the field of pollen allergy.

Chapter 2 Materials and Methods

2.1 Materials

2.1.1 Solvents

The following solvents were used in the scope of this work (Table 2.1).

Table 2.1 Table of solvents.

Name	Grade and Information from the Supplier	Supplier	Use
Acetone	For analysis EMSURE®	Merck, Darmstadt, Germany	HPLC/UPLC
Acetonitrile	ChromAR® HPLC	Macron Fine Chemicals, Radnor, PA, USA	HPLC
Acetonitrile	Lichrosolv®	Merck, Darmstadt, Germany	HPLC/UPLC
Dichloromethane (DCM)	grade for GC residual analysis	Scharlab, Barcelona, Spain	Resin Experiment
Dimethylformamide (DMF)	AnalaR NORMAPUR	VWR, Radnor, PA, USA	Resin Synthesis
Dimethyl sulfoxide (DMSO)	Extra pure	Scharlab, Barcelona, Spain	Resin Experiment, Sample Preparation
DMSO-d6	D-enrichment ≥ 99.95 %	Acros Organics, Geel, Belgium	NMR
Ethanol (EtOH)	absolute GPR RECTAPUR	VWR, Radnor, PA, USA	Resin Synthesis
Formic acid (FA)	98 % pure	Acros Organics, Geel, Belgium	HPLC
FA	99 % pure	Biosolve, Dieuze, France	HPLC/UPLC
n-Hexane	Re-distilled		Resin Experiment
Isopropyl alcohol (2-PrOH)	suitable for LC and UV spectrophotometry	Macron Fine Chemicals, Radnor, PA, USA	HPLC/UPLC
Methanol (MeOH)	Re-distilled		Extract Generation
MeOH	HPLC grade	Reuss Chemie, Tägerig, Switzerland	Resin Experiment
MeOH	anhydrous	Macron Fine Chemicals, Radnor, PA, USA	Resin Experiment
Tetrahydrofuran (THF)		Macherey-Nagel	Extract Generation

2.1.2 Reagents

The following reagents were used in the scope of this work (Table 2.2).

Table 2.2 Table of reagents.

Name	Supplier	Use
Cl-TCP(Cl)-resin	CEM Corporation, Matthews, NC, USA	Resin Synthesis
2-Chlorotriyl chloride resin	Bachem, Bubendorf, Switzerland	Resin Synthesis
Diisopropylcarbodiimide (DIC)	Sigma-Aldrich, Buchs, Switzerland	Resin Synthesis
<i>N,N</i> -diisopropylethylamine (DIPEA)	Sigma-Aldrich, Buchs, Switzerland	Resin Synthesis
5,5'-Dithiobis-(2-nitrobenzoic acid) (Ellman's Reagent)	Sigma-Aldrich, Buchs, Switzerland	Electrophile and Cysteine Quantification
DTT	Sigma-Aldrich, Buchs, Switzerland	<i>In Situ</i> Detection
1,2-Ethanedithiol	Sigma-Aldrich, Buchs, Switzerland	Nucleophilic Peptide Synthesis
Fmoc-Ala-OH	CEM Corporation, Matthews, NC, USA	Resin Synthesis
Fmoc-Asp(OtBu)-OH	CEM Corporation, Matthews, NC, USA	Nucleophilic Peptide Synthesis
(Fmoc-Cys-OH) ₂	Bachem, Bubendorf, Switzerland	Resin Synthesis
Fmoc-His(Trt)-OH	Bachem, Bubendorf, Switzerland	Nucleophilic Peptide Synthesis
Hexafluoroisopropyl alcohol (HFIP)	Sigma-Aldrich, Buchs, Switzerland	Resin Experiment
2-Mercaptoethanol (BME)	Sigma-Aldrich, Buchs, Switzerland	Resin Experiment
Methionine	Axonlab, Baden-Dättwil, Switzerland	Resin Experiment
1-Methyl-2-pyrrolidinone (NMP)	Sigma-Aldrich, Buchs, Switzerland	Resin Synthesis
piperazine	Sigma-Aldrich, Buchs, Switzerland	Resin Synthesis
Potassium iodide	Hänseler AG, Herisau, Switzerland	Resin Synthesis
Triethylamine (TEA)	Sigma-Aldrich, Buchs, Switzerland	Electrophile Quantification
Trifluoroacetic acid (TFA)	Sigma-Aldrich, Buchs, Switzerland	Nucleophilic Peptide Synthesis, Resin Experiment
Triisopropylsilane (TIS)	Sigma-Aldrich, Buchs, Switzerland	Nucleophilic Peptide Synthesis

Chapter 2

2.1.3 Buffers

The following chemicals were used for buffers (Table 2.3).

Table 2.3 Table of buffer chemicals.

Name	Supplier	Use
Potassium dihydrogen phosphate	Merck, Darmstadt, Germany	<i>In situ</i> Detection
di-Potassium hydrogen phosphate	Merck, Darmstadt, Germany	<i>In situ</i> Detection

2.1.4 Model Compounds

The following model compounds were used in the scope of this work (Table 2.4).

Table 2.4 Table of model compounds.

Name	Supplier
NAC	Sigma-Aldrich, Buchs, Switzerland
Alantolactone	Sigma-Aldrich, Buchs, Switzerland
Atropine	Sigma-Aldrich, Buchs, Switzerland
Berberine chloride	Sigma-Aldrich, Buchs, Switzerland
Cnicin	Carbosynth Limited, Staad, Switzerland
Cynaropicrin	Extrasynthese, Genay Cedex, France
Cysteine	Roth, Karlsruhe, Germany
Forskolin	Extrasynthese, Genay Cedex, France
GSH	Sigma-Aldrich, Buchs, Switzerland
Glutathione disulfide (GSSG)	Sigma-Aldrich, Buchs, Switzerland
Mangiferin	Sigma-Aldrich, Buchs, Switzerland
<i>N</i> -(1-naphthyl)- <i>N</i> -phenylmethacrylamide	Alfa Aesar, Haverhill, MA, United States
Parthenolide	Chengdu Biopurify Phytochemicals. Chengdu, China
Penicillin V	Sigma-Aldrich, Buchs, Switzerland
Valerenic acid	Extrasynthese, Genay Cedex, France

2.1.5 Plant Material

Tiliae flos conc. Ph. Eur. was purchased from Dixia, St. Gallen Switzerland. All pollen plant material in Table 2.5 was sourced from Greer Laboratories, Lenoir, NC, United States.

Table 2.5 Table of plant pollen materials.

Species	Lot Number
<i>Ambrosia psilostachya</i>	P3701938-2
<i>Ambrosia psilostachya</i>	P3757208
<i>Ambrosia psilostachya</i>	P4129072-1
<i>Ambrosia psilostachya</i>	P4576841
<i>Ambrosia artemisiifolia</i>	P3024704-3
<i>Ambrosia artemisiifolia</i>	P3744652-2
<i>Ambrosia artemisiifolia</i>	P3396120-3
<i>Ambrosia artemisiifolia</i>	P335440-18
<i>Ambrosia artemisiifolia</i>	P3392522-19
<i>Phleum pratense</i>	P319351-7
<i>Phleum pratense</i>	P3280848-1
<i>Phleum pratense</i>	P3743977-1
<i>Phleum pratense</i>	P3929196-1
<i>Betula pendula</i>	P3317516-1
<i>Betula pendula</i>	P3317540-1
<i>Betula pendula</i>	P3752220
<i>Urtica dioica</i>	P3730565
<i>Urtica dioica</i>	P4079048-1
<i>Urtica dioica</i>	P4889415
<i>Corylus avellana</i>	P976555-1
<i>Corylus avellana</i>	P1330035-2
<i>Corylus avellana</i>	P4530617

2.2 Methods

2.2.1 Extract Preparation

Commercially obtained plant parts were milled using a M20 universal mill (IKA, Staufen, Germany). If the supplier provided powdered product, then the subsequent extraction step was performed without prior milling.

All extracts with source material of less than 6 g were generated by Accelerated Solvent Extraction (ASE) utilising a Dionex ASE200 Accelerated Solvent Extractor. For each extraction, three cycles of solvent were added to fill the cell size and the extraction occurred at 70 °C and 120 bar. In the case of pollen extracts, pollen was extracted with the following three solvents in sequence of increasing polarity: n-hexane, THF and MeOH. *Tiliae Flos* MeOH extract was prepared by only extracting with MeOH.

One batch of *Ambrosia psilostachya* (batch number P4129072-1) was ordered in bulk (105 g) and is designated as P4129072-1'. 5 g of that batch were extracted using the ASE method detailed previously, the rest (100 g) was extracted using a serial percolation at ambient pressure and temperature. The solvents used were n-hexane (800 ml), THF (1000 ml) and MeOH (1500 ml).

2.2.2 Sample Drying

In order to render samples of any kind solvent-free, a series of different techniques was employed according to the size and nature of the samples.

Rotary evaporation. Two types of rotary evaporators were used. One type was a Rotavapor R-215 coupled with a Vacuum Controller V-850, a Heating Bath B-491 (all BÜCHI, Flawil, Switzerland) and a PC 3000 series vacuum pump (vacuubrand, Wertheim, Germany) cooled by a Unichiller (Huber, Offenburg, Germany). The other type was a multiway rotary evaporator, Multivapor P-12, coupled with a Vacuum Controller V-855 and Vacuum Pump V-700 (all BÜCHI) and cooled by a polystat cc1 (Huber), for the simultaneous evaporation of larger sample bulks.

Centrifugal Evaporation. An EZ-2 Plus Genevac (SP Industries, Warminster, PA, United States) was used for centrifugal evaporation. Standard settings were used at a maximum temperature of 35 °C.

Evaporation under Nitrogen Flow. For small sample sizes, a PIAG Evapor equipped with a heating block (Portman Instruments, Biel-Benken, Switzerland) set to 30 °C under nitrogen flow was used for solvent removal.

Lyophilisation. A Gamma 1-16 LSC ice condenser (Christ, Osterode am Harz, Germany) was used for lyophilisation. Prior to lyophilisation, the samples were made free of organic solvent by rotary evaporation and frozen over an ethanol ice bath or in a freezer at -20 °C.

2.2.3 Liquid Chromatography (LC) Analysis

All the LC methods used for the work presented in this dissertation are summarised in this chapter.

Samples were made particle free by centrifugation for 10 min at 16'168 x *g* (13'200 rpm) at 20 °C using a MiniSpin plus (Vaudaux Eppendorf, Schönenbuch, Switzerland) to sediment residual particles before taking an aliquot for analysis.

2.2.3.1 Analytical High Pressure Liquid Chromatography (HPLC)

Analytical profiling was carried out on two different instruments, one a Shimadzu system, the other a Waters system.

The Shimadzu HPLC System (Kyoto, Japan) consisted of a degasser, a binary pump, a column thermostat, a photodiode array (PDA) detector (SPD-M20A) with a temperature-controlled UV cell that was connected to a triple quadrupole mass spectrometer with ESI and APCI interface (LCMS-8030) and an Alltech 3300 evaporative light scattering detector (BÜCHI, Flawil, Switzerland) via a T split. The MS conditions were as follows: positive and negative ion spectra were recorded simultaneously in the range of *m/z* 250 to *m/z* 2000; capillary voltage: 4.5 kV; scan speed: 15000 u/s; event time: 0.150 s. Evaporative light scattering detector conditions were as follows: nitrogen flow: 3.0 l/min, temperature: 45 °C. Data acquisition and analysis were performed with LabSolutions 5.89 software (Shimadzu, Kyoto, Japan). The column used for analysis was the Waters SunFire™ C18 (3.5 µm 3.0 mm × 150 mm i.d.) coupled to a guard column (10 mm × 3.0 mm i.d.). Mobile phases were 0.1 % FA in water (eluent A) and 0.1 % FA in acetonitrile (eluent B). The gradient was 5 % B for 2.0 min, then up to 100 % B in 30.0 min, at 100 % for 5.0 min, down to 5 % in 0.1 min, following by a re-equilibration at 5 % for 7.9 min, with total run time of 45 min.

Chapter 2

Other HPLC analyses were performed on an ACQUITY UPLC system coupled to an ACQUITY TQD (Waters, Milford, MA, USA) under lower pressure HPLC conditions. The cooling light-protected autosampler was set at 10 °C in-between runs, at 20 °C for runs and the column oven was set at 45 °C. A Waters SunFire™ C18 column (3.5 µm 3 mm × 150 mm i.d.) was used for qualitative analysis of the samples. Mobile phases were 0.1 % FA in acetonitrile:water (5:95) (eluent A), and 0.1 % FA in acetonitrile (eluent B). For qualitative analysis a linear gradient of 5 % to 100 % B in 8 min was used. The exact method details, conditions and tune settings can be found in the method section of the Appendix. Data acquisition and analysis were performed with MassLynx 4.1 software (Waters).

2.2.3.2 Semi-preparative HPLC

Three different systems were used for isolation depending on availability and detector requirements: an Agilent system with a PDA and MS detector, an Alliance system with a PDA detector and another Agilent system with a PDA detector.

The first system consisted of a 1200 series binary pump, a 1290 Infinity II series injection module with a 10-port rotary valve that connected to a 1100 series PDA detector (all Agilent, Basel, Switzerland). A dynamic splitter (split ratio 3:40, model 691 Series Adjustable Makeup-Flow Splitter, ASI, Richmond, USA) led to a collection port and to a 6120 series quadrupole mass spectrometer (all Agilent). Make-up flow for the spectrometer was delivered by a 1290 Infinity II series quaternary pump. The column used was a Waters SunFire™ C18 (5 µm 10 mm × 150 mm i.d.) equipped with a guard column (10 mm × 10 mm i.d.). The mobile phase was water (eluent A) and acetonitrile (eluent B), and the make-up flow for the T split was 0.1 % FA in acetonitrile:water (1:1). MS detection was performed with a scan range from m/z 100 to m/z 1000. Data acquisition and analysis was performed with OpenLAB 2.3 and ChemRTD 1.2 software (both Agilent).

The second system semi-preparative system was an Alliance system consisting of a 2690 Separation Module and a Waters 996 PDA (all Waters). Mobile phases and columns were the same as above. Data acquisition and analysis was performed with Empower 2 software (Waters)

The third system was an 1100 series instrument consisting of pump, sample manager, column heater and PDA detector (Agilent). Mobile phases and columns were the

same as above. Data acquisition and analysis was performed with OpenLab CDS ChemStation Edition (Agilent).

2.2.4 Spectrophotometric Assay

Samples were dissolved in DMSO to obtain a solution of 50 mg/ml. If solubility was an issue, lower concentrations were utilised. A solution of parthenolide (1.13 mg/ml in DMSO) was used as a standard for construction of the calibration curve. Extract samples were both measured with and without Ellman's Reagent. The calibration curve included five different concentrations (cal10, cal20, cal30, cal50 and cal100) and a blank (cal0). For the preparation of the blanks and cal0 for the calibration curve, 100 μ l of DMSO was used as sample. For both the extract sample blanks and the extract samples, 20 μ l of extract (50 mg/ml) was dispensed into 80 μ l of DMSO. Parthenolide was chosen as a calibrant because its reaction with NAC is stoichiometric and goes to completion. The calibration curve samples contained 10 μ l, 20 μ l, 30 μ l, 50 μ l and 100 μ l of parthenolide solution (1.13 mg/ml) in DMSO which were then made up to a total volume of 100 μ l using DMSO.

The experiment outline detailed in Table 2.6 was followed.

Table 2.6 Experimental procedure of the spectrophotometric assay

Experimental Procedure	
1st step	1. The sample (100 μ l) is pipetted into the vial.
	2. NAC (0.429 mg/ml) in MeOH (200 μ l) is added.
	3. TEA (40 μ l) is added.
Incubation for at least 40 minutes	
2nd step	4. 0.1 M Monobasic/dibasic phosphate buffer at pH 8.0 (30 μ l) is added to blanks, Ellman's Reagent (16 mg/ml) in 0.1 M monobasic/dibasic phosphate buffer at pH 8.0 is added to samples and calibration curve samples.
	5. The mixture is washed into a volumetric flask (10 ml) and the volume is made up to 10 ml with MeOH.
The samples were measured thrice on a multiplate reader at 416 nm.	

As only a limited number of volumetric flasks was available for the final dilution step, the extract sample blanks were measured first while the remaining samples were stored in the fridge (-4 °C) for their prolonged incubation time. The samples were measured on a Plate CHAMELEON Multilabel Detection Platform (Hidex, Turku, Finland) equipped with a 415-4416 Absorption filter 416 nm BW10 12.5 mm. This experiment was repeated on three separate days to give three independent data sets

that were ultimately analysed together. The results are reported as averaged out over the three data sets.

2.2.5 Nuclear Magnetic Resonance (NMR) Analysis

NMR spectra were recorded on two different instruments.

One was a 500 MHz Avance III™ spectrometer (Bruker BioSpin, Fällanden, Switzerland) operating at 500.13 MHz for ¹H and 125.77 MHz for ¹³C nuclei. ¹H NMR data and correlation spectroscopy (COSY), heteronuclear single quantum coherence (HSQC), and heteronuclear multiple bond correlation (HMBC) spectra were measured at 23 °C in a 1 mm TXI probe with a z-gradient. Standard pulse sequences of the software package Topspin 3.5pl7 were used.

The other instrument was a Bruker Avance III Neo 600 MHz NMR spectrometer equipped with a QCI 5 mm Cryoprobe and a SampleJet automated sample changer (Rheinstetten, Germany). The frequency for ¹H NMR was 600 MHz, the frequency for ¹³C NMR was 151 MHz.

Spectra were analysed using Bruker TopSpin 3.5pl7 and ACDLabs Spectrus Processor (Toronto, Canada).

2.2.6 *In Situ* Detection Methods

2.2.6.1 GSH Experiment with Parthenolide

GSH was tested as potential nucleophile for the project against a model electrophile, parthenolide. GSSG was used as a negative control for GSH. Parthenolide solutions was prepared in DMSO (2 mg/ml), GSH and GSSG solutions were prepared in 0.1 M phosphate buffer at pH 7.4 (10 mg/ml). The following samples were prepared and measured in HPLC-MS (Table 2.7).

Table 2.7 Sample composition for the GSH experiment with parthenolide.

Sample Number	Buffer content (15 µl)	DMSO content (15 µl)
1	Buffer	DMSO
2	Buffer	DMSO containing parthenolide
3	Buffer containing GSH	DMSO
4	Buffer containing GSSG	DMSO
5	Buffer containing GSH	DMSO containing parthenolide
6	Buffer containing GSSG	DMSO containing parthenolide

Additionally, another sample was prepared with the same composition as sample 6 (Table 2.7) and injected three consecutive times to see if there are any kinetic differences. This sample was mixed, and the injection method was started 5 minutes later. HPLC-MS conditions used for this chapter are the same as described in Chapter 2.2.3.1.

2.2.6.2 GSH Experiment with *Ambrosia psilostachya* Extract

Ambrosia psilostachya extract (P3757208) was tested with GSG and GSSG in the same manner as described in Chapter 2.2.6.1, but with different concentrations. The extract was used at 50 mg/ml in DMSO and GSH and GSSG were used at concentrations of 5 mg/ml in 0.1 M phosphate buffer at pH 7.4. HPLC-MS conditions used for this chapter are the same as described in Chapter 2.2.3.1.

2.2.6.3 *In Situ* Detection Using Tandem Mass Spectrometry (MSMS) Methods

For the NLS and PIS experiments, a separate MS method was written in MassLynx. In NLS mode, neutral losses of m/z 129 were recorded in negative mode with a collision energy of 30 V. The scan range of was m/z 131-1000. In PIS mode, the precursor ions of m/z 272 were recorded in negative mode with a collision energy of 40 V. The scan range was m/z 103-1000.

2.2.7 Methods for the Assessment of Affinity-Tag Assisted Electrophile Detection

2.2.7.1 Synthesis of Nucleophilic Peptide

The nucleophilic peptide was synthesised by solid-phase peptide synthesis (SPPS) was performed on a Liberty Blue™ instrument (CEM). Unless stated otherwise, followed the User Guide published by the manufacturer was followed. More details on the methods can be found in the Appendix. Cl-TCP(Cl) ProTide Resin (0.1 mmol equivalent) was used. Fmoc-His(Trt)-OH, Fmoc-Asp(OtBu)-OH and Fmoc-Cys(Trt)-OH were dissolved in DMF at a concentration of 0.2 M in DMF. 0.5 M DIC in DMF was used as activator. 10 % piperazine (w/v) in EtOH:NMP (10:90) was used as deprotection reagent. Upon completion of the procedure, the synthesised resin was transferred out of the reaction vessel by rinsing with DMF. Cleavage was performed outside of the Liberty Blue with TFA/TIS/H₂O/1,2-ethanedithiol (92.5/2.5/2.5/2.5). The reaction mixture was agitated for 3.5 h at RT. By application of the cleavage cocktail to the resin beads, the peptide was cleaved off the resin and the Trt-protecting groups were removed in the same step. The resin beads were removed by filtration. The

Chapter 2

peptide was precipitated in ether and sedimented as a pellet by centrifugation at 13'200 rpm for 5 min. The supernatant was removed.

The peptide mass was checked by HPLC-MS on the ACQUITY UPLC system (Chapter 2.2.3.1).

2.2.7.2 Experiments with Nucleophilic Peptide

2.2.7.2.1 Experiments with C6His and 6His

Peptides C6His and 6His were used immediately for analysis with parthenolide. Peptide, L-histidine and L-cysteine concentrations for this experiment were 10 mM in DMSO, parthenolide was used as a 10 mM solution in DMSO, DTT was used as a 200 mM solution in water. When no DTT was used, the missing volume was made up with water instead. The following samples were prepared (Table 2.8). HPLC-MS analysis was performed on the ACQUITY UPLC system (Chapter 2.2.3.1).

Table 2.8 Sample composition for the pilot experiment with the nucleophilic probe.

Sample Number	Electrophile (20 µl)	Test Nucleophile (20 µl)	Reducing Agent (20 µl)	Additional Solvent (20 µl)
1	Parthenolide in DMSO	DMSO	None	DMSO
2	Parthenolide in DMSO	L-Histidine in DMSO	None	DMSO
3	Parthenolide in DMSO	L-Histidine in DMSO	DTT	DMSO
4	Parthenolide in DMSO	L-Cysteine in DMSO	None	DMSO
5	Parthenolide in DMSO	L-Cysteine in DMSO	DTT	DMSO
6	Parthenolide in DMSO	6His in DMSO	None	DMSO
7	Parthenolide in DMSO	6His in DMSO	DTT	DMSO
8	Parthenolide in DMSO	C6His in DMSO	None	DMSO
9	Parthenolide in DMSO	C6His in DMSO	DTT	DMSO

2.2.7.2.2 Experiments with CD6His

Purification of CD6His was performed using semi-preparative HPLC as described in Chapter 2.2.3.2. The eluents were water and 0.1 % FA (eluent A) and acetonitrile and 0.1 % FA (eluent B), the gradient was 1 % B isocratic for 5 min, then up to 100% in 20 min, the column used was a semi-preparative Atlantis T3 column (5 µm 10 mm × 150 mm i.d.).

HPLC-MS analysis was performed on the ACQUITY UPLC system (Chapter 2.2.3.1).

2.2.8 Experiments with the Solid-Supported Nucleophilic Probe

2.2.8.1 Synthesis of the Solid-Supported Nucleophilic Probe

The synthesis of the solid-supported nucleophilic probe was performed on a Liberty Blue™ instrument (CEM) and, unless stated otherwise, followed the User Guide and the Cl-MPA ProTide and Cl-TCP(Cl) ProTide Resin Loading Procedure of the manufacturer. Fmoc-Ala-OH in DMF was used at a concentration of 0.2 M in DMF, and (Fmoc-Cys-OH)₂ was used at a concentration of 0.1 M in DMF due to solubility. 1.0 M DIPEA with 0.125 M KI solution was used as loading reagent, and 10 % piperazine (w/v) in EtOH:NMP (10:90) was used as deprotection reagent. Two types of resins were synthesised, one that coupled Cl-TCP(Cl) to alanine, abbreviated as Ala-TCP, and the other to a cysteine dimer, abbreviated as Cys-TCP. Fmoc-Ala-OH (0.2 M in DMF) was used for the synthesis of Ala-TCP, and (Fmoc-Cys-OH)₂ (0.1 M in DMF) was used for Cys-TCP. Upon completion of the procedure, the synthesised resin was transferred out of the reaction vessel by rinsing with DMF. The resin was used within two days of synthesis.

2.2.8.2 Pilot Study Utilising the Solid-Supported Nucleophilic Probe

2.2.8.2.1 Pilot Experiment Procedure

Sample stock solutions (10 mM in DMSO) were prepared for this experiment. The synthesised resin (0.1 mmol equivalent) was resuspended in DMF to be split into four aliquots. The aliquots were transferred into SPE cartridges (CHROMABOND® reservoir columns, 2 ml, with PE frits, Macherey-Nagel, Düren, Germany). The cartridges were fitted onto a standard 12-port model Supelco Visiprep™ SPE Vacuum Manifold (Merck).

The following procedure was followed:

- i. Wash resin with 10 ml THF
- ii. Wash resin with 10 ml MeOH
- iii. Add 5 ml 2 M 2-BME in MeOH and leave to incubate for 30 min. Wash resin with 7 ml 2 M 2-BME in MeOH, collect the flow-through. Wash resin with another 3 ml MeOH
- iv. Add sample (12.5 µl for single compound test, 2 × 12.5 µl for compound mixture) the glass vial with another 600 µl DMSO that is added to resin as

well. The mixture is left to incubate for 17.5 h at RT. Collect the flow-through. Wash with 10 ml THF

- v. Wash resin with 10 ml MeOH
- vi. Add with 1 % TFA in MeOH (5 ml). Leave the mixture to incubate for 1 h, then, collect the flow-through. Wash resin with 10 ml MeOH
- vii. Wash resin with 10 ml THF

For each step, the flow-through was collected and dried on a PIAG Evapor equipped with a heating block (Portman Instruments, Biel-Benken, Switzerland) set to 30 °C under nitrogen flow. The leftover dried residue was redissolved in DMSO (325 µl) for HPLC analysis.

2.2.8.2.2 Pilot Experiment Repeat

The synthesised resin (0.1 mmol equivalent) was resuspended in MeOH and transferred into SPE cartridges (CHROMABOND® reservoir columns, 6 ml, with PE frits, Macherey-Nagel, Düren, Germany). The cartridges were fitted onto a standard 12-port model Supelco Visiprep™ SPE Vacuum Manifold (Merck).

The following procedure was followed:

- i. Wash resin with 5 ml MeOH
- ii. Wash resin with 5 ml MeOH
- iii. Wash resin with 5 ml MeOH
- iv. Add 50 µl 2-BME and 5 ml MeOH, leave the mixture to stir for 1 h at RT. Wash resin with 10 ml.
- v. Add parthenolide (12 mg) in DMSO (2 ml) and leave to mixture incubate for 17.5 h. Wash with 10 ml MeOH and 10 ml DCM.
- vi. Wash resin with 10 ml MeOH
- vii. Add with 1 % TFA in MeOH (5 ml). Leave the mixture to incubate for 30 min, then collect the flow-through. Wash resin with 10 ml MeOH and 10 ml DCM.
- viii. Wash resin with 10 ml THF

For each step, the flow-through was collected and dried on a PIAG Evapor equipped with a heating block (Portman Instruments, Biel-Benken, Switzerland) set to 30 °C under nitrogen flow. The leftover dried residue was redissolved in DMSO (325 µl) for HPLC analysis. When adduct formation was observed, the sample collected from step (vii) was used for purification by semi-preparative HPLC (Chapter 2.2.3.2) with solvents water (eluent A) and acetonitrile (eluent B) with the following gradient: 5 % to 20 % B in 10 min, isocratic at 20 % for 10 min.

2.2.8.2.3 Adapted Method for Spectroscopic Cysteine Quantification

This method used the same stock solutions as the previous method described in Chapter 2.2.4. Two sample sets were prepared, a 'blank' set and a set that was reacted with Ellman's Reagent, called 'sample' set. The samples were prepared in HPLC vials. For the calibration curve (0, 0.000010, 0.000025, 0.000050, 0.000100, 0.000250 and 0.000500 mmol), 200 µl of NAC solution in MeOH of the appropriate concentration was added into the vial; 200 µl of MeOH was added to the blanks and the analyte samples. 50 µl of DMSO was added to all calibration curve samples and the blanks. 30 µl DMSO and 20 µl of sample (500 mg/ml in DMSO) were added into analyte samples. 30 µl of 0.1 M phosphate buffer at pH 8.0 was added to the 'blank' series; 30 µl of Ellman's Reagent containing buffer solution was added to the 'sample' series. 200 µl of MeOH was used to wash down any remaining droplets in the vial. 200 µl of each sample were pipetted into a 96-well-plate for spectroscopic measurement on the Plate CHAMELEON Multilabel Detection Platform (Hidex).

2.2.8.3 Method Optimisation

2.2.8.3.1 Adjustment of Cleavage Conditions

Previous cleavage conditions of 1 % TFA in MeOH for 30-60 min in Chapter 2.2.8.2 were replaced with HFIP:DCM (1:4 v/v) for 5 h at RT. An experiment with this new cleavage step was conducted. The remaining method steps were the same as described in Chapter 2.2.8.2.3.

2.2.8.3.2 Wash Solvent Optimisation

2.2.8.3.2.1 Preliminary Dead Volume Experiment

Untreated Cl-TCP(Cl) ProTide resin (0.1 mmol equivalent, 192 mg dry residue for loading capacity 0.52 mmol/g) was weighed out, resuspended in DMF and transferred into an SPE cartridge (2 ml). Methylene blue (0.1 % in DMSO) solution was added until the clear solvent in the cartridge was completely displaced with blue dye in order to determine the approximate dead volume.

Chapter 2

The differences in wash behaviour of DCM, n-hexane, acetone, ethyl acetate and MeOH were observed. The solvent to be tested was added to the cartridge and left to percolate slowly until no more change could be observed. The behaviour was noted, then methylene blue was added to replenish the dye on the resin so that the next solvent could be tested.

2.2.8.3.2.2 Solvent Tests

Due to manual nature of the SPE set-up utilised, the flow rates were recorded for each step and kept lower than 1 ml/min. Cl-TCP(Cl) resin (0.192 g) weighed into an Eppendorf tube (1.5 ml) was left to swell in DMF (1.2 ml). The mixture was resuspended and 300 μ l of the mixture was transferred into each of the four prepared cartridges. The Eppendorf tube was washed with DMF (850 μ l), and an aliquot of the resuspended mixture (200 μ l) was transferred into each cartridge. The cartridge was washed out with MeOH (10 ml) to replace DMF and the elute was collected as X1 (X is a placeholder for A/B/C/D and DCM/n-hexane/acetone/ethyl acetate respectively). The analyte mixture (1.25 mM) was then loaded onto the cartridge and left to incubate for 17 h. DMSO (200 μ l) was layered on top the cartridge to prevent the cartridge from drying out. After incubation, a wash of MeOH (10 ml) was performed to confirm that all the resin-cartridge set-ups behave the same. The elute was collected as sample X2. The cartridge was then washed with 3 \times 10 ml test solvent and the elute of each wash was collected as samples X3-X5. Two final washes with MeOH (2 \times 10 ml) were performed and collected as X6 and X7. The samples were dried under nitrogen and reconstituted in DMSO (325 μ l) for HPLC-MS analysis.

2.2.8.3.3 Cysteine Quantification by Ultra Performance Liquid Chromatography (UPLC)-MSMS

A UPLC-MSMS method for determining the quantity of reactive cysteine-dimer-coupled resin by quantifying the released cysteine from reduction with 2-BME was developed. The same Waters system as for HPLC analysis was used for UPLC quantification; an ACQUITY UPLC system coupled to an ACQUITY TQD (Waters, Milford, MA, USA) with the cooling light-protected autosampler set at 10 °C in-between runs, at 20 °C for runs and the column oven set at 45 °C. A Waters ACQUITY UPLC® HSS T3 column (1.8 μ m 2.1 mm \times 100 mm i.d.) with corresponding pre-column was used for quantification. The injection solvent used for this quantification was a mixture of 65 % A (0.1 % FA in water) and 35 % B (0.1 % FA in acetonitrile). All standards and analytes were prepared in injection solvent. The calibration curve

was prepared using cysteine, the candidates evaluated as internal standard (IS) were methionine, NAC and atropine. The multiple reaction monitoring (MRM) transitions for cysteine were m/z 121.50>75.92 as quantifier and m/z 121.50>58.89 as qualifier. The methionine transition was m/z 149.80>104.00. The NAC transition was m/z 163.90>122.00. The atropine transition was m/z 289.50>123.90. For the calibration curve, 8 cysteine serial dilutions (0.00 $\mu\text{g/ml}$, 0.25 $\mu\text{g/ml}$, 1.25 $\mu\text{g/ml}$, 2.50 $\mu\text{g/ml}$, 5.0 $\mu\text{g/ml}$, 10.00 $\mu\text{g/ml}$, 20.00 $\mu\text{g/ml}$ and 25.00 $\mu\text{g/ml}$) and three quality control preparations (0.75 $\mu\text{g/ml}$, 12.50 $\mu\text{g/ml}$ and 20.00 $\mu\text{g/ml}$) were prepared. The IS working solution was prepared by serial dilution to give a 10 $\mu\text{g/ml}$ solution. The samples used for quantification were a 1:1 mixture of cysteine-containing standard or analyte and IS solution that was vortexed and spun down. Separation was performed with a gradient of 5 % to 10 % B in 1.5 min. The detailed conditions can be found in the method section of the Appendix. The QuanLynx add-on for MassLynx 4.1 (Waters) was used for analysis.

2.2.8.4 Updated Method Utilising the Solid-Supported Nucleophilic Probe

The resin was transferred into SPE cartridges (CHROMABOND® reservoir columns, 6 ml, with PE frits, Macherey-Nagel, Düren, Germany) containing magnetic stirrers. The cartridges were fitted onto a standard 12-port model Supelco Visiprep™ SPE Vacuum Manifold (Merck). The prepared resin was transferred into the SPE cartridge by resuspension in DCM:MeOH (1:1).

The following procedure was followed:

- i. Wash resin with 10 ml DCM:MeOH (1:1)
- ii. Wash resin with 10 ml DCM:MeOH (1:1)
- iii. Wash resin with 10 ml DCM:MeOH (1:1)
- iv. Wash resin with 2 ml MeOH to remove previous solvent, then add 200 µl BME and 2 ml MeOH, leave the mixture to stir for 60 min at RT, then, the flow-through is collected. The resin is washed with 50 ml DCM:MeOH (1:1)
- v. Wash resin with 400 µl DMSO to remove previous solvent, then add the dissolved sample from the HPLC glass vial, wash the glass vial with another 600 µl DMSO that is added to resin as well. The mixture is left to stir for 17.5 h at RT then, the flow-through is collected. The resin is washed with 50 ml DCM:MeOH (1:1)
- vi. Wash resin with 10 ml DCM:MeOH (1:1)
- vii. Add 1 ml of HFIP and 4 ml of DCM. Leave the mixture to stir for 5 h, then, the flow-through is collected. The resin is washed with 50 ml DCM:MeOH (1:1)
- viii. Wash resin with 10 ml DCM:MeOH (1:1)

For each step, the flow-through was collected and dried on a PIAG Evapor equipped with a heating block (Portman Instruments, Biel-Benken, Switzerland) set to 30 °C under nitrogen flow. The leftover dried residue was weighed and redissolved in DMSO or injection solvent to give a concentration of 1 mg/ml for HPLC analysis.

2.2.8.5 Reactions with Model Reactions

2.2.8.5.1 Model Reactions with Cysteine

Model compounds (1-3 mg) were dissolved in DMSO to give a 0.01 M solution. Equimolar amounts of cysteine solution (0.01 M in DMSO) were added and the samples were shaken in a BioShake iQ (Quantifoil Instruments, Jena, Germany) at 200 rpm at room temperature (RT) for 17.5 h. The samples were diluted 1:100 in DMSO prior to HPLC analysis.

2.2.8.5.2 Purification of Model Compound Adducts

Purification occurred via semi-preparative HPLC (Chapter 2.2.3.2). The reacted adduct compounds were purified using water (eluent A) and acetonitrile (eluent B) with the following gradients: alantolactone (isocratic 32 % B), cynaropicrin (5 % to 16 % B in 10 min followed by isocratic at 16 % for 18 min), *N*-(1-Naphthyl)-*N*-phenylmethacrylamide (5 % to 65 % B in 10 min, isocratic at 65 % for 2 min), penicillin V (30 % B for 10 min, to 55 % in 10 min, 55 % for 8 min, to 100 % in 5 min).

2.2.8.5 Adapted Method for the Processing of the Larger Batch

Cys-TCP was synthesised in batches until a total of 1.25 g was obtained, in the same manner as described in Chapter 2.2.8.1. The cartridge size was larger to accommodate for the larger amount of resin. For this experiment, 3.74 g of *Ambrosia psilostachya* was used.

The following procedure was followed:

- i. Wash resin with 30 ml DCM:MeOH (1:1)
- ii. Wash resin with 30 ml DCM:MeOH (1:1)
- iii. Wash resin with 30 ml DCM:MeOH (1:1)
- iv. Wash resin with 5 ml MeOH to remove previous solvent, then add 1.5 ml BME and 5 ml MeOH, leave the mixture to stir for 60 min at RT, then, the flow-through is collected. The resin is washed with 90 ml DCM:MeOH (1:1)
- v. Wash resin with 1 ml DMSO to remove previous solvent, then add the dissolved sample from the HPLC glass vial. The mixture is left to stir for 17.5 h at RT then, the flow-through is collected. The resin is washed with 180 ml DCM:MeOH (1:1)
- vi. Wash resin with 30 ml DCM:MeOH (1:1)
- vii. Add 2 ml of HFIP and 8 ml of DCM. Leave the mixture to stir for 5 h, then, the flow-through is collected. The resin is washed with 90 ml DCM:MeOH (1:1)
- viii. Wash resin with 30 ml DCM:MeOH (1:1)

For each step, the flow-through was collected and dried on a PIAG Evapor equipped with a heating block (Portman Instruments, Biel-Benken, Switzerland) set to 30 °C under nitrogen flow. The leftover dried residue was weighed and redissolved in injection solvent to give a concentration of 1 mg/ml for HPLC analysis.

Chapter 3 Quantifying Electrophiles in Extracts

3.1 Introduction

Previous research in this laboratory by Alen Božičević has yielded that electrophiles are present in numerous allergenic plant pollen (Figure 3.1)²⁸⁴.

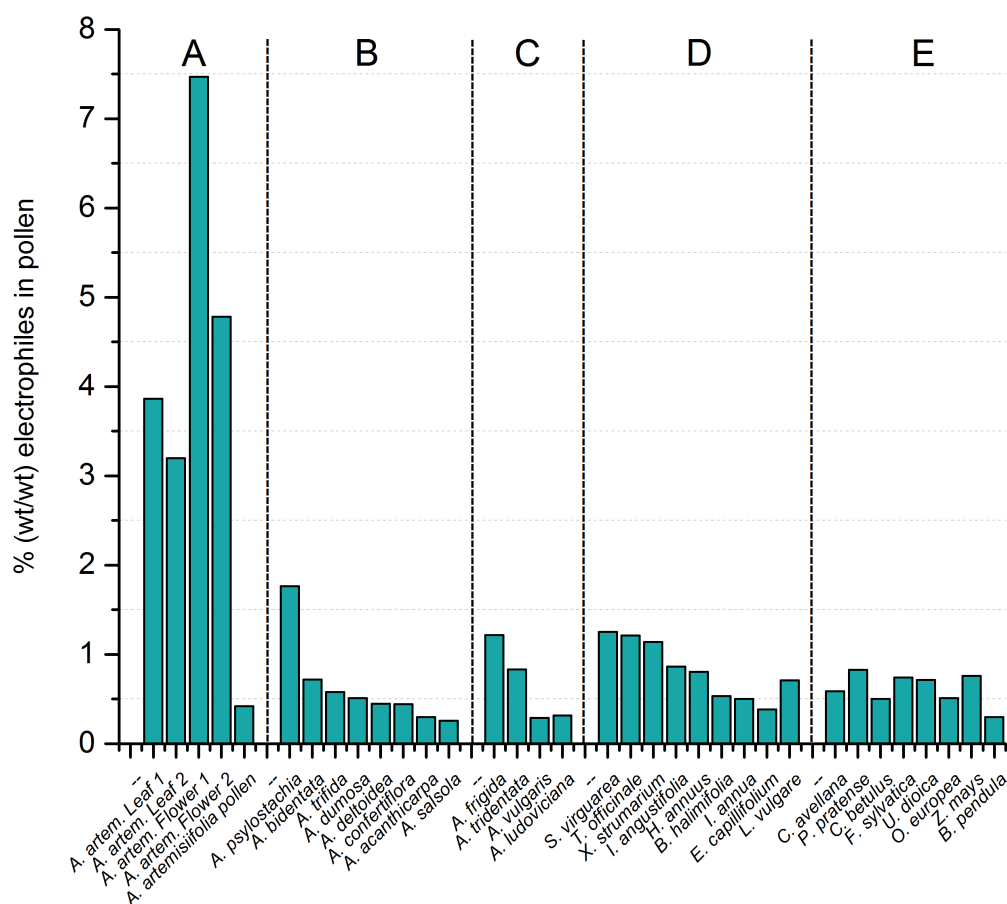


Figure 3.1 Electrophile content of *Ambrosia artemisiifolia* plant parts and pollen from a selection of other plant species. Reproduced with permission^{††}, copyright American Chemical Society.

A common class of electrophilic natural products are sesquiterpene lactones, which feature α,β -unsaturated carbonyls and are therefore UV-active²⁸⁵. In order to find out whether sesquiterpene lactones could be the electrophiles present in pollen extracts, extracts were subjected to PDA measurements (Figure 3.2). Whilst pollen of the Asteraceae family showed absorption at 254 nm, non-Asteraceae did not show

^{††} Reproduced with permission from Božičević, A., De Mieri, M., Nassenstein, C., Wiegand, S., Hamburger, M., Secondary metabolites in allergic plant pollen samples modulate afferent neurons and murine tracheal rings, *J. Nat. Prod.* 80 (2017), 2953-2961. Copyright (2017) American Chemical Society.

absorbance. This meant that non-Asteraceae plant pollen contained electrophiles that were not sesquiterpene lactones.

A more in-depth analysis on *Ambrosia artemisiifolia* and *Ambrosia psilostachya* plant pollen showed that pollen of these species both contain electrophilic sesquiterpene lactones and polyamines. Non-Asteraceae pollen were not investigated, so it is not known what electrophiles they could contain. In order to shed some light on what these electrophiles were, pollen extract batches from plant species of interest needed to be examined in more detail. This chapter will discuss the selection of the pollen samples, their extraction and their characterisation.

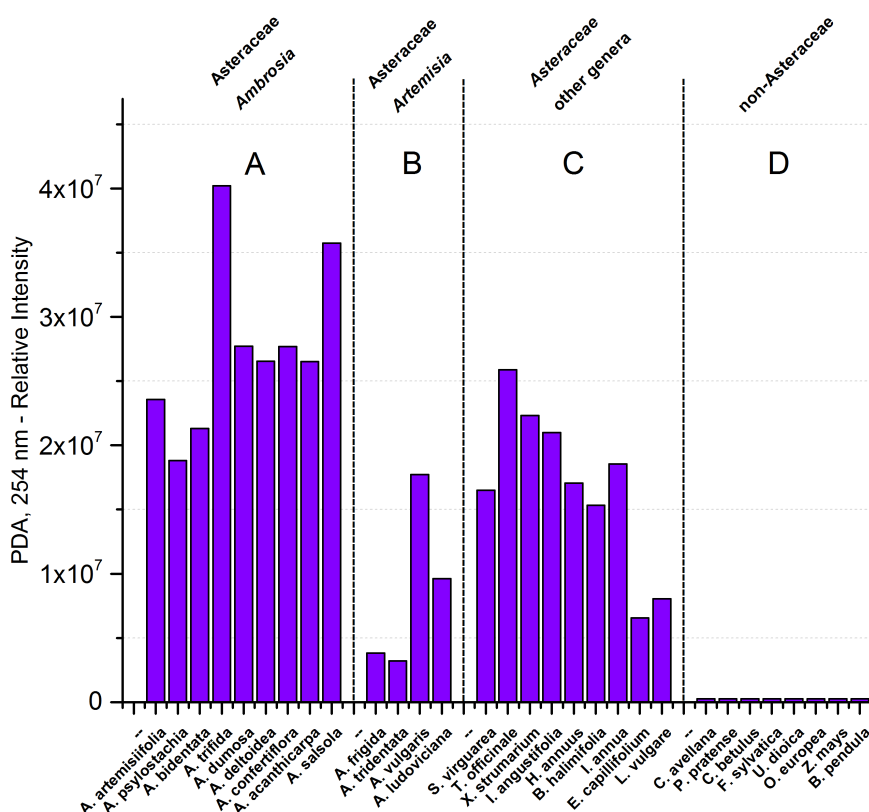


Figure 3.2 PDA measurement results of plant pollen extracts at 254 nm. Reproduced with permission^{‡‡}, copyright American Chemical Society.

3.2 Pollen Batches and Extract Generation

Pollen species of particular interest were the ones that have electrophile content but no absorbance at 254 nm. From the ones tested in previous research, four were

^{‡‡} Reproduced with permission from Božičević, A., De Mieri, M., Nassenstein, C., Wiegand, S., Hamburger, M., Secondary metabolites in allergic plant pollen samples modulate afferent neurons and murine tracheal rings, *J. Nat. Prod.* 80 (2017), 2953-2961. Copyright (2017) American Chemical Society.

selected: *Betula pendula*, *Corylus avellana*, *Phleum pratense* and *Urtica dioica*. For testing purposes, two batches of the Asteraceae family were also included. *Ambrosia psilostachya* and *Ambrosia artemisiifolia* were chosen for two reasons: i) continued interest in the natural compounds of the *Ambrosia* family and ii) previous research on these two plant pollen extracts had given insight on their composition, therefore they would constitute ideal test extracts in the method development process.

Since the quantities of previously tested pollen batches were not enough to start a new series of experiments, new batches had to be ordered. For each plant species pollen, several batches were ordered in order to account for batch to batch variability and to make sure that at least one of the batches would contain electrophiles (Table 2.5). The extracts were prepared by ASE as described in Chapter 2.2.1, the yields can be found in Table 3.1. Every pollen batch generated three extracts by serial extraction with three different solvents: n-hexane, THF and MeOH.

Table 3.1 Pollen extract yields of the pollen batches ordered. Total yield corresponds to quantity of residue extracted of all solvents combined.

Species	Lot Number	Solvent	Isolated Mass (mg)	Pollen Starting Material (g)	Total Yield(%)
<i>Ambrosia psilostachya</i>	P3701938-2	Hexane	21.3	4.8503	
<i>Ambrosia psilostachya</i>	P3701938-2	THF	286.3	4.8503	30.2
<i>Ambrosia psilostachya</i>	P3701938-2	MeOH	1157.8	4.8503	
<i>Ambrosia psilostachya</i>	P3757208	Hexane	10.8	4.8331	
<i>Ambrosia psilostachya</i>	P3757208	THF	287.7	4.8331	23.6
<i>Ambrosia psilostachya</i>	P3757208	MeOH	840.4	4.8331	
<i>Ambrosia psilostachya</i>	P4129072-1	Hexane	34.3	4.8460	
<i>Ambrosia psilostachya</i>	P4129072-1	THF	405.2	4.8460	27.2
<i>Ambrosia psilostachya</i>	P4129072-1	MeOH	880.7	4.8460	
<i>Ambrosia psilostachya</i>	P4576841	Hexane	4.8	4.9961	
<i>Ambrosia psilostachya</i>	P4576841	THF	298.0	4.9961	29.1
<i>Ambrosia psilostachya</i>	P4576841	MeOH	1149.0	4.9961	
<i>Ambrosia artemisiifolia</i>	P3024704-3	Hexane	299.6	2.4207	
<i>Ambrosia artemisiifolia</i>	P3024704-3	THF	159.2	2.4207	38.4
<i>Ambrosia artemisiifolia</i>	P3024704-3	MeOH	470.3	2.4207	
<i>Ambrosia artemisiifolia</i>	P3744652-2	Hexane	16.8	2.2009	
<i>Ambrosia artemisiifolia</i>	P3744652-2	THF	156.4	2.2009	32.6
<i>Ambrosia artemisiifolia</i>	P3744652-2	MeOH	545.3	2.2009	
<i>Ambrosia artemisiifolia</i>	P3396120-3	Hexane	203.0	2.6142	
<i>Ambrosia artemisiifolia</i>	P3396120-3	THF	172.8	2.6142	33.6
<i>Ambrosia artemisiifolia</i>	P3396120-3	MeOH	502.9	2.6142	
<i>Ambrosia artemisiifolia</i>	P335440-18	Hexane	238.7	2.1557	
<i>Ambrosia artemisiifolia</i>	P335440-18	THF	172.2	2.1557	37.8
<i>Ambrosia artemisiifolia</i>	P335440-18	MeOH	404.3	2.1557	

Chapter 3

<i>Ambrosia artemisiifolia</i>	P3392522-19	Hexane	286.6	2.5406	
<i>Ambrosia artemisiifolia</i>	P3392522-19	THF	164.2	2.5406	38.2
<i>Ambrosia artemisiifolia</i>	P3392522-19	MeOH	520.3	2.5406	
<i>Phleum pratense</i>	P319351-7	Hexane	82.2	4.6518	
<i>Phleum pratense</i>	P319351-7	THF	266.0	4.6518	15.3
<i>Phleum pratense</i>	P319351-7	MeOH	365.9	4.6518	
<i>Phleum pratense</i>	P3280848-1	Hexane	30.0	4.3511	
<i>Phleum pratense</i>	P3280848-1	THF	118.5	4.3511	15.8
<i>Phleum pratense</i>	P3280848-1	MeOH	540.4	4.3511	
<i>Phleum pratense</i>	P3743977-1	Hexane	41.9	4.5290	
<i>Phleum pratense</i>	P3743977-1	THF	126.1	4.5290	11.4
<i>Phleum pratense</i>	P3743977-1	MeOH	351.1	4.5290	
<i>Phleum pratense</i>	P3929196-1	Hexane	47.1	4.4900	
<i>Phleum pratense</i>	P3929196-1	THF	93.7	4.4900	18.3
<i>Phleum pratense</i>	P3929196-1	MeOH	681.5	4.4900	
<i>Betula pendula</i>	P3317516-1	Hexane	163.3	4.6534	
<i>Betula pendula</i>	P3317516-1	THF	441.2	4.6534	32.3
<i>Betula pendula</i>	P3317516-1	MeOH	900.6	4.6534	
<i>Betula pendula</i>	P3317540-1	Hexane	181.6	4.7336	
<i>Betula pendula</i>	P3317540-1	THF	394.3	4.7336	30.2
<i>Betula pendula</i>	P3317540-1	MeOH	853.0	4.7336	
<i>Betula pendula</i>	P3752220	Hexane	147.7	4.6252	
<i>Betula pendula</i>	P3752220	THF	438.5	4.6252	31.5
<i>Betula pendula</i>	P3752220	MeOH	868.5	4.6252	
<i>Urtica dioica</i>	P3730565	Hexane	48.8	4.7094	
<i>Urtica dioica</i>	P3730565	THF	356.7	4.7094	36.9
<i>Urtica dioica</i>	P3730565	MeOH	1334.5	4.7094	
<i>Urtica dioica</i>	P4079048-1	Hexane	48.2	4.7758	
<i>Urtica dioica</i> ^a	P4079048-1	THF	109.7	4.7758	29.9
<i>Urtica dioica</i>	P4079048-1	MeOH	1148.9	4.7758	
<i>Urtica dioica</i>	P4889415	Hexane	32.1	4.6652	
<i>Urtica dioica</i>	P4889415	THF	182.1	4.6652	29.1
<i>Urtica dioica</i>	P4889415	MeOH	1145.6	4.6652	
<i>Corylus avellana</i>	P976555-1	Hexane	28.7	4.5384	
<i>Corylus avellana</i>	P976555-1	THF	401.9	4.5384	34.2
<i>Corylus avellana</i>	P976555-1	MeOH	1120.9	4.5384	
<i>Corylus avellana</i>	P1330035-2	Hexane	27.4	4.6923	
<i>Corylus avellana</i>	P1330035-2	THF	344.0	4.6923	29.2
<i>Corylus avellana</i>	P1330035-2	MeOH	998.8	4.6923	
<i>Corylus avellana</i>	P4530617	Hexane	20.7	4.5102	
<i>Corylus avellana</i>	P4530617	THF	309.2	4.5102	28.1
<i>Corylus avellana</i>	P4530617	MeOH	938.2	4.5102	

^a Extract yield lowered due to a post-extraction contamination before yield determination. The yield recorded is for the residue that was salvaged.

Generally, the batches of the same species showed similar patterns of absolute extraction yields for the individual solvents. The pollen batches had been defatted by the supplier, so the low yields for the n-hexane extracts were not surprising. After extract generation, the next step was quality control by HPLC.

3.3 Extract Analysis by HPLC

The extract profiles were measured on two separate instruments coupled to mass analysers. An aliquot of dry extract was dissolved in DMSO and measured on the Shimadzu HPLC System (Chapter 2.2.3.1), another aliquot was dissolved in injection solvent (Chapter 2.2.8.3.3) and measured on the ACQUITY UPLC system (Chapter 2.2.3.1). This was done for quality control reasons and to check how similar the individual species batches were (data not shown).

Although the general profiles of pollen batch extracts within a species were the same, there were differences in peak areas and thus abundancies of individual constituents. The electrophile content of all the extracts generated needed to be measured to know how much electrophile content could be expected. Furthermore, it was decided to reorder a larger quantity of the batch of *Ambrosia psilostachya* that contained the highest amount of electrophiles, in order to have a pollen test extract to use for method development and to have a larger batch to work with for a later isolation. The next chapter will discuss the spectrophotometric quantification of electrophile content of the pollen extracts generated.

3.4 Spectrophotometric Quantification with Ellman's Reagent

Previous quantification of electrophile content in plant extracts in this group was performed using a spectrophotometric method adapted from Salapovic *et al* (Chapter 2.2.4)²⁸⁶. In this method, the sample's reactive potential was quantified with an excess of NAC, which was used as a proxy for electrophile content. This approximation was in line with our interest to identify electrophiles that were reactive in a physiological setting, since cysteine and other thiolates are one of the sources of endogenous nucleophilicity.



Figure 3.3 Reaction of Ellman's reagent with free thiols.

Samples were first left to react with a known quantity of excess NAC for 40 min, then, Ellman's Reagent was added to react with the remaining NAC, resulting in a quantifiable colour change. The basis of this spectrophotometric assay is the reactivity of Ellman's reagent with free thiol moieties to give a coloured reaction product, 2-nitro-5-chlorobenzoate dianion, that has a characteristic absorption at 412 nm (Figure 3.3).

Consequently, by measuring absorbance at 412 nm and thus the abundance of the coloured product, the amount of NAC that previously reacted with the sample could be indirectly quantified. Due to the constraints in the wavelength adjustment of the equipment available, the measurements were carried out at 416 nm, which still allowed for construction of a calibration curve. The calibration curve was constructed using a model electrophile, parthenolide. The graph compiled for *Phleum pratense* is shown in Figure 3.4. The remaining graphs for the other plant species can be found in the Appendix (Figure S.1 to Figure S.5)

Phleum pratense

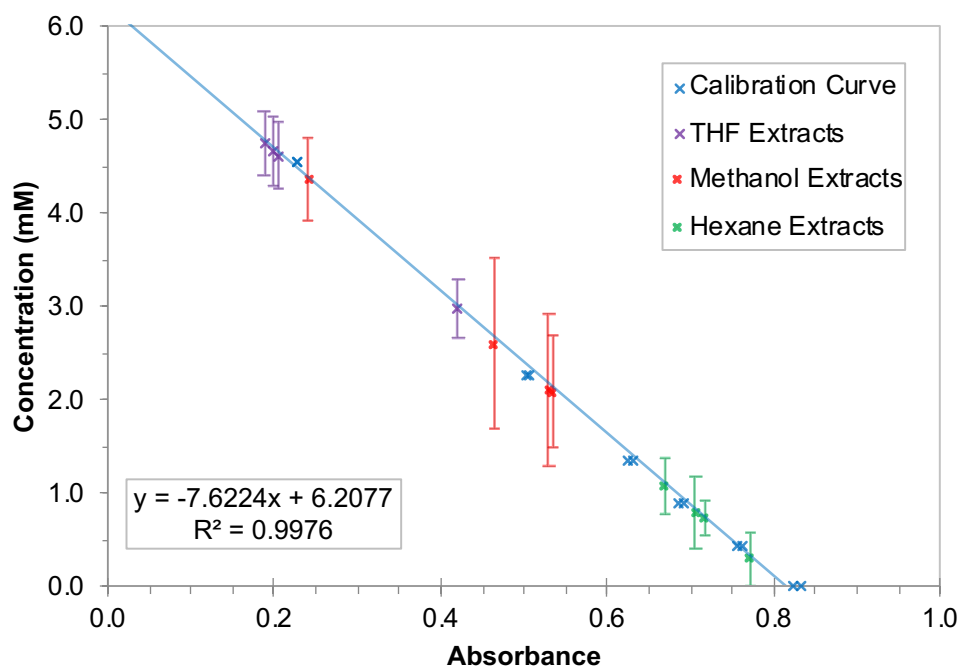


Figure 3.4 Calibration curve and interpolated data points for *Phleum pratense*.

The tabulated results for n-hexane, THF and MeOH extracts tested are reported in the Appendix (Table S.1) and the results are graphically represented in Figure 3.5. It was found that different plant species showed distinct characteristic distribution patterns of relative electrophile content. In *Ambrosia artemisiifolia* and *Betula pendula*, electrophilicity was solely located in the THF extract. *Corylus avellana*

P976555-1 (Lot #1) had some electrophilicity in the n-hexane extract, but apart from that outlier, this species also had all its electrophilic content in the THF extract. *Urtica*

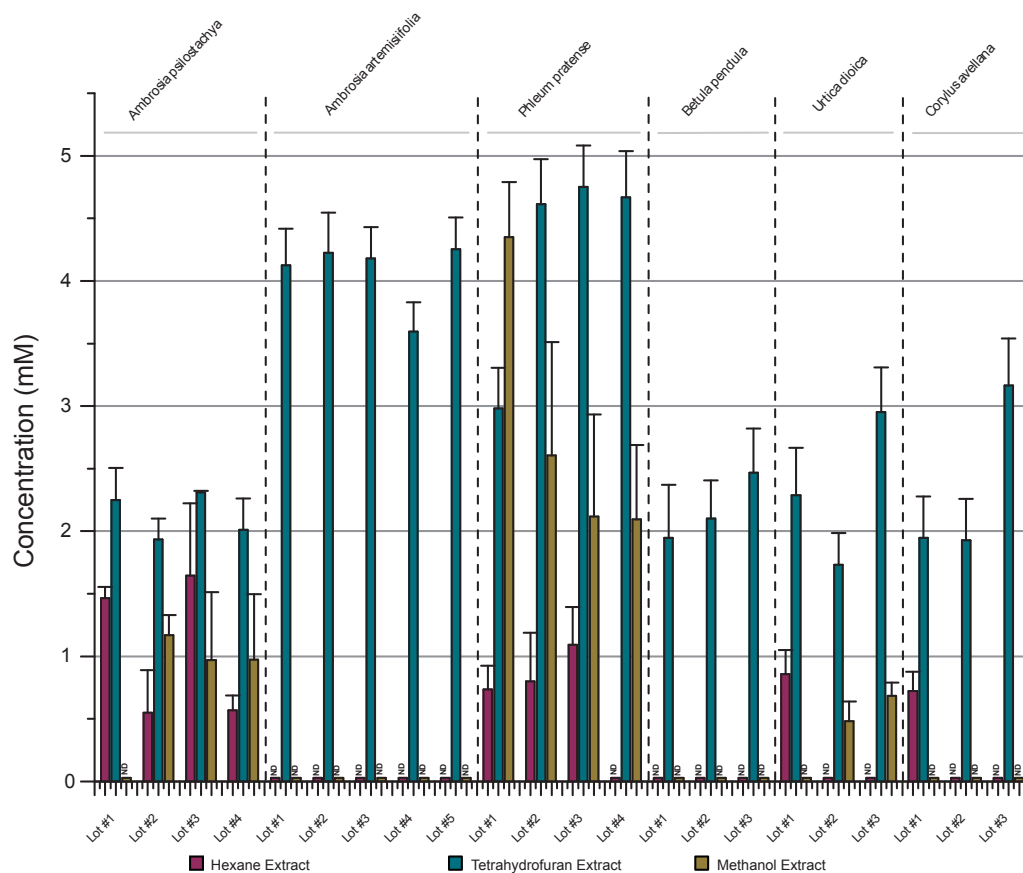


Figure 3.5. Electrophilic content of the individual pollen extracts generated by serial extraction with hexane, THF and MeOH, plotted as a bar chart, as result of the NAC-based spectrophotometric assay. The concentration of electrophiles was plotted in reference to the standard utilised, parthenolide, by means of a calibration curve. The samples where the electrophile content fell underneath the threshold for quantification, i.e. below 0.45 mM, were denoted as ND for not determined. Lot numbers are abbreviated to single digits in this figure. The numbers follow the batch number sequence of Table 3.1.

dioica had most of its electrophilicity concentrated in the THF extract as well. *Ambrosia psilostachya* and *Phleum pratense* had their electrophilic content split up between the solvent extracts, with some electrophilicity found in each solvent extract, but the majority remained in the THF extract.

From these measurements, it could be concluded that the majority of the electrophilic compounds were moderately polar as they were located in the THF extract. Analyses would therefore focus on the THF extracts of these pollen batches. Based on the

electrophile content in the THF extracts of the different *Ambrosia psilostachya* batches, it was decided to reorder 100 g of batch P4129072-1. This batch was extracted by percolation as detailed in Chapter 2.2.1. Since this extraction method is different from the original extraction, which was performed with ASE, these two extracts were not merged. The newly ordered batch was denoted as P4129072-1'.

A putative gram formula mass (GFM) can be used to estimate the total amount of electrophiles in mg. GFM 250 g mol^{-1} and GFM 400 g mol^{-1} were chosen as example masses since secondary metabolite GFMs often fall into the mass range between 250 g mol^{-1} and 400 g mol^{-1} . Combining data of the THF extract yields and the quantification of electrophile content with the putative masses, Table 3.2 was generated.

Table 3.2 Electrophile content estimation of the THF extracts by extrapolation with putative GFM 250 g mol^{-1} and GFM 400 g mol^{-1} . The second batch of P4129072-1 ordered is listed as a separate entry P4129072-1' at the end of the table, as the extraction method was different. The electrophile content of P4129072-1' was extrapolated from P4129072-1.

Species	Lot Number	Extract Mass (mg)	Electrophile Concentration (mM)	Total Electrophile Content (μmol)	Mass for GFM 250 (mg)	Mass for GFM 400 (mg)
<i>Ambrosia psilostachya</i>	P3701938-2	286.3	2.250	6.44	1.61	2.58
<i>Ambrosia psilostachya</i>	P3757208	287.7	1.934	5.56	1.39	2.23
<i>Ambrosia psilostachya</i>	P4129072-1	405.2	2.311	9.37	2.34	3.75
<i>Ambrosia psilostachya</i>	P4576841	298.0	2.012	6.00	1.50	2.40
<i>Ambrosia artemisiifolia</i>	P3024704-3	159.2	4.125	6.57	1.64	2.63
<i>Ambrosia artemisiifolia</i>	P3744652-2	156.4	4.225	6.61	1.65	2.64
<i>Ambrosia artemisiifolia</i>	P3396120-3	172.8	4.180	7.22	1.81	2.89
<i>Ambrosia artemisiifolia</i>	P335440-18	172.2	3.595	6.19	1.55	2.48
<i>Ambrosia artemisiifolia</i>	P3392522-19	164.2	4.255	6.99	1.75	2.79
<i>Phleum pratense</i>	P319351-7	266.0	2.981	7.93	1.98	3.17
<i>Phleum pratense</i>	P3280848-1	118.5	4.612	5.47	1.37	2.19
<i>Phleum pratense</i>	P3743977-1	126.1	4.751	5.99	1.50	2.40
<i>Phleum pratense</i>	P3929196-1	93.7	4.667	4.37	1.09	1.75
<i>Betula pendula</i>	P3317516-1	441.2	1.948	8.59	2.15	3.44
<i>Betula pendula</i>	P3317540-1	394.3	2.100	8.28	2.07	3.31
<i>Betula pendula</i>	P3752220	438.5	2.468	10.82	2.71	4.33
<i>Urtica dioica</i>	P3730565	356.7	2.288	8.16	2.04	3.26
<i>Urtica dioica</i>	P4079048-1	109.7	1.732	1.90	0.47	0.76
<i>Urtica dioica</i>	P4889415	182.1	2.953	5.38	1.34	2.15
<i>Corylus avellana</i>	P976555-1	401.9	1.945	7.82	1.95	3.13
<i>Corylus avellana</i>	P1330035-2	344.0	1.927	6.63	1.66	2.65
<i>Corylus avellana</i>	P4530617	309.2	3.166	9.79	2.45	3.92

<i>Ambrosia psilostachya</i>	P4129072-1'	5240.0	2.311	121.11	30.28	48.44
------------------------------	-------------	--------	-------	--------	-------	-------

Based on this analysis, it was evident that only very small amounts of active electrophiles were present in each extract. This meant that the method for detecting, purifying and identifying electrophiles needed to be able to work on very small amounts.

3.5 Conclusions

Pollen batches were selected and extracted by ASE. HPLC analyses were performed on the extracts and their electrophile content was quantified using UV spectroscopy. Extracts of the same species overall seemed to contain the same type of compounds and had the same reactivity profile but had differences in abundance and therefore in electrophile content. Based on the analysis, batch P4129072-1 was reordered and processed as P4129072-1'. After calculating the total electrophile content, it became evident that only very small amounts of electrophiles were present in each extract. This needed to be considered during the method development process. Method development first took an *in situ* approach as LC methods require only very small amounts of compound, which will be described in Chapter 4.

Chapter 4 *In situ* Detection of Electrophiles in Chromatography

4.1 Introduction

Due to the limited amount of extract material available for study, method development first focused around the detection and identification *in situ* via LC methods. LC allows for analysis of complex samples by separation according to their interaction with the column stationary phase.

The presence of an electrophile can be confirmed by the reaction with a nucleophile. Comparing a pre-reaction sample to a post-reaction sample by using an LC-coupled detector would potentially enable the detection of electrophiles in extract samples, as structural changes of molecules, like adduct formation, can result in a change in *rt*. Additionally, different LC detectors can be leveraged in the same way, as structural changes can also affect other physicochemical properties, e.g. mass or UV absorption that could be detected by MS or UV/Vis detectors respectively. This can render adduct structures easily detectable. Thus, by carefully choosing the nucleophile, it is possible to further modify the electrophile in a way that a resulting adduct can be easily identified as the product of a nucleophilic addition.

Detection of electrophiles with LC detection methods can be addressed in a number of different ways, and this chapter serves to recount the different approaches that were attempted in order to find a method that could work in the context of natural product research. In Chapter 4.2, methods utilising MS Scan will be discussed, in Chapter 4.3 MSMS methods will be the subject.

4.2 *In Situ* Detection by Mass Spectrometry (MS) Scan

The earliest stage of the project focused solely on identifying the compounds by means of qualitative assessment by comparing pre- and post-reaction samples.

As raised in the introduction, formation of an adduct could result in a change in *rt* and mass that could be quantified using LC-MS. This change can be observed by comparison of a sample that has not been exposed to the nucleophile (pre-reaction) with a sample that has been exposed to the nucleophile (post-reaction), as demonstrated in Figure 4.1.

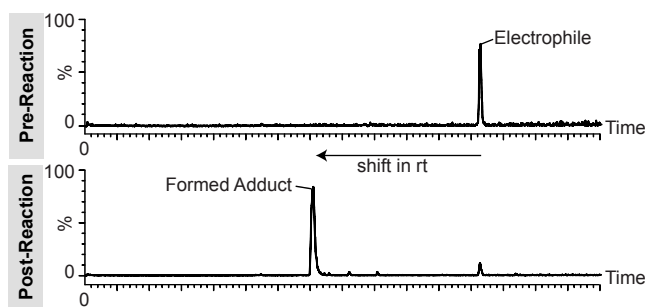


Figure 4.1 Sample LCMS comparison of a pre-reaction and a post-reaction sample. In this example the electrophile reacts with an added nucleophile to form an adduct. The reaction does not entirely go to completion as can be seen by the remaining electrophile peak in the post-reaction chromatogram.

Signals that appear in the post-reaction chromatogram that are not present in the pre-reaction chromatogram are adducts, whereas signals that are present in the pre-reaction chromatogram but disappear in the post-reaction chromatogram should be electrophiles. The spectral data recorded by LC-coupled detectors can be analysed. The work presented in this dissertation utilised two commonly used detector types, MS and UV/Vis, which will now both be discussed.

MS measures the mass-to-charge ratio of ions. This gives information about the mass of the whole molecule as well as its most commonly formed fragments, depending on the ionisation mode used. Since an adduct is formed, both the rt and the mass should differ from the starting material. MS could give information about both the electrophile and the adduct mass, which could be valuable information for compound identification.

The second detection method used in the work of this thesis was UV/Vis. UV/Vis detection is a standard method to detect UV/Vis-active compounds in mixtures. Organic compounds that have conjugated double bonds or aromatic rings can absorb energy from light in the region of UV/Vis, which enables their detection. Using a nucleophile that in itself is UV/Vis active could enable facile detection. Furthermore, UV/Vis spectra can give valuable information on the compound structure as some compound classes have characteristic absorption spectra²⁸⁷.

If an identification could not be made based on the already available data, the isolation of the peaks of interest for further analysis, e.g. NMR, would become necessary. There were two options for pursuing further analysis: a) isolating the electrophiles from an unreacted, i.e. pre-reaction, sample or b) isolating the adducts from a post-

reaction sample. If the unreacted electrophiles could be isolated, it would be possible to elucidate the native structure of the electrophiles in the sample. Conversely, one could also isolate the adducts formed after the reaction, which could be an option if the former option was not possible due to the complexity of the pre-reaction sample mixture. Another reason for isolating the post-reaction adducts would be analysing the mechanism of adduct formation by figuring out at which site of adduct formation occurred.

Reactive electrophiles that enter the body are usually quickly quenched by the body's nucleophilic 'safety net', GSH. The GSH reservoir regulates oxidation and reduction in the body. It is involved in many biological processes, examples being transport, metabolism and protection of cells²⁸⁸. GSH is the most abundant nonprotein intracellular thiol in the body and its biological function also includes the scavenging of reactive electrophiles²⁸⁹. Often, GSH and its analogues are used for the characterisation of metabolic stability²⁹⁰⁻²⁹³. Thus, as it was planned to characterise electrophiles that could possibly be reactive *in vivo*, this physiologically relevant nucleophile was the logical first choice.

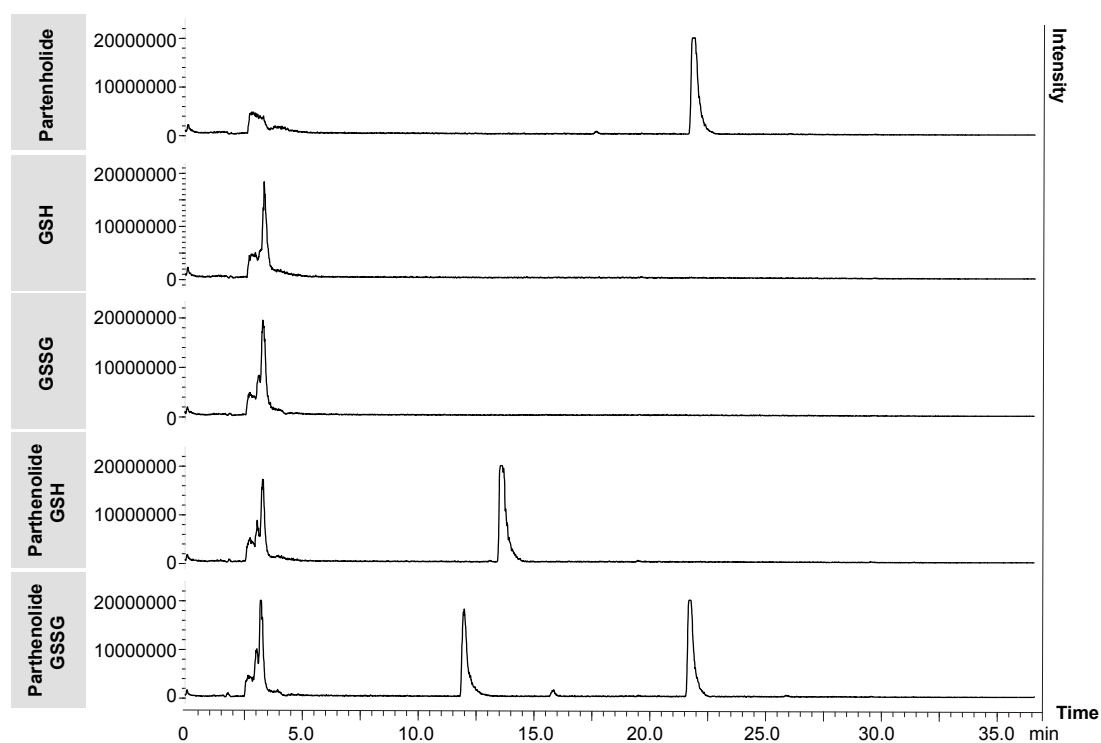


Figure 4.2 Reaction of model compound parthenolide with GSH and GSSG. HPLC-MS traces (positive ion mode) were recorded with a scan range m/z 160-1000. Intensity scaled to max peak.

GSSG is the disulfide formed from two GSH molecules and hence should have no activity as a nucleophile, which is why it was chosen as a negative control. These two compounds were tested as described in Chapter 2.2.6.1 against an electrophilic model compound, parthenolide (Figure 4.2).

GSH was found at rt 3.0 min with m/z 308 $[M+H]^+$. In the same sample, another mass was found, namely m/z 307 $[M+2H]^{2+}$ and m/z 613 $[M+H]^+$ at rt 3.4 min, which corresponds to the mass of GSSG. This meant that GSH could form GSSG *in situ* via oxidation at ambient conditions. In the GSSG sample, GSSG was found at rt 3.4 min with m/z 307 $[M+H]^+$ and m/z 613 $[M+2H]^{2+}$. Parthenolide (m/z 249 $[M+H]^+$, rt 22.1 min) showed to be reactive with GSH, forming an adduct with had an m/z that was the sum of parthenolide plus GSH (m/z 556 $[M+H]^+$, rt 13.8 min). Interestingly, in the sample with GSSG, one can find the unreacted parthenolide (m/z 249 $[M+H]^+$, rt 22.1 min) but also another peak (m/z 431 $[M+2H]^{2+}$ and m/z 861 $[M+H]^+$) with rt 12.1 min. Judging by the m/z value observed, it seemed that GSSG reacted with parthenolide as well; this mass corresponded to the sum of the masses of GSSG and parthenolide. This indicated that GSSG could not be used as a non-nucleophilic control for GSH.

In the course of this experiment, the kinetics of the reaction of parthenolide with GSH was also examined. A reaction mixture of GSH and parthenolide was injected three consecutive times directly after mixing (Figure 4.3). It was found that the reaction of parthenolide with GSH was fast; there was no unreacted parthenolide in any of the runs, which meant that this particular reaction was not only spontaneous but also practically instantaneous.

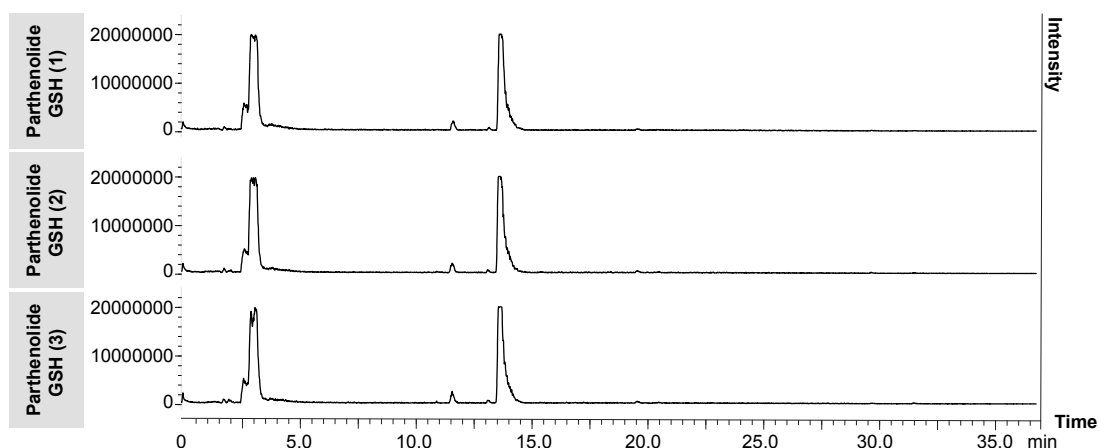


Figure 4.3 Reaction of parthenolide with GSH. (1) was injected 5 min after mixing. Each run took a total of 45 min, (1), (2) and (3) were injected one after another. HPLC-MS traces (positive ion mode) were recorded with a scan range m/z 160-1000. Intensity scaled to max peak.

With these results, an experiment was launched with an extract (Chapter 2.2.6.2), the THF extract *Ambrosia psilostachya* (Lot P3757208). This extract had been previously shown to have high electrophile content in the quantification experiment (Figure 4.4).

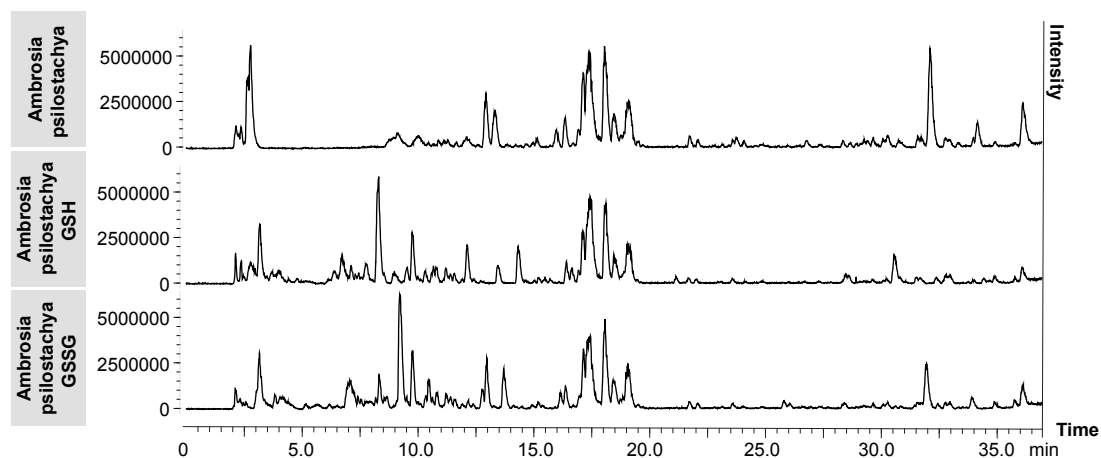


Figure 4.4 Top: blank *Ambrosia psilostachya* extract; centre: reaction of *Ambrosia psilostachya* extract with GSH; bottom: reaction of *Ambrosia psilostachya* extract with GSSG. HPLC-MS traces (positive ion mode) were recorded with a scan range m/z 160-1000. Intensity scaled to max peak.

What could be observed from this experiment was that there were a number of peaks that appeared in the reactions with both GSH and GSSG between rt 6.0 min and rt 12.5 min which were previously not in the blank extract sample. GSH is a big molecule and influences the rt of its adducts, which explained this shift to an earlier rt . GSSG was previously shown to be reactive, therefore observing a similar shift with the extract as GSH was expected.

The *Ambrosia psilostachya* extract is known to contain electrophilic sesquiterpene lactones. These sesquiterpene lactones in the extract likely reacted with GSH, which explained the surge in signals around rt 6.0 min to 12.5 min. By comparing the pre- and post-reaction samples, it was not possible to tell which exact peaks in the pre-reaction sample corresponded to electrophiles that would be interesting to purify. This stemmed from the inherent complexity of extracts, but it could also be that reactive compounds do not react fully with the nucleophile and instead form an equilibrium, like in the example figure shown previously (Figure 4.1). This made an interpretation of the obtained data difficult, even though some electrophiles in this extract had been previously reported²⁸⁴.

The newly formed adducts in the post-reaction sample were also too convoluted and too similar in rt to consider a purification. GSH, being a rather large molecule,

influenced the *rt* of the formed adduct greatly and thus caused the majority of the formed adducts to aggregate around similar *rt*. The *m/z* values found in the post-reaction sample could not be mapped clearly to known masses of compounds reported in *Ambrosia psilostachya*. Furthermore, multiple addition of GSH was also an option, since GSH was not added in a stoichiometric manner.

To consolidate the findings of this experiment, the reaction of GSH with parthenolide worked very well, however, working with an extract proved to be difficult. GSH is a big molecule that influenced the *rt* of formed adducts greatly, which was why many of the adducts ultimately had very similar *rt* and overlap. From there, figuring out which masses were relevant was very difficult. A way to circumvent this would be using a different type of tag, perhaps a smaller one that would not influence the *rt* so greatly. Additionally, there was the possibility of multiple reactions with more than one stoichiometric equivalent of GSH.

This experiment had shown that the qualitative approach to this problem may not work. The biggest problem was the fact that it was not possible to force reaction to go to completion under the used reaction conditions. This made the analysis more difficult because every peak would have to be evaluated individually by all the mass peaks that they include. To make this task less tedious and time-consuming, automated mass tables could be generated with the LabSolutions software and a quantitative approach could be utilised.

In terms of the experimental setup, in order to compare two states of an extract (reacted vs. unreacted) it would be essential to make sure that the changes were statistically relevant, i.e. measuring replicates by injecting the same sample several times. What could also help in this part of the experiment is the use of an internal standard that could confirm the comparability of the measurements in terms of *rt*, mass accuracy, integrated area. Other things to consider would be isobaric masses, ionisation states and isomers, as at that stage of the project the premise essentially was that structures with the same mass and the same *rt* were the same compound. Thus, shifting these experiments to MSMS might be very insightful e.g. in the case of isomers with close *rt*.

A possible solution would be moving the MS analysis from HPLC to UPLC. This would reduce measuring times and would potentially solve the problem of not being able to see full peak disappearance of the electrophile upon addition of the nucleophile as NLS could be used. After consultation, it became clear that in order to make any

assessment of the small changes observed in the chromatograms, it would be necessary to average them out over several measurements, $n \geq 6$. This would increase the measuring time considerably, even with a method transfer to UPLC.

4.3 *In Situ* Detection by MSMS Methods

MSMS approaches were investigated in parallel with the experiments detailed in the previous chapter. Mentioned briefly in Chapter 1.2.3.1 of the Introduction, MSMS enables additional scan modes. In this chapter, the potential use of PIS and NLS are investigated.

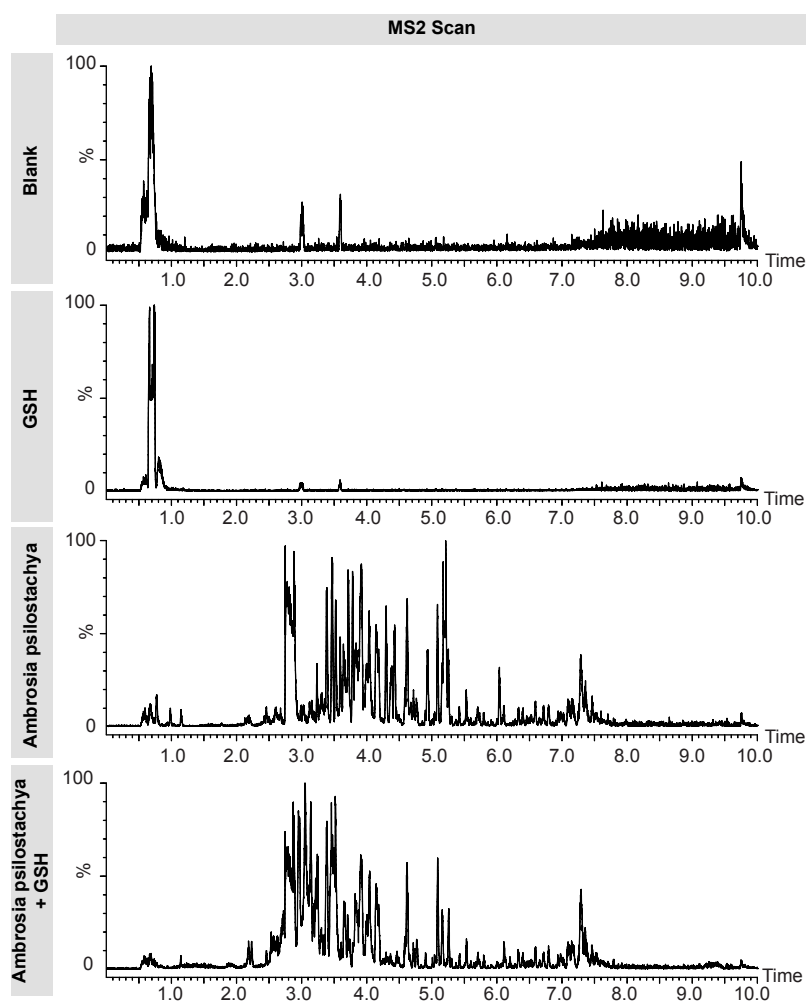


Figure 4.5 MS2 Scan of the samples. HPLC-MS traces (positive ion mode) were recorded with a scan range m/z 121-1000. Intensity scaled to max peak.

GSH is a commonly used molecule for conjugation reactions, thus MSMS fragmentation of GSH conjugates have been reported²⁹⁴. In positive mode, GSH is reported to undergo a neutral loss of pyroglutamic acid (loss of 129 Da)²⁷³. In negative

mode, and a fragment ion of m/z 272 is lost, corresponding to deprotonated γ -glutamyl-dehydroalanyl-glycine²⁹⁵. An experiment was devised to test the applicability of these methods with the instrumentation available (Chapter 2.2.6.3).

In this experiment, a blank sample, GSH, *Ambrosia psilostachya* extract, and a mixture of *Ambrosia psilostachya* and GSH were measured in MS2 Scan (Figure 4.5) and then subjected to NLS (Figure 4.6) and PIS (Figure 4.7), tuned to the fragments previously stated. These experiments were performed on a UPLC system under HPLC conditions, which enabled the shorter run time.

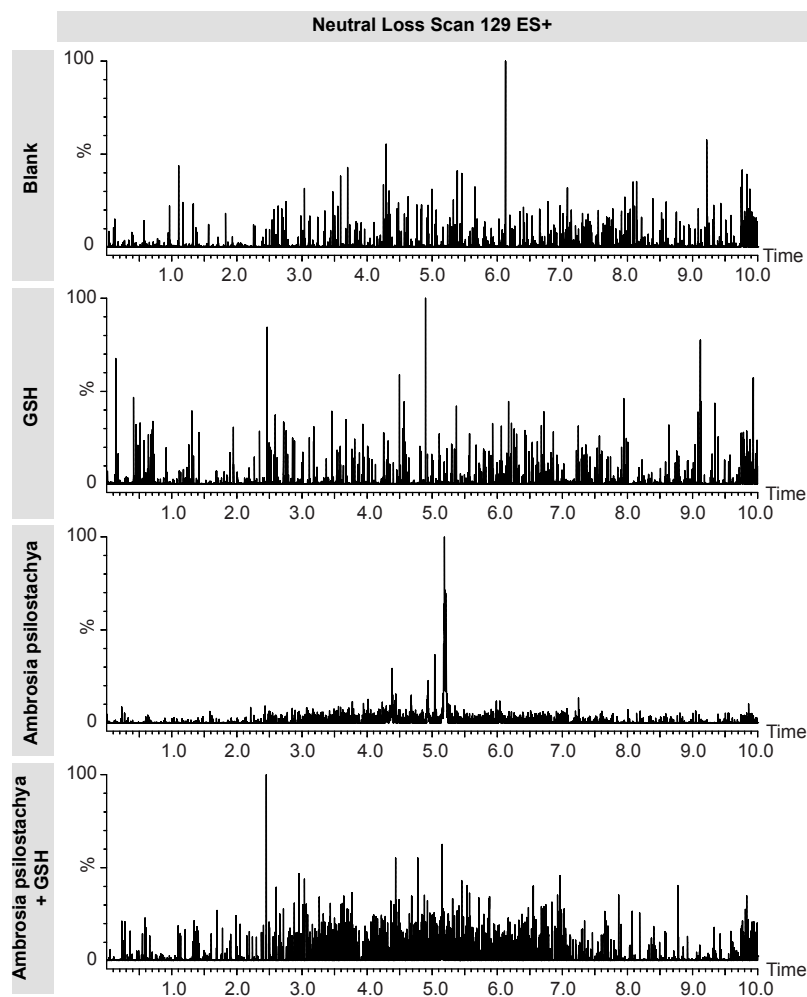


Figure 4.6 NLS for the fragment 129 ES+ of the samples. HPLC-MS traces (positive ion mode) were recorded with a scan range m/z 131-1000. Intensity scaled to max peak.

The MS2 Scan data showed that peaks from the chromatogram shifted to an earlier rt upon reaction with GSH (Figure 4.5), same as the experiments in the previous chapter (Figure 4.4). NLS of the same samples only showed noise with the exception of the unreacted *Ambrosia psilostachya* extract (Figure 4.6); neutral loss could be

observed at rt 5.19 min. This is interesting as no GSH was in this sample, thus this must be the result of a fragment formed by extract endogenous substances. The *Ambrosia psilostachya* and GSH containing sample did not show any peaks in NLS.

At the same time as recording NLS, PIS was also recorded (Figure 4.7). Unlike in NLS, the PIS spectrum of GSH showed GSH elution around rt 0.78 min. Furthermore, there seemed to be an accumulation of signal intensity in the *Ambrosia psilostachya* sample which was shifted to an earlier rt in the *Ambrosia psilostachya* mixed with GSH sample. These signals, however, were not clear and thus not very useful in the further investigation of electrophiles in this extract.

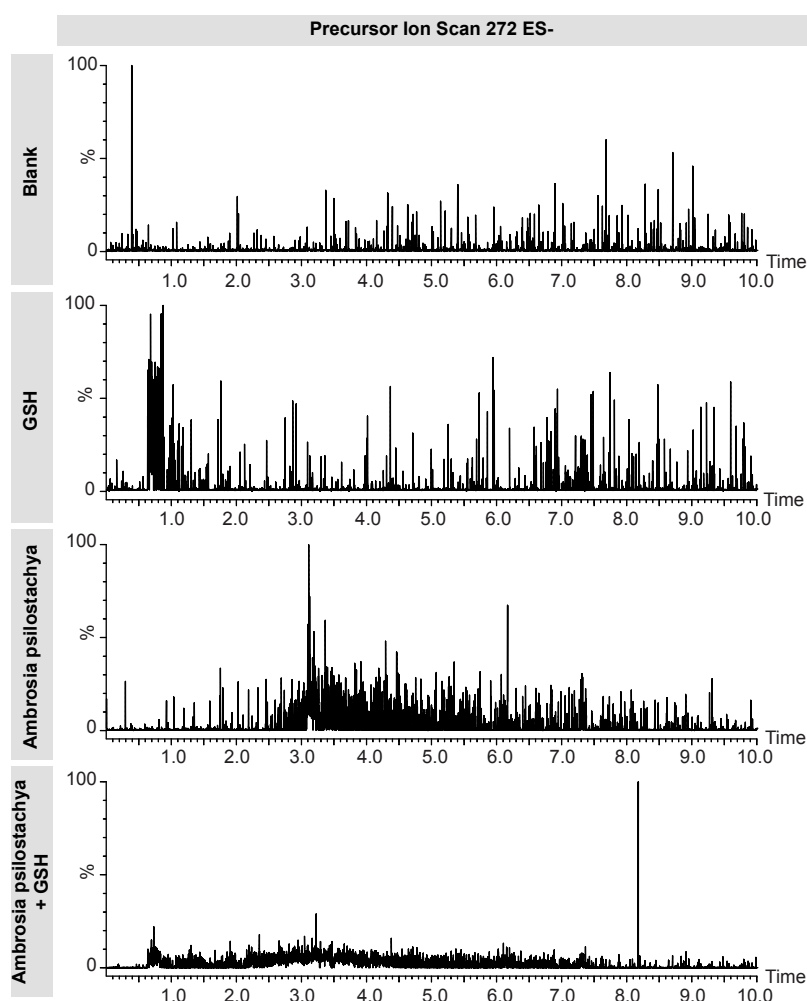


Figure 4.7 PIS for the fragment 272 ES- of the samples. HPLC-MS traces (negative ion mode) were recorded with a scan range m/z 103-1000. Intensity scaled to max peak.

4.4 Conclusions

This chapter illustrated the different approaches that were examined in the context of *in situ* detection with one model compound, GSH. Another model compound, NAC, was also investigated, but the results were similarly inconclusive. The main problem that had been identified was the fact that the spectra were difficult to deconvolute as extracts are complex mixtures and the reactive compounds might be minor compounds. Additionally, it was very likely that structural confirmation of reacted electrophiles would be required in the future, which meant that purification of either electrophiles from a pre-reaction sample or adducts from a post-reaction sample would be unavoidable. Provided the reactive compounds in each extract sample amounted to 1-2 mg in each extract sample and these were, at the time of purification, still present inside a complex extract mixture, purifying pure compound would be very difficult. The next chapter will address the approach that was investigated next, namely affinity tag-assisted electrophile detection and purification.

Chapter 5 Affinity Tag-Assisted Electrophile Detection and Purification

5.1 Introduction

As *in situ* methods did not prove to be successful due to the complexity of the samples, tag-assisted electrophile pull-down was investigated as the next step. It was recognised that due to the small amount of active electrophilic content, purification could become very difficult and structural confirmation would be required. The idea was that the nucleophile could be a tagged probe with properties that would allow a subsequent purification step selective for formed adducts. This was the first attempt to link detection and purification in order to minimise the loss of compound.

5.2 Probe Design

Affinity tag-assisted purification is commonly used in biochemistry for protein isolation after recombinant protein expression²⁹⁶. Over the years, many different approaches have been developed in order to facilitate the purification process. Some already established methods could be adapted for the use in this project. A probe that would be useful within the scope of this project would contain a suitable affinity-tag linked to a moiety with a nucleophilic centre for reaction. Since the tag would have to be designed and assembled *de novo*, the probe could be designed specifically for this project. Ideally, the nucleophile would consist of three sections: a nucleophilic section for reacting with electrophiles of interest, a section that enables targeted purification, and potentially a linking section that connects the two aforementioned parts (Figure 5.1). This chapter will address each element of the probe in turn before revealing the final probe design.



Figure 5.1 Elements required for probe design.

5.2.1 Affinity Tag

There are many different ligands used in affinity chromatography which are each specialised to retain a different type of target molecule. Many of these methods were

optimised for specific uses that were not relevant for this project. Therefore, only two of the affinity tags that are commonly used will be discussed, namely the biotin and the poly-histidine tag.

Both of these tags have specialised, commercially available resins and columns; the biotin tag can be retained on immobilised avidin or streptavidin, and the poly-histidine tag can be retained by immobilised nickel-nitrilotriacetic acid (Ni-NTA). The retention is achieved by different interactions. The biotin-avidin/streptavidin interaction involves multiple hydrogen bonds and van der Waals interactions that allow biotin to be buried inside the protein²⁹⁷⁻²⁹⁸. The poly-histidine tag is retained on Ni-NTA supports due to chelation to the Ni²⁺ ions (Figure 5.2). Biotin was commercially available whereas poly-histidine could not be purchased in a project-relevant form.

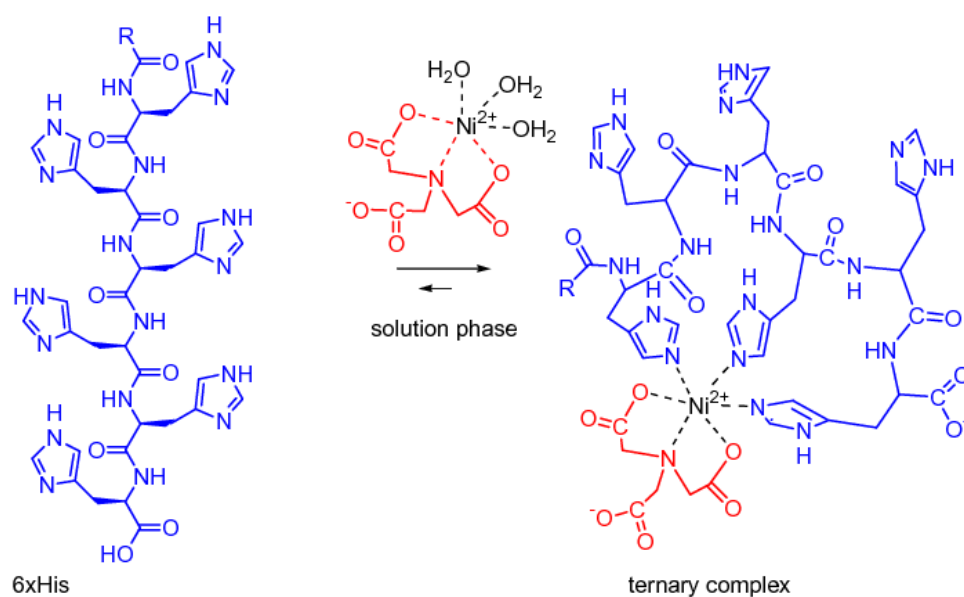


Figure 5.2 Ni-NTA interaction with a poly-histidine tag. Reproduced with permission²⁹⁹, copyright Elsevier.

5.2.2 Linker

The affinity tag and the probe could be directly covalently bound to each other without a specific linking moiety binding them. This, however, could be a missed opportunity, as the linking section could serve as more than just as a connector between the nucleophilic and the purification part – it could be designed as a cleavable linker.

The reason why a cleavable linking section would be beneficial was that the affinity tag could be cleaved from the adduct after affinity purification. Both the biotin and the poly-histidine tag suggested in the previous subchapter are very bulky tags that could

complicate an NMR analysis post-purification. If the affinity tag could be cleaved off, the only remaining part attached to the electrophile would be the nucleophilic centre and potentially a remainder of the cleavable section.

5.2.3 Nucleophilic Centre

The intention was to remain with a nucleophile that is physiologically relevant, such as GSH. Since the body utilises soft cysteine-bearing nucleophiles, and the nucleophilicity of GSH is also linked to its cysteine building block, the reactive moiety could be a cysteine residue or another thiol nucleophile. The nucleophilic moiety would have to be already part of the molecule that could be selectively purified or synthetically introduced into the molecule.

5.2.4 Probe Structure Considerations

Weighing in all the earlier ideas and considerations from the previous subchapters, a final structure for pilot studies needed to be decided on. This subchapter will discuss the deliberations that were made to decide on the final structure.

Biotin was considered as affinity tag. It possesses a carboxylic acid moiety that can be functionalised with a nucleophilic centre. Since the process of functionalisation could potentially be cumbersome, options that were commercially available were researched first. Thiolated biotin polyethylene glycol (PEG) derivatives and biocytin, which is the amide formed from biotin and lysine, were found as potential candidates. Both of these options were rather expensive at the time, so they were dismissed.

The other tag that was considered was poly-histidine. A commonly used number of histidines for a poly-histidine tag is six, a tag that is also called a hexa histidine(6His)-tag. Although not commercially available, its synthesis was possible via SPPS, which could also be used for the incorporation of a nucleophilic centre. Thus, it was decided to work with a 6His-tag for the design of this nucleophilic probe. Since 6His could not be readily bought as a tag, it needed to be synthesised.

The next step was deciding on a nucleophilic centre. Remaining close to physiological nucleophiles, like GSH, the obvious choice for a small molecule that could be incorporated was cysteine. Cysteine is an amino acid and could be easily attached to the 6His-tag in the same SPPS process. Furthermore, it is the most nucleophilic amino acid and therefore in line with the previously tested nucleophiles GSH and NAC.

Having determined both the affinity tag and the nucleophilic centre, there was the possibility to include a linking moiety. It was also possible to skip a potential linker entirely and to bind the 6His-tag directly to cysteine, which would give H₂N-HHHHHHC-OH (C6His). The resulting short nucleophilic peptide made for an interesting design choice, as GSH is a peptide as well. The other option was to include a cleavable linker. Staying faithful to the peptidic design, aspartic acid could be introduced between the 6His-tag and cysteine as a guiding motif for enzymatic cleavage. Endoprotease AspN could be used to cleave aspartic acid N-terminally to release bound adducts without the 6His-tag, e.g. In H₂N-HHHHHHDC-OH (CD6His), AspN would cleave 6His. It was decided that before investigating the possibility of a cleavable linker, the concept of using an affinity tag needed to be tested first by synthesising and testing a simple test peptide.

Alternatively to C6His, the peptide structure H₂N-CHHHHHH-OH could be synthesised, with cysteine bound N-terminally instead of C-terminally. Cysteine would have an adjacent electron-withdrawing group regardless at which terminus of the histidine chain it would be placed; thus, the assumption was made that the difference in the pK_a of the thiolates of the two possible structures would be similar. Another idea was to mimic the situation in GSH, i.e. a reactive cysteine situated not at a terminus, but inside the peptide chain. This idea was dismissed for two reasons: i) this would not be compatible with building in a cleavage site for removal of the 6His-tag in the future and ii) the steric hindrance caused by the histidine side chains could make the thiolate less reactive.

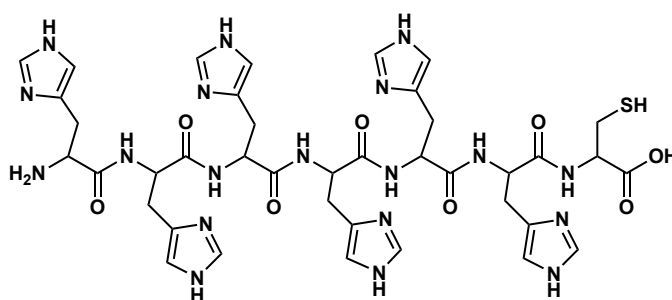


Figure 5.3 C6His Structure.

Finally, it was decided to synthesise C6His (Fig 5.3) as a first test peptide and investigate CD6His at a later stage.

5.3 Nucleophilic Peptide Probe Pilot Study

SPPS was used for the synthesis of C6His, and also a control peptide, 6His. 6His was designed as a negative control to account for nonspecific binding with the histidine residues. These two peptides would be used as crude test peptides to quickly assess whether this approach was feasible at all. Once a test had confirmed this could be a valid method for electrophile detection, purified CD6His would be used for the actual pilot study that would also test the affinity purification and the tag cleavage.

The Liberty Blue peptide synthesiser used for SPPS utilises the Fmoc synthetic strategy. This synthetic strategy is now the most commonly used one in small scale SPPS, as it proceeds at milder conditions than the previously discovered Boc strategy³⁰⁰. The Fmoc strategy utilises Fmoc-protected amino acids in order to achieve consecutive chain extension with amino acid building blocks from C- to N-terminus. SPPS uses a solid support to enable consecutive reagent additions and washes in a facile manner. After each coupling step, the Fmoc-protected N-terminus of the newly coupled amino acid building block is deprotected for the next coupling, until full chain extension is achieved. During this whole process, reactive side chains need to be orthogonally protected in order to prevent side reactions. After the last coupling, the side chains are usually deprotected in the same step as the

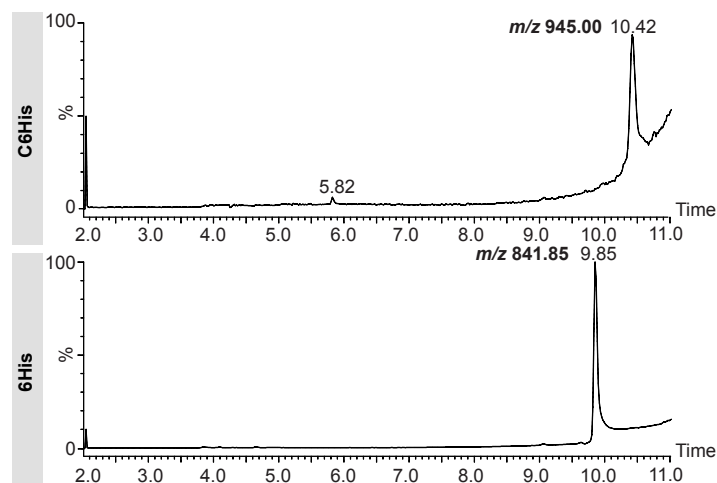


Figure 5.4 Injection of C6His and 6His post-synthesis. HPLC-MS traces (positive ion mode) were recorded using selected ion recording mode.

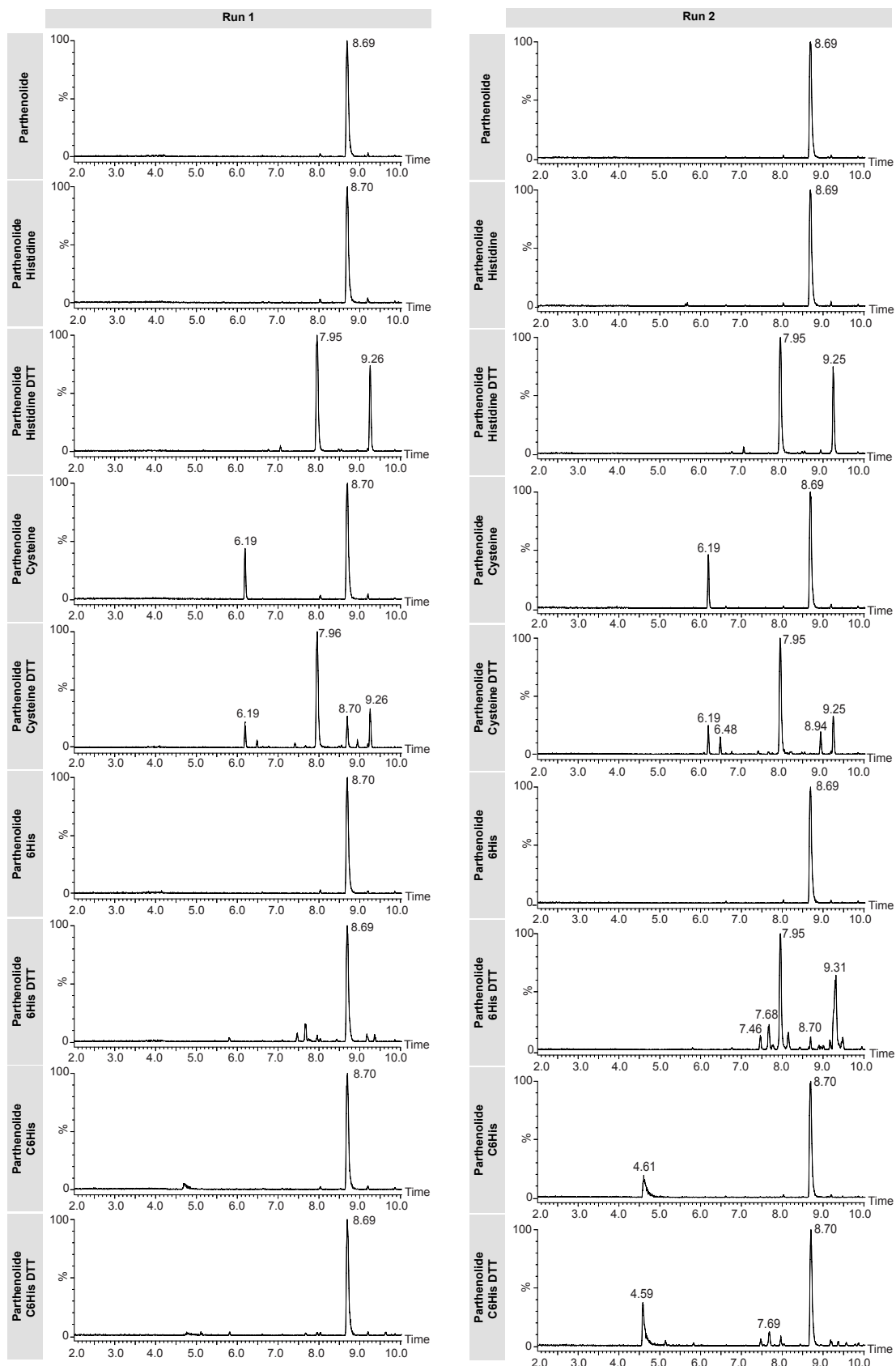


Figure 5.5 Parthenolide tests with L-histidine, L-cysteine, 6His, C6His with and without DTT. HPLC-MS traces (positive ion mode) were recorded with a scan range m/z 121-1900. Intensity scaled to max peak.

Chapter 5

cleavage from the solid support. For the synthesis of C6His, both cysteine and histidine needed to have Trt-protected side chains.

The peptides C6His and 6His were synthesised using the procedure detailed in Chapter 2.2.7.1. After peptide precipitation, the peptides were immediately used for a test without being lyophilised. Aliquots were weighed out to make a 5 mg/ml solution and were first injected on the Waters instrument to check whether the peptides synthesised had the correct mass (Figure 5.4).

The masses were confirmed to be m/z 945 and m/z 842 for C6His and 6His respectively. The peak at *rt* 5.82 min on the C6His chromatogram seemed to be the product forming an intermolecular disulfide bridge, giving the C6His-dimer. Based on this result it was decided to add DTT in subsequent tests. As a next step, both peptides were tested against the model compound parthenolide (Figure 5.5, left side; Chapter 2.2.7.2.1). Their constituent amino acids L-histidine and L-cysteine were tested in the same experiment.

Based on this analysis, it was concluded that the incubation time of 1 h was not enough, thus, the same samples were reinjected on the next day, to give the results shown in Figure 5.5, right side.

The parthenolide peak was found at *rt* 8.69 min with m/z 249 $[M+H]^+$. No reaction was observed with L-histidine. The L-cysteine parthenolide adduct could be found at *rt* 6.19 min and m/z 370 $[M+H]^+$. Further, the C6His-parthenolide adduct was found at *rt* 4.60 with m/z 1193 $[M+H]^+$ and m/z 597 $[M+2H]^{2+}$. There was a peak with m/z 420 and m/z 828 at *rt* 7.96 min which occurred in all the DTT-containing reaction mixtures, which led to the conclusion that this peak was likely caused by a reaction between parthenolide and DTT. It was unclear what product had formed. In the chromatogram with C6His, parthenolide and DTT, this peak was not so prominent, likely due to the competing reduction of C6His-dimer. Generally speaking, all the DTT-containing samples had fragment peaks in the area between 6.40 min and 9.40 min, which were hypothesised to be due to unwanted side reactions occurring in the presence of DTT.

As this experiment showed promising results for the reactivity of C6His and also showed no adduct formation for 6His, it was decided to move forward and synthesise CD6His as well (Chapter 2.2.7.2.2). CD6His was purified on a semi-preparative system to give 31.6 mg peptide. The peptide was again injected into the Waters system to see whether purity was achieved (Figure 5.6).

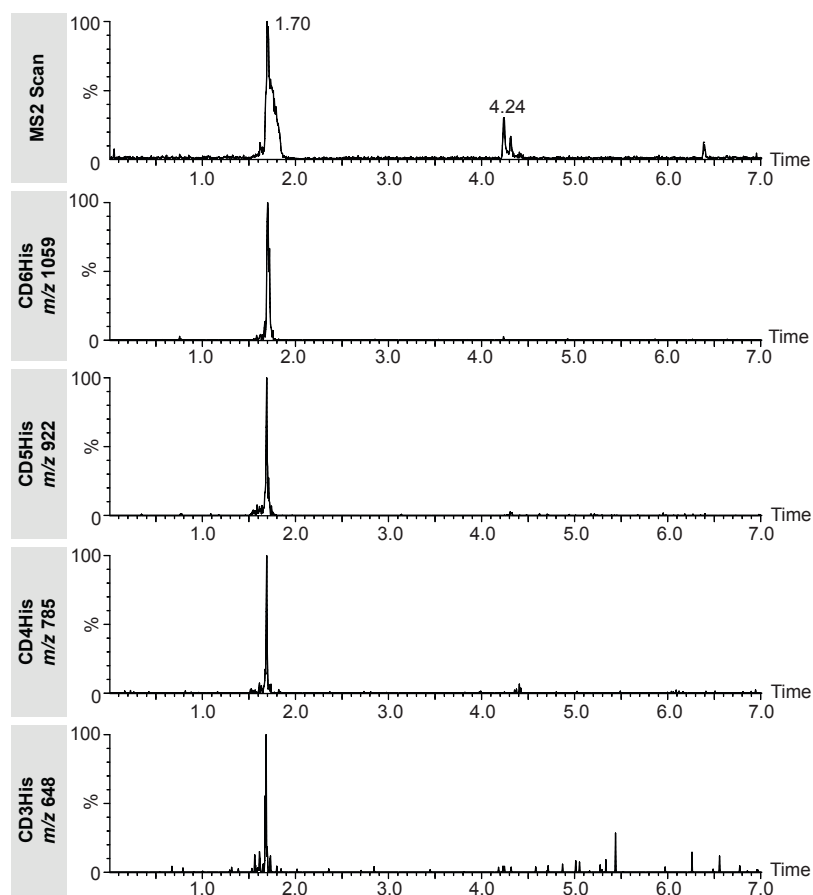


Figure 5.6 Quality control of CD6His. Different mass extracts corresponding to the CD5His, CD4His and CD3His were generated for this chromatogram. HPLC-MS traces (positive ion mode) were recorded with a scan range m/z 121-1900.

At first it seemed that the peptide degraded since the peak was not sharp. The conditions under which the peptide was synthesised and handled, however, were standard conditions, so this seemed unlikely. After examining potential side reactions or side products of the synthesis, it was discovered that the additional peaks were not caused from degradation but caused by the synthesis itself. Whilst it was attempted to synthesise CD6His, CD5His and CD4His were also part of the product mixture. This is attributed to the fact that coupling histidine consecutively is problematic due to the steric bulk of both the extending chain and the incoming amino acid building block. This steric hindrance makes each coupling step not 100 % effective, leaving some chains unextended and thus giving the shorter peptide chains like 5His and 4His as side products. Purification of CD6His was attempted but due to the very close *rt*s and no observable separation, this was not further pursued.

5.4 Conclusions

This section of the thesis examined the possibility of using a nucleophilic peptide probe that could form adducts with electrophiles and be selectively purified. Whilst this seemed like a promising way to link detection and purification, this part of the project was aborted due to the inability of synthesising the nucleophilic peptide and the control peptide in a pure manner in order to properly conduct a proof-of-concept experiment. Another reason why this method development approach was halted was because a more promising lead was discovered, which will be discussed in Chapter 6.

Chapter 6 Solid-Supported Nucleophilic Probe Development and Optimisation

6.1 Introduction

In the exploratory experiments with the nucleophilic peptide probe CD6His, synthesising the pure histidine chains remained a roadblock to properly conduct a proof of concept experiment. During a discussion on the strategy moving forward, the idea of taking advantage of the resin beads used in SPPS surfaced. The idea was that instead of coupling a nucleophile that could be retained on a column, the nucleophile could be tethered onto a solid support, such as a resin bead. Immobilising a nucleophile on solid-support by using resin beads for SPPS would have the following advantages: i) the captured electrophiles would be linked to a solid, thus unreacted compounds can be easily washed off and ii) in many resin beads for SPPS there is an in-built peptide release mechanism that we could utilise to release reacted electrophiles.

6.2 Solid-Supported Nucleophilic Probe Design

For the design of the immobilised probe, as with the previous nucleophilic peptide approach, we needed to decide on three separate parts for the design: a section that enabled targeted purification, a linking section that connected and could be cleaved, as well as a nucleophilic section for reacting with electrophiles of interest. These sections could also be termed anchor, linker and probe (Figure 6.1). Unlike in the previous peptide design, the linking section of the solid support needed to be cleavable. The following subchapters will discuss the individual sections of the solid-supported nucleophilic probe.

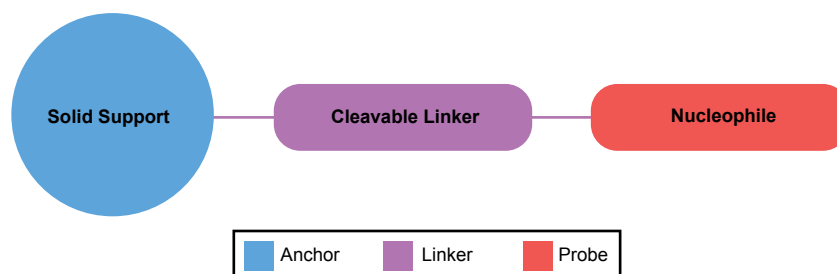


Figure 6.1 Solid-supported nucleophilic probe design.

6.2.1 Anchor

In this solid-supported probe, the section that enabled the targeted purification was the polymer aggregate used in SPPS. This polymer aggregate will be addressed as 'resin' for discussion in this thesis. A commonly used resin is polystyrene, which was also used for all the previous syntheses of nucleophilic peptide. The only factors that are important for a solid support are chemical stability and reactive inertness, which are both characteristics of commercially available polystyrene resins.

6.2.2 Linker

Commercial resins are manufactured for the use in SPPS, thus already have an in-built chemical release mechanism which is triggered upon addition of a cleavage cocktail. Standard resins used in Fmoc strategy SPPS are cleaved with TFA-containing cocktails. Therefore, building this cleavage mechanism *de novo* was not required, as it was possible to choose among options offered by commercially available resins. A standard resin used for the SPPS of the nucleophilic peptide is the rink amide resin, which has a polystyrene and PEG core connected to Rink Amide linkers (Figure 6.2A). The recommended cleavage cocktail for this resin is TFA/TIS/H₂O/dioxa-1,8-octane-dithiol (92.5/2.5/2.5/2.5).

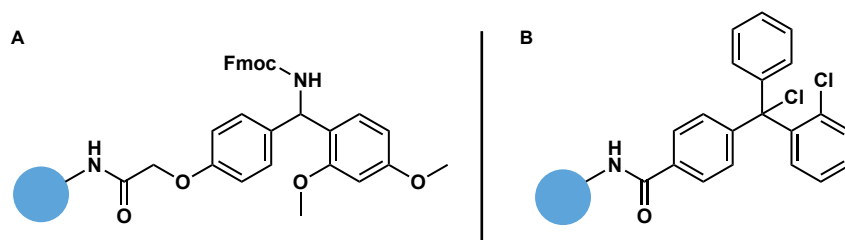


Figure 6.2 Linker structures, drawn as found on the supplier website of CEM. The polystyrene core and PEG linkers are not shown and represented by the bead. **A:** Rink Amide ProTide Resin; **B:** Cl-TCP(Cl) ProTide Resin.

Whilst these cleavage conditions are tolerated by peptides, they are too harsh for natural product adducts. This is why in this case we opted for a linker with milder cleavage conditions: a trityl linker containing resin, Cl-TCP(Cl) ProTide Resin, was chosen, which can be readily cleaved with 1 % TFA (Figure 6.2B) and was also previously used for the synthesis of the nucleophilic peptide.

6.2.3 Probe

As for the nucleophilic probe, it was decided to keep cysteine as the nucleophile, resulting in the following final product Cys-TCP (Figure 6.3).

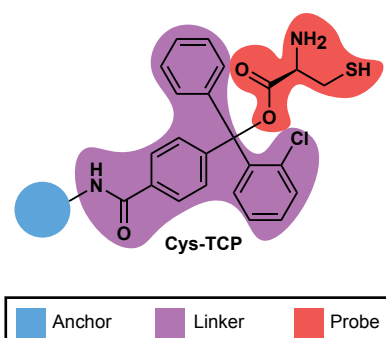


Figure 6.3 Structure of the cysteinyl probe immobilised on solid support.

6.3 Solid-Supported Nucleophilic Probe Pilot Experiment

6.3.1 Solid-supported Cysteinyl Probe Synthesis

Cys-TCP would be synthesised using the Fmoc synthetic strategy. The standard cysteine building block for Fmoc-protected synthesis is Fmoc-Cys(Trt)-OH. The Trt-protecting group protects the reactive thiol side chain of cysteine and only cleaves at high percentages of TFA. Usually, the Trt-protecting group is cleaved at the same time as the peptide is released from the resin.

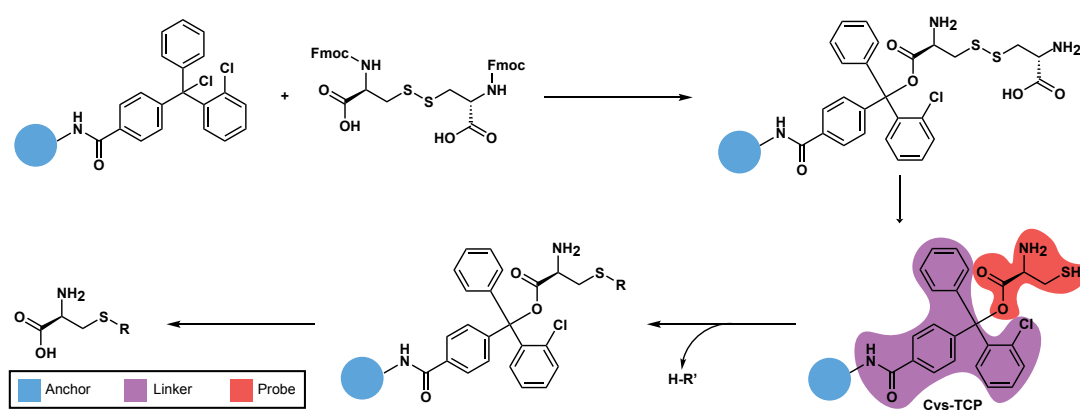


Figure 6.4 Strategy for the synthesis and application of Cys-TCP.

For our purposes, however, a different protecting group was required that could be cleaved separately and under milder conditions than 1 % TFA in order to not break the trityl linker. In search of a suitable building block for the incorporation of cysteine,

Fmoc-protected cysteine dimer, (Fmoc-Cys-OH)₂, was found. This molecule features Fmoc-protected N-termini essential for the Fmoc synthetic strategy and a disulfide bridge that protects the thiol groups. The disulfide bond can be easily and orthogonally cleaved with a reducing agent. The following strategy for the synthesis and application was devised (Figure 6.4).

The scheme shows the coupling of (Fmoc-Cys-OH)₂ to the Cl-TCP(Cl) ProTide Resin, giving cysteine dimer-coupled resin 'protected Cys-TCP' which is then activated to form 'reactive/activated Cys-TCP'. Reactive Cys-TCP then can be used for the capture of electrophiles and release of cysteine-electrophile adducts.

The first step was to synthesise protected Cys-TCP by SPPS. Cl-TCP(Cl) ProTide Resin has a dedicated technical note by the manufacturer CEM, detailing how to best use it for synthesis. The recommendations of CEM were generally followed (Chapter 2.2.8.1). The only change that had to be made was concentration of the reagent (Fmoc-Cys-OH)₂. This compound was not soluble at the recommended concentration of 0.2 M and was therefore halved to 0.1 M. A 0.1 mmol batch of protected Cys-TCP was synthesised for each sample in the pilot experiment.

6.3.2 Solid-Phase Extraction (SPE) Set-Up

A pilot experiment was devised to test the concept and determine the practical details for the use of Cys-TCP. Knowing that repeated washes would be required, the experiment was designed to be carried out in SPE cartridges. In this way, the solid resin beads would be kept inside the cartridge while solvent and unbound species could be removed from the cartridge. Further, this set-up would allow multiple experiments in tandem, as the SPE vacuum manifold used featured 12 ports and each port could be used for a separate experiment. The addition of reagent and solvent would occur in a percolation-like manner, with solvent and reagent passing through the cartridge. It was assumed that the application of reduced pressure by a vacuum pump might be necessary to obtain the samples with sufficient speed; this, however, was not found to be the case, and all the samples were generated without the application of reduced pressure.

The samples to be analysed in a first pilot experiment were a blank, parthenolide, atropine and a mixture of parthenolide and atropine. The blank would enable assessment of what peaks are present even without sample present. Parthenolide, a reactive electrophile, was chosen as positive control for the reactivity of Cys-TCP.

Atropine, a non-electrophilic compound, was chosen as negative control. The mixture of both parthenolide and atropine was also tested in order to assess whether the resin could react selectively with parthenolide in the presence of non-reactive atropine. The steps (i)-(vii) were planned ahead (Table 6.1).

Table 6.1 Pilot experiment outline, showing the samples A-D and the procedure steps (i)-(vii).

	Sample	(i)	(ii)	(iii)	(iv)	(v)	(vi)	(vii)
A	Blank DMSO	THF wash	MeOH wash	Deprotection with 2 M 2-BME in MeOH and wash	Incubation and subsequent wash with THF	Wash with MeOH	Cleavage with 1% TFA in MeOH and subsequent MeOH wash	Wash with THF
B	Parthenolide 5 mg/ml in DMSO							
C	Atropine 5 mg/ml in DMSO							
D	Parthenolide + Atropine 5 mg/ml in DMSO respectively							

Steps (i) and (ii) served to wash the protected Cys-TCP and remove residual DMF left from the synthesis. Step (iii) was the activation step in which the cysteine dimer was reduced with 2-BME to give activated Cys-TCP. A MeOH wash was performed after the reduction with 2-BME to remove any 2-BME and cleaved cysteine present. Step (iv) was the incubation with sample, followed by a wash with THF to remove any unreacted compound. Step (v) was another wash with MeOH. Step (vi) was the cleavage with 1 % TFA in MeOH, followed by a wash with MeOH. Step (vii) was a final wash with THF to confirm all the cleaved product was washed off. The experiment was conducted as described in Chapter 2.2.8.2.1. The results of the experiment are shown in Figure 6.5 and Figure 6.6.

It was observed that in the experiment with parthenolide, a peak was visible at *rt* 6.14 min with *m/z* 274 after incubation, and another two peaks were found in the sample after cleavage from the resin at *rt* 5.38 min and *rt* 5.55 min with *m/z* 231/249 and *m/z* 370 respectively (Figure 6.5, right side). The peak with *m/z* 370 [M+H]⁺ corresponded to the parthenolide-adduct. Both the mass, which was the molecular ion of parthenolide (*m/z* 249) with an *m/z* increase of +121 corresponding to the mass of cysteine, and the observed *rt* (5.55 min) corresponded to previous measurements in Chapter 5.3. The other two peaks, however, could not be assigned. It was not known what the source of the peak at *rt* 6.14 min with *m/z* 274 was, perhaps

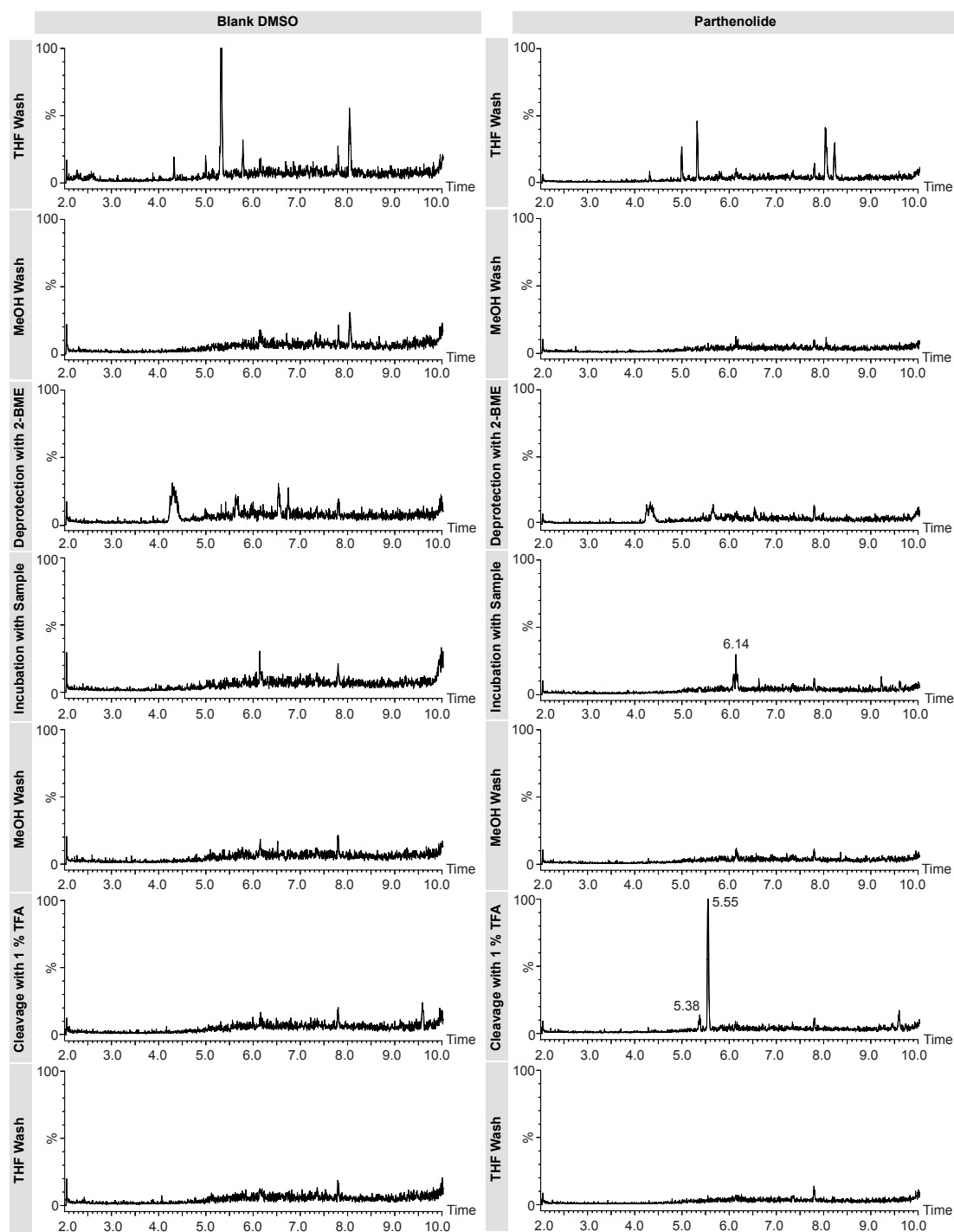


Figure 6.5 HPLC-MS data from the first pilot experiment. Left: data from the experiment with blank DMSO, chromatograms scaled to $8.5E6$; right: data from the experiment with parthenolide, chromatograms scaled to $1.5E7$. HPLC-MS traces (positive ion mode) were recorded with a scan range m/z 121-1000.

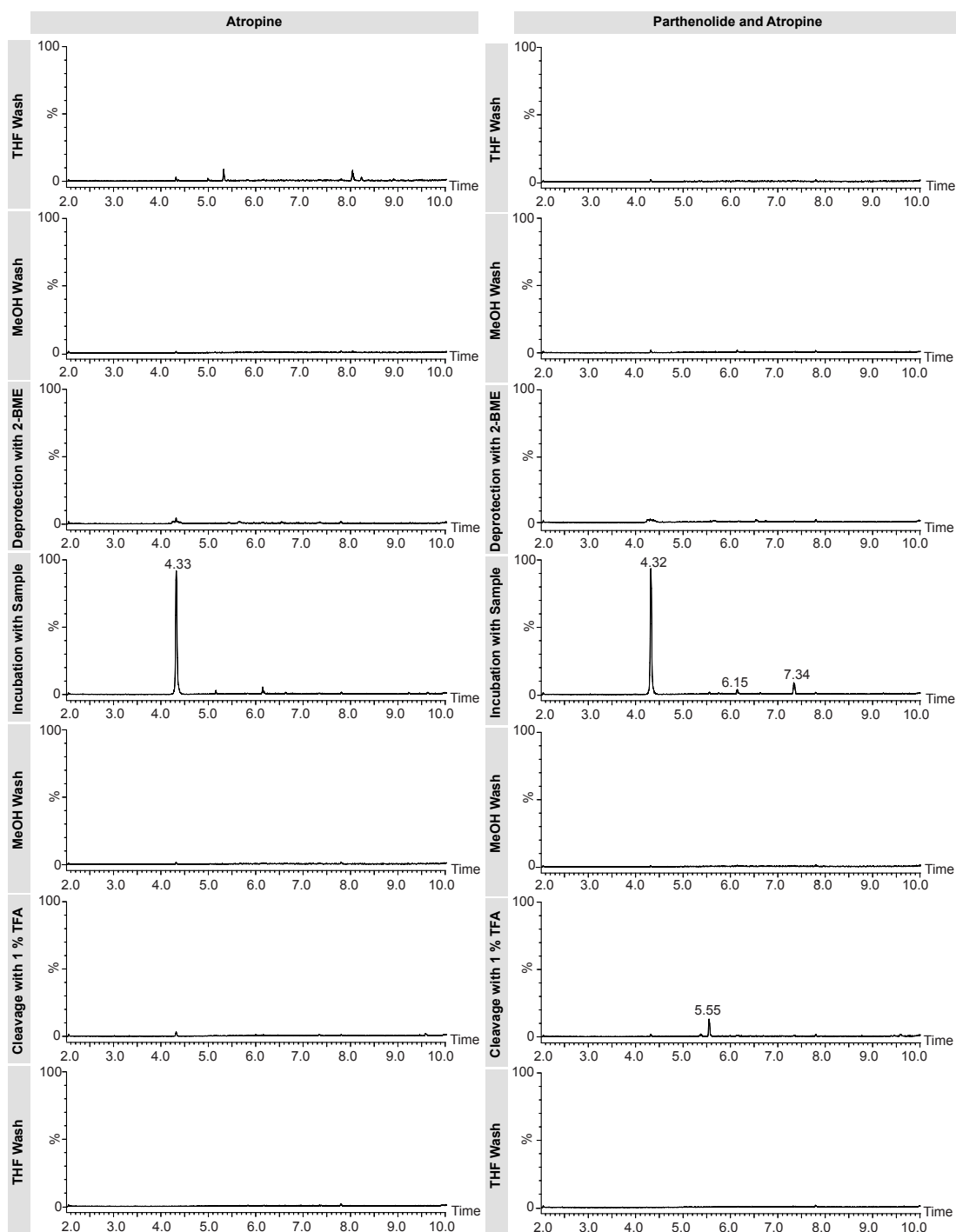


Figure 6.6 HPLC-MS data from the first pilot experiment. Left: data from the experiment with atropine, chromatograms scaled to $1.0E8$; right: data from the experiment with parthenolide and atropine, chromatograms scaled to $1.0E8$. HPLC-MS traces (positive ion mode) were recorded with a scan range m/z 121-1000.

it had occurred due to a contamination. As for the peak at 5.38 min with m/z 231/249, m/z 249 would correspond to the $[M+H]^+$ mass of parthenolide, however, parthenolide should elute later than the adduct, which indicates that this peak is likely something

different. The experiment was repeated with parthenolide to confirm that these peaks were not a by-product of contamination (Chapter 6.3.3).

In the experiment with atropine, one peak was visible at *rt* 4.33 min with *m/z* 290. No other peaks were visible in subsequent samples, which was consistent with the hypothesis that atropine does not react with Cys-TCP.

In the experiment with the mixture of parthenolide and atropine, after incubation, three peaks were visible at *rt* 4.32 min, *rt* 6.15 min and *rt* 7.34 min, with *m/z* 290, *m/z* 274 and *m/z* 349 respectively. *M/z* 290 corresponded to the $[M+H]^+$ mass of atropine, *m/z* 274 appeared to be the same peak as previously observed in the experiment with parthenolide and *m/z* 349 is a mass that had not been previously observed and also could not be rationalised. In the sample after cleavage, a peak was observed at *rt* 5.55 min with *m/z* 370 which corresponded to the $[M+H]^+$ of the formed parthenolide-adduct.

In conclusion, this experiment gave interesting insights into how Cys-TCP can be incorporated into the method. Although a parthenolide peak was not observed, a peak of its formed adduct was in the sample after the cleavage step. In general, there seemed to be an issue with the parthenolide aliquot that was used in this experiment as masses were observed that were not expected and not explained. Therefore, this experiment had to be repeated with a fresh aliquot. Atropine proved to be a valid negative control.

6.3.3 Purification of Parthenolide-Adduct

The experiment with parthenolide needed to be repeated for two reasons: i) the confidence in the previously obtained data was not high, as unexpected and unexplained *m/z* values were observed in the mass spectrum, and ii) we wanted to isolate the parthenolide-adduct in order to know where binding of the cysteine occurred. Furthermore, the quantity previously used was not sufficient for purification. Based on the *m/z* observed, it seemed that cysteine added to parthenolide through nucleophilic addition, resulting in a mass increase of 121 Da. It was suspected that this addition proceeded via the exomethylene group of parthenolide.

At that point, a change of solvents was considered, as well as testing different protocol parameters to see their effect. In addition, higher quantities of resin and test compound had to be used for isolation. The method described in Chapter 2.2.8.2.2 was followed and the following data was obtained (Figure 6.7)

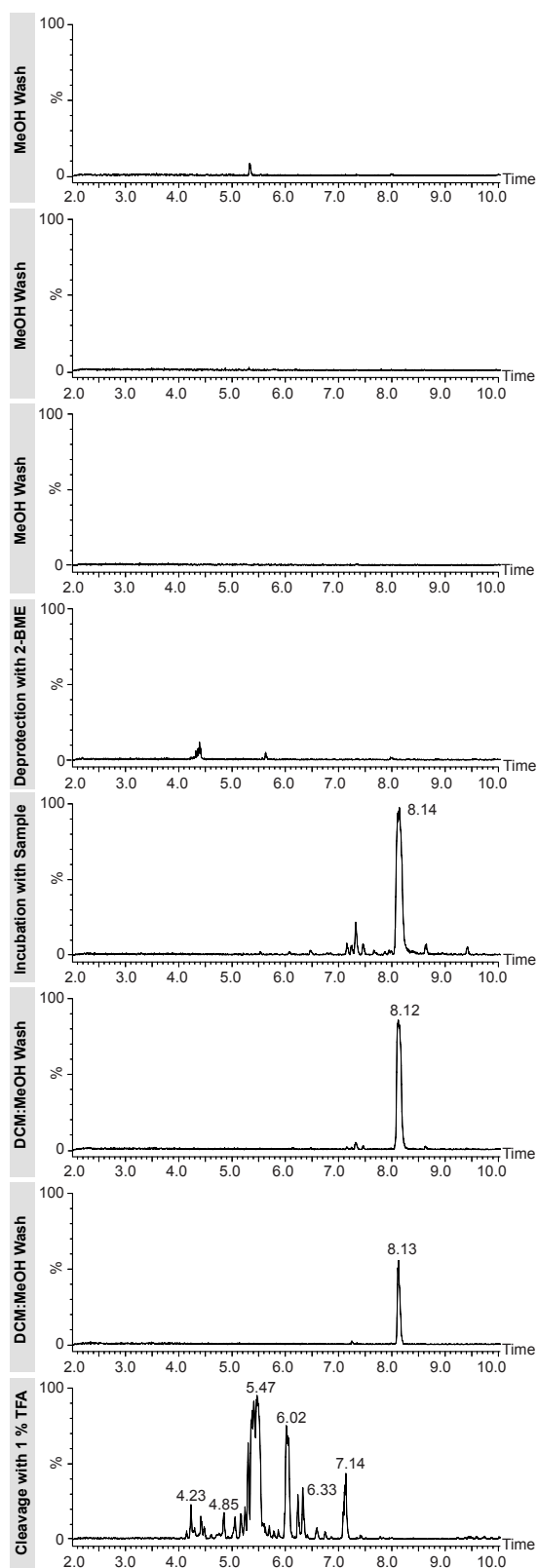


Figure 6.7 HPLC-MS data from the add-on experiment for the pilot experiment, chromatograms scaled to 1.0E8. HPLC-MS traces (positive ion mode) were recorded with a scan range m/z 121-1000.

The parthenolide peak was found around *rt* 8.23 min with *m/z* 249. This *rt* was different than observed in the previous experiment. This was in agreement with the hypothesis that there had been a contamination in the parthenolide aliquot used in the last experiment. Additionally, major differences were observed in this experiment: i) the solvent mixture of DCM:MeOH apparently had difficulties washing out the remaining parthenolide after the incubation step and ii) there were a number of peaks with *m/z* 370, the expected mass, in the sample after the cleavage with 1 % TFA. This was unexpected since only one product was anticipated, namely an adduct with cysteine bound to the exomethylene group. The adducts were purified in order to find out more about their nature and determine why so many adducts were formed. Purification was performed on a semi-preparative HPLC-UV-MS system as described in Chapter 2.2.3.2 to give the following separation profile (Figure 6.8).

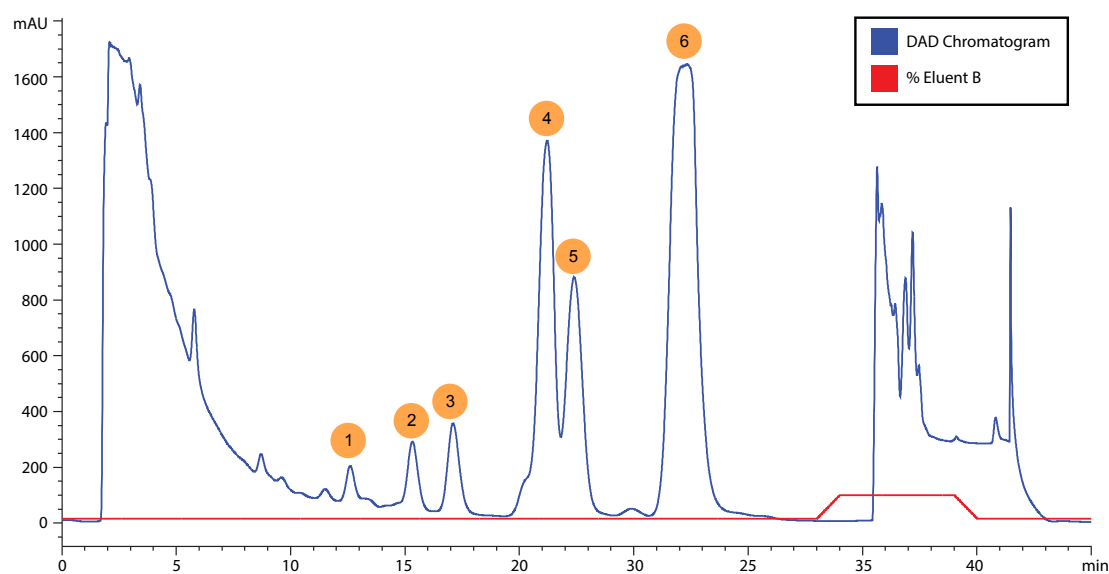


Figure 6.8 HPLC-UV trace of a semi-preparative purification of parthenolide adducts from the pilot Cys-TCP experiment, released by treatment with 1 % TFA in MeOH. PDA trace, max plot displayed in graph. The peaks that were isolated are marked 1-6.

The adducts were collected and NMR spectra in DMSO- d_6 were recorded (Figure 6.9). From the NMR spectra, it was gathered that addition had in fact occurred at the exomethylene position as originally had been predicted; however, some other change had occurred in the parthenolide structure. Searching through published literature of parthenolide, it was found that Castañeda-Acosta and Fischer had previously described Lewis acid-initiated rearrangements of parthenolide, resulting in six different products³⁰¹. The release of formed cysteine-adducts had occurred in the

presence of Lewis acid, 1 % TFA. The use of TFA could have caused the

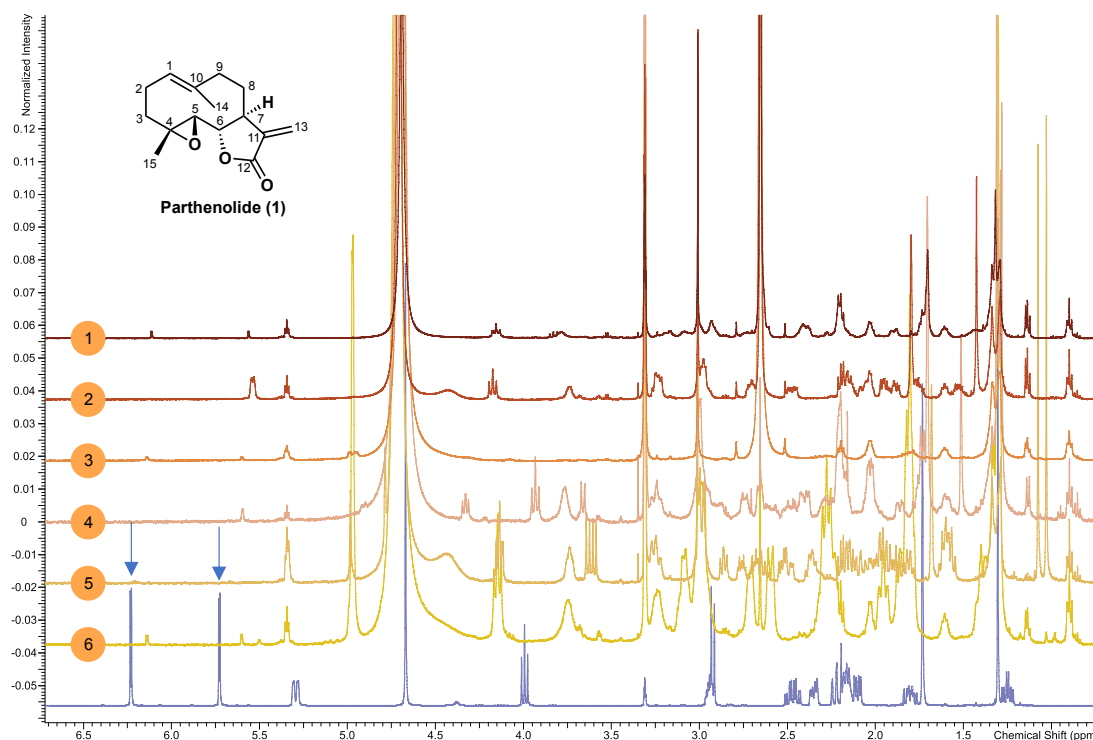


Figure 6.9 ^1H NMR spectra in DMSO- d_6 of isolated peaks 1-6 in Figure 6.8, in comparison to the ^1H spectrum of unreacted parthenolide (spectrum at bottom, blue). The signals at 5.73 and 6.23 ppm corresponding to the exomethylene protons at C-13 (marked with an arrow) disappear in the product spectra.

rearrangement of the only parthenolide-adduct that was formed initially, in order to give six rearranged products with cysteine bound at the site where the exomethylene group used to be. This explanation was plausible, so in future optimisation steps the cleavage conditions needed to be adjusted in order to prevent any Lewis acid-induced rearrangements from happening.

6.3.4 Spectroscopic Quantification of Cysteine

Quantification of cysteine was an important step as we had no other method to confirm whether the coupling of the resin with the Fmoc-protected cysteine dimer had worked and or how many activated Cys-TCP sites were actually available for reaction with electrophiles. The intention was to quantify the amount of liberated cysteine from the 2-BME reductive step using a spectroscopic method similar to the one used in Chapter 3.4. The formerly used protocol with Ellman's reagent for the quantification of electrophiles, however, was an indirect quantification of electrophile content. This time, the analytes that needed to be quantified were not electrophiles, but cysteines. Therefore, NAC was used for the calibration curve instead of parthenolide, and the

whole method was adapted as described in Chapter 2.2.8.2.3 in order to directly quantify the amount of cysteines.

In the indirect quantification method, the highest point in the calibration was represented by 200 μ l NAC (0.429 mg/ml in MeOH). All the other calibration curve points had a lower cysteine concentration, since they are reduced by reaction with the calibration curve standard for electrophilicity, parthenolide. For a direct quantification method, the concentration of NAC directly correlates to the concentration of reacted Ellman's reagent in solution and thus the coloured side product. This meant that a calibration curve could be directly constructed by increasing and decreasing the concentration of NAC. Furthermore, TEA could be removed completely from the procedure since it was previously used to facilitate the reaction between NAC and reactive electrophiles in solution. The aggregate data from three separate runs is shown in Figure S.6, the associated multiplate reader data can be found in Table S.2 of the Appendix. Judging by the plotted data, this adapted assay was not suitable for the quantification of cysteine. The linear regression curve had an R^2 value of 0.95 and the samples that were measured were at the limit of quantification. Therefore, the cysteine quantification method had to be adapted.

6.3.5 Learnings from the Pilot Experiment

The pilot experiment showed that the concept of using a solid-supported nucleophilic probe was promising. The Anchor-Linker-Probe concept was tested and was shown to be successful. Adduct formation with the model compound occurred as predicted, and the release mechanism was found to work, although the cleavage conditions resulted in the rearrangement of the formed adduct. The SPE set-up enabled processing of several samples at once and the cartridge system combined with the resin beads allowed sequential washes and reagent additions and facile collection of eluates. Further, the quantity of released cysteine in the reduction step with 2-BME could not be determined by using an adapted version of the assay with Ellman's Reagent; it was clear that the reduction step was successful based on the chromatograms obtained from the experiment, but in order to quantify the active Cys-TCP sites, a new method for quantification needed to be established.

6.4 Method Optimisation

After the first pilot experiment, there were a number of details in the procedure that needed to be further optimised or changed completely before settling on a procedure for future experiments. These optimisation steps will be discussed in this chapter.

6.4.1 Adjustment of Cleavage Conditions

First and foremost, the cleavage conditions needed to be adjusted (Chapter 2.2.8.3.1). The cleavage conditions that were used in the pilot experiment resulted in the rearrangement of parthenolide, which indicated that 1 % TFA was too harsh. This meant that alternative cleavage options for the linker needed to be testing. Literature research revealed that trityl linkers may also be cleaved using HFIP:DCM (1:4 v/v)³⁰². Following this lead, an experiment was conducted to test these conditions on the Cys-TCP (Figure 6.11).

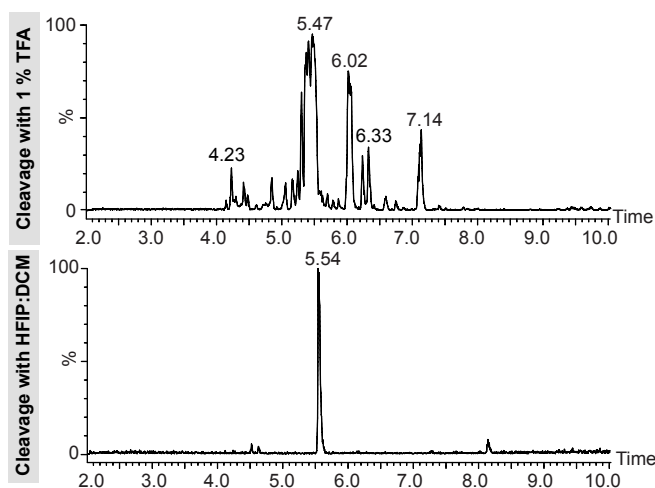


Figure 6.11 Comparison of the samples after cleavage using 1 % TFA (top) and HFIP:DCM (1:4 v/v) (bottom). Intensity scaled to max peak. HPLC-MS traces (positive ion mode) were recorded with a scan range m/z 121-1000.

Unlike in the previous experiment, only a single adduct was formed with m/z 370. Purification and NMR analysis (Table S.3) of this parthenolide adduct revealed that the site of reaction in fact was indeed at the C-13 position of parthenolide, resulting in a disappearance of the proton signals of the exomethylene group (Figure 6.12). This was consistent with reports from literature indicating that the most reactive site of parthenolide is the exomethylene group²⁵⁰.

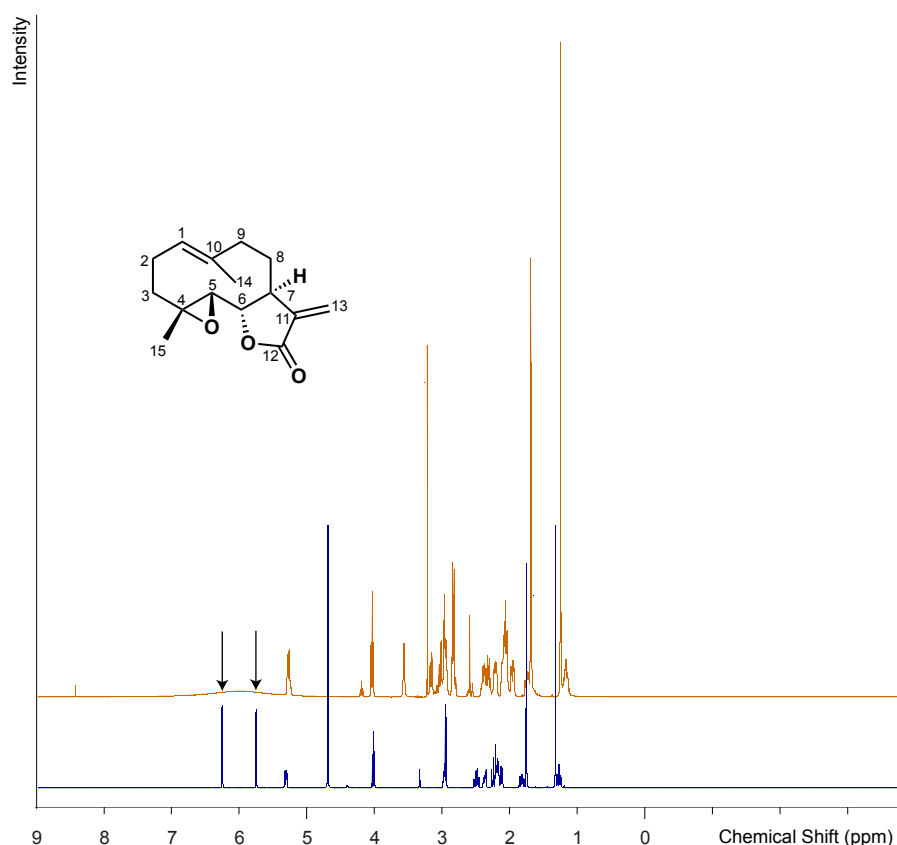


Figure 6.12 Disappearance of the C-13 exomethylene group ^1H signals in ^1H NMR.

In conclusion, HFIP:DCM (1:4 v/v) would be used for the proof-of-concept experiment as it was found to be a more suitable cleavage condition than 1 % TFA in MeOH for the cleavage of cysteine-adducts of natural products, as it did not result in the Lewis acid-induced rearrangement of parthenolide.

6.4.2 Wash Solvent Optimisation

In the previous pilot experiment, the wash solvents were THF and MeOH. THF was chosen because the extracts to be tested in the future were THF extracts, and MeOH was selected in order to have a polar wash. Both solvents were chosen as a starting point to conduct a pilot experiment, but needed to be re-evaluated. It was decided to keep MeOH as a polar wash but replace THF with a more suitable solvent. In the experiment that was performed with MeOH and a mixture of DCM:MeOH (Figure 6.7), the washes did not remove compound in the same manner as in the initial pilot experiment (Figure 6.5). It was unclear whether this happened due to the solvents used, their volume, or due to the flow rate of the washes. In both previous experiments, the flow rates were not recorded, so this, additionally to solvent identity,

needed to be tested. The experimental details for this can be found in Chapter 2.2.8.3.2.

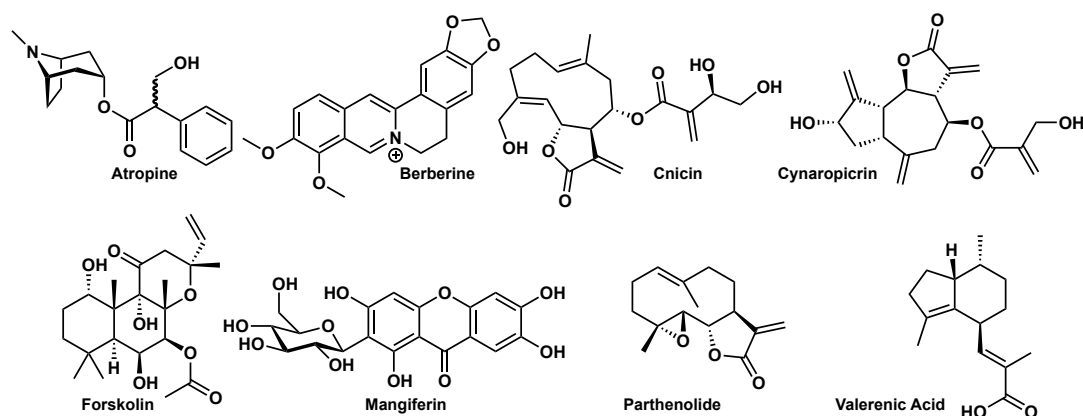


Figure 6.13 The structures of atropine, berberine, cnicin, cynaropicrin, forskolin, mangiferin, parthenolide and valeric acid.

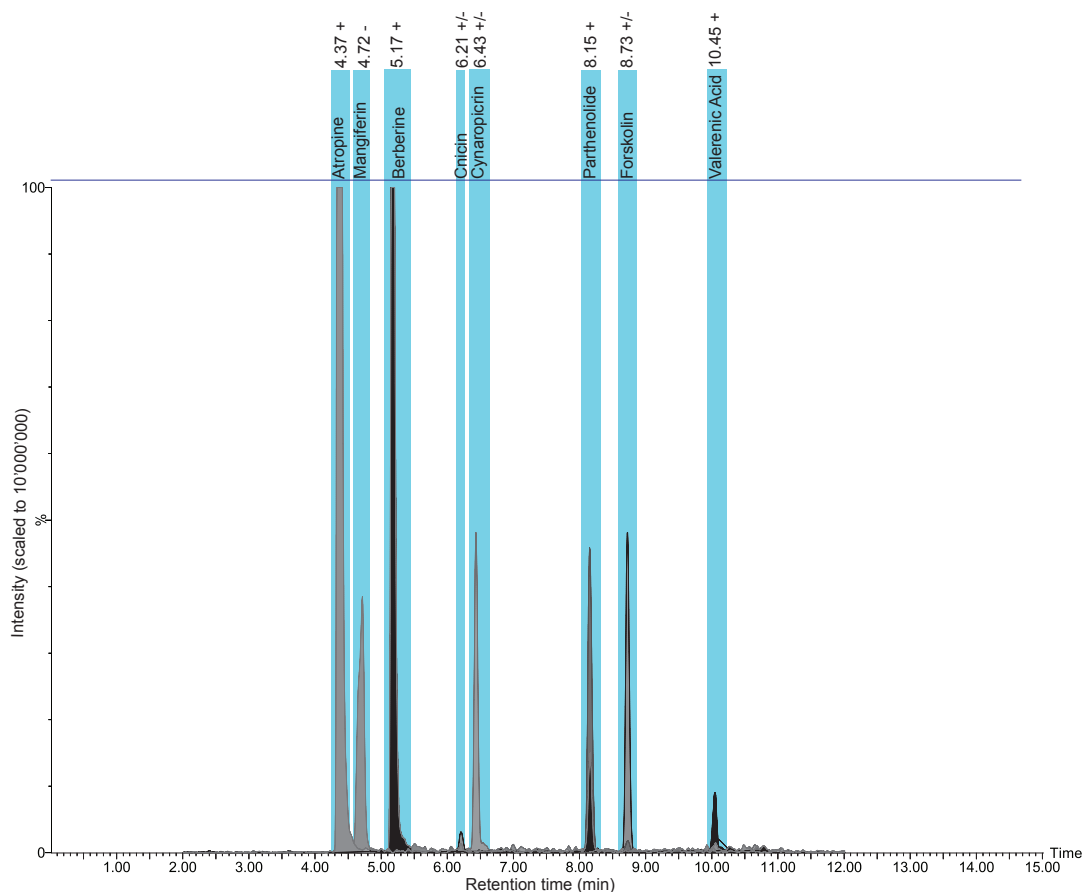


Figure 6.14 Assembled HPLC-MS traces of atropine, berberine, cnicin, cynaropicrin, forskolin, mangiferin, parthenolide and valeric acid. This chromatogram is an overlay of individual injections of each compound. Next to the peak assignment, the *rt* and which ionisation mode the compound can be visible in is indicated. ES- traces are shown for cnicin (m/z 377 [M-H]⁻), forskolin (m/z 409 [M-H]⁻),

Chapter 6

mangiferin (m/z 421 [M-H]⁻); ES⁺ traces are shown for atropine (m/z 290 [M+H]⁺), berberine (m/z 336 [M+H]⁺), cynaropicrin (m/z 227 [2M+H]⁺), parthenolide (m/z 249 [M+H]⁺), valerenic acid (m/z 235 [M+H]⁺).

The solvents DCM, hexane, acetone and ethyl acetate were tested. As the solvent was required to be able to elute a variety of different compounds, a mixture of eight compounds was assembled: atropine, berberine, cnicin, cynaropicrin, forskolin, mangiferin, parthenolide and valerenic acid (Figure 6.13). This compound mixture will be referred to as 'mixture of eight compounds' in the subsequent text.

These compounds were tested on HPLC-MS so that subsequent analysis of the solvent experiment would not be complicated by peak overlap (Figure 6.14).

Further, a preliminary experiment to determine the dead volume was designed in order to know how much solvent volume had to be loaded onto the cartridge for optimal overlap with the resin. Spiking DMSO with methylene blue gave the advantage that resin coverage by the analyte could be visually confirmed and the dead volume could be examined immediately. The approximate dead volume of a resin batch size of 0.1 mmol with loading capacity 0.52 mmol/g was determined to be 20 μ l for a sample dissolved in DMSO.

Since the dye was already loaded onto the resin in the cartridge, the differences in wash behaviour of DCM, hexane, acetone, ethyl acetate and MeOH were tested qualitatively. The solvent to be tested was added to the cartridge and left to percolate slowly until no more change could be observed. The behaviour was noted, then methylene blue was added to replenish the dye on the resin. Whilst all the other solvents tested struggled to remove the blue hue of the resin, DCM washed methylene blue out completely and returned the resin back to its original colour. Two additional striking observations were made: i) no channels could be observed in the packing of the resin and ii) the resin swelling changed with different solvents and when the solvent was DCM, the resin occupied the biggest volume due to its swelling and was visually observed to have the same size as in DMF. Conversely, when MeOH was the solvent, the resin bead size visually shrunk. In hexane, the resin looked almost 'dried out'; in acetone and ethyl acetate the resin beads had approximately the same size as in MeOH. The conclusions drawn from this were the following: i) swelling can change immensely depending on solvent, ii) hexane does not seem to be an ideal solvent due to its swelling properties, iii) the activation of Cys-TCP with 2-BME should occur before the packing of the cartridge, especially since 2-BME is added with MeOH and its swelling properties could affect the reaction if the resin is simply left to stand

without motion, and iv) the resin packing did not seem to be affected by swelling and de-swelling since no channels were observed, with the exception of hexane.

Next, the mixture of eight compounds was added the untreated resin in order to see which solvent would be the best to replace THF. The flow rates were controlled manually by twisting the cartridge port until a satisfactory flow was achieved. The times required for 10 ml of solvent to pass the resin-filled cartridge was recorded in order to calculate the flow rate (Table 6.2)

Table 6.2 Elution time range and flow rate ranges recorded for the experiment. The elution time indicates the fastest and the slowest elution time for each sample set which were then used to calculate the range of flow rates.

Wash	Elution time for 10 ml	Flow Rate Range(ml/min)
X1: MeOH (0)	12 min 17 s + 1 min 50 s	0.814 – 0.708
X2: MeOH (1)	19 min 52 s + 2 min 28 s	0.503 – 0.448
X3: Test Solvent (1)	18 min 4 s + 2 min 39 s	0.553 – 0.483
X4: Test Solvent (2)	21 min 27 s + 1 min 36 s	0.466 – 0.434
X5: Test Solvent (3)	13 min 56 s + 2 min 16 s	0.718 – 0.617
X6: MeOH (2)	9 min 12 s + 1 min 24 s	1.087 – 0.943
X7: MeOH (3)	13 min 10 s + 2 min 26 s	0.759 – 0.641

The samples were analysed by HPLC-MS (Figure 6.15). The following observations were made: i) the DMSO used for the reconstitution of the samples seemed to be contaminated with a peak around rt 7.20 min, confirmed by a blank; ii) there were no differences between the solvents, although there was an unidentified peak in the ethyl acetate wash at rt 9.49 min, perhaps due to impurities in the solvent; iii) as previously observed, hexane had a de-swelling effect on the resin that made it look dry and thus was excluded as a solvent replacement for THF.

As a conclusion, it was found the flow rate of the wash determined much of the quality of the wash. No nonspecific binding was confirmed for the resin, so most solvents should be able to draw out the compounds that the cartridge was subjected to. It was decided to perform future washes with MeOH and DCM at a flow rate of around 0.5 ml/min.

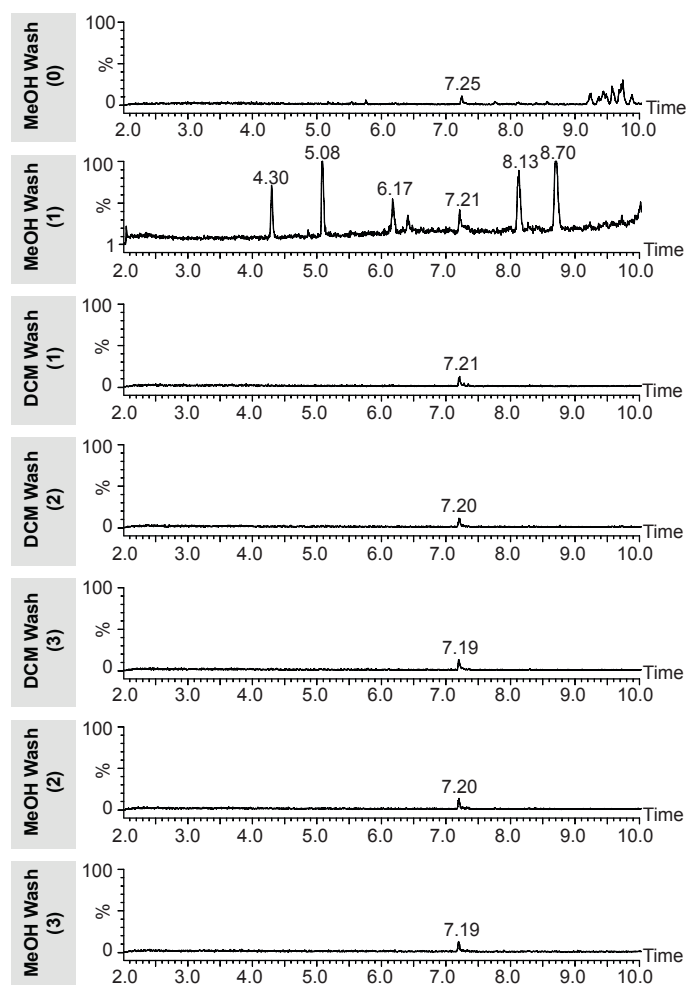


Figure 6.15 HPLC-MS data example of a solvent wash experiment, scaled to 5.0E6. HPLC-MS traces (positive ion mode) were recorded with a scan range m/z 121-1000.

6.4.3 SPE Set-Up

Up until now, the SPE set-up was used to conduct the experiment. The reagents were added in a manner that resembled percolation, and incubation was essentially letting the resin stand for an extended period of time with the reagent in solution. Adding an element of motion to the reaction mixture could potentially increase the rate of reaction by increasing the chances of collision of the reactants and ensure that every resin bead is equally exposed to the reagent.

The SPE vacuum manifold consisted of an SPE-stand that was fitted with ports with screw-type valves that served as connecting points for the SPE cartridges, and a glass container which held the tubes for the collection of elute and could be connected to a vacuum pump for the application of vacuum. The SPE-stand could be detached from the glass container. This meant that if magnetic stirrers were inserted into the SPE cartridges and the stand was moved on top of a magnetic stirrer plate, the resin

bead reagent mixture could be agitated. This had an additional benefit that dead volumes and resin bead packing no longer needed to be considered.

After checking that such a set-up would indeed be feasible by assembling it without any resin beads, it was decided to make use of magnetic stirrers in the experiment procedure in the future.

6.4.4 Quantification of Cysteine Residues as Quality Control

The experimental details for this subchapter can be found in Chapter 2.2.8.3.3. Previously, cysteine quantification was attempted using the adapted Ellman's procedure. The results for this experiment, however, were not convincing since the regression line was an R^2 value of 0.95 and generally departed from linearity (Figure S.6). Another way to achieve this quantification was to perform MRM quantification. Cysteine is a commonly used compound and was found to be the quantified analyte in a number of papers³⁰³⁻³⁰⁵. These papers quantified cysteine with a structural analogue as IS, methionine or NAC. It was attempted to use these compounds as IS for the quantification of cysteine (Figure 6.16 and Figure 6.17, Figure S.7 and Figure S.8, Table S.4 and Table S.5).

Compound name: Methionine
 Response Factor: 958.7
 RRF SD: 621.795, % Relative SD: 648581
 Response type: External Std, Area
 Curve type: RF

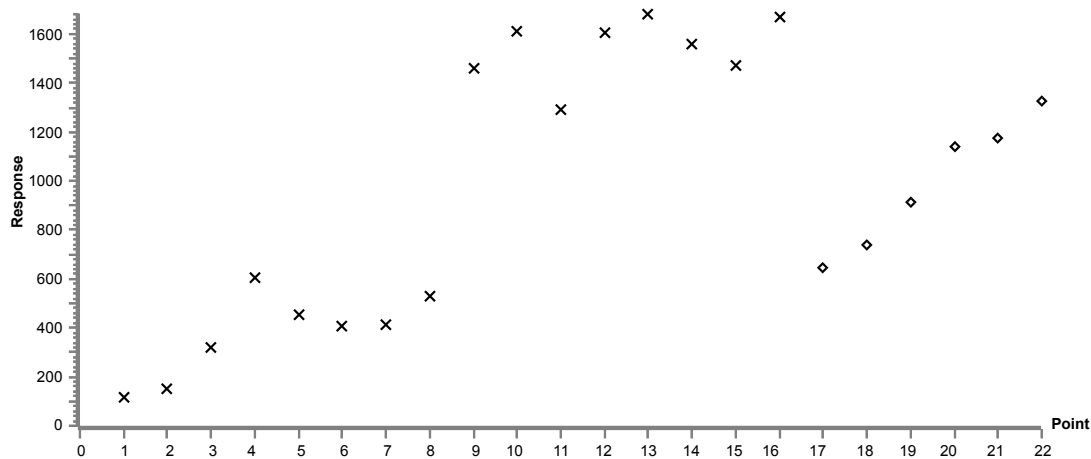


Figure 6.16 Methionine IS levels for calibration curve samples (crosses) and quality controls (squares).

Chapter 6

Compound name: N-acetylcysteine
Response Factor: 2589.27
RRF SD: 1187.74, % Relative SD: 45.8715
Response type: External Std, Area
Curve type: RF

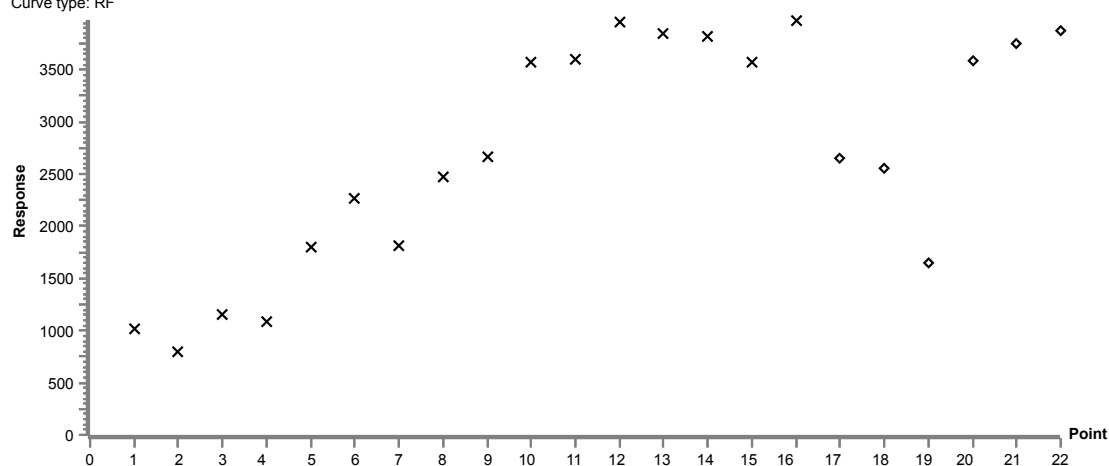


Figure 6.17 NAC IS levels for calibration curve samples (crosses) and quality controls (squares).

The IS levels of methionine and NAC were never stable, which was unexpected since the same IS had been used in literature. It seemed that in both the case of methionine and NAC, the IS levels both increased gradually until saturation was reached (Table S.4 and Table S.5). Finally, a non-structural analogue that also was known to not interact with cysteine was chosen instead: atropine (Figure 6.18 and Figure 6.19; Table S.6).

Compound name: Atropine
Response Factor: 241987
RRF SD: 11034.3, % Relative SD: 4.55987
Response type: External Std, Area
Curve type: RF

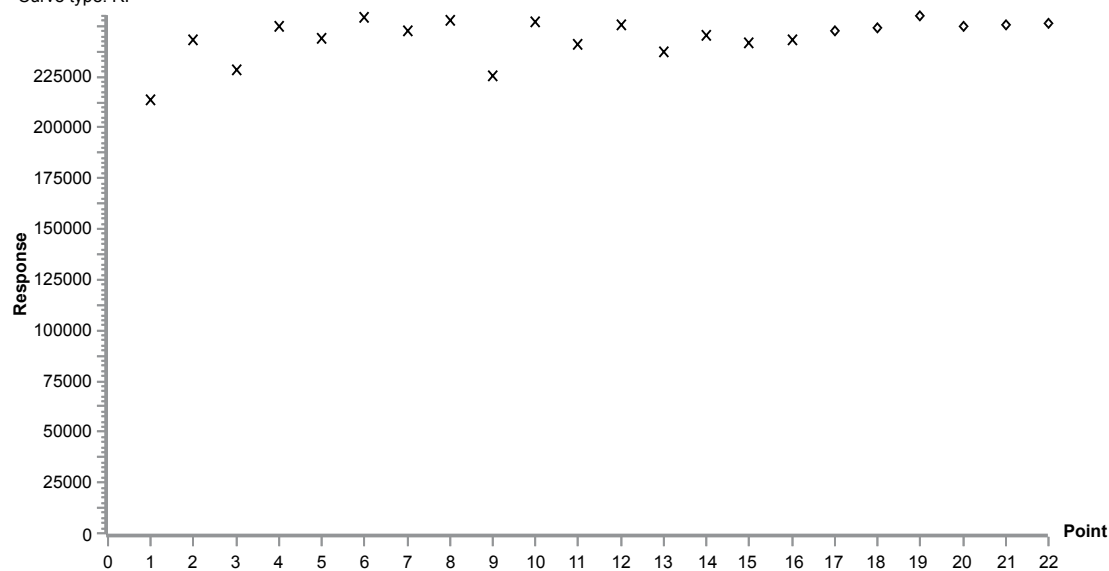


Figure 6.18 Atropine IS levels for calibration curve samples (crosses) and quality controls (squares).

Compound name: Cysteine
 Coefficient of Determination: $R^2 = 0.998577$
 Calibration curve: $-2.82417e-005 * x^2 + 0.010116 * x + -0.000674618$
 Response type: Internal Std (Ref 2), Area * (IS Conc. / IS Area)
 Curve type: 2nd Order, Origin: Include, Weighting: Null, Axis trans: None

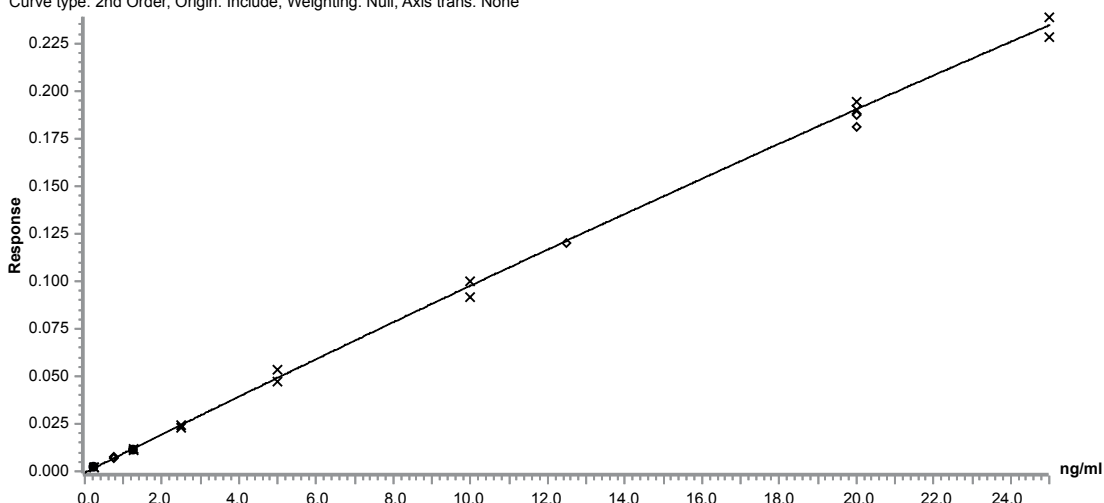


Figure 6.19 Calibration curve of the cysteine quantification experiment. The calibration curve samples are represented by crosses, the quality control samples as squares. R^2 value = 0.998577. Table with data points and standard deviations found in Table S.6.

Atropine gave stable IS levels and standardised the cysteine curve. This curve shows a satisfactory R^2 value, the associated data points showed acceptable standard deviation (standard deviation of each data point within $\pm 15\%$), and the quality control points were in range of the curve (standard deviation standard deviation of each data point within $\pm 15\%$), which meant that the quantification experiment was successful. Therefore, this method was used for quantification of cysteine-containing samples in the proof-of-concept experiment discussed in Chapter 6.5.

6.5 Proof-Of-Concept

The findings from method optimisation were consolidated in a procedure described in Chapter 2.2.8.4. This experimental procedure was followed for the proof-of-concept experiment described in this chapter.

As before, this proof-of-concept would test Cys-TCP (0.0750 mmol equivalent) against a blank (DMSO), parthenolide (positive control), atropine (negative control) and a mixture of parthenolide and atropine. All samples were used at half of the Cys-TCP stoichiometric equivalent (0.0375 mmol). Furthermore, alanine coupled to Cl-TCP(Cl) ProTide Resin (Ala-TCP) would be synthesised as a control for nonspecific binding caused by the resin beads. Ala-TCP would be tested against the a blank

(DMSO), parthenolide and atropine. The amounts were the same as in the Cys-TCP experiment.

One last part of this proof-of-concept experiment sequence was pulling out a small amount of parthenolide. For the previous experiments, an equimolar amount of compound to resin total loading capacity was tested, which, i) given that the true number of active sites on Cys-TCP was lower and can change between batch sizes and ii) since natural products tend to be present at much lower amounts, did not reflect what the method was intended for. This is why in this experiment 1 mg of parthenolide, as opposed to 9.3 mg (0.0375 mmol) in the previous experiment, would be used as a sample in order to see whether the method can succeed in detection, purification and NMR analysis of small amounts.

The samples of these experiments were analysed by HPLC-MS. The chromatograms for these experiments can be found in the Appendix as Figure S.9 to Figure S.12. The key findings will now be discussed with key chromatograms extracted from the figures in the Appendix.

First, the experiment between Cys-TCP and parthenolide will be discussed (Figure 6.20). The method procedure was changed to a sequence of three washes, the reduction step with 2-BME, incubation with sample, a wash to remove unreacted compounds, release of cysteine-bound adduct, and a wash to confirm everything had been washed out.

Based on Figure 6.20, the capture of parthenolide and the release of parthenolide adduct was successful. The adduct mass, m/z 370 $[M+H]^+$, was seen in at rt 5.55 min. The mass of parthenolide, m/z 249 $[M+H]^+$, was found in at rt 8.15 min both in the sample collected after incubation with the sample and also in the sample after the cleavage step, at rt 8.14 min. The wash performed between those two samples showed no peaks, therefore all the excess parthenolide from the incubation had been washed out. Any parthenolide found after the cleavage step must have been formed by the adduct via a retro-1,4-Michael reaction. This was supported by literature reporting that the retro-1,4-Michael reaction to parthenolide had been previously observed³⁰⁶.

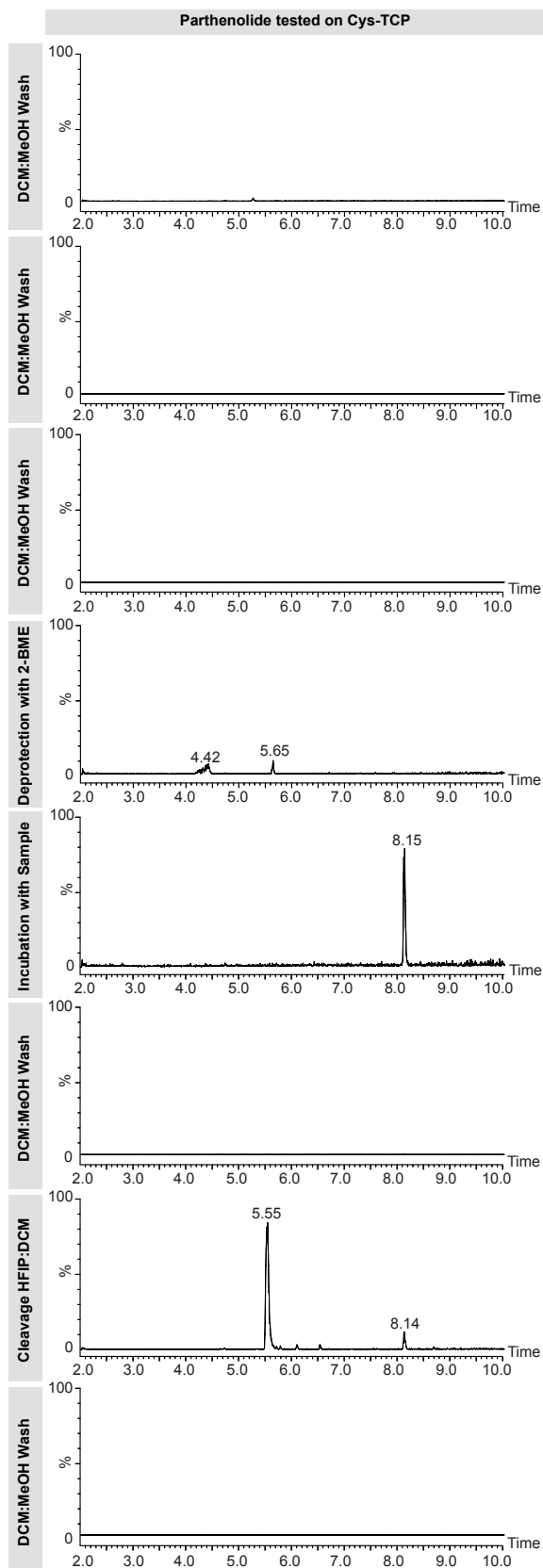


Figure 6.20 Experiment with Cys-TCP and parthenolide. HPLC-MS traces (positive ion mode) were recorded with a scan range m/z 121-1000.

Moving on to the other samples tested on Cys-TCP, the reactions with the blank sample, atropine and the mixture of atropine and parthenolide will now be discussed.

The sample reaction with the blank (DMSO) sample was performed in order to know which peaks were present when no compound was in the sample (Figure S.9, left side). The experiment did not show any notable abnormalities, besides confirming that the peaks at *rt* 4.41 min and *rt* 5.65 min were standard peaks in the reduction process with 2-BME.

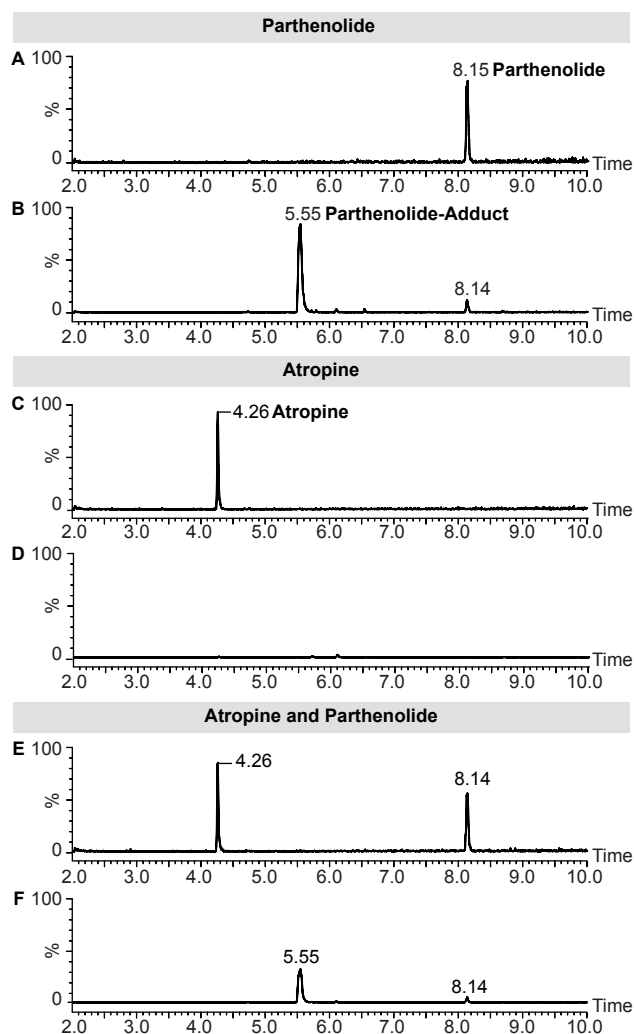


Figure 6.21 HPLC-MS traces of experiments with Cys-TCP and equimolar amounts of parthenolide (A and B, scaled to $1.0E8$), equimolar amounts of atropine (C and D, scaled to $9.0E7$), and equimolar amounts of a stoichiometric mixture of parthenolide and atropine (E and F, scaled to $3.6E7$). HPLC-MS traces (positive ion mode) were recorded with a scan range m/z 121-1000.

Figure 6.21 shows the chromatograms of the eluate from the incubation (Figure 6.21ACE) and the eluate from the cleavage step with HFIP:DCM (1:4 v/v) (Figure 6.21BDF) for the reactions with parthenolide, atropine and the mixture of atropine and

parthenolide. The two chromatograms from the previous parthenolide reaction in Figure 6.20 are shown again in Figure 6.21 in order to enable side-by-side comparison.

The negative control atropine did not react with the cysteinyl probe and eluted completely after incubation, as could be seen by the peak at *rt* 4.26 min in Figure 6.21C and the absence of peaks in Figure 6.21D.

In the reaction with Cys-TCP and the mixture of atropine and parthenolide, essentially a combination of the separate reactions with atropine and parthenolide occurred. Non-electrophilic atropine eluted without reaction, whereas electrophilic parthenolide reacted to give parthenolide-adduct, which was released after the cleavage. This confirmed that Cys-TCP selectively reacted with electrophiles like parthenolide, whereas non-electrophilic compounds like atropine were washed off after incubation. The full data for the experiments with Cys-TCP can be found in Figure S.9 to Figure S.10.

The full data for the experiments conducted with Ala-TCP can be found in the Appendix as Figure S.11 to Figure S.12. These experiments showed that any binding previously observed for the Cys-TCP experiments were not due to non-specific interactions of the resin, validating that binding via the nucleophilic cysteine was the only way in which molecules could be retained on Cys-TCP after incubation.

The last experiment in this series of proof-of-concept experiments was the experiment with 1 mg of parthenolide (Figure S.12, right side). In this experiment, no parthenolide eluted after the incubation step since all of the starting material had reacted with the resin. Parthenolide formed by retro-Michael-addition was observed at *rt* 8.14 min with *m/z* 249, and parthenolide-adduct was observed after the cleavage step at *rt* 5.55 min with *m/z* 370. Subsequent purification the sample yielded 1.5 mg of parthenolide-adduct which equated to complete conversion of starting material into adduct.

Lastly, for the experiments with Cys-TCP, the amount of cysteine released in the reduction step with 2-BME was quantified using the MSMS method. The yield was found to be 8.65 ± 2.65 % (Table S.6). This yield was rather low and could potentially be increased by further optimisation, e.g. by re-examining the reduction step with 2-BME and using the quantification method for yield monitoring. The results of this experiment served as quality control and were used to determine the quantity of Cys-TCP required for future experiments.

6.6 Conclusions

In this chapter, the potential of a solid-supported nucleophilic probe Cys-TCP was evaluated. Cys-TCP featured a reactive moiety that could be selectively activated, form adducts with electrophiles in a sample and then cleaved off selectively to release the formed adducts.

The probe was synthesised using SPPS and tested in a pilot experiment in an SPE set-up. This set-up facilitated consecutive washes and reagent additions to Cys-TCP and enabled removal of eluate for sample collection without having to disturb Cys-TCP. Purification of the adducts from the experiment was attempted, as was assessment of the amount of activated Cys-TCP by quantification of the released cysteines in the 2-BME reduction step. From analysis of this first pilot experiment, it was concluded that the method showed promise but needed optimisation. In the optimisation process, various aspects of the method were re-examined in order to streamline the process, resulting in the adjustment of the cleavage conditions, investigation of solvent effects, changing the SPE set-up and the MRM method development for the quantification of released cysteine with the IS atropine.

Having consolidated the findings of optimisation, a new method was assembled for experiments with Cys-TCP which formed the foundation for a series of proof-of-concept experiments. The proof-of-concept experiments demonstrated that the solid-supported nucleophilic probe worked as expected with positive and negative controls and excluded matrix effects by testing a non-reactive probe, Ala-TCP. Furthermore, it was demonstrated that Cys-TCP could also work with a small amount of reactive material.

The next step for this method would be the application on other compounds and extracts, which will be discussed in the next chapter.

Chapter 7 Application of the Cysteinyl Probe

7.1 Introduction

The previous chapter focused on the method development and the proof-of-concept experiment of the immobilised cysteinyl probe. This chapter will discuss the experiments that were conducted with the probe, starting tests with model compounds, then test with a model compound spiked into a test extract, and lastly the experiments with the pollen extracts that were discussed in Chapter 3.

7.1 Model Compounds

So far, Cys-TCP had only been tested with parthenolide and atropine. It was important to see how Cys-TCP would interact with compounds that may be structurally different from parthenolide in order to have a better understanding of how Cys-TCP would react. Subchapter 7.1.1 will address how those compounds were selected and subchapter 7.1.2. will detail the experiments with Cys-TCP.

7.1.1 Model Compound Selection

It was important to select electrophiles that were structurally different. To this end, the compounds shown in Figure 7.1 were selected. These compounds were first reacted with stoichiometric amounts of cysteine in order to assess their reactivity with no resin present (refer to Chapter 2.2.8.5.1 for the method). These cysteine reactions were analysed by HPLC-MS (Figure 7.2).

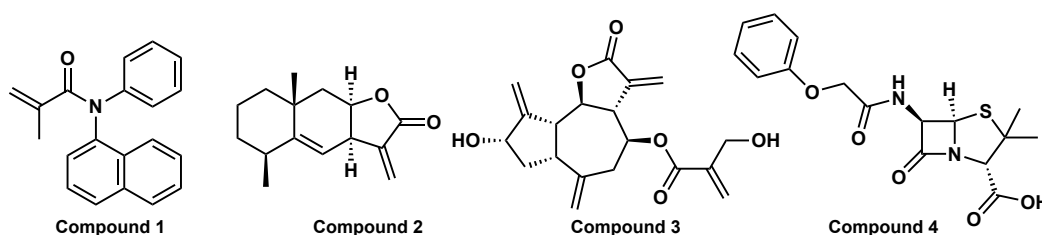


Figure 7.1 Chemical structures of model compounds; 1: *N*-(1-naphthyl)-*N*-phenylmethacrylamide; 2: alantolactone; 3: cynaropicrin; 4: penicillin V.

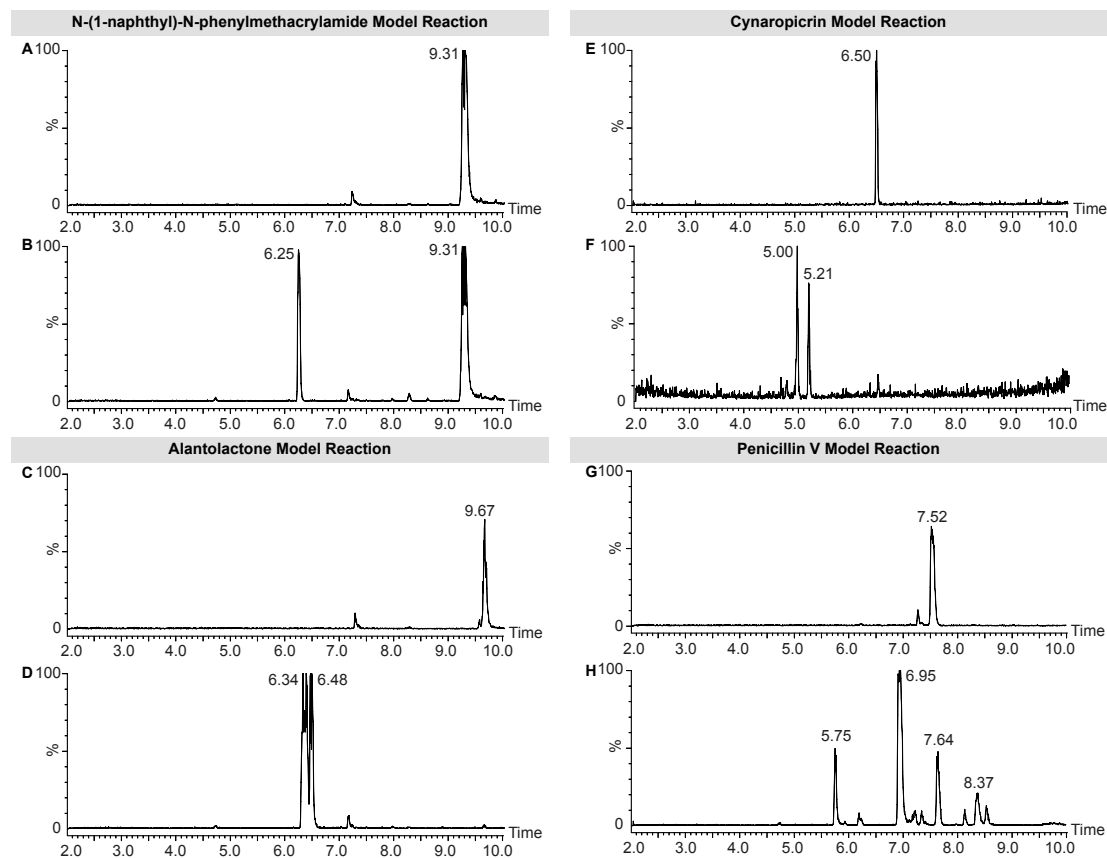


Figure 7.2 Model reactions with cysteine, HPLC-MS traces (positive ion mode) were recorded with a scan range m/z 121-1000. Reactions of model compounds 1-4 with cysteine. A, C, E, G: HPLC-MS analysis of unreacted model compound; B, D, F, H: HPLC-MS analysis of reaction with cysteine. A-B scaled to signal intensity $9.0E7$, C-D scaled to $9.0E7$, E scaled to $1.1E7$, F scaled to $6.7E6$, G-H scaled to $1.0E8$. HPLC-MS traces (positive ion mode) were recorded with a scan range m/z 121-1000.

Compound 1 had rt 9.31 min with m/z 288 and formed one adduct with rt 6.25 min with m/z 409 (Figure 7.2AB). Alantolactone had rt 9.67 min with m/z 233 and formed two adducts, one with rt 6.34 min and one with rt 6.48 min, with m/z 354 and m/z 354 respectively. These two adducts were likely diastereoisomers formed by addition to the Michael acceptor site of alantolactone. Cynaropicrin had rt 6.50 min with m/z 347 and formed two adducts, one with rt 5.00 min and one with 5.21 min, with m/z 468 and m/z 468. These two products were likely formed at two different reactive sites in cynaropicrin. Penicillin V had rt 7.52 min with m/z 351 and formed a product with m/z 472 at rt 6.95. The peak at rt 5.75 min had m/z 591 and could potentially be a double-adduct. For the peaks formed around rt 8.37 min no clear m/z could be assigned.

All of the compounds shown in Figure 7.2 showed reactivity with cysteine and were therefore found to be appropriate for the use in model reactions with Cys-TCP that are described in the subsequent chapter.

7.1.2 Experiments with Model Compounds

In theory, only mono-addition should be possible due to the catch-and-release mechanism of Cys-TCP. The earlier experiment with parthenolide only showed mono-addition. This, however, could be because parthenolide does not have another reactive site that is electrophilic enough to react with another stoichiometric equivalent of cysteine. Another observation made previously was that adduct formation proceeded through nucleophilic addition of cysteine via its thiol group, resulting in a change of mass by +121 Da.

The next experiments with model compounds should be able to confirm whether mono-adduct formation was a by-product of the probe design, as cynaropicrin has several reactive sites, and if a mass increase of +121 Da is observed for all compounds.

The experiment with compound **1** followed the method described in Chapter 2.2.8.2.2. For all other experiments with Cys-TCP, the same experiment protocol was followed as for the proof-of-concept experiment (Chapter 2.2.8.4), but with varying batch sizes. The full data for this experiment can be found in the Appendix as Figure S.13 to Figure S.16. Selected chromatograms are shown to illustrate the main findings (Figure 7.3).

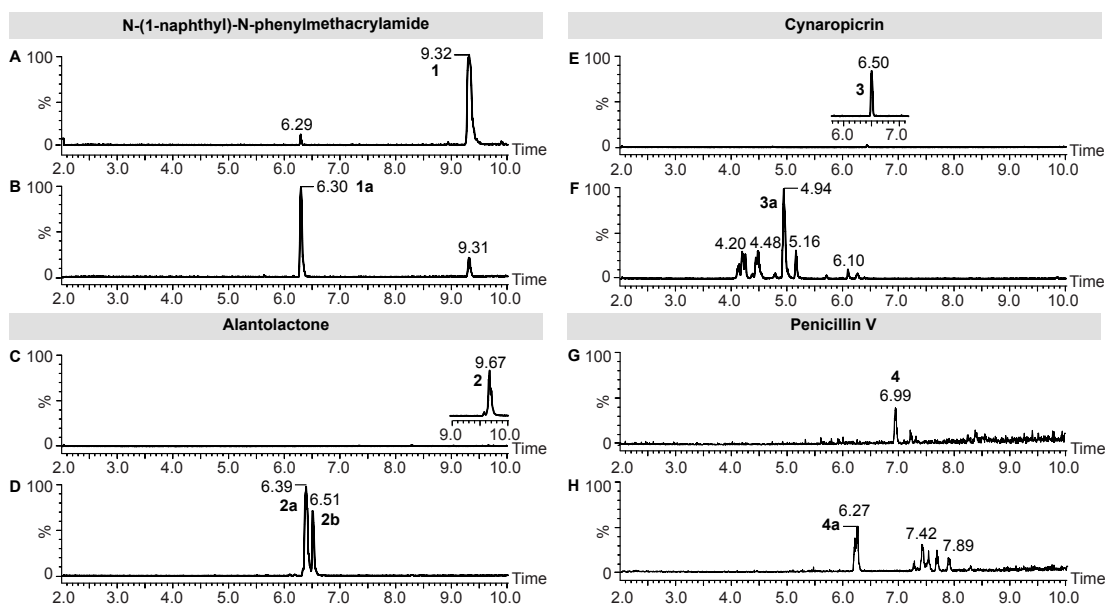


Figure 7.3 Model compound reactions with Cys-TCP. **A, C, E, G**: HPLC-MS analysis of flow-through after incubation with sample, washing off unreacted and excess sample (step v); **B, D, F, H**: HPLC-MS analysis of released cysteine adducts after cleavage with HFIP:DCM (1:4) (step vii). **A-B** scaled to signal intensity $9.0E7$, **C-D** scaled to $9.0E7$, **E-F** scaled to $5.0E7$, **G-H** scaled to $1.2E8$. Inserts in

Chapter 7

chromatograms **C** and **E** show peak rt of pure compound since no excess compound was washed out. HPLC-ESIMS traces (positive ion mode) were recorded with a scan range m/z 121-1000.

The main compounds were isolated by semi-preparative HPLC and analysed by NMR (Figure 7.3). The following section now will discuss each model compound in order to explain the data shown in Figure 7.3 and Figure 7.4.

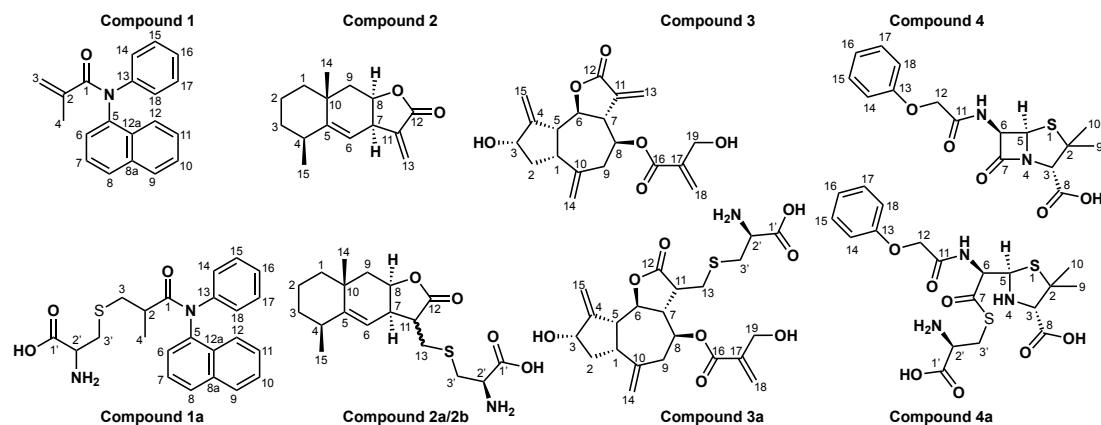


Figure 7.4 Chemical structures of model compounds and their confirmed adducts.

The synthetic compound *N*-(1-naphthyl)-*N*-phenylmethacrylamide (**1**, m/z 288, $[M+H]^+$) formed a single adduct **1a** (m/z 409, $[M+H]^+$) (Figure 7.2AB). The adduct structure was confirmed by NMR (Table S.7), but the configuration at the site of the addition was not determined. This case is similar to parthenolide, which also only formed a single product.

Alantolactone (**2**) is a sesquiterpene lactone with a reactive α,β -unsaturated carbonyl group at C-13. The reaction of **2** (m/z 233, $[M+H]^+$) went to completion (Figure 7.3C) and formed two products, **2a** and **2b** (Figure 7.3D), both with m/z 354, $[M+H]^+$. They corresponded to the two diastereoisomers formed upon addition. Due to overlapping signals of H-7 and H-11 in the HSQC spectra of adducts **2a** (Table S.8) and **2b** (Table S.9) the relative stereochemistry at C-11 could not be established in this sample. In order to be able to clearly assign relative compound structures by NMR methods, a better signal-to-noise ratio in a purer sample or measuring a Nuclear Overhauser Effect spectroscopy spectrum would have been required.

Next, the sesquiterpene lactone cynaropicrin (**3**) (m/z 347, $[M+H]^+$, Figure 7.3EF) was tested as a model for a natural product possessing three reactive sites at C-13, C-15 and C-18, as demonstrated by the model reactions in Chapter 7.1.1. In this case, one

major adduct **3a** was formed, with *rt* 4.94 min and *m/z* 468, $[M+H]^+$, corresponding to a mono-adduct at C-13, as confirmed by NMR data (Table S.10). Smaller peaks in the HPLC-MS chromatogram at *rt* 4.48 min and 5.16 min also showed a molecular ion at *m/z* 468, and they likely corresponded to the other two possible mono-adducts. The peaks at *rt* 6.10 min and 6.27 min exhibited *m/z* 410 and *m/z* 480, respectively, but could not be further characterised due to low abundance. Surprisingly, several peaks around *rt* 4.20 min showed *m/z* 589, which would correspond to adducts with two cysteine residues. The ^1H NMR data of the isolated compounds from *rt* 4.20 showed that not only the $\Delta_{11,13}$ but also the $\Delta_{17,18}$ double bond had disappeared, indicating addition of cysteine residues at C-13 and C-18. Considering the design of the resin and its loading capacity multiple addition of cysteine residues to a typical 'small molecule' such as a plant secondary metabolite was unlikely. We assumed that the compounds with *m/z* 589 are formed by reaction of a mono-adduct with cysteine liberated during the decomposition of adducts via retro-thia-Michael addition. The retro-Michael reaction is often observed to be reversible, and was previously also observed with parthenolide. This reversibility is also reported in literature to be the cause for decomposition that makes compounds difficult to isolate³⁰⁷. Similarly, for the compounds found at *rt* 4.48 min and 5.16 min, even though uncharacterised, it was hypothesised that these were products of decomposition.

Penicillin V (**4**; *m/z* 351, $[M+H]^+$) is not a Michael acceptor, but was selected because of its highly electrophilic beta-lactam ring. Penicillin V reacted to give one major compound (**4a**) at *rt* 6.96 min (*m/z* 472, $[M+H]^+$) (Fig. 7.3GH). The structure of **4a** was confirmed by NMR spectral data (Table S.11). The peaks between *rt* 7.30 and 7.89 min had MS spectra that could not be assigned, and isolation was not successful. We assume that these were the result of decomposed adducts, similar to what occurred to cynaropicrin (**3**). The yields of all the purifications are reported in Table S.12.

This chapter examined the reaction of Cys-TCP with a range of model compounds, showing cases where the analysis was very straightforward, like the cases of parthenolide and compound **1**, but also cases where the analysis was more complex, like the cases of cynaropicrin and penicillin V. As before, formation of the mono-adduct with a mass increase of +121 Da was generally observed. A cynaropicrin adduct that was isolated had the mass of a bi-addition product, but this adduct was likely the side product of a decomposition. Multiple reactive sites can make the

problem more complex; however, when weighing this method against the purification from an extract, this may be a trade-off that ultimately still makes isolation easier. An interesting aspect about multiple reactive sites was that the abundance of the products in principle showed a distribution according to reactivity. Cysteine is a soft nucleophile, therefore favours soft electrophilic sites for bond formation. 1,4-addition was observed for 1-3 as this addition was thermodynamically favourable. In the case of cynaropicrin (3), other products were observed, and since the thia-Michael reaction is reversible, these abundances of the products should be determined by thermodynamic stability. This is feature that could potentially be interesting for other investigations into the reactivity of compounds.

7.2 Model Compound Spiked in a Test Extract

The aim of this method development process was the application on plant extracts. Therefore, it was necessary to demonstrate that Cys-TCP could isolate an electrophile from a complex mixture of compounds, e.g. a test extract.

Tiliae flos MeOH extract is known to contain phenolic compounds such as flavonoids and phenylpropanoids, which are not known to be particularly electrophilic. In this experiment, *Tiliae flos* MeOH extract (200 mg) and parthenolide spiked into *Tiliae flos* MeOH (0.0375 mmol parthenolide and 200 mg extract) extract were tested on Cys-TCP (0.075 mmol). The procedure described in Chapter 2.2.8.4 were followed. As before, the full data can be found in the Appendix (Figure S.17). The key chromatograms for the experiment outcome are shown in Figure 7.4, together with a chromatogram of untreated *Tiliae flos* MeOH extract.

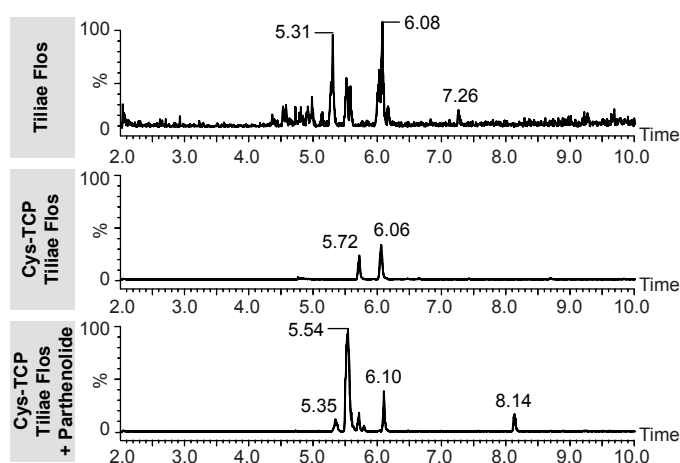


Figure 7.4 Capture of parthenolide from a spiked *Tiliae flos* MeOH extract. Top: chromatogram of the extract. Centre: cysteine adducts from a Cys-TCP experiment with the extract, after cleavage with

HFIP:DCM (1:4 v/v) (step vii). Bottom: cysteine adducts from a Cys-TCP experiment with extract spiked with parthenolide, after cleavage with HFIP:DCM (1:4 v/v) (step vii). Signal intensity percentage scaled to highest peak. HPLC-MS traces (positive ion mode) were recorded with a scan range m/z 121-1000.

Parthenolide could be observed in the HPLC-MS analysis at rt 5.54 min with m/z 370, and was isolated with a purified adduct yield of 0.7 mg, sufficient for a clean NMR. Two other peaks were observed in Cys-TCP treated *Tiliae Flos* extract (Figure 7.4, centre) at rt 5.72 min (m/z 396 $[M+H]^+$) and rt 6.06 min (m/z 410 $[M+H]^+$), which were also found in the spiked extract (Figure 7.4, bottom) with a retention shift. It was attempted to isolate these two adducts, but the low amounts that were obtained were not enough for a *de novo* characterisation.

This experiment demonstrated that this method was able to pull out parthenolide from an extract matrix and give enough purified adduct for a clean NMR spectrum. Some low abundance electrophile-adducts were also found in the eluate of the cleavage step; however, an elucidation of their structure was not possible. This showed that even though this method can successfully pull out spiked compounds, minor compounds in extracts can still be challenging due to their low abundance.

7.3 Testing Pollen Extracts

The pollen extracts from Chapter 3 were tested on Cys-TCP next. Due to supplier issues, CI-TCP(CI) ProTide Resin was exchanged for 2-chlorotriyl chloride resin by Bachem. The exact differences between these two resins are not known since only limited information was available from both suppliers. The previously used resin had a 2-chlorotriyl linker bound to PEG-ylated polystyrene via an amide moiety. For the new resin the exact chemical structure beside the 2-chlorotriyl linker is unknown. Before using this new resin systematically for all extracts, it needed to be tested. Two batches of Cys-TCP were synthesised using this resin and tested against parthenolide and *Ambrosia psilostachya* P4129072-1. This extract batch was chosen as test extract since it had been reordered this batch for a larger scale experiment, thus the risk of using this extract was the lowest. For all the experiments, except for the large batch P4129072-1', a resin batch size equivalent to 0.25 mmol was used.

The experiment results for parthenolide and *Ambrosia psilostachya* P4129072-1 are shown in Appendix Figure S.18 and Figure S.19. A problem was identified, where parthenolide adduct was found in the sample after incubation (Figure S.18). This meant that the linker on the new resin was likely more acid-sensitive than the one

previously used. In order to reduce premature cleavage the MeOH used for these experiments was changed to anhydrous MeOH. Another interesting observation from this experiment was that Cys-TCP synthesised from the new resin changed its colour from the usual yellow orange to dark red upon addition of HFIP:DCM (1:4 v/v).

After this experiment, the other pollen extracts were tested in batches of three to five. The tested extract amounts are recorded in Table S.13 of the Appendix. The chromatograms for these experiments are shown in Figure S.20 of the Appendix; in this case, due to the large volume of data, only the extract profile and the sample after cleavage from step (vii) are shown, not the full data. For each extract, the sample from step (vii) was subjected to semi-preparative analysis and purification on the HPLC-MS instrument with a dynamic splitter (described in Chapter 2.2.3.2). This chapter will first discuss all the smaller batches of pollen extract and then discuss the large batch P4129072-1'.

Even with Cys-TCP to aid in the purification process, it was not possible to isolate any adduct species formed in these experiments due to the limited amount of extract and the low abundance of electrophilic content, as was shown in Table 3.2. The electrophile content was already low to begin with, and additionally, those electrophiles were likely also a mixture of products, making the purification difficult at best. The adduct masses observed in the purification process, however, were recorded in Appendix Table S.14.

It was attempted to match the adduct masses with reported compounds from the respective plant species. This was done based on the assumption that adducts are formed by nucleophilic addition with cysteine. A mass of m/z 122 (corresponding the $[M+H]^+$ of cysteine) was deducted from the adduct mass $[M+H]^+$ in order to give the putative original mass of the electrophile, $[M]$ i.e. GFM. This highly speculative method was met with varying degrees of success, as some masses could be mapped to known structures (Figure 7.5), but the majority of the masses could not be explained. In *Ambrosia psilostachya*, the adduct masses m/z 384, 386 and 402 could correspond to parthenin (GFM 262 gmol^{-1}), coronopilin (GFM 264 gmol^{-1}) and psilostachyin (GFM 280 gmol^{-1}), all compounds previously reported to be isolated from this plant^{284,308}. Interestingly, the most prominent peak in these extracts had m/z 600, which would correspond to GFM 478 gmol^{-1} , and it could not be mapped to any reported compound. Similarly, another albeit smaller peak with m/z 616 could also find no matching reported mass.

The *Ambrosia artemisiifolia* also showed a number of peaks, but none of the masses were found to correspond to any reported compounds. Interestingly though, pollen extracts from this species also showed peaks with m/z 600 and m/z 616, just like *Ambrosia psilostachya*. This could be due to those plants belonging to the same family, hence having similar secondary metabolites.

In the case of *Phleum pratense*, no masses matched up except m/z 462, which would translate to GFM 340 g mol^{-1} . Gamahonolide B with GFM 340 g mol^{-1} was previously reported in association with *Phleum pratense*³⁰⁹.

Betula pendula has many reported natural products, but only one m/z matched up, namely putative GFM 474 g mol^{-1} for 12,20,25-trihydroxydammar-23-en-3-one³¹⁰.

Among the m/z values observed for *Urtica dioica*, only one matched to a known compound, namely putative GFM 354 g mol^{-1} , which corresponded to the mass of chlorogenic acid³¹¹.

The final pollen species of pollen species examined was *Corylus avellana*. There, putative GFMs 284 g mol^{-1} , and 354 g mol^{-1} matched to the reported masses of kaempferol and giffonin³¹²⁻³¹³.

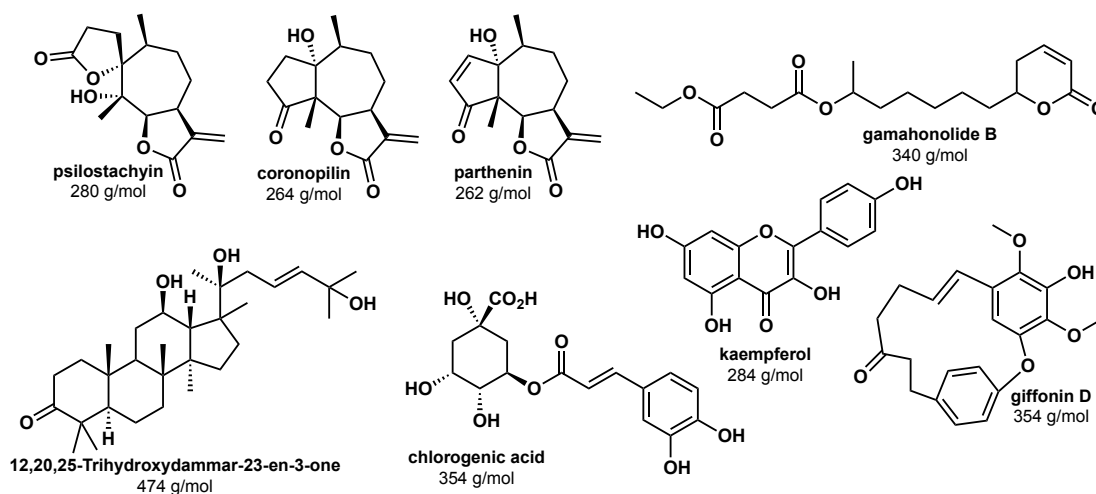


Figure 7.5 Chemical structures of mapped compounds.

The experiment with the batch P4129072-1' was adapted to accommodate for the larger amount of extract and the quantity of the resin beads. The exact procedure is detailed in Chapter 2.2.8.5. The chromatogram of the HPLC-MS analysis is shown in Figure 7.6.

A major peak with m/z 600 was observed at rt 6.27 min during the HPLC-MS analysis. Purification was performed as in the previous experiments and gave a number of samples. The majority had yields that were too low for further analysis. Two samples, **5a** and **5b** (both m/z 600) with yields of 0.7 mg and 0.9 mg respectively, were submitted for NMR analysis on a cryoprobe. The spectral data can be found in Appendix Figure S.21 to Figure S.23. The spectral data of **5b** (data not included) was considerably worse than the data set of **5a**, and they seemed to be structurally related compounds, thus the analysis focused on **5a**.

At first glance, two things could be said: i) the sample was not pure and ii) **5a** seemed to be a coumaroyl spermine or spermidine-type structure (Figure 7.7); this impression was based two distinct areas in the HSQC where the peaks aggregated, the first in the area of 1H 1.50-3.47 ppm and ^{13}C 27.17-47.86 pm, indicating short chains of CH_2 that are close to heteroatoms, and the second in the area of 1H 6.38-7.37 ppm and ^{13}C 116.19-139.15 pm, indicating an aromatic or double bond conjugated environment. Furthermore, this hypothesis was also based on the fact coumaroyl spermidine structures had been previously isolated from *Ambrosia psilostachya*²⁸⁴.

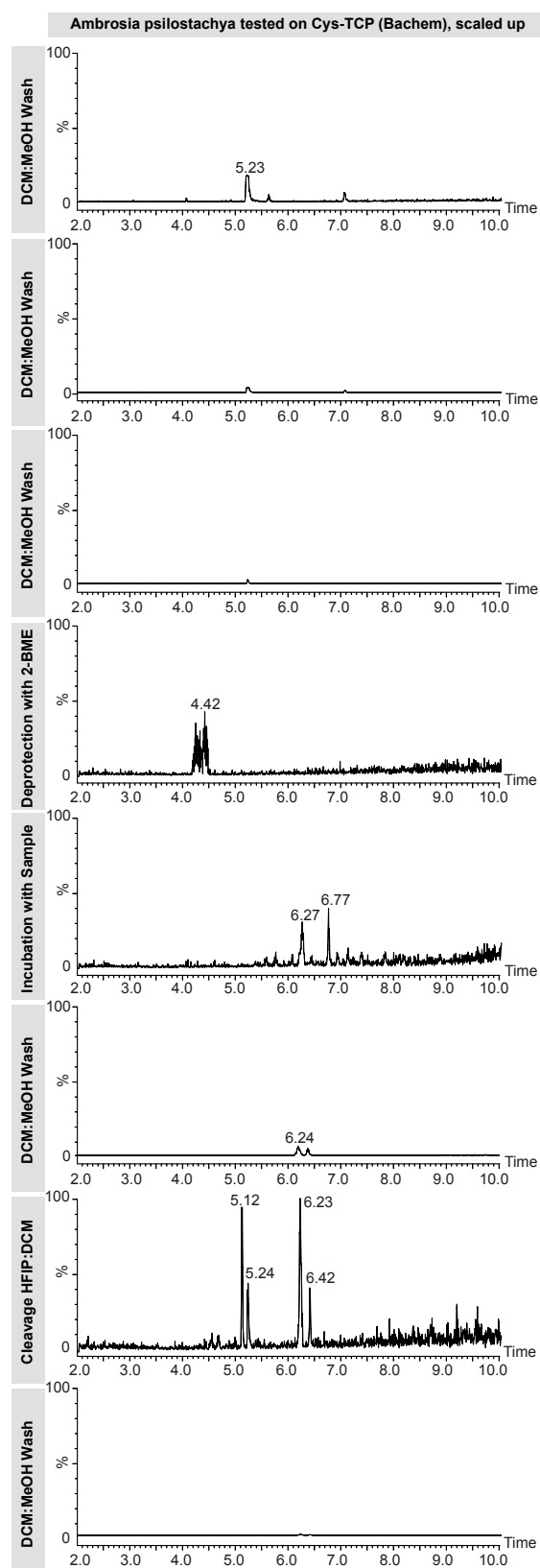


Figure 7.6 Cys-TCP experiment with *Ambrosia psilostachya* batch P4129072-1'. Signal intensity percentage scaled to 1.0×10^7 . HPLC-MS traces (positive ion mode) were recorded with a scan range m/z 121-1000.

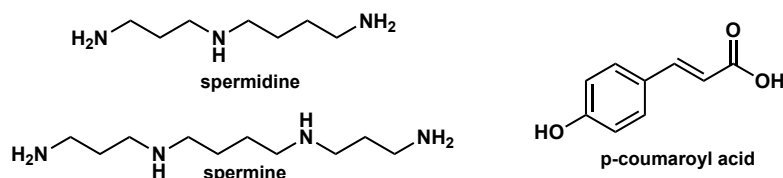


Figure 7.7 Chemical structures of spermine, spermidine and p-coumaroyl acid

The m/z observed for **5a** was 600, which, if a molecular ion peak $[M+H]^+$, would correspond to a putative GFM of 599 g mol^{-1} , which is interesting piece of information, as this can tell us about the potential of nitrogen atoms in the structure. The nitrogen rule states that organic compounds containing only the elements H, C, N, O, Si, P, S and the halogens have an odd nominal mass if there is an odd number of nitrogen atoms present, but an even one if an even number of nitrogen atoms are present. Based on the previous hypothesis that this is indeed spermine or spermidine-type structure, the original structure **5** (putative GFM 478 g mol^{-1}) must have an even number of nitrogen atoms. The two possible options are that the original structure **5** has either two nitrogen atoms or four.

In the area of the short CH_2 -chain signal, three patches of signals could be observed in HSQC, one around ^{13}C 27 ppm, one around ^{13}C 35 ppm and one around ^{13}C 47 ppm. These seemed to be different types of CH_2 -environments, which could indicate that there were three different types of short CH_2 -chains, which could be adjacent to nitrogen atoms (Figure 7.8).

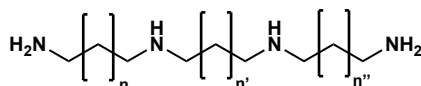


Figure 7.8 Example of a spermine/spermidine-type structure.

Accommodating for the signals observed in the aromatic area and based on putative GFM of 599 g mol^{-1} , two coumaroyl side chains were added. In the HSQC, there were four signals in the area that were the most intense (^1H - ^{13}C ppm as follows: 6.38-119.21 ppm; 6.77-116.19 ppm; 7.31-139.15 ppm; 7.37-129.66 ppm). The other signals in this area have less intensity. An explanation would be that those coumaroyl substituents are substituted at different nitrogen atoms in the spermine/spermidine-like structure and that those intense signals are attributable to the most abundant compound. Another explanation would be that those coumaroyl-substituents are not

necessarily all para-substituted. These two explanations could account for the quantity of peaks in the aromatic region and be consistent with previous findings, i.e. that this sample was not pure but the compounds in the sample all had the same m/z and the same r_t during purification. This sample could indeed be a mixture of spermine/spermidine-like structures with coumaroyl groups substituted on different nitrogen atoms in the structure, of which some coumaroyl groups that are not para-substituted.

Since **5a** is the NMR spectrum of a compound that, according to the method used, should be cysteine-adduct, it was necessary to account for this cysteine. Cysteine-adducts were isolated previously, therefore a range into which the ^1H and ^{13}C shifts could fall was known. The cysteine CH ^1H shift ranged from 3.30-4.40 ppm and the ^{13}C shift ranged from 53.5-55.4 ppm. The cysteine CH_2 ^1H shift ranged from 2.75-3.20 ppm and the ^{13}C shift ranged from 25.2-36.8 ppm. In the HSQC of **5a**, a signal could be found at 3.16 ppm-37.00 ppm, that could correspond to the CH-group of bound cysteine. The peak that could correspond to the CH_2 -signal, however, was not observed. All the observed CH_2 -signals did not match the expected values. This was problematic since absence of this CH_2 -signal could mean that the compound is not, in fact, bound to cysteine at all. If cysteine was bound to this structure, it would be unlikely for cysteine to be connected to one of the coumaroyl-substituents since this would break the chain of conjugated double bonds, which would be visible in the NMR spectrum. The more likely binding spot in the currently constructed structure would be one of the nitrogen atoms.

Combining all of the findings, a putative structure was constructed in order to match the observed mass, featuring two coumaroyl groups and a cysteine bound to the thermospermine-like structure (Figure 7.9).

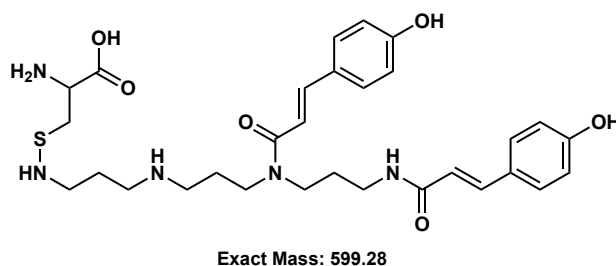


Figure 7.9 Putative chemical structure for **5a**.

The sample was too impure to confirm the proposed structure for **5a**. Further, it was not possible to ascertain through which exact mechanism such a nucleophilic addition

of cysteine could have occurred. What could be said for certain is that **5a** is a likely a coumaroyl spermidine-like structure and this is in line with previous findings from this group²⁸⁴.

7.4 Conclusions

Model compounds were successfully tested on Cys-TCP. The main adducts formed were isolated and characterised by NMR. Next, parthenolide spiked into the model extract, *Tiliae Flos* MeOH, was tested on Cys-TCP. The parthenolide adduct was successfully formed by the probe and allowed purification with a yield of 0.7 mg, enough for the compound structure to be confirmed by NMR. Lastly, pollen extract batches were tested on Cys-TCP. Due to the limited amount of electrophilic content in these extracts, it was not possible to isolate and identify any compounds for certain. The observed *m/z* masses of these pollen extract experiments were used for finding out if compounds of corresponding masses had been previously found. This highly speculative analysis based on the assumption that adduct formation with cysteine always resulted in a mass increase of +121 Da was met with varying degrees of success. Furthermore, a big batch of *Ambrosia psilostachya* pollen extract was tested on Cys-TCP. Two compounds were isolated with sufficient amount for NMR submission, and were found to be structurally related. Based on the NMR analysis of these compounds, it concluded that these structures were likely coumaroyl spermidine-like structures.

Chapter 8 Conclusions and Future Perspectives

Pollen allergy is a multicausal, complex disease that affects millions of people worldwide. Treatment options for this disease currently consist of mainly symptom management rather than addressing the disease directly. The only treatment regimen that addresses the disease directly is allergen-specific immunotherapy, a treatment approach to achieve desensitisation to an allergen, leading to cessation of allergic symptoms. This treatment regimen is lengthy, requires regular medical attention and furthermore, often does not offer permanent relief of the disease, as symptoms can resurface years after stopping the treatment. The process of desensitisation, although clinically observed, is not well-understood; the same holds true for the process that actually triggers allergic disease, sensitisation, and the nature of the exacerbative episodes of the disease. Since sensitisation and desensitisation are likely inextricably linked, understanding one will potentially lead to a deeper understanding of the other, which could result in a greater overall understanding of the disease that could translate into new treatment options.

Many hypotheses have been made in an attempt to understand the underlying causes of the disease. Amongst these hypotheses are two, the hapten theory and the danger model, that lead to believe that small molecules associated to allergens could be involved in the sensitisation process. Reactive small molecules in pollen represent an underresearched area in comparison to their protein counterparts and investigating them could shed some light on the sensitisation process and the exacerbative episodes of the disease. They could be involved in the disease via immunological mechanisms in the allergic cascade and also elicit a physiological reaction in the human body and thus aggravate the disease. Therefore, this project aimed to develop a method that could detect and identify pathophysiologically relevant electrophiles in pollen extracts, as this could serve as a starting point to gain new learnings in the field of pollen allergy.

After compiling a selection of extracts and characterising their electrophile content, method development started out as an *in situ* approach. It was recognised that electrophiles make up a very small proportion of the total extract, thus using LC-MS-based methods for the detection and identification of electrophiles seemed appealing. The nucleophiles used for the identification of electrophiles were GSH and NAC. After testing the nucleophiles with the electrophilic model compound parthenolide and a model extract of *Ambrosia psilostachya*, it was discovered that although this approach

may work with model compounds, extracts were too complex to be analysed in this manner since i) there were many overlapping peaks, making it difficult to discern which mass peaks were the most important, ii) the addition of nucleophiles to electrophiles could potentially be nonstoichiometric and not result in a simple m/z change of adding the respective masses of the reactants, therefore calculating the original mass after having identified an adduct mass was not possible, and iii) the reactions with nucleophiles may not go to completion, which meant that identifying which peaks belonged to electrophiles of interest was difficult. Furthermore, it was realised that isolation and subsequent structure elucidation would be required to confirm electrophile identity, so the efforts then focused on linking detection and purification.

In an attempt to combine detection and purification, a nucleophile, cysteine, was linked via an aspartic acid residue, that served as a guiding motif for enzymatic cleavage, to an affinity tag, 6His, that would potentially facilitate a subsequent purification step after LC analysis. The resulting nucleophilic probe was the peptide CD6His. The synthesis of the nucleophilic probe via SPPS turned out to be challenging due to the histidine chain. It was presumed that the bulky side chains lowered the coupling efficiency.

Another approach to link detection and purification was taken, namely tethering the nucleophile onto a solid support via a cleavable linker. By taking advantage of materials already in use in SPPS, a polystyrene-supported nucleophilic probe with a hyperacid sensitive linker attached to cysteine, Cys-TCP, was constructed and tested in a pilot experiment. After promising results in this pilot experiment, further optimisations were performed before conducting a proof-of-concept experiment. Cys-TCP was shown to capture the model electrophile parthenolide, not react with the negative control atropine and release formed parthenolide-adducts after application of a cleavage cocktail. In the course of the experiment, it was also discovered that the thia-Michael reaction with parthenolide is reversible due to the presence of starting material found after cleavage. Matrix effects were excluded by testing an unreactive probe, Ala-TCP. The ability to pull out small amounts of electrophiles was also demonstrated by testing 1 mg of parthenolide which resulted in the isolation of 1.5 mg parthenolide adduct. Furthermore, a quality control step was engineered into the probe in order to be able to quantify the amount of reactive nucleophilic probes

available on the solid support, which showed that 8.65 ± 2.65 % of the reactive sites were available for reaction.

As a next step, another series of model compounds were tested on Cys-TCP. These experiments showed that adduct formation was usually accompanied with a m/z increase of +121 Da and that generally, mono-addition is observed, unless the thia-Michael reaction was reversible and resulted in the formation of side products as part of the decomposition process. The main adducts of each reaction were purified and characterised. The next experiment was with a *Tiliae flos* MeOH extract and with *Tiliae flos* MeOH extract spiked with parthenolide. In this experiment, it was demonstrated that an electrophile in an extract could be selectively pulled out and purified. This was followed by the final round of experiments using the pollen extracts that had been prepared at the beginning. The experiments showed that isolating low abundance molecules is difficult, even with a probe to assist in purification. The problem encountered was that although the total electrophile content was extrapolated to 1-2 mg per extract batch, ultimately those compounds themselves were a mixture of products and it was not possible to single out any adducts formed for structure elucidation except in the case of one larger batch of *Ambrosia psilostachya* extract, where a coumaroyl spermidine structure was isolated. Although the exact structure could not be confirmed, this was in agreement with previous findings in this extract.

In this thesis method development for the detection and identification of pathophysiologically relevant electrophiles in pollen was investigated. Ultimately, this method development process was an odyssey of trial and error, where different approaches were tested and evaluated. The best approach developed was a solid-supported nucleophilic probe that i) can be selectively activated and the number of active sites can be quantified by MRM, ii) reacts with its cysteine moiety in a mono-additive fashion, and iii) has a hyperacid sensitive linker for the release of formed adducts. By using the tools that have been already developed, like the quantification assay for quality control, that this probe and method could be further developed in order to give better yields for future experiments.

Retrospectively analysing the journey, there are both learnings from the experiments that could improve experiments in the future, and also further experiments that would be interesting to pursue in the future.

Starting with the former, a fact that had become very clear especially towards the end was that the amount of reactive content in pollen extracts is very small, similar to minor compounds in plant extracts from other plant parts. The difference here, however, is that unlike in standard natural product research, this work started out with an amount of pollen, 5 g per batch, which is very little when the end goal is compound isolation and NMR characterisation. This naturally is a restriction imposed by the nature of pollen, as they are not easy to collect, thus are expensive. Nonetheless, starting out with larger amounts may allow future researchers to be more successful in the endeavour of isolating and characterising new structures. During the optimisation of the method, more factors could have been optimised in order to increase the yield of active Cys-TCP, if it were not for time constraints. An example for this is the reduction step with 2-BME that was not further optimised, which could have made a big impact in the yield of active Cys-TCP sites after deprotection. Isolating minor compounds from plant extracts is a very difficult task, hence making sure the method is as effective as possible is crucial. The quantification method for cysteine released after the 2-BME step could give insights into the effectiveness of various optimisation aspects. Another challenge that came up towards the end was having had to switch supplier for the resin beads that were used in synthesis. From the experiments conducted, it seemed that the new resin linker was more acid sensitive than the previously used one, which naturally impacted the experiments. All in all, there were lessons to be learned and findings that will improve future experiments.

The experiments in this dissertation mainly focused on using MS methods in order to detect and purify formed adducts. Experiments that would be interesting to pursue in the future would involve using UV/Vis detection additionally to MS detection. Incorporating an additional UV/Vis active tag into the probe could have improved detection sensitivity and made purification of the released adduct via UV/Vis detection possible.

Furthermore, once interesting electrophiles in pollen extracts are identified, they could be tested in both immune response models and in physiological cell models to gauge their effect on a cellular level. It is our hope that by investigating small reactive molecules in pollen, our understanding of the disease can be furthered and translated into future treatment options.

Appendix

Methods

Liberty Blue methods. SPPS methods included three different types of steps: the coupling step of the first amino acid, the standard coupling step and the final deprotection step.

First amino acid coupling step: the resin was left to swell in DMF for 10 min before starting the reaction. Then, both the chloride loading solution (1.0 M DIPEA and 0.125 M KI) (2 ml) and the building block to be coupled (0.2 M in DMF, 5 ml) were added and the mixture was microwaved at 80 °C with 75 W for 60 s as ramping stage and then settled at 90 °C at 20 W for another 540 s. After microwaving, a manifold wash was performed with 5 ml DMF, then, the sample was washed with 4 ml DMF with drain time 5 s for four times.

Standard coupling step: 4 ml deprotection cocktail (10 % piperazine (w/v) in EtOH:NMP 10:90) was added to the resin reaction chamber, then microwaved at 75 °C with 155 W for 15 s as ramping stage and then settled at 90 °C at 30 W for another 50 s. After microwaving, the sample was washed with 4 ml DMF with drain time 5 s for 4 times. The next amino acid building block to be coupled (0.2 M in DMF, 2.5 ml) was added, left at 25 °C for 120 s and then microwaved at 50 °C at 35 W for another 480 s.

Final deprotection step: 5 ml of deprotection cocktail (10 % piperazine (w/v) in EtOH:NMP 10:90) was added, then microwaved at 75 °C with 155 W for 15 s as ramping stage and then settled at 90 °C at 30 W for another 50 s. After microwaving, the sample was washed with 4 ml DMF with drain time 5 s for 4 times.

Waters system data acquisition - Qualitative. Standard qualitative analysis was performed on the UPLC system under HPLC conditions with a SunFire™ C18 (3.5 µm 3 mm × 150 mm i.d.). Weak wash solution was 0.2 % TFA in acetonitrile and water (1:1). Strong wash solution was 0.2 % in a mixture of acetonitrile, 2-PrOH, and acetone (4:3:3). Seal wash solution was a mixture of acetonitrile and water (1:9). The pressure limit was set to 6000 psi. The wash solution volumes were set to 600 µl for weak wash and 200 µl for strong wash. The sample manager was set to 20 °C, the column oven to 45 °C. The injector was set to partial loop injection. The gradient used

Appendix

was as follows (flow rate of 0.6 ml/min): 5 % B for 2 min, up to 100 % B of 8 min, at 100 % B for 2 min, to 5 % B in 0.1 min, at 5 % B for 2.9 min.

Detection was performed with both PDA and MS. The PDA was set to scan wavelengths from 210 – 400 nm, the resolution was set to 1.2 nm and the recording speed was 20 points/s. The MS method was set to scan in both positive and negative ion mode for m/z values of 121 – 1000. The detection time window was set between 2.00 – 12.00 min. The tune file conditions were as follows:

Capillary	4.00 kV
Cone	30 V
Extractor	1 V
RF Lens	0.1 V
Source Temperature	150 °C
Desolvation Temperature	400 °C
Gas Flow	800 l/h
Cone Gas Flow	10 l/h
LM Resolution 1	15.0
HM Resolution 1	15.0
Ion Energy 1	3.0
Entrance	50
Collision	3
Exit	50.0
LM Resolution 2	15.0
HM Resolution 2	15.0
Ion Energy	0.5
Gain	2.00

Waters system data acquisition - Quantitative. Quantification of cysteine was performed on the UPLC system with an ACQUITY UPLC® HSS T3 (1.8 µm 2.1 mm × 100 mm i.d.) with the matching pre-column (both Waters). Flow rate was set to 0.4 ml/min. The pressure limit was set to 15000 psi. The wash solution volumes were set to 800 µl for weak wash and 200 µl for strong wash. The sample manager was set to 20 °C, the column oven to 45 °C. The injector was set to partial loop injection. The inlet method was configured as follows: 5 % B for 0.50 min, up to 10 % B of 1.50 min, to 100 % B in 0.50 min, at 100 % for 0.20 min, to 5 % B in 0.29 min, at 5 % B for 0.51 min.

Detection was performed with MSMS. The MS method was set to scan in positive ion mode. The detection time window was set between 0.50 – 3.10 min. The tune file conditions were as follows:

Capillary	2.90 kV
Cone	36 V
Extractor	3 V
RF Lens	0.1 V
Source Temperature	150 °C
Desolvation Temperature	350 °C
Gas Flow	500 l/h
Cone Gas Flow	10 l/h
LM Resolution 1	4.5
HM Resolution 1	14.6
Ion Energy 1	0.4
Entrance	1
Collision	20
Exit	0.5
LM Resolution 2	12.8
HM Resolution 2	15.4
Ion Energy	0.5
Gain	1.00

The MS file for the detection of cysteine with IS methionine was as follows:

Compound	Transition	Dwell Time (s)	Cone (V)	Collision (V)
Cysteine	121.50>75.92	0.103	20	18
	121.50>58.89	0.103	20	20
Atropine	289.50>123.90	0.103	44	24

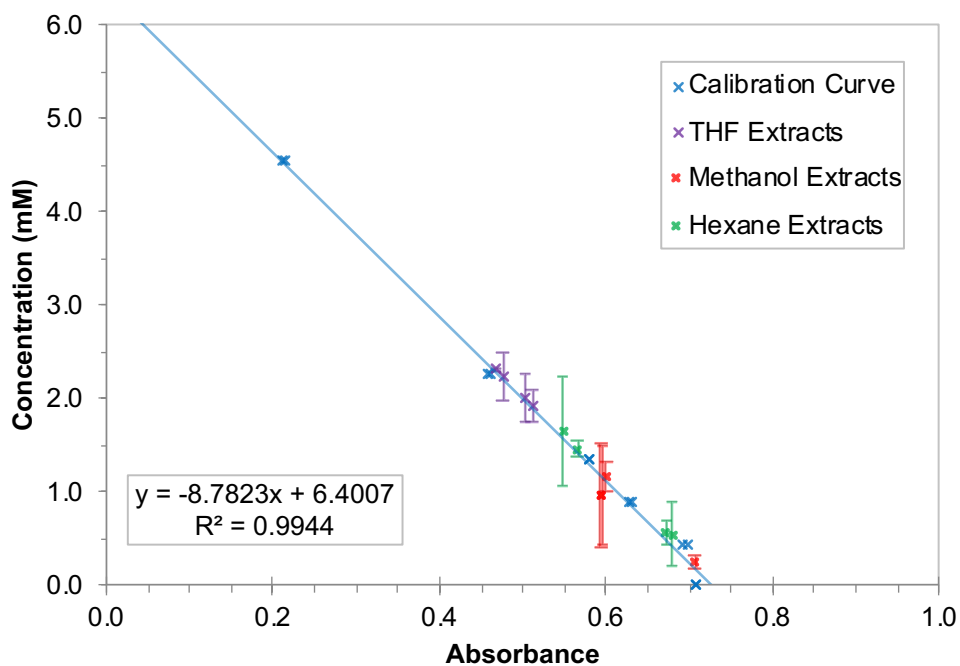
Shimadzu Conditions. Needle wash solution was acetonitrile/MeOH/isopropyl alcohol/water (1:1:1:1).

Agilent Conditions for Semi-Preparative Purification. Seal wash was MeOH:2-PrOH/water (1:1:1). The sample and the column were at RT. The MS detection in positive ion mode settings were as follows:

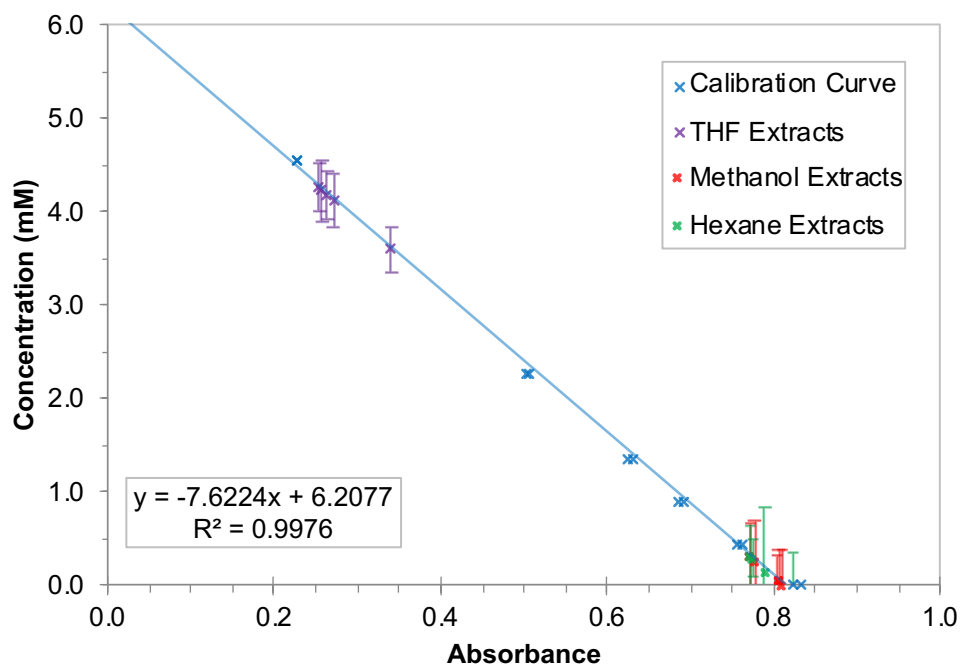
Mass Low	Mass High	Fragmentor	Gain	Threshold	Stepsize	Speed (u/s)
100	1000	125	1.00	150	0.10	1733

Ion source was set to API-ES, peak width 0.050 min, cycle time 0.54 s/cycle.

Ambrosia psilostachya

Figure S.1 Calibration curve and interpolated data points for *Ambrosia psilostachya*.

Ambrosia artemisiifolia

Figure S.2 Calibration curve and interpolated data points for *Ambrosia artemisiifolia*.

Betula pendula

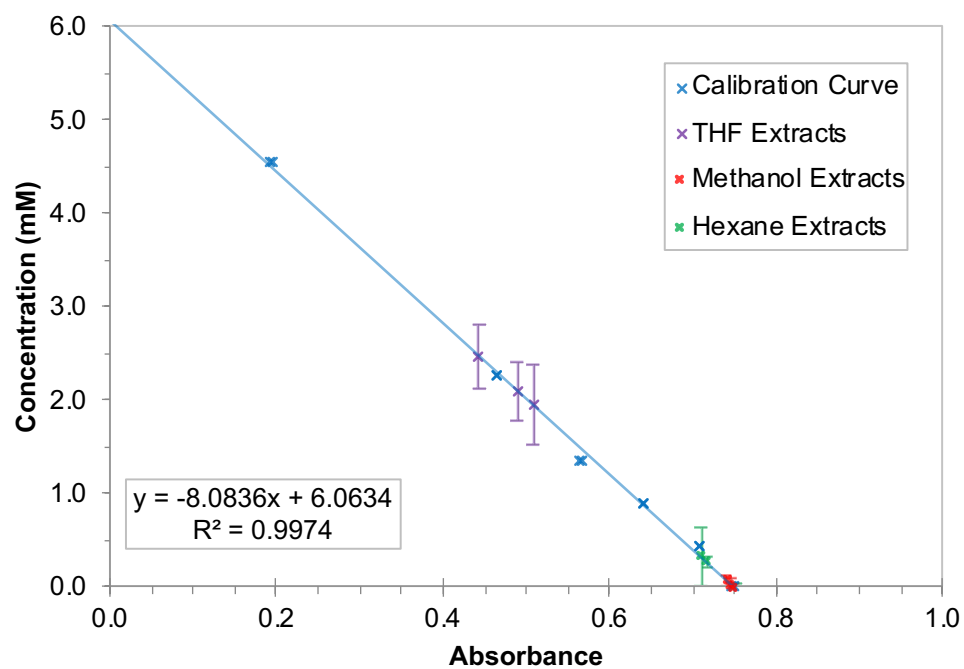


Figure S.3 Calibration curve and interpolated data points for *Betula pendula*.

Urtica dioica

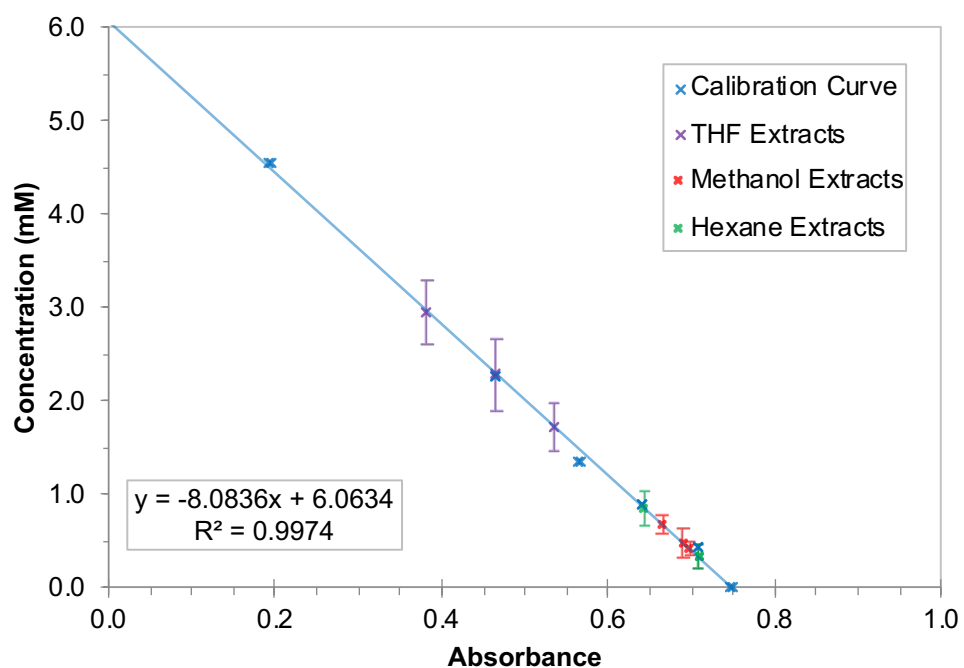


Figure S.4 Calibration curve and interpolated data points for *Urtica dioica*.

Corylus avellana

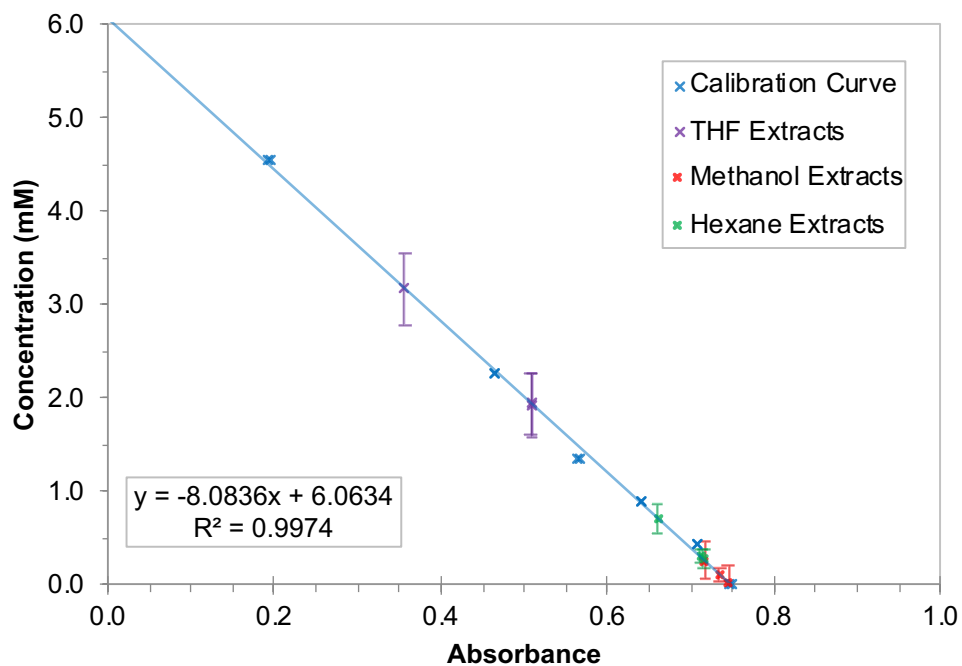


Figure S.5 Calibration curve and interpolated data points for *Corylus avellana*.

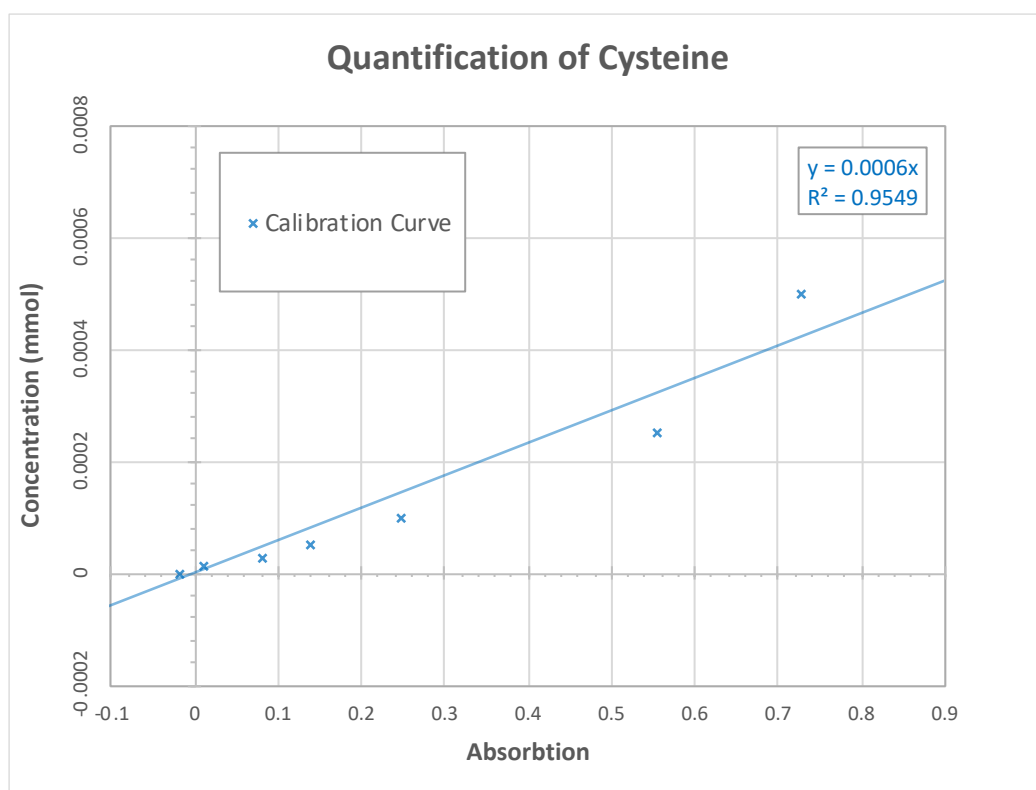


Figure S.6 Calibration curve of the adapted version of the indirect method previously used to quantify electrophile content.

Compound name: Cysteine
 Coefficient of Determination: $R^2 = 0.952472$
 Calibration curve: $0.0106864 * x^2 + 0.45027 * x + -0.129142$
 Response type: Internal Std (Ref 2), Area * (IS Conc. / IS Area)
 Curve type: 2nd Order, Origin: Include, Weighting: Null, Axis trans: None

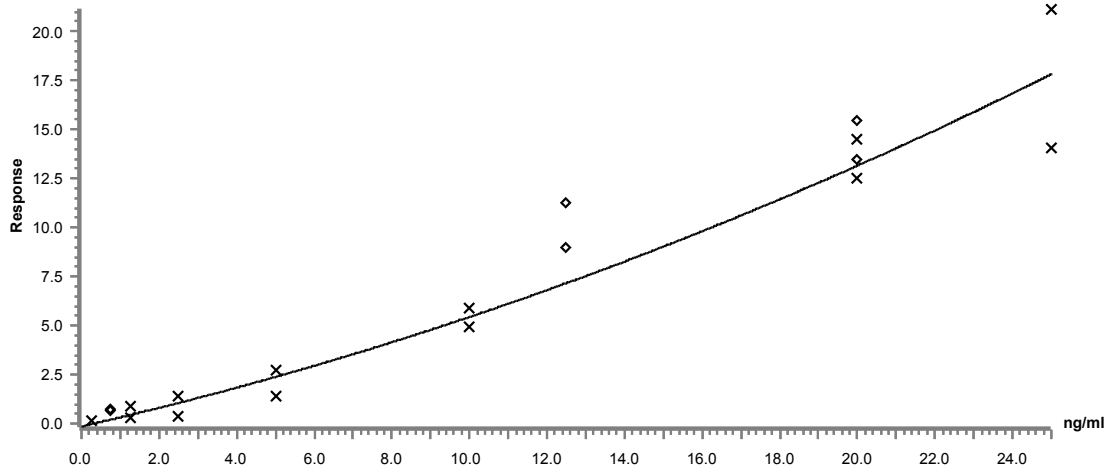


Figure S.7 Cysteine calibration curve with IS methionine. Data found in Table S.3.

Compound name: Cysteine
 Coefficient of Determination: $R^2 = 0.880262$
 Calibration curve: $-8.95963e-005 * x^2 + 0.253676 * x + 0.0346365$
 Response type: Internal Std (Ref 2), Area * (IS Conc. / IS Area)
 Curve type: 2nd Order, Origin: Include, Weighting: Null, Axis trans: None

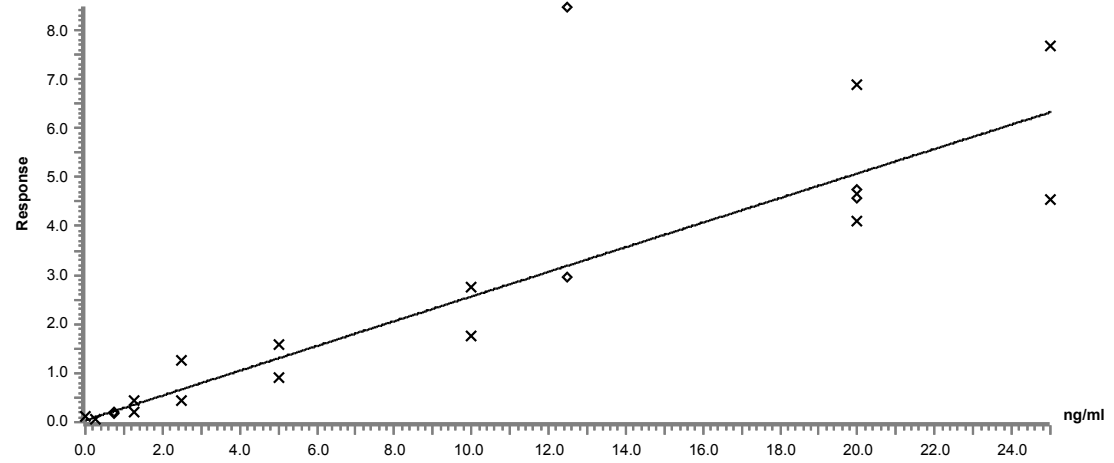


Figure S.8 Cysteine calibration curve with IS NAC. Data found in Table S.4.

Appendix

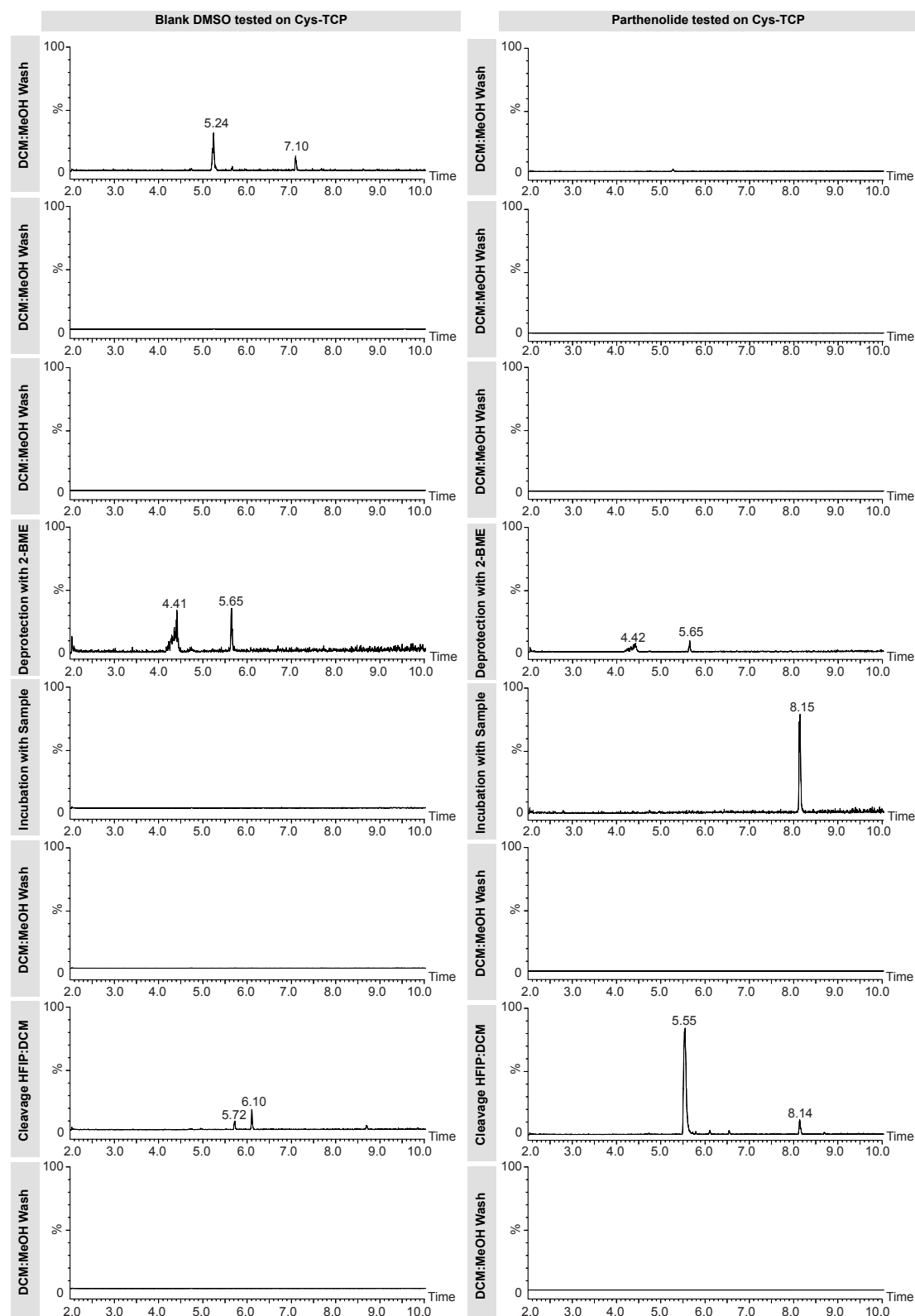


Figure S.9 Data from Cys-TCP proof-of-concept experiment. Left: data from the experiment with blank DMSO, chromatograms scaled to $1.4E7$; right: data from the experiment with parthenolide, chromatograms scaled to $1.0E8$. HPLC-MS traces (positive ion mode) were recorded with a scan range m/z 121-1000.

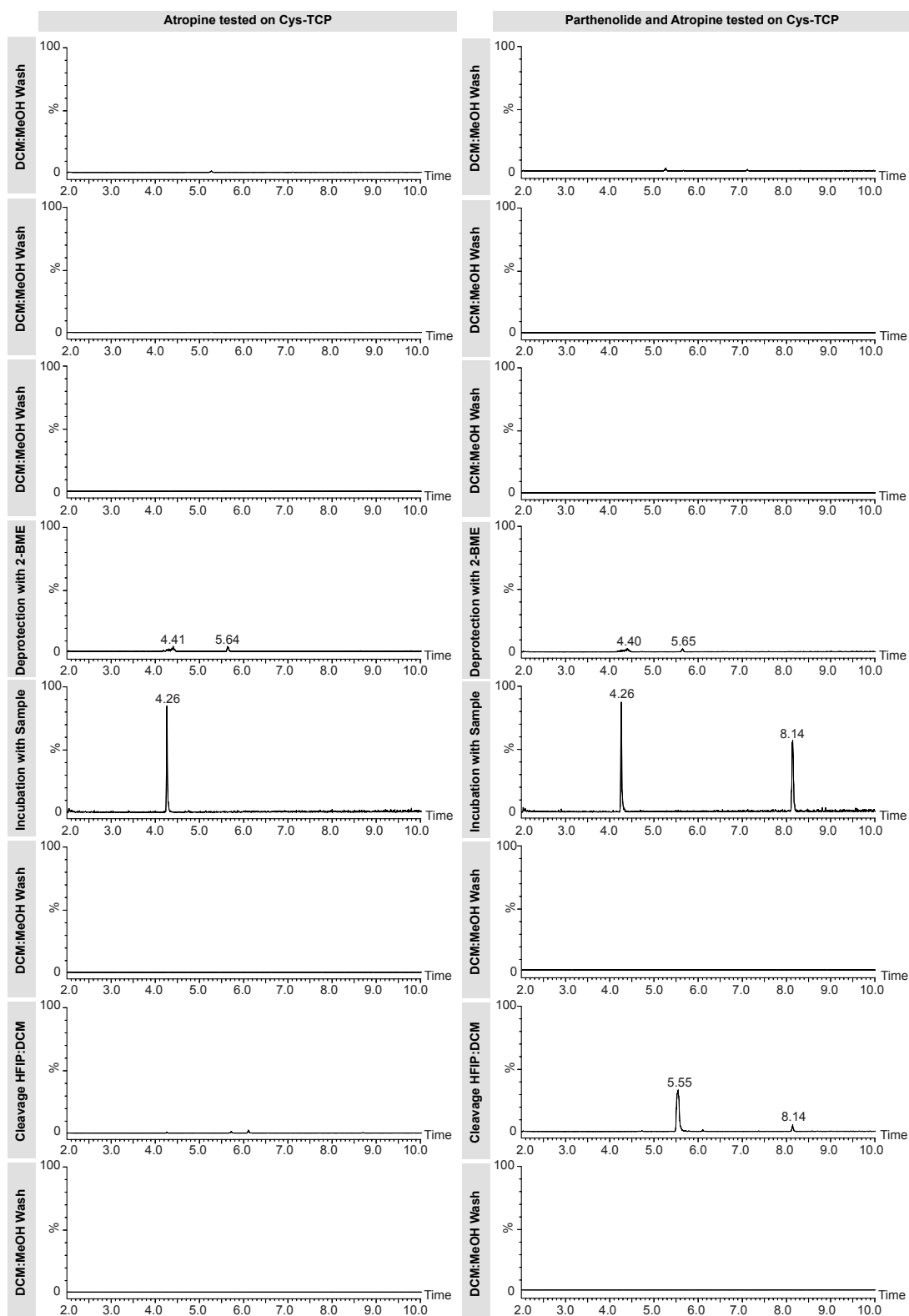


Figure S.10 Data from Cys-TCP proof-of-concept experiment. Left: data from the experiment with atropine, chromatograms scaled to $9.0E7$; right: data from the experiment with parthenolide and atropine, chromatograms scaled to $3.6E7$. HPLC-MS traces (positive ion mode) were recorded with a scan range m/z 121-1000.

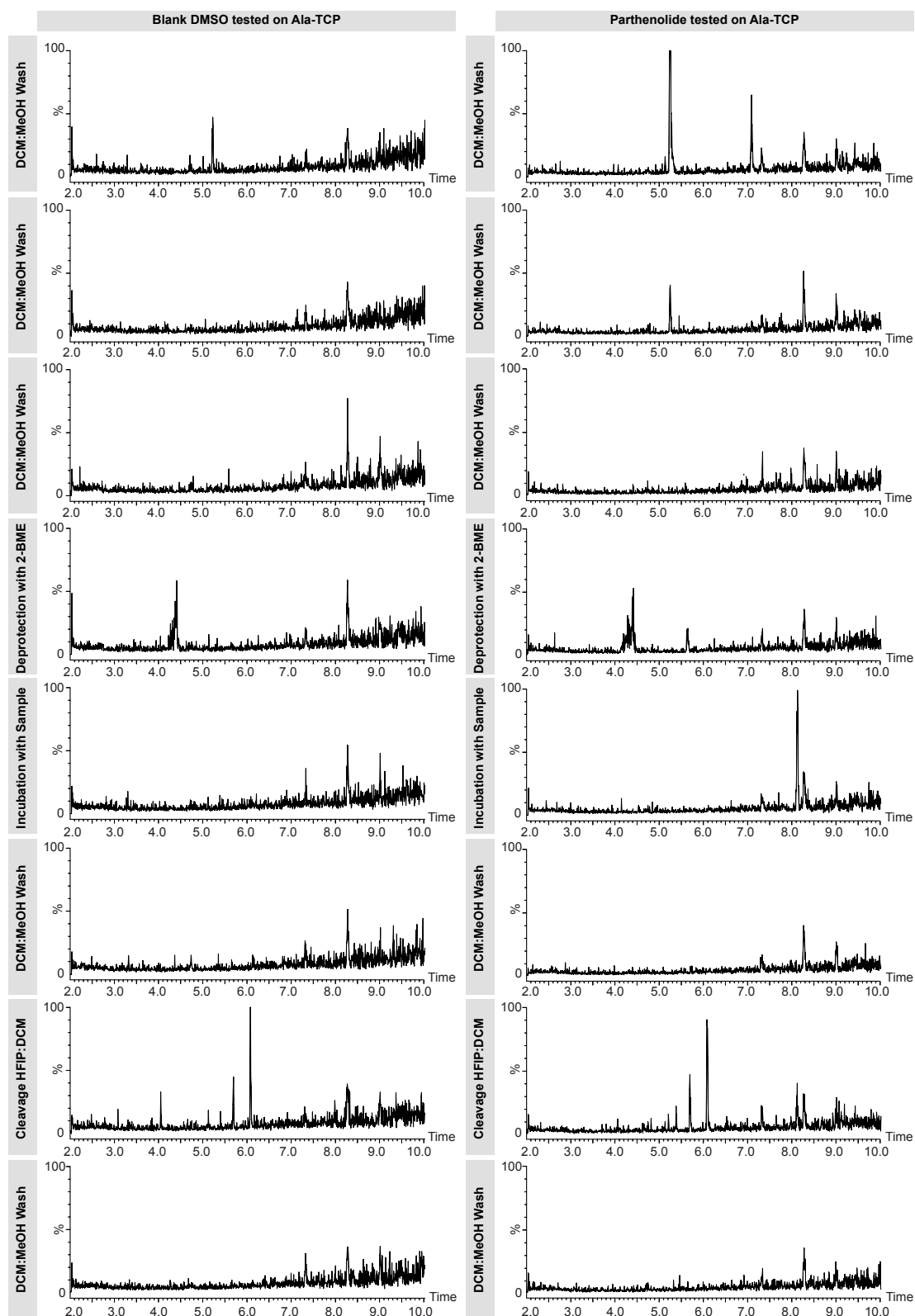


Figure S.11 Data from Ala-TCP proof-of-concept experiment. Left: data from the experiment with blank DMSO, chromatograms scaled to $4.0E6$; right: data from the experiment with parthenolide, chromatograms scaled to $5.5E6$. HPLC-MS traces (positive ion mode) were recorded with a scan range m/z 121-1000.

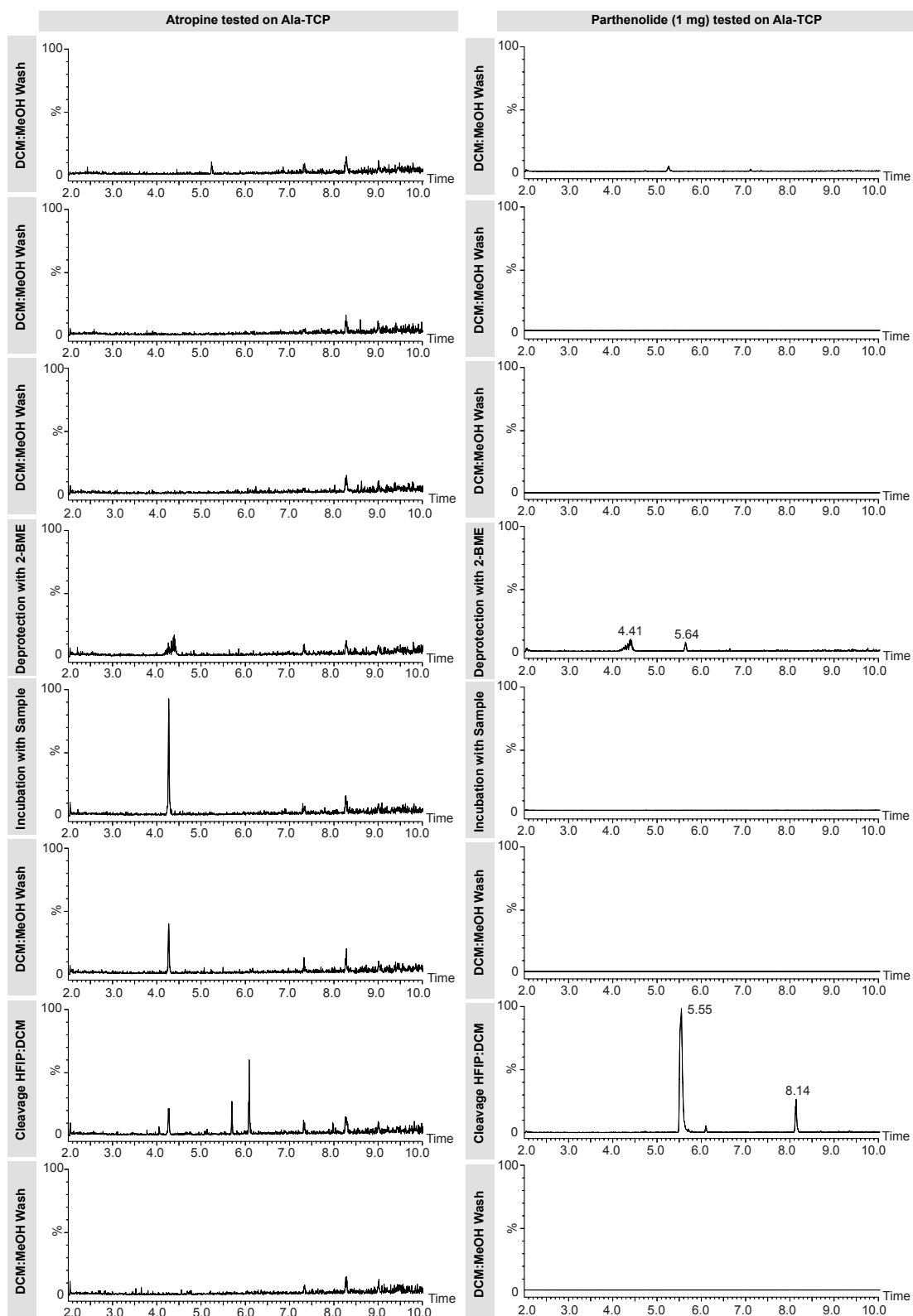


Figure S.12 Data from proof-of-concept experiment. Left: data from the Ala-TCP experiment with atropine, chromatograms scaled to 1.3×10^7 ; right: data from the Cys-TCP experiment with 1 mg parthenolide, chromatograms scaled to 8.5×10^7 . HPLC-MS traces (positive ion mode) were recorded with a scan range m/z 121-1000.

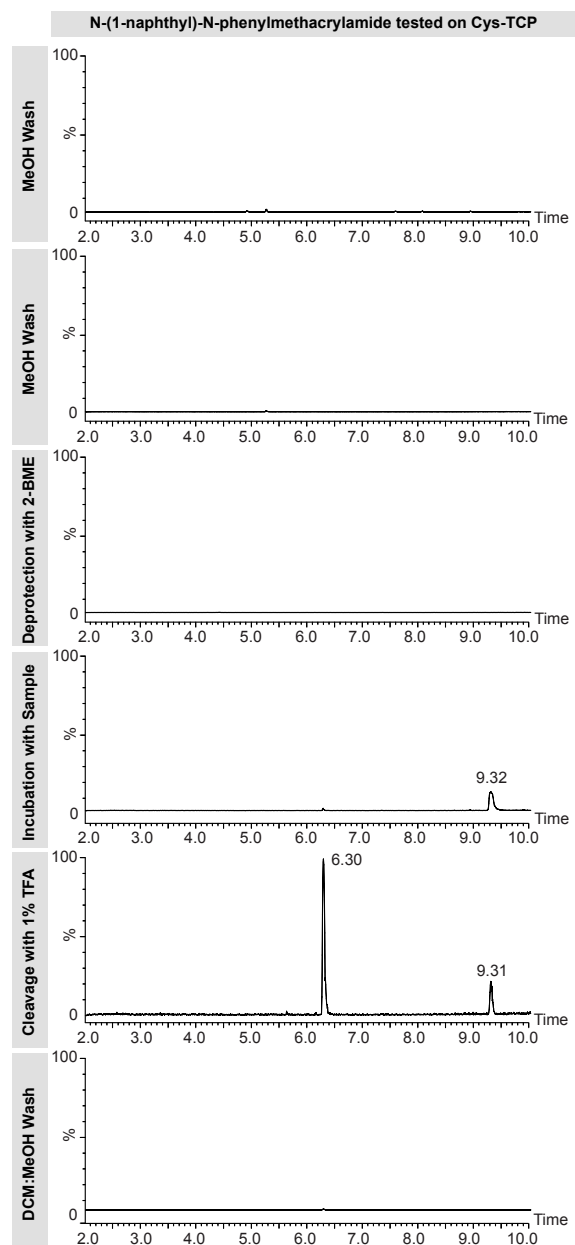


Figure S.13 Data from the Cys-TCP experiment with *N*-(1-naphthyl)-*N*-phenylmethacrylamide (1), scaled to 9.0E7. HPLC-MS traces (positive ion mode) were recorded with a scan range m/z 121-1000. The sample from the third wash step at the beginning and the final wash after incubation with compound were not recorded.

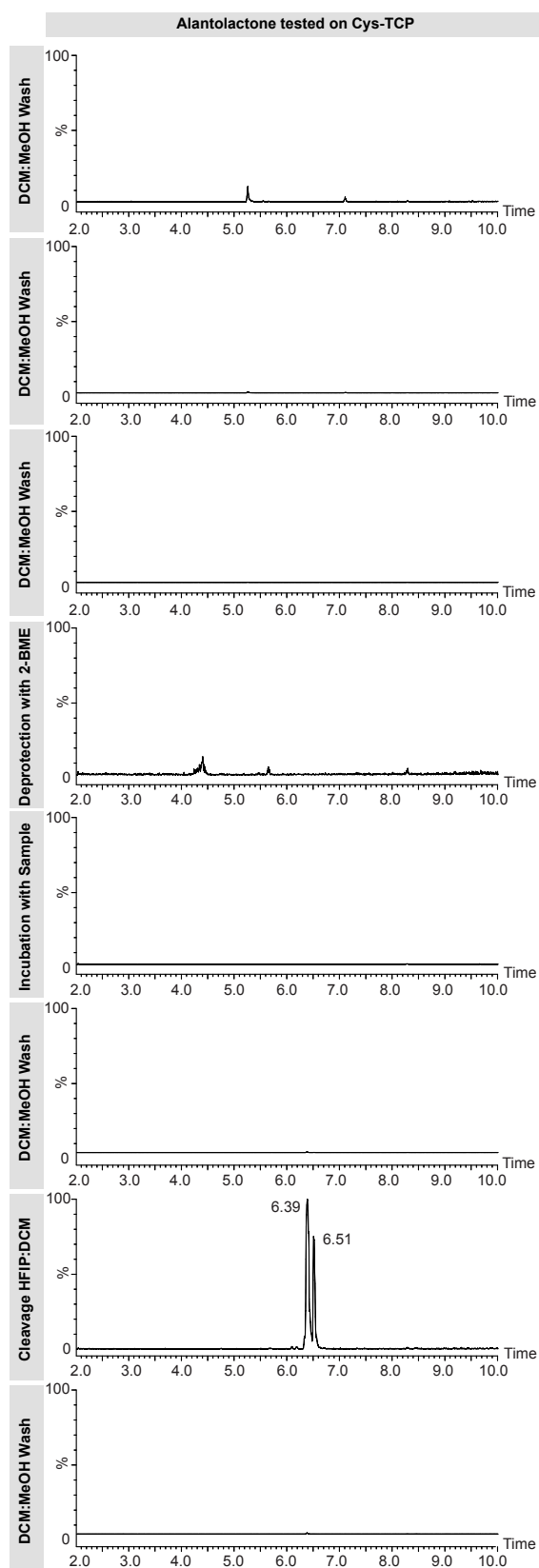


Figure S.14 Data from the Cys-TCP experiment with alantolactone (**2**), scaled to $9.0E7$. HPLC-MS traces (positive ion mode) were recorded with a scan range m/z 121-1000.

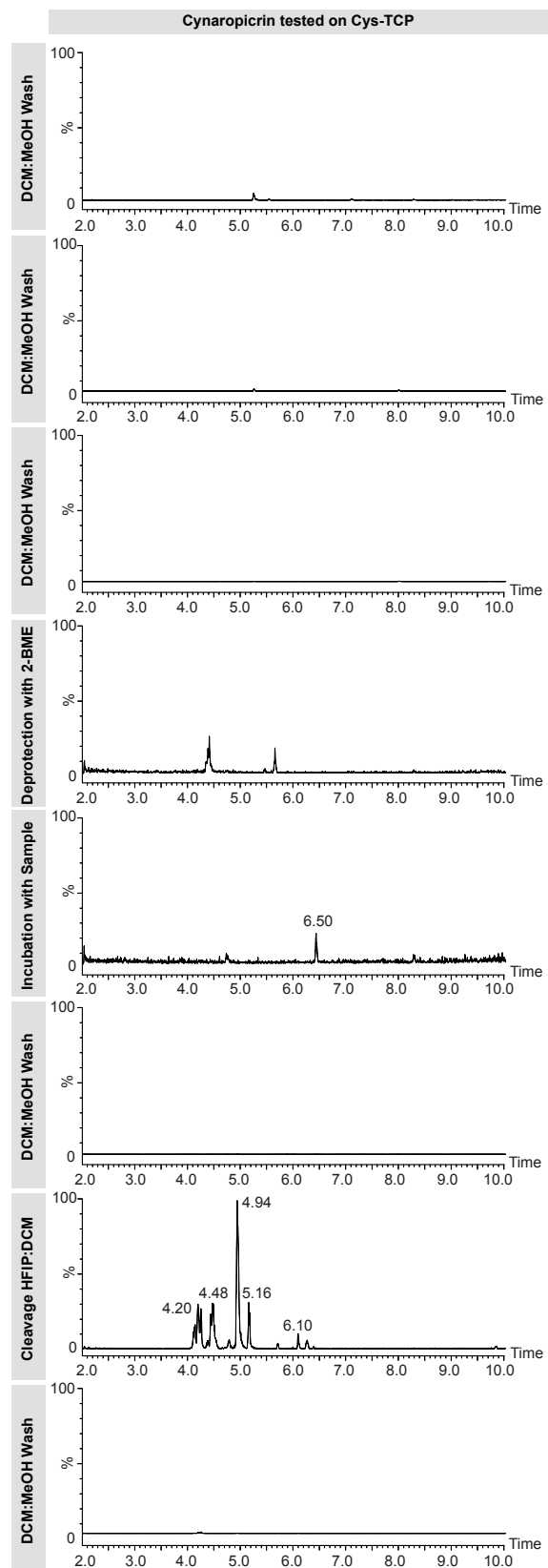


Figure S.15 Data from the Cys-TCP experiment with cynaropicrin (**3**), scaled to 5.0E7. HPLC-MS traces (positive ion mode) were recorded with a scan range m/z 121-1000.

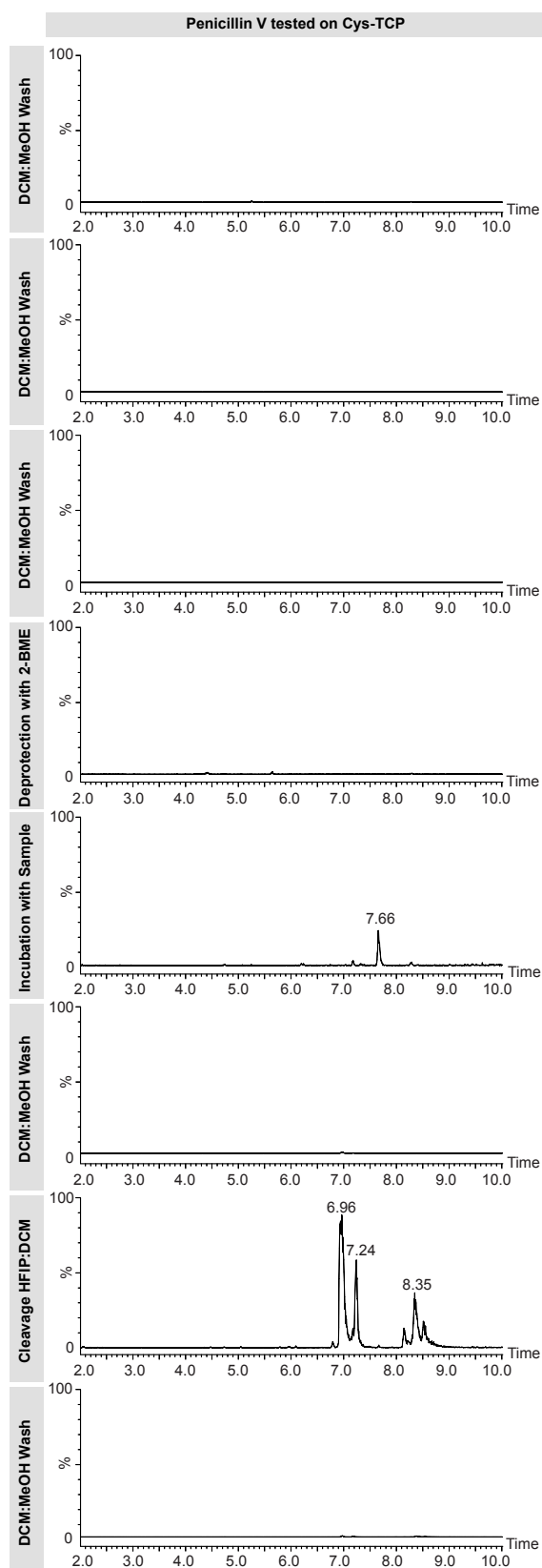


Figure S.16 Data from the Cys-TCP experiment with penicillin V (**4**), scaled to 1.2E8. HPLC-MS traces (positive ion mode) were recorded with a scan range m/z 121-1000.

Appendix

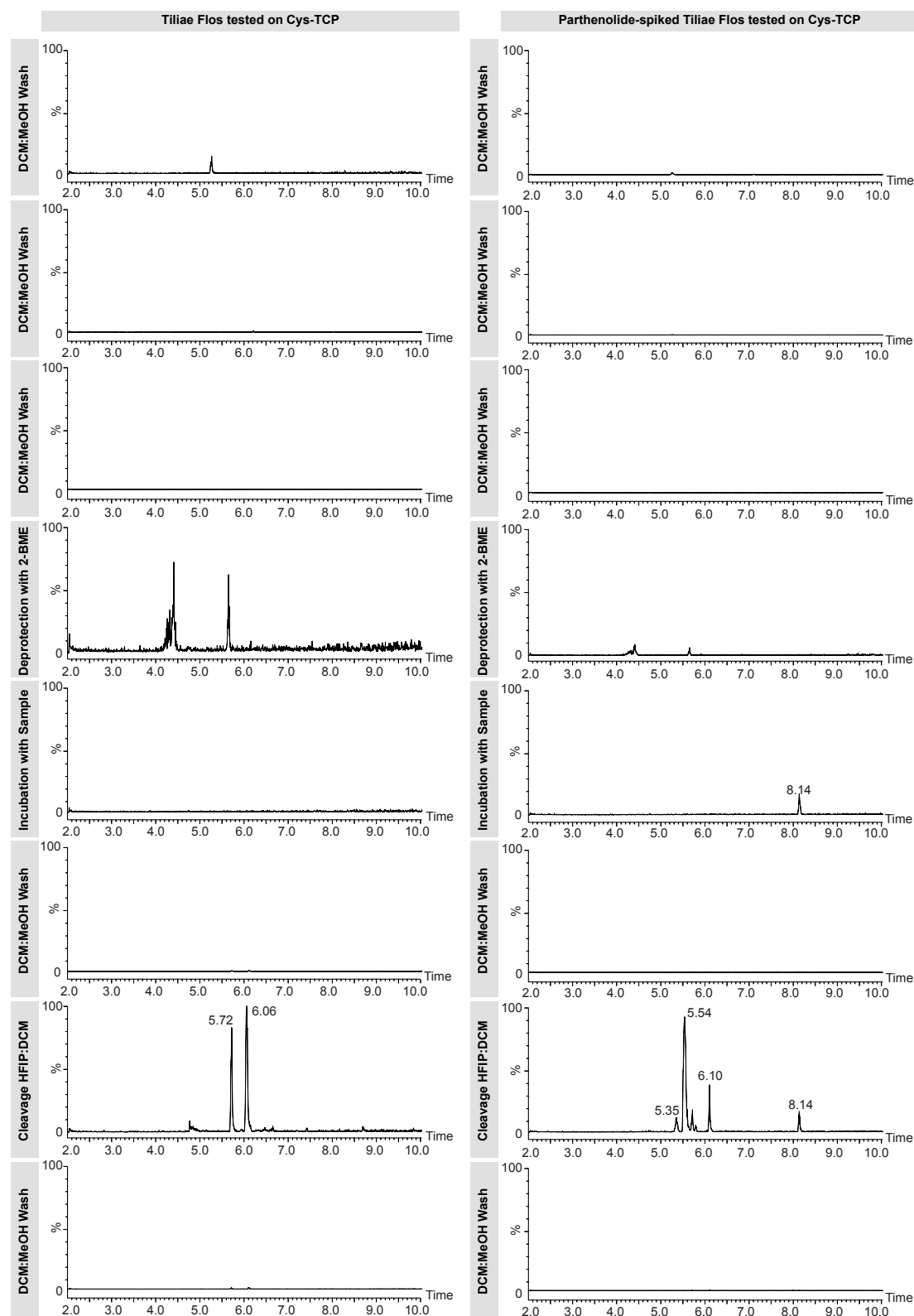


Figure S.17 Left: data from the Cys-TCP experiment with *Tiliae Flos* MeOH extract, chromatograms scaled to $4.0E7$; right: data from the Cys-TCP experiment with *Tiliae Flos* MeOH extract spiked with parthenolide, chromatograms scaled to $8.0E7$. HPLC-MS traces (positive ion mode) were recorded with a scan range m/z 121-1000.

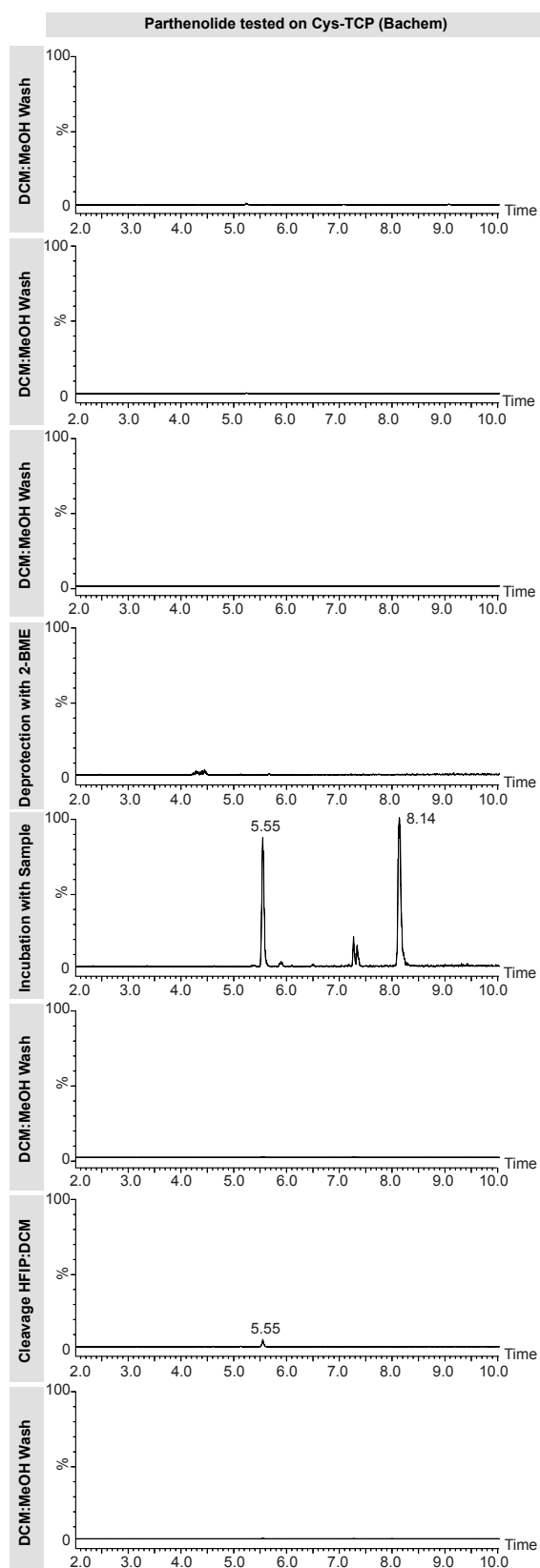


Figure S.18 Experiment of Cys-TCP made from Bachem resin with parthenolide, chromatograms scaled to $8.0E7$. HPLC-MS traces (positive ion mode) were recorded with a scan range m/z 121-1000.

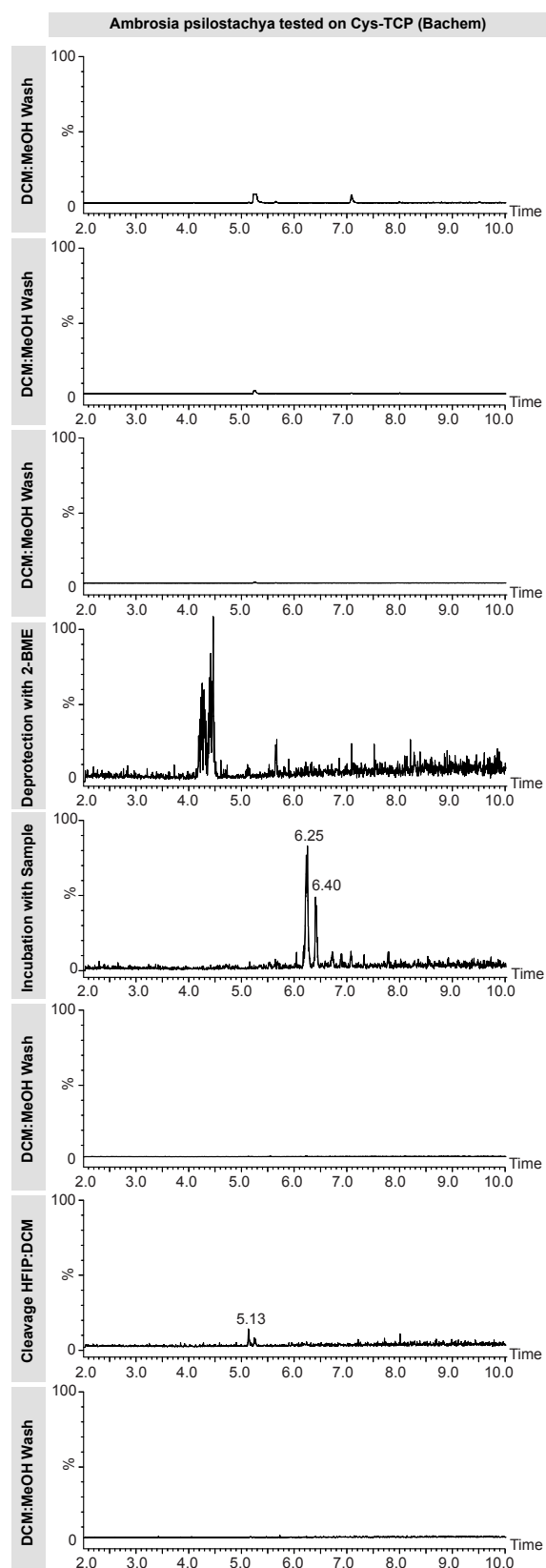


Figure S.19 Experiment of Cys-TCP made from Bachem resin with *Ambrosia psilostachya* extract (Lot P4129072-1), chromatograms scaled to $1.0E7$. HPLC-MS traces (positive ion mode) were recorded with a scan range m/z 121-1000.

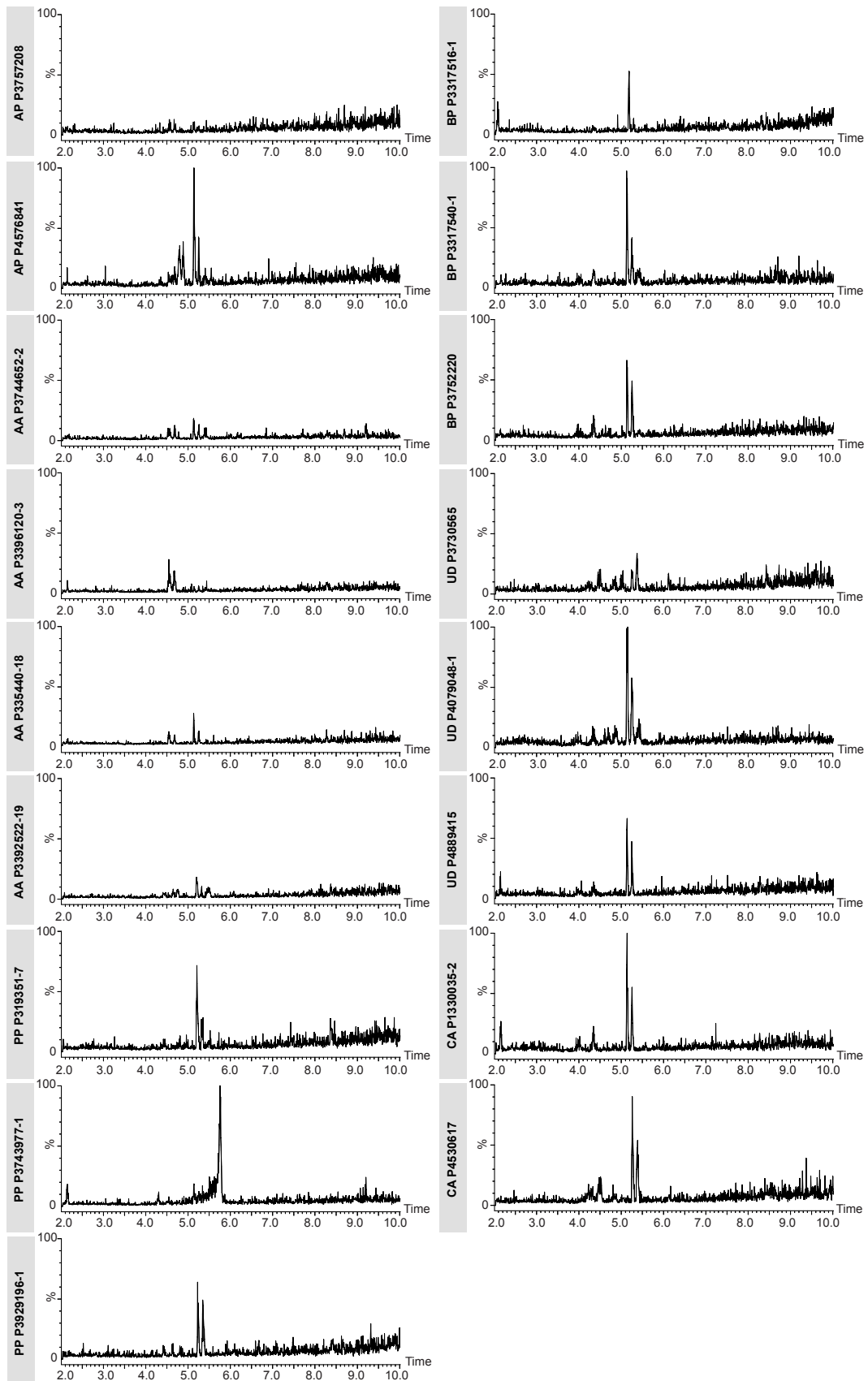


Figure S.20 Pollen extract experiments. Abbreviations: AP (*Ambrosia psilostachya*); AA (*Ambrosia*

Appendix

artemisiifolia); PP (*Phleum pratense*); BP (*Betula pendula*); CA (*Corylus avellana*). AA chromatograms scaled to 1.0E7, PP P3743977-1 scaled to 8.0E6, the remaining scaled to 5.0E6. HPLC-MS traces (positive ion mode) were recorded with a scan range m/z 121-1000.

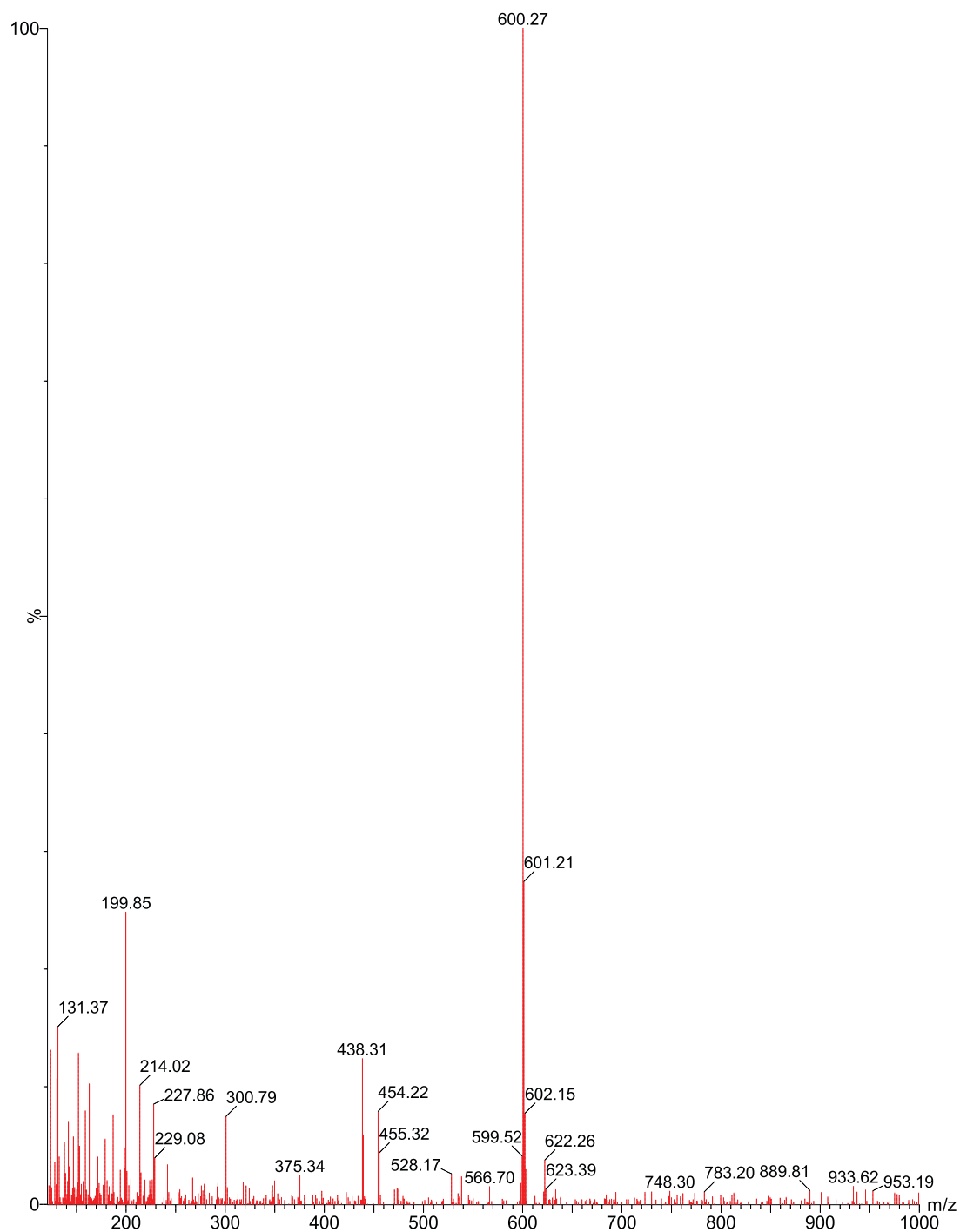


Figure S.21 MS data of compound **5a**, scaled to highest intensity.

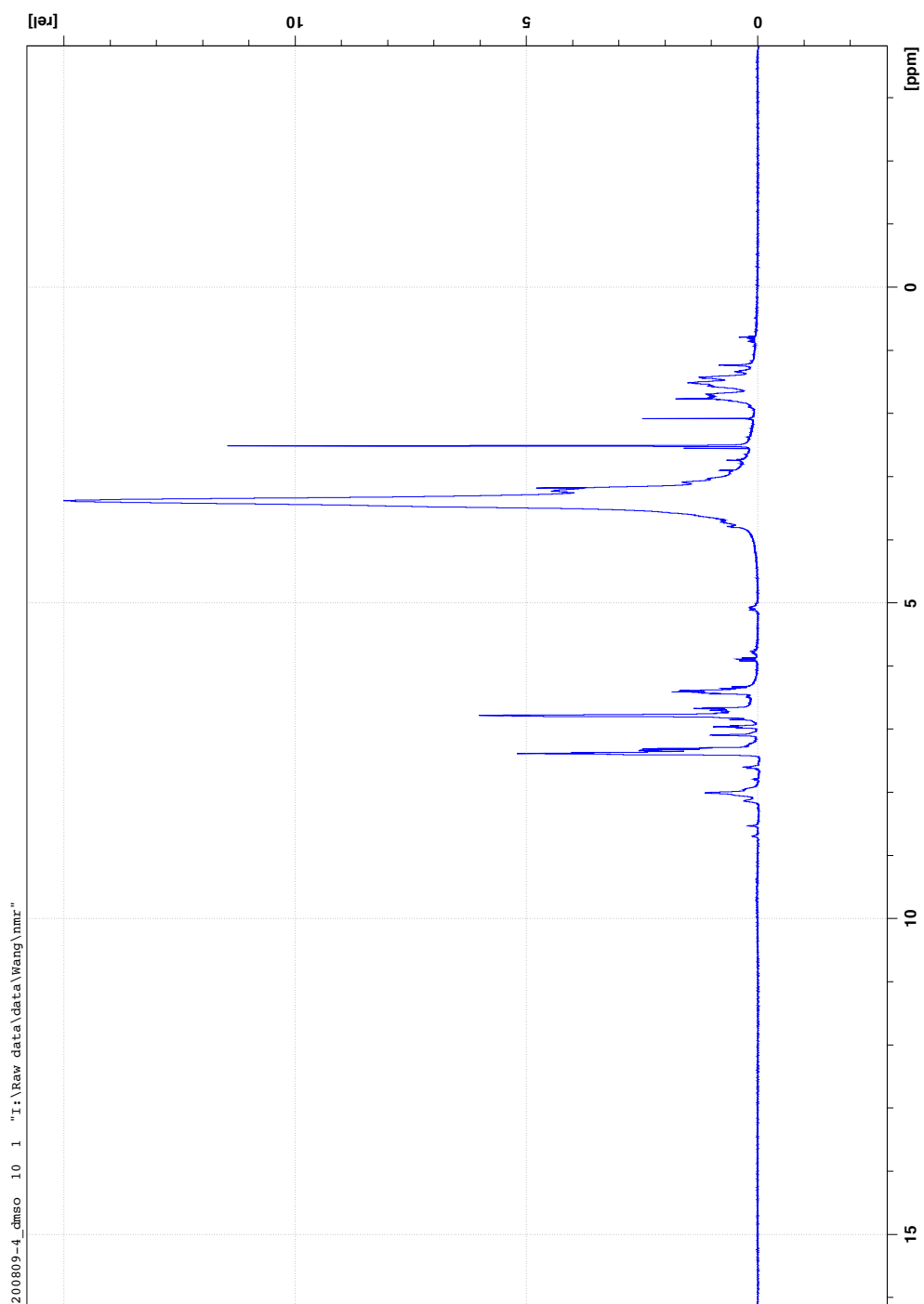


Figure S.22 ^1H spectrum of compound **5a**, recorded on the 500 MHz Avance IIITM spectrometer described in Chapter 2.2.5.

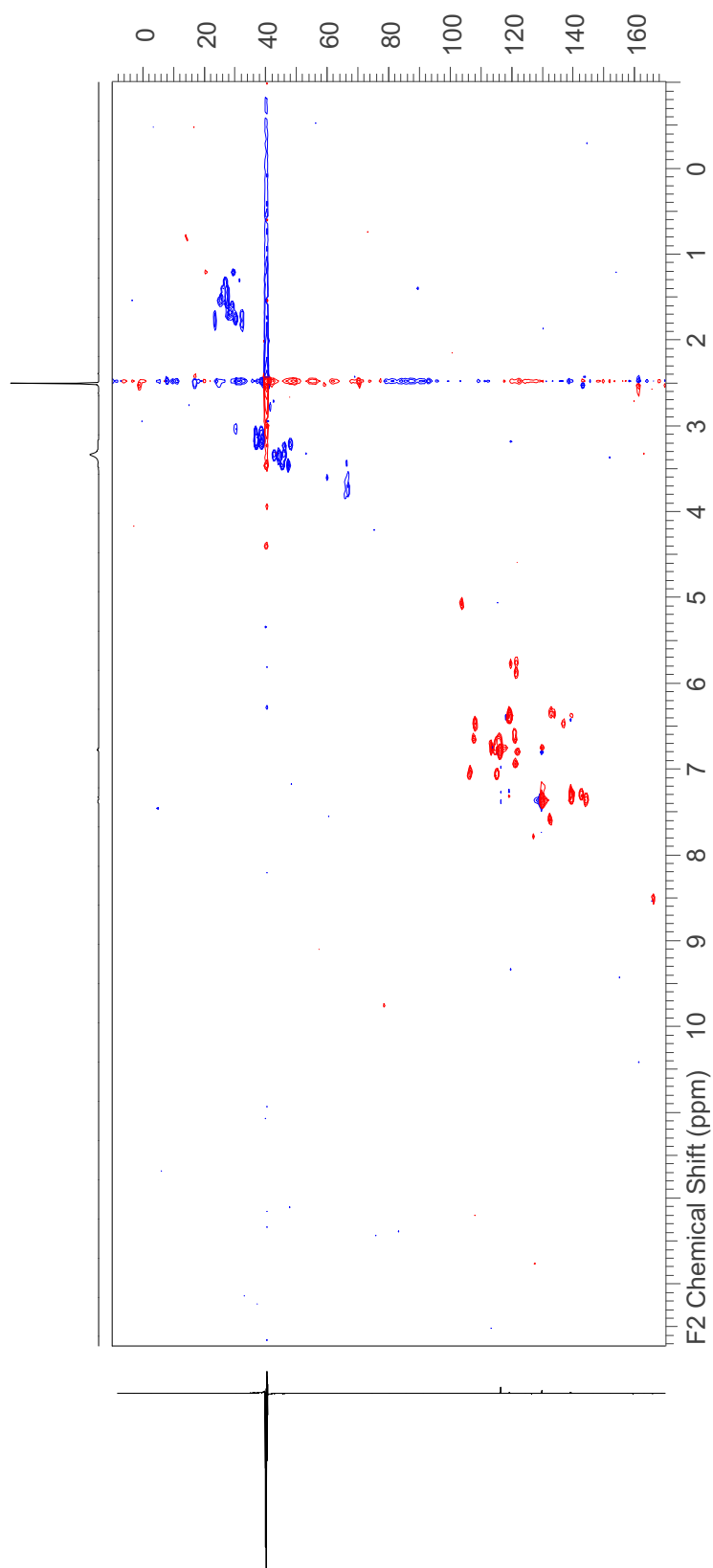


Figure S.23 NMR HSQC data of compound **5a**, recorded on the Bruker Avance III Neo 600 MHz NMR spectrometer described in Chapter 2.2.5.

Tables

Table S.1 PDA measurement results and interpolated concentrations for all the plant extracts measured.

Species	Lot Number	Solvent	Absorbance	Calculated Concentration (mM)	Standard Deviation (mM)
<i>Ambrosia psilostachya</i>	P3701938-2	Hexane	0.722	1.47	0.89
<i>Ambrosia psilostachya</i>	P3701938-2	THF	0.713	2.25	2.55
<i>Ambrosia psilostachya</i>	P3701938-2	MeOH	0.737	0.26	0.67
<i>Ambrosia psilostachya</i>	P3757208	Hexane	0.733	0.55	3.41
<i>Ambrosia psilostachya</i>	P3757208	THF	0.717	1.93	1.69
<i>Ambrosia psilostachya</i>	P3757208	MeOH	0.726	1.17	1.62
<i>Ambrosia psilostachya</i>	P4129072-1	Hexane	0.720	1.64	5.81
<i>Ambrosia psilostachya</i>	P4129072-1	THF	0.713	2.31	0.11
<i>Ambrosia psilostachya</i>	P4129072-1	MeOH	0.728	0.97	5.44
<i>Ambrosia psilostachya</i>	P4576841	Hexane	0.733	0.57	1.20
<i>Ambrosia psilostachya</i>	P4576841	THF	0.716	2.01	2.49
<i>Ambrosia psilostachya</i>	P4576841	MeOH	0.728	0.97	5.21
<i>Ambrosia artemisiifolia</i>	P3024704-3	Hexane	0.771	0.31	3.15
<i>Ambrosia artemisiifolia</i>	P3024704-3	THF	0.271	4.13	2.91
<i>Ambrosia artemisiifolia</i>	P3024704-3	MeOH	0.804	0.06	2.54
<i>Ambrosia artemisiifolia</i>	P3744652-2	Hexane	0.774	0.29	2.03
<i>Ambrosia artemisiifolia</i>	P3744652-2	THF	0.257	4.23	3.20
<i>Ambrosia artemisiifolia</i>	P3744652-2	MeOH	0.810	0.01	3.69
<i>Ambrosia artemisiifolia</i>	P3396120-3	Hexane	0.822	-0.09	4.32
<i>Ambrosia artemisiifolia</i>	P3396120-3	THF	0.264	4.18	2.50
<i>Ambrosia artemisiifolia</i>	P3396120-3	MeOH	0.777	0.26	4.51
<i>Ambrosia artemisiifolia</i>	P335440-18	Hexane	0.873	-0.47	4.43
<i>Ambrosia artemisiifolia</i>	P335440-18	THF	0.341	3.59	2.35
<i>Ambrosia artemisiifolia</i>	P335440-18	MeOH	0.806	0.05	3.47
<i>Ambrosia artemisiifolia</i>	P3392522-19	Hexane	0.789	0.14	7.09
<i>Ambrosia artemisiifolia</i>	P3392522-19	THF	0.254	4.25	2.52
<i>Ambrosia artemisiifolia</i>	P3392522-19	MeOH	0.772	0.30	3.80
<i>Phleum pratense</i>	P319351-7	Hexane	0.717	0.74	1.88
<i>Phleum pratense</i>	P319351-7	THF	0.420	2.98	3.24
<i>Phleum pratense</i>	P319351-7	MeOH	0.240	4.35	4.41
<i>Phleum pratense</i>	P3280848-1	Hexane	0.706	0.80	3.86
<i>Phleum pratense</i>	P3280848-1	THF	0.206	4.61	3.62
<i>Phleum pratense</i>	P3280848-1	MeOH	0.464	2.61	9.06
<i>Phleum pratense</i>	P3743977-1	Hexane	0.669	1.09	3.03
<i>Phleum pratense</i>	P3743977-1	THF	0.188	4.75	3.32

Appendix

<i>Phleum pratense</i>	P3743977-1	MeOH	0.530	2.12	8.18
<i>Phleum pratense</i>	P3929196-1	Hexane	0.771	0.31	2.87
<i>Phleum pratense</i>	P3929196-1	THF	0.198	4.67	3.69
<i>Phleum pratense</i>	P3929196-1	MeOH	0.535	2.09	5.95
<i>Betula pendula</i>	P3317516-1	Hexane	0.328	0.33	3.23
<i>Betula pendula</i>	P3317516-1	THF	1.948	1.95	4.22
<i>Betula pendula</i>	P3317516-1	MeOH	0.042	0.04	0.53
<i>Betula pendula</i>	P3317540-1	Hexane	0.272	0.27	0.59
<i>Betula pendula</i>	P3317540-1	THF	2.100	2.10	3.06
<i>Betula pendula</i>	P3317540-1	MeOH	0.014	0.01	0.35
<i>Betula pendula</i>	P3752220	Hexane	-0.011	-0.01	0.47
<i>Betula pendula</i>	P3752220	THF	2.468	2.47	3.54
<i>Betula pendula</i>	P3752220	MeOH	0.083	0.08	0.55
<i>Urtica dioica</i>	P3730565	Hexane	0.856	0.86	1.94
<i>Urtica dioica</i>	P3730565	THF	2.288	2.29	3.79
<i>Urtica dioica</i>	P3730565	MeOH	0.421	0.42	0.68
<i>Urtica dioica</i>	P4079048-1	Hexane	0.336	0.34	1.26
<i>Urtica dioica</i>	P4079048-1	THF	1.732	1.73	2.54
<i>Urtica dioica</i>	P4079048-1	MeOH	0.481	0.48	1.57
<i>Urtica dioica</i>	P4889415	Hexane	0.336	0.34	1.26
<i>Urtica dioica</i>	P4889415	THF	2.953	2.95	3.54
<i>Urtica dioica</i>	P4889415	MeOH	0.685	0.69	1.04
<i>Corylus avellana</i>	P976555-1	Hexane	0.724	0.72	1.54
<i>Corylus avellana</i>	P976555-1	THF	1.945	1.95	3.34
<i>Corylus avellana</i>	P976555-1	MeOH	0.266	0.27	1.92
<i>Corylus avellana</i>	P1330035-2	Hexane	0.307	0.31	0.71
<i>Corylus avellana</i>	P1330035-2	THF	1.927	1.93	3.33
<i>Corylus avellana</i>	P1330035-2	MeOH	0.042	0.04	1.83
<i>Corylus avellana</i>	P4530617	Hexane	0.282	0.28	1.06
<i>Corylus avellana</i>	P4530617	THF	3.166	3.17	3.75
<i>Corylus avellana</i>	P4530617	MeOH	0.121	0.12	0.67

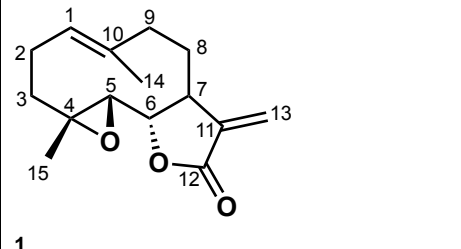
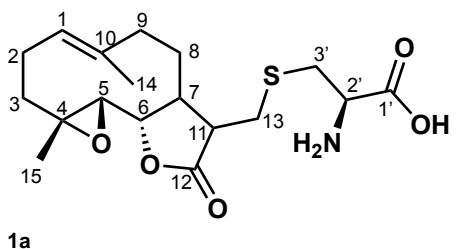
Table S.2 Spectroscopic quantification of cysteine by using an adapted version of the indirect method previously used to quantify electrophile content.

Calibrants	Absorbance Run 1		Absorbance Run 2		Absorbance Run 3		Average Absorbance	10 ³ mmol	
cal6	6.61E-01		7.51E-01		7.74E-01		7.29E-01	5.00E-01	
cal5	4.18E-01		6.49E-01		6.01E-01		5.56E-01	2.50E-01	
cal4	2.07E-01		2.60E-01		2.75E-01		2.48E-01	1.00E-01	
cal3	7.57E-02		1.74E-01		1.66E-01		1.38E-01	5.00E-02	
cal2	8.70E-02		6.97E-02		8.67E-02		8.11E-02	2.50E-02	
cal1	-1.77E-02		1.43E-02		3.20E-02		9.56E-03	1.00E-02	
cal0	9.00E-03		-4.97E-02		-1.17E-02		-1.74E-02	0.00E+00	
Samples	Absorbance	[c10 ³ mmol]	Absorbance	10 ³ mmol	Absorbance	10 ³ mmol	Average Absorbance	10 ³ mmol	St. Dev.
1	2.39E-01	1.47E-04	1.61E-01	8.05E-05	ND	ND	2.00E-01	1.14E-01	3.34E-05
2	-3.33E-04	-2.02E-05	-5.40E-02	-2.70E-05	ND	ND	-2.72E-02	-2.36E-02	3.38E-06
3	4.33E-03	-1.70E-05	-7.80E-02	-3.90E-05	ND	ND	-3.68E-02	-2.80E-02	1.10E-05
4	3.00E-02	1.00E-06	1.15E-01	5.74E-05	ND	ND	7.24E-02	2.92E-02	2.82E-05

ND: Sample amount not sufficient for a 3rd run

Appendix

Table S.3 ^1H and ^{13}C NMR Spectroscopic Data (500 MHz) for parthenolide (**1**) (measured in methanol- d_4) and adduct **1a** (measured in DMSO-d_6).

	 1		 1a	
position	δ_{C} , type ^a	δ_{H} (J in Hz)	δ_{C} , type ^a	δ_{H} (J in Hz)
1	126.5, CH	5.30, br dd (12.2, 2.4)	124.6, CH	5.22, m
2	25.5, CH_2	2.16, m 2.47, m	23.7, CH_2	2.34 ^b 2.06 ^b
3	37.9, CH_2	2.1, ddd (12.6, 5.3, 2.0) 1.25, m	36.1, CH_2	2.01 ^b 1.12, m
4	63.7, C		61.2, C	
5	68.1, CH	2.92, br s	65.4, CH	2.78 ^b
6	84.7, CH	3.99, m	81.6, CH	3.98, t (9.0)
7	49.1, CH	2.94, m	47.0, CH	2.26 ^b
8	32.0, CH_2	2.18, s 1.80, m	28.8, CH_2	1.69 ^b 1.91, m
9	42.6, CH_2	2.22, m 2.35, m	40.4, CH_2	2.16 ^b 2.03, m
10	136.7, C		134.4, C	
11	141.8, C		47.5, CH	2.78 ^b
12	172.1, C		175.8, C	
13	122.1, CH_2	5.73, d (3.1) 6.23, d (4.0)	30.1, CH_2	2.98 ^b 2.91 ^b
14	17.6, CH_3	1.73, s	16.6, CH_3	1.64, s
15	18.1, CH_3	1.31, s	16.8, CH_3	1.20, s
1'			169.6, C	
2'			53.8, CH	3.51, m
3'			34.8, CH_2	2.91, m 3.11, dd (13.8, 3.8)

^a Chemical shifts extracted from HSQC and HMBC

^b Overlapping signals

Table S.4 Calibration curve of cysteine with IS methionine, automatic integration, no manual adjustment.

Name	Type	Std. Conc.	RT	Area	ng/ml	IS Area
Blank1-1	Blank					
Cal0-1	Standard	0				113.673
Cal1-1	Standard	0.25				151.665
Cal2-1 ^a	Standard	1.25	0.62	104.793	1	319.716
Cal3-1	Standard	2.5	0.62	248.616	1.2	606.439
Cal4-1	Standard	5	0.62	654.743	3.2	453.013
Cal5-1	Standard	10	0.62	1993.823	9.2	405.767
Cal6-1	Standard	20	0.62	5958.632	21.5	411.14
Cal7-1	Standard	25	0.62	11162.282	28.2	528.621
Blank2-1	Blank					
QCL1	QC	0.75	0.62	436.709	1.7	646.048
QCL2	QC	0.75	0.62	537.852	1.8	740.657
QCM1	QC	12.5	0.62	10289.195	17.8	915.663
QCM2	QC	12.5	0.62	10196.908	14.9	1138.746
QCH1	QC	20	0.62	18123.584	22.5	1175.375
QCH2	QC	20	0.62	17884.93	20.4	1328.296
Blank1-2	Blank					
Cal0-2	Standard	0				1459.471
Cal1-2 ^a	Standard	0.25	0.62	219.607	0.6	1613.934
Cal2-2	Standard	1.25	0.62	1192.096	2.2	1292.29
Cal3-2	Standard	2.5	0.62	2328.191	3.3	1605.632
Cal4-2	Standard	5	0.62	4596.884	5.6	1681.016
Cal5-2	Standard	10	0.62	9192.807	10.7	1556.723
Cal6-2	Standard	20	0.62	18481.809	19.3	1473.529
Cal7-2	Standard	25	0.62	23438.531	21	1666.578
Blank2-2	Blank					

Appendix

Table S.5 Calibration curve of cysteine with IS NAC, automatic integration, no manual adjustment.

Name	Type	Std. Conc.	RT	Area	ng/ml	IS Area
Blank1-1	Blank					
Cal0-1	Standard	0				113.673
Cal1-1	Standard	0.25				151.665
Cal2-1 ^a	Standard	1.25	0.62	104.793	1	319.716
Cal3-1	Standard	2.5	0.62	248.616	1.2	606.439
Cal4-1	Standard	5	0.62	654.743	3.2	453.013
Cal5-1	Standard	10	0.62	1993.823	9.2	405.767
Cal6-1	Standard	20	0.62	5958.632	21.5	411.14
Cal7-1	Standard	25	0.62	11162.282	28.2	528.621
Blank2-1	Blank					
QCL1	QC	0.75	0.62	436.709	1.7	646.048
QCL2	QC	0.75	0.62	537.852	1.8	740.657
QCM1	QC	12.5	0.62	10289.195	17.8	915.663
QCM2	QC	12.5	0.62	10196.908	14.9	1138.746
QCH1	QC	20	0.62	18123.584	22.5	1175.375
QCH2	QC	20	0.62	17884.93	20.4	1328.296
Blank1-2	Blank					
Cal0-2	Standard	0				1459.471
Cal1-2 ^a	Standard	0.25	0.62	219.607	0.6	1613.934
Cal2-2	Standard	1.25	0.62	1192.096	2.2	1292.29
Cal3-2	Standard	2.5	0.62	2328.191	3.3	1605.632
Cal4-2	Standard	5	0.62	4596.884	5.6	1681.016
Cal5-2	Standard	10	0.62	9192.807	10.7	1556.723
Cal6-2	Standard	20	0.62	18481.809	19.3	1473.529
Cal7-2	Standard	25	0.62	23438.531	21	1666.578
Blank2-2	Blank					

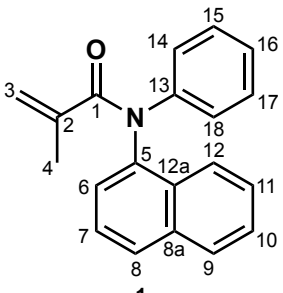
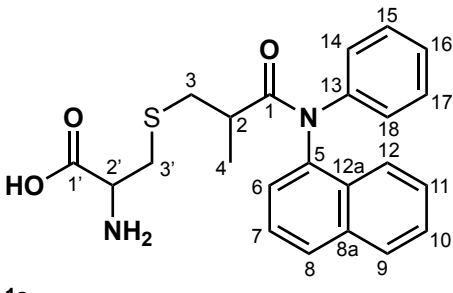
Table S.6 Quantification of cysteine in proof-of-concept samples with Cys-TCP (scale 0.15 mmol) with IS atropine, manual integration.

Name	Type	Std. Conc.	RT	Area	ng/ml	IS Area
Blank1-1	Blank					
Cal0-1	Standard	0				213858.688
Cal1-1	Standard	0.25	0.64	523.925	0.3	243332.578
Cal2-1 ^a	Standard	1.25	0.64	2484.117	1.1	228677.844
Cal3-1	Standard	2.5	0.64	5709.601	2.3	250124.828
Cal4-1	Standard	5	0.64	11604.783	4.8	244169.5
Cal5-1	Standard	10	0.64	23296.49	9.4	254312.063
Cal6-1	Standard	20	0.65	47050.141	20	247741.609
Cal7-1	Standard	25	0.64	57804.887	24.3	252900.813
Blank2-1	Blank					
QCL1	QC	0.75	0.65	1795.896	0.8	247570.25
QCL2	QC	0.75	0.64	1877.264	0.8	248872.813
QCM1	QC	12.5	0.64	30555.596	12.3	255019.609
QCM2	QC	12.5	0.64	29894.703	12.3	249559.953
QCH1	QC	20	0.64	45520.68	19	250940.969
QCH2	QC	20	0.64	46983.484	19.6	250982.125
Blank1-2	Blank					
Cal0-2	Standard	0				225349.156
Cal1-2 ^a	Standard	0.25	0.65	608.576	0.3	251773.75
Cal2-2	Standard	1.25	0.64	2788.772	1.2	240800.719
Cal3-2	Standard	2.5	0.64	6169.033	2.5	250480.953
Cal4-2	Standard	5	0.64	12669.277	5.4	237431.156
Cal5-2	Standard	10	0.64	24615.508	10.3	245491.969
Cal6-2	Standard	20	0.64	47031.488	20.4	241995.328
Cal7-2	Standard	25	0.64	58106.133	25.5	243358.406
Blank2-2	Blank					
Proof-of-concept Blank	Analyte	1	2.03	241201.172	1.0	241201.172
Proof-of-concept Parthenolide	Analyte	1	2.03	261820.078	1.1	261820.078
Proof-of-concept Atropine	Analyte	1	2.04	288932.281	1.2	288932.281
Proof-of-concept Parthenolide and Atropine	Analyte	1	2.03	262343.281	1.1	262343.281
Proof-of-concept Tiliae Flos	Analyte	1	2.04	257624.938	1.1	257624.938
Proof-of-concept Tiliae Flos spiked with Parthenolide	Analyte	1	2.03	257943.766	1.1	257943.766
Proof-of-concept 1 mg Parthenolide	Analyte	1	2.04	252070.359	1.0	252070.359

^a excluded

Appendix

Table S.7 ¹H and ¹³C NMR Spectroscopic Data (500 MHz) for *N*-(1-naphthyl)-*N*-phenylmethacrylamide (**1**) (measured in DMSO-d₆) and adduct **1a**^a (measured in CDCl₃).

	 1		 1a	
position	δ _c , type ^b	δ _H (J in Hz)	δ _c , type ^c	δ _H (J in Hz)
1			Not observed	
2			38.5, CH	2.59 ^d
3		5.18, 5.04, br s	36.0, CH ₂	2.58 ^d 3.01 ^d
4		1.81, m	18.5, CH ₃	1.06, m
5			Not observed	
6		7.17, quin (4.3)	125.6, CH	7.08, m
7		7.55 ^d	125.5, CH	7.47 ^d
8		7.55 ^d	127.1, CH	7.57, m
8a			Not observed	
9		7.93, m	122.9, CH	8.08, m
10		7.55 ^d	126.3, CH	7.52 ^d
11		7.55 ^d	126.3, CH	7.52 ^d
12		7.31, d (4.3)	128.3, CH	7.85, m
12a			Not observed	
13			Not observed	
14		7.31, d (4.3)	128.4, CH	7.52 ^d
15		8.00 ^d	128.5, CH	7.24 ^d
16		7.31, d (4.3)	128.4, CH	7.52 ^d
17		8.00 ^d	128.5, CH	7.24 ^d
18		7.31, d (4.3)	128.4, CH	7.52 ^d
1'			Not observed	
2'			53.9, CH	3.88, m
3'			33.7, CH ₂	3.01 ^d

^a Only ¹H spectrum recorded

^b Data not recorded

^c Chemical shifts extracted from HSQC and HMBC

^d Overlapping signals

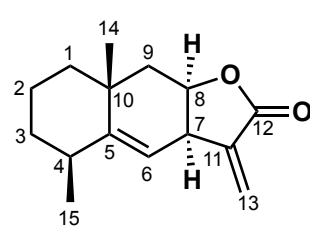
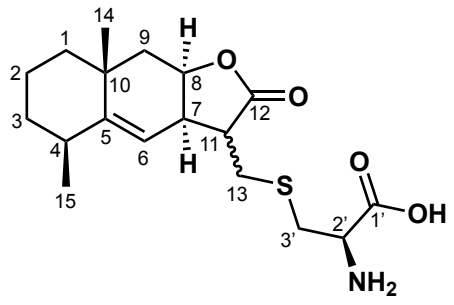
Table S.8. ¹H and ¹³C NMR Spectroscopic Data (500 MHz) for alantholactone (**2**) and adduct **2a** (both measured in DMSO-d₆).

position	2		2a	
	δ_c , type ^a	δ_H (J in Hz)	δ_c , type ^a	δ_H (J in Hz)
1	40.7, CH ₂	1.11, m 1.53, m	42.3, CH ₂	1.58, br d (3.7) 1.13, m
2	15.9, CH ₂	1.40, m 1.78, m	17.2, CH ₂	1.64, m 1.58, m
3	31.9, CH ₂	1.52, br d (1.5)	33.1, CH ₂	1.55, m
4	36.4, CH	2.45, m	38.5, CH	2.52, m
5	147.3, C		Not observed	
6	119.3, CH	5.22, d (4.3)	116.1, CH	5.32, d (2.8)
7	38.2, CH	3.67, dddd (6.6, 4.3, 1.9, 1.9)	37.8, CH	3.19, br d (5.5)
8	75.4, CH	4.86, ddd (6.7, 3.1, 3.1)	77.1, CH	4.81, m
9	41.7, CH ₂	1.53, m 1.99, dd (15.0, 3.8)	43.0, CH ₂	1.54, br s 2.01, m
10	31.7, C		Not observed	
11	139.5, C		49.1, CH	2.52, m
12	169.2, C		Not observed	
13	121.1, CH ₂	6.03, d (1.8) 5.76, d (1.5)	29.1, CH ₂	2.49, m 2.93, br d (1.8)
14	27.9, CH ₃	1.11, s	29.2, CH ₃	1.18, m
15	22.1, CH ₃	1.06, d (7.3)	23.4, CH ₃	1.13, d (7.6)
1'			Not observed	
2'			55.4, CH	3.36, m
3'			36.8, CH ₂	2.77, m 3.03, m

^a Chemical shifts extracted from HSQC and HMBC

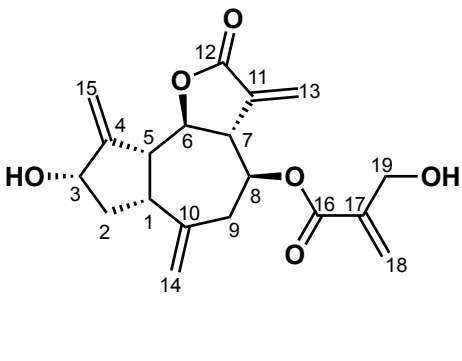
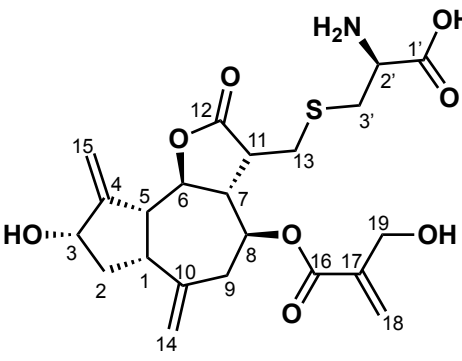
Appendix

Table S.9. ^1H and ^{13}C NMR Spectroscopic Data (500 MHz, DMSO- d_6) for alantholactone (**2**) and adduct **2b**.

	 2		 2b	
position	δ_{C} , type ^a	δ_{H} (J in Hz)	δ_{C} , type ^a	δ_{H} (J in Hz)
1	40.7, CH ₂	1.11, m 1.53, m	41.1, CH ₂	1.12, m 1.54, m
2	15.9, CH ₂	1.40, m 1.78, m	16.1, CH ₂	1.40, br d (13.4) 1.79, br d (13.1)
3	31.9, CH ₂	1.52, br d (1.5)	32.1, CH ₂	1.53, m
4	36.4, CH	2.45, m	36.8, CH	2.46, m
5	147.3, C		147.3, C	
6	119.3, CH	5.22, d (4.3)	120.0, CH	5.22, d (3.4)
7	38.2, CH	3.67, dddd (6.6, 4.3, 1.9, 1.9)	38.8, CH	3.00, m
8	75.4, CH	4.86, ddd (6.7, 3.1, 3.1)	76.2, CH	4.96, m
9	41.7, CH ₂	1.53, m 1.99, dd (15.0, 3.8)	41.8, CH ₂	1.51, m 1.97, dd (14.7, 3.1)
10	31.7, C		Not observed	
11	139.5, C		48.0, CH	2.51, m
12	169.2, C		176.5, C	
13	121.1, CH ₂	6.03, d (1.8) 5.76, d (1.5)	31.6, CH ₂	2.91, m
14	27.9, CH ₃	1.11, s	28.1, CH ₃	1.16, s
15	22.1, CH ₃	1.06, d (7.3)	22.1, CH ₃	1.11, d (7.3)
1'			Not observed	
2'			53.5, CH	3.36, m
3'			33.9, CH ₂	2.82, m 3.06, br d (11.9)

^a Chemical shifts extracted from HSQC and HMBC

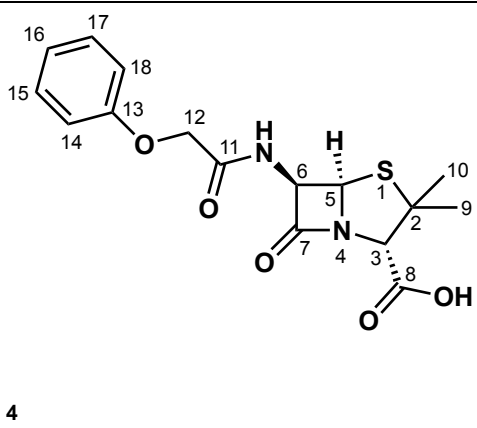
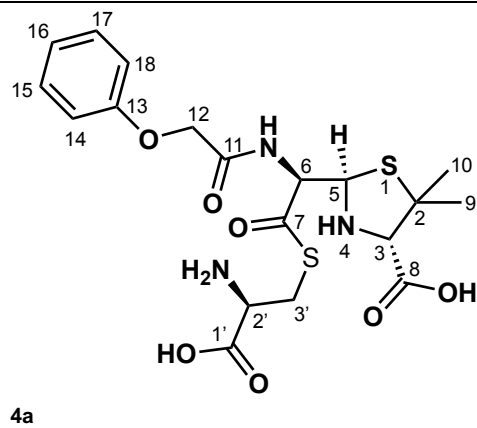
Table S.10 ¹H and ¹³C NMR Spectroscopic Data (500 MHz, DMSO-d₆) for cynaropicrin (**3**) and adduct **3a**.

				
position	δ_c , type ^a	δ_H (J in Hz)	δ_c , type ^a	δ_H (J in Hz)
1	43.7, CH	2.92 ^b	43.0, CH	2.90 ^b
2	38.3, CH ₂	1.95, m 1.64, m	38.3, CH ₂	1.58, m 2.06, m
3	71.7, CH	4.36, m	71.8, CH	4.35, m
4	153.2, C		Not observed	
5	49.4, CH	2.87 ^b	49.3, CH	2.76 ^b
6	77.9, CH	4.35, br s	78.6, CH	4.21, m
7	46.1, CH	3.22, m	47.3, CH	2.70 ^b
8	73.3, CH	5.09 ^b	75.3, CH	5.03 ^b
9	36.3, CH ₂	2.27, dd (14.3, 3.7) 2.67, dd (14.3, 5.2)	39.4, CH ₂	2.65, m 2.21 ^b
10	142.6, C		Not observed	
11	137.8, C		46.3, CH	3.04 ^b
12	168.3, C		Not observed	
13	120.5, CH ₂	5.52, d (3.1) 6.02, d (3.1)	31.6, CH ₂	2.75 ^b 2.93, m
14	116.5, CH ₂	4.84, m 5.09 ^b	116.0, CH ₂	4.90 ^b 5.05, m
15	110.0, CH ₂	5.232, m	109.2, CH ₂	5.16 ^b
16	164.5, C		Not observed	
17	140.6, C		Not observed	
18	123.8, CH ₂	6.18, m 5.91, m	124.3, CH ₂	6.15, m 5.88, m
19	59.3, CH ₂	4.18, s	59.6, CH ₂	4.33, m
1'			Not observed	
2'			54.1, CH	3.31 ^b
3'			35.6, CH ₂	2.75 ^b 3.02 ^b

^a Chemical shifts extracted from HSQC and HMBC^b Overlapping signals

Appendix

Table S.11 ¹H and ¹³C NMR Spectroscopic Data (500 MHz, DMSO-d₆) for penicillin V (**4**) and adduct **4a**

				
position	δ _c , type ^a	δ _H (J in Hz)	δ _c , type ^a	δ _H (J in Hz)
1				
2	63.4, C		57.7, C	
3	69.9, CH	4.30, s	72.4, CH	3.61 s
5	66.9, CH	5.53, m	65.8, CH	5.03, br s
6	57.9, CH	5.56, m	56.6, CH	4.47, br s
7	172.6, C		Not observed	
8	168.4, C		Not observed	
9	30.7, CH ₃	1.59, s	26.3, CH ₃	1.20, s
10	26.2, CH ₃	1.50, s	26.7, CH ₃	1.52, s
11	167.3, C		167.4, C	
12	66.1, CH ₂	4.63, d (2.4)	66.5, CH ₂	4.55, br s 4.60, br s
13	157.3, C		157.3, C	
14	114.4, CH	6.94 ^b	114.4, CH	6.97 ^b
15	129.1, CH	7.29 ^b	129.0, CH	7.28, br t (7.8), ^b
16	121.0, CH	6.96, m	120.9, CH	6.96 ^b
17	129.1, CH	7.29 ^b	129.0, CH	7.28, br t (7.8) ^b
18	114.4, CH	6.94 ^b	114.4, CH	6.97 ^b
1'			Not observed	
2'			54.3	4.36, m
3'			25.2	2.80, m 2.89, m

^a Chemical shifts extracted from HSQC and HMBC^b Overlapping signals

Table S.12. Yield table of experiments with Cys-TCP.

Sample	Starting Resin (mmol)	Starting Material (mg)	Crude Yield (mg)	Post-Purification Yield (mg)
Compound 1a	0.100	57.4	21.7	6.5
Compound 2a	0.150	5.7	3.9	0.2
Compound 2b	0.150	5.7	3.9	0.4
Compound 3a	0.225	15	8.0	2.5
Compound 4a	0.225	16.7	14.7	1.2

Table S.13 Table of tested pollen extract amounts on Cys-TCP.

Species	Lot Number	Mass (mg)
<i>Ambrosia psilostachya</i>	P3757208	131.0
<i>Ambrosia psilostachya</i>	P4129072-1	187.7
<i>Ambrosia psilostachya</i>	P4576841	272.9
<i>Ambrosia artemisiifolia</i>	P3744652-2	110.1
<i>Ambrosia artemisiifolia</i>	P3396120-3	143.8
<i>Ambrosia artemisiifolia</i>	P335440-18	147.5
<i>Ambrosia artemisiifolia</i>	P3392522-19	50.0
<i>Phleum pratense</i>	P319351-7	50.0
<i>Phleum pratense</i>	P3743977-1	109.4
<i>Phleum pratense</i>	P3929196-1	78.6
<i>Betula pendula</i>	P3317516-1	351.0
<i>Betula pendula</i>	P3317540-1	331.1
<i>Betula pendula</i>	P3752220	413.9
<i>Urtica dioica</i>	P3730565	293.5
<i>Urtica dioica</i>	P4079048-1	71.5
<i>Urtica dioica</i>	P4889415	165.5
<i>Corylus avellana</i>	P1330035-2	315.3
<i>Corylus avellana</i>	P4530617	254.0

Appendix

Table S.14 Masses observed during purification of the pollen extract cleavage (step vii) samples.

Ambrosia psilostachya		Ambrosia artemisiifolia		Pheum pratense		Betula pendula		Urtica dioica		Corylus avellana	
Observed m/z	Putative GFM	Observed m/z	Putative GFM	Observed m/z	Putative GFM	Observed m/z	Putative GFM	Observed m/z	Putative GFM	Observed m/z	Putative GFM
346	224	324	202	260	138	251	129	300	178	324	202
358	236	332	210	291	169	268	146	321	199	406	284
370	248	366	244	300	178	300	178	370	248	413	291
384	262	406	284	332	210	321	199	385	263	416	294
386	264	410	288	343	221	324	202	406	284	427	305
394	272	415	293	354	232	332	210	426	304	476	354
398	276	426	304	370	248	336	214	427	305	546	424
402	280	437	315	383	261	338	216	476	354	558	436
410	288	438	316	385	263	350	228	488	366	588	466
415	293	439	317	402	280	415	293	496	374		
416	294	455	333	410	288	420	298	546	424		
418	296	476	354	419	297	426	304	558	436		
428	306	480	358	426	304	436	314	566	444		
430	308	496	374	453	331	437	315	578	456		
432	310	501	379	462	340	438	316	588	466		
449	327	546	424	476	354	455	333	589	467		
471	349	578	456	480	358	476	354	616	494		
476	354	584	462	490	368	488	366	628	506		
488	366	600	478	496	374	506	384	697	575		
501	379	616	494	508	386	546	424	698	576		
508	386	622	500	512	390	558	436	768	646		
535	413	628	506	546	424	588	466	785	663		
546	424	686	564	558	436	596	474				
566	444	698	576	698	576	616	494				
584	462					628	506				
589	467					698	576				
600	478										
616	494										
641	519										
648	526										
659	537										
768	646										
787	665										

References

1. von Pirquet, C. Allergy. In: Gell, P. G. H., Coombs, R. R. A., eds. Clinical aspects of immunology. Oxford, England: Blackwell Scientific, 1963.
2. Kay, A. B., Allergy and Allergic Diseases – First of Two Parts, N. Engl. J. Med. 344 (2001) 30-37.
3. Kormelink, T. G., Thio, M., Blokhuis, B. R., Nijkamp, F. P., Redegeld, F. A., Atopic and non-atopic allergic disorders: current insights into the possible involvement of free immunoglobulin light chains, Clin. Exp. Allergy 39 (2008) 33-42.
4. Suphioglu, C., Singh, M. B., Taylor, P., Bellomo, R., Holmes, P., Puy, R., Knox, R. B., Mechanism of grass-pollen-induced asthma, The Lancet 339 (1992) 569-572.
5. Taylor, P. E., Flagan, R. C., Valenta, R., Glovsky, M. M., Release of allergens as respirable aerosols: A link between grass pollen and asthma, J. Allergy Clin. Immunol. 109 (2002) 51-56.
6. Boulet, L.-P., Cartier, A., Thomson, N. C., Roberts, R. S., Dolovich, J., Hargreave, F. E., Asthma and increases in nonallergic bronchial responsiveness from seasonal pollen exposure, J. Allergy Clin. Immunol. 71 (1983) 399-406.
7. Darrow, L. A., Hess, J., Rogers, C. A., Tolbert, P. E., Klein, M., Sarnat, S. E., Ambient pollen concentrations and emergency department visits for asthma and wheeze, J. Allergy Clin. Immunol. 130 (2012) 630-638.
8. Taylor, P. E., Jacobson, K. W., House, J. M., Glovsky, M. M., Links between pollen, atopy and the asthma epidemic, Int. Arch. Allergy Immunol. 144 (2007) 162-170.
9. Krämer, U., Weidinger, S., Darsow, U., Möhrensclager, M., Ring, J., Behrendt, H., Seasonality in symptom severity influenced by temperature or grass pollen: results of a panel study in children with eczema, J. Invest. Dermatol. 124 (2005) 514-523.
10. Darsow, U., Behrendt, H., Ring, J., Gramineae pollen as trigger factors of atopic eczema: evaluation of diagnostic measures using the atopy patch test, Brit. J. Dermatol. 137 (1997) 201-207.
11. Nanagas, V. C., Baldwin, J. L., Karamched, K. R., Hidden causes of anaphylaxis, Curr. Allergy Asthma Rep. 17 (2017) 44.
12. Eifan, A. O., Keles, S., Bahceciler, N. N., Barlan, I. B., Anaphylaxis to multiple pollen allergen sublingual immunotherapy, Allergy 61 (2007) 567-568.
13. Robledo-Retana, T., Mani, B. M., Teran, L. M., *Ligustrum* pollen: New insights into allergic disease, World Allergy Organ. J. 13 (2020).
14. Passali, D., Cingi, C., Staffa, P., Passali, F., Muluk, N. B., Bellussi, M. L., The international study of the allergic rhinitis survey: outcomes from 4 geographical regions, Asia Pac. Allergy 8 (2018) 7.
15. Behrendt, H., Becker, W.-M., Localization, release and bioavailability of pollen allergens: the influence of environmental factors, Curr. Opin. Immunol. 13 (2001) 709-715.
16. Morgenstern, V., Zutavern, A., Cyrys, J., Brockow, I., Koletzko, S., Krämer, U., Behrendt, H., Herbarth, O., von Berg, A., Bauer, C. B., Wichmann, H.-E., Heinrich, J., Atopic diseases, allergic sensitization, and exposure to traffic-related air pollution in children, A. J. Resp. Crit. Care 177 (2008) 1331-1337.

References

17. D'Amato, G., Pawankar, R., Vitale, C., Lanza, M., Molino, A., Stanziola, A., Sanduzzi, A., Vatrella, A., D'amato, M., Climate change and air pollution: effects on respiratory allergy, *Allergy Asthma Immunol. Res.* 8 (2016) 391-395.
18. D'Amato, G., Baena-Cagnani, C. E., Cecchi, L., Annesi-Maesano, I., Nunes, C., Ansotegui, I., D'Amato, M., Liccardi, G., Sofia, M., Canonica, W. G., Climate change, air pollution and extreme events leading to increasing prevalence of allergic respiratory diseases, *Multidiscip. Respir. Med.* 8 (2013) 12.
19. Lake, I. R., Jones, N. R., Agnew, M., Goodness, C. M., Giorgi, F., hamaoui-Laguel, L., Semenov, M. A., Solomon, F., Storkey, J., Vautard, R., Epstein, M. M., Climate change and future pollen allergy in Europe, *Environ. Health Perspect.* 125 (2017) 385-391.
20. Blomme, K., Tomassen, P., Lapeere, H., Huvenne, W., Bonny, M., Acke, F., Bachert, C., Gevaert, P., Prevalence of allergic sensitization versus allergic rhinitis symptoms in an unselected population, *Int. Arch. Allergy Immunol.* 160 (2013) 200-207.
21. Selgrade, M. K., Lemanske Jr., R. F., Gilmour, M. I., Neas, L. M., Ward, M. D. W., Henneberger P. K., Weissman, D. N., Hoppin, J. A., Dietert, R. R., Sly, P. D., Geller, A. M., Enright, P. L., Backus, G. S., Bromberg, P. A., Germolec, D. R., Yeatts, K. B., Induction of asthma and the environment: What we know and need to know, *Environ. Health Perspect.* 144 (2006) 615-619.
22. Gould, H. J., Sutton, B. G., IgE in allergy and asthma today, *Nat. Rev. Immunol.* 8 (2008) 205-217.
23. Murphy, K., Weaver, C., (2016). *Janeway's immunobiology*, 9th edition. New York, Garland Science/Taylor & Francis.
24. Moon, T. C., St Laurent, C. D., Morris, K. E., Marcet, C., Yoshimura, T., Sekar, Y., Befus, A. D., Advances in mast cell biology: new understanding of heterogeneity and function, *Mucosal Immunol.* 3 (2010) 111-128.
25. Galli, S. J., Gaudenzio, N., Tsai, M., Mast cells in inflammation and disease: recent progress and ongoing concerns, *Annu. Rev. Immunol.* 38 (2020) 49-77.
26. Nathan, C., Neutrophils and immunity: challenges and opportunities, *Nat. Rev. Immunol.* 6 (2006) 173-182.
27. Akuthota, P., Wang, H., Weller, P. F., Eosinophils as antigen-presenting cells in allergic upper airway disease, *Curr. Opin. Allergy Clin. Immunol.* 10 (2010) 14-19.
28. Mikhak, Z., Luster, A. D., The emergence of basophils as antigen-presenting cells in Th2 inflammatory response, *J. Mol. Cell Biol.* 1 (2009) 69-71.
29. Spellberg, B., Edwards, J. E. Jr., Type 1/type 2 immunity in infectious diseases, *Clin. Infect. Dis.* 32 (2001) 76-102.
30. Gordon, S., Alternative activation of macrophages, *Nat. Rev. Immunol.* 3 (2003) 23-35.
31. Banchereau, J., Steinman, R. M., Dendritic cells and the control of immunity, *Nature* 392 (1998) 245-252.
32. Banchereau, J., Briere, F., Caux, C., Davoust, J., Lebecque, S., Liu, Y.-J., Pulendran, B., Palucka, K., Immunobiology of dendritic cells, *Annu. Rev. Immunol.* 18 (2000) 767-811.
33. Burton, O. T., Oettgen, H. C., Beyond immediate hypersensitivity: evolving roles for IgE antibodies in immune homeostasis and allergic diseases, *Immunol. Rev.* 242 (2011) 128-143.
34. Kraft, S., Kinet, J.-P., New developments in FcεRI regulation, function and inhibition, *Nat. Rev. Immunol.* 7 (2007) 365-378.

35. Romagnani, S., The Th1/Th2 paradigm and allergic disorders, *Allergy* 53 (1998) 12-15.
36. Thornton, C. A., Holloway, J. A., Popplewell, E. J., Shute, J. K., Boughton, J., Warner, J. O., Fetal exposure to intact immunoglobulin E occurs via gastrointestinal tract, *Clin. Exp. Allergy* 33 (2003) 306-311.
37. Galli, S. J., Grimaldeston, M., Tsai, M., Immunomodulatory mast cells: negative, as well as positive, regulators of immunity, *Nat. Rev. Immunol.* 8 (2008) 478-486.
38. Sutton, B. J., Gould, H. J., The human IgE network, *Nature* 366 (1993) 421-428.
39. He, J.S., Narayanan, S., Subramaniam, S., Ho, W.Q., Lafaille, J.J., and Curotto de Lafaille, M.A., Biology of IgE production: IgE cell differentiation and the memory of IgE responses, *Curr. Opin. Microbiol. Immunol.* 388 (2015) 1-19.
40. Gauchat, J.-F., Henchoz, S., Mazzei, G., Aubry, J.-P., Brunner, T., Blasey, H., Life, P., Talabot, D., Flores-Romo, L., Thompson, J., Kishi, K., Butterfield, J., Dahinden, C., Bonnefoy, J.-Y., Induction of human IgE synthesis in B cells by mast cells and basophils, *Nature* 365 (1993) 340-343.
41. Mikhak, Z., Luster, A.D., The emergence of basophils as antigen-presenting cells in Th2 inflammatory responses. *J. Mol. Cell Biol.* 1 (2009) 69-71.
42. Nelms, K., Keegan, A. D., Zamorano, J., Ryan, J. J., Paul, W. E., The IL-4 receptor: signaling mechanisms and biologic functions, *Annu. Rev. Immunol.* 17 (1999) 701-738.
43. Galli, S. J., Tsai, M., IgE and mast cells in allergic disease, *Nat. Med.* 18 (2012) 693-704.
44. Geha, R. S., Jabara, H. H., Brodeur, S. R., The regulation of immunoglobulin E class-switch recombination, *Nat. Rev. Immunol.* 3 (2003) 721-732.
45. Furuichi, K., Rivera, J., Isersky, C., The receptor for immunoglobulin E on rat basophilic leukemia cells: Effect of ligand binding on receptor expression, *Proc. Natl. Acad. Sci. USA* 82 (1985) 1522-1525.
46. Hsu, C., MacGlashan, D. Jr., IgE antibody up-regulates high affinity IgE binding on murine bone marrow-derived mast cells, *Immunol. Lett.* 52 (1996) 129-134.
47. Yamaguchi, M., Lantz, C. S., Oettgen, H., Katona, I. M., Fleming, T., Miyajima, I., Kinet, J.-P., Galli, S. J., IgE enhances mouse mast cell FcεRI expression in vitro and in vivo: evidence for a novel amplification mechanism in IgE-dependent reactions, *J. Exp. Med.* 185 (1997) 663-672.
48. Borkowski, T. A., Jouvin, M.-H., Lin, S.-Y., Kinet, J.-P., Minimal requirements for IgE-mediated regulation of surface FcεRI, *J. Immunol.* 167 (2001) 1290-1296.
49. Ouyang, W., Löhning, M., Gao, Z., Assenmacher, M., Ranganath, S., Radbruch, A., Murphy, K. M., Stat6-independent GATA-3 autoactivation directs IL-4-independent Th2 development and commitment, *Immunity* 12 (2000) 27-37.
50. Usui, T., Nishikomori, R., Kitani, A., Strober, W., GATA-3 suppresses Th1 development by downregulation of Stat4 and not through effects on IL-12Rβ2 chain or T-bet, *Immunity* 18 (2003) 415-428.
51. Szabo, S. J., Kim, S. T., Costa, G. L., Zhang, X., Fathman, C. G., Glimcher, L. H., A novel transcription factor, T-bet, directs Th1 lineage commitment, *Cell* 100 (2000) 655-669.
52. Platzer, B., Baker, K., Vera, M. P., Singer, K., Panduro, M., Lexmond, W. S., Turner, D., Vargas, C. O., Kinet, J.-P., Maurer, D., Baron, R. M., Blumberg, R. S., Fiebiger, E., Dendritic cell-bound IgE functions to restrain allergic inflammation at mucosal sites, *Mucosal Immunol.* 8 (2015) 516-532.

References

53. Moiseeva, E.P., Bradding, P. Mast cells in lung inflammation. *Adv. Exp. Med. Biol.* 716 (2011) 235–269.
54. Gilfillan, A. M., Tkaczyk, C., Integrated signalling pathways for mast-cell activation, *Nat. Rev. Immunol.* 6 (2006) 218-230.
55. Galli, S. J., Tsai, M., Mast cells in allergy and infection: Versatile effector and regulatory cells in innate and adaptive immunity, *Eur. J. Immunol.* 40 (2010) 1843-1851.
56. Boyce, J. A., Mast cells and eicosanoid mediators: a system of reciprocal paracrine and autocrine regulation, *Immunol. Rev.* 217 (2007) 168-185.
57. Galli, S. J., Nakae, S., Tsai, M., Mast cells in the development of adaptive immune responses, *Nat. Immunol.* 6 (2005) 135-142.
58. Repka-Ramirez, M. S., New concepts of histamine receptors and actions, *Curr. Allergy Asthm. R.* 3 (2003) 227-231.
59. Rivera, J., Gilfillan, A. M., Molecular regulation of mast cell activation, *J. Allergy Clin. Immunol.* 117 (2006) 1214-1225.
60. Wershil, B. K., Wang, Z. S., Gordon, J. R., Galli, S. J., Recruitment of neutrophils during IgE-dependent cutaneous late phase reactions in the mouse is mast cell-dependent. Partial inhibition of the reaction with antiserum against tumor necrosis factor-alpha, *J. Clin. Invest.* 87 (1991) 446-453.
61. Nagai, H., Abe, T., Yamaguchi, I., Mito, K., Tsunematsu, M., Kimata, M., Inagaki, N., Role of mast cells in the onset of IgE-mediated late-phase cutaneous response in mice, *J. Allergy Clin. Immunol.* 106 (2000) S91-S98.
62. Galli, S. J., Tsai, M., Piliponsky, A. M., The development of allergic inflammation, *Nature* 454 (2008) 445-454.
63. Mari, A., Multiple pollen sensitization: A molecular approach to the diagnosis, *Int. Arch. Allergy Immunol.* 125 (2001) 57-65.
64. Beck, L. A., Leung, D. A. M., Allergen sensitization through the skin induced systemic allergic responses, *J. Allergy Clin. Immunol.* 106 (2000) 258-263.
65. Liu, A. H., Hygiene theory and allergy and asthma prevention, *Paediatr. Perinat. Ep.* 21 (2007) 2-7.
66. Platts-Mills, T. A. E., Mitchell, E. B., Nock, P., Tovey, E. R., Moszoro, H., Wilkins, S. R., Reduction of bronchial hyperreactivity during prolonged allergen avoidance, *Lancet* 320 (1982) 675-678.
67. Peroni, D. G., Boner, A. L., Vallone, G., Antolini, I., Warner, J. O., Effective allergen avoidance at high altitude reduces allergen-induced bronchial hyperresponsiveness, *Am. J. Respir. Crit. Care Med.* 149 (1994) 1442-1446.
68. Custovic, A., Simpson, A., Chapman, M. D., Woodcock, A., Allergen avoidance in the treatment of asthma and atopic disorders, *Thorax* 53 (1998) 63-72.
69. Cipriani, F., Calamelli, E., Ricci, G., Allergen avoidance in allergic asthma, *Front. Pediatr.* 5 (2017) 103.
70. Platts-Mills, T. A. E., Allergen avoidance, *J. Allergy Clin. Immunol.* 113 (2004) 388-391.
71. Uermösi, C., Beerli, R. R., Bauer, M., Manolova, V., Dietmeier, K., Buser, R. B., Kündig, T. M., Saudan, P., Bachmann, M. F., Mechanisms of allergen-specific desensitization, *J. Allergy Clin. Immunol.* 126 (2010) 375-383.

72. Hedlin, G., Graff-Lonnevig, V., Heilborn, H., Lilja, G., Norrlind, K., Pegelow, K., Sundin, B., Lowenstein, H., Immunotherapy with cat- and dog-dander extracts, V. effects of 3 years of treatment, *J. Allergy Clin. Immunol.* 87 (1991) 955-964.
73. Krishna, M. T., Huissoon, A. P., Clinical immunology review series: an approach to desensitization, *Clin. Exp. Immunol.* 163 (2011) 131-146.
74. Rocklin, R. E., Shedder, A. L., Greineder, D. K., Melmon, K. L., Generation of antigen-specific suppressor cells during allergy desensitization, *N. Engl. J. Med.* 302 (1980) 1213-1219.
75. Walker, S. M., Pajno, G. B., Lima, M. T., Wilson, D. R., Durham, S. R., Grass pollen immunotherapy for seasonal rhinitis and asthma: a randomized, controlled trial. *J. Allergy Clin. Immunol.* 107 (2001) 87-93.
76. Penagos, M., Eifan, A. O., Durham, S. R., Scadding, G. W., Duration of allergen immunotherapy for long-term efficacy in allergic rhinoconjunctivitis, *Curr. Treat. Options Allergy* 5 (2018) 275-290.
77. Durham, S. R., Walker, S. M., Varga, E.-M., Jacobson, M. R., O'Brien, F., Noble, W., Till, S. J., Hamid, Q. A., Nouri-Aria, K. T., Long-term clinical efficacy of grass-pollen immunotherapy, *N. Engl. J. Med.* 341 (1999) 468-475.
78. Lichtenstein, L. M., Holtzman, N. A., Burnett, L. S., A quantitative in vitro study of the chromatographic distribution and immunoglobulin characteristics of human blocking antibody, *J. Immunol.* 101 (1968) 317-324.
79. Palmqvist, M., Persson, G., Lazer, L., Rosenborg, J., Larsson, P., Lötvall, J., Inhaled dry-powder formoterol and salmeterol in asthmatic patients: Onset of action, duration of effect and potency, *Eur. Respir. J.* 10 (1997) 2484-2489.
80. Cao, R., Dong, X.-W., Jiang, J.-X., Yan, X.-F., He, J.-S., Deng, Y.-M., Li, F.-F., Bao, M.-J., Xie, Y.-C., Chen, X.-P., Xie, Q.-M., M₃ muscarinic receptor antagonist bencycloquidium bromide attenuates allergic airway inflammation, hyperresponsiveness and remodeling in mice, *Eur. J. Pharmacol.* 655 (2011) 83-90.
81. Lewis, R. A., Austen, K. F., Soberman, R. J., Leukotrienes and other products of the 5-lipoxygenase pathway. Biochemistry and relation to pathobiology in human diseases, *N. Engl. J. Med.* 323 (1990) 645-55.
82. Drazen, J. M., Israel, E., O'Byrne, P. M., Treatment of asthma with drugs modifying the leukotriene pathway, *N. Engl. J. Med.* 340 (1999) 197-206.
83. Philip, G., Malmstrom, K., Hampel Jr, F. C., Weinstein, S. F., LaForce, C. F., Ratner, P. H., Malice, M.-P., Reiss, T. F., Montelukast for treating seasonal allergic rhinitis: a randomized, double-blind, placebo-controlled trial performed in the spring, *Clin. Exp. Allergy* 32 (2002) 1020-1028.
84. Taylor, I. K., O'Shaughnessy, K. M., Fuller, R. W., Dollery, C., Effect of cysteinyl-leukotriene receptor antagonist ICI 204.219 on allergen-induced bronchoconstriction and airway hyperreactivity in atopic subjects, *Lancet* 337 (1991) 690-694.
85. Diamant, Z., Grootendorst, D. C., Veselic-Charvat, M., Timmers, M. C., De Smet, M., Leff, J. A., Seidenberg, B. C., Zwinderman, A. H., Peszek, I., Sterk, P. J., The effect of montelukast (MK-0476), a cysteinyl leukotriene receptor antagonist, on allergen-induced airway responses and sputum cell counts in asthma, *Clin. Exp. Allergy* 29 (1999) 42-51.
86. Barnes, P. J., Therapeutic strategies for allergic diseases, *Nature* 402 (1999) 31-38.
87. Israel, E., Cohn, J., Dubé, L., Effect of treatment with zileuton, a 5-lipoxygenase inhibitor, in patients with asthma, *JAMA* 275 (1996) 931-936.

References

88. Israel, E., Dermarkarian, R., Rosenberg, M., Sperling, R., Taylor, G., Rubin, P., Drazen, J. M., The effects of a 5-lipoxygenase inhibitor on asthma induced by cold, dry air, *N. Engl. J. Med.* 323 (1990) 1740-1744.
89. Knapp, H. R., Reduced allergen-induced nasal congestion and leukotriene synthesis with an orally active 5-lipoxygenase inhibitor, *N. Engl. J. Med.* 323 (1990) 1745-1748.
90. Ducharme, Y., Blouin, M., Brideau, C., Châteauneuf, A., Gareau, Y., Grimm, E. L., Juteau, H., Laliberté, S., MacKay, B., Massé, F., Ouellet, M., Salem, M., Styhler, A., Friesen, R. W., The discovery of setileuton, a potent and selective 5-lipoxygenase inhibitor, *ACS Med. Chem. Lett.* 1 (2010) 170-174.
91. Cevikbas, F., Braz, J. M., Wang, X., Solorzano, C., Sulk, M., Buhl, T., Steinhoff, M., Basbaum, A. I., Synergistic antipruritic effects of gamma aminobutyric acid A and B agonists in a mouse model of atopic dermatitis, *J. Allergy Clin. Immunol.* 140 (2017) 454-464.
92. Duthey, B., Hübner, A., Diehl, S., Boehncke, S., Pfeffer, J., Boehncke, W.-H., Anti-inflammatory effects of the GABA_B receptor agonist baclofen in allergic dermatitis, *Exp. Dermatol.* 19 (2010) 661-666.
93. Blaiss, M. S., Gelfand, E., Gilmore, T., Harvey, P. D., Hindmarch, I., Simons, F. E. R., Spangler, D. L., Szefer, S. J., Terndrup, T. E., Waldman, S. A., Weiler, J., Wong, D. F., First do no harm: Managing antihistamine impairment in patients with allergic rhinitis, *J. Allergy Clin. Immunol.* 111 (2003) 835-842.
94. Zhang, T., Finn, D. F., Barlow, J. W., Walsh, J. J., Mast cell stabilisers, *Eur. J. Pharmacol.* 778 (2016) 158-168.
95. Finn, D. F., Walsh, J. J., Twenty-first century mast cell stabilizers, *Brit. J. Pharmacol.* 170 (2013) 23-37.
96. Krauth, M. T., Mirkina, I., Herrmann, H., Baumgartner, C., Kneidinger, M., Valent, P., Midostaurin (PKC412) inhibits immunoglobulin E-dependent activation and mediator release in human blood basophils and mast cells, *Clin. Exp. Allergy* 39 (2009) 1711-1720.
97. Jensen, B. M., Beaven, M. A., Iwaki, S., Metcalfe, D. D., Gilfillan, A. M. Concurrent inhibition of kit- and FcεRI-mediated signaling: coordinated suppression of mast cell activation, *J. Pharmacol. Exp. Ther.* 324 (2008) 128-138.
98. Norton, S. K., Dellinger, A., Zhou, Z., Lenk, R., Macfarland, D., Vonakis, B., Conrad, D., Kepley, C. L., A new class of human mast cell and peripheral blood basophil stabilizers that differentially control allergic mediator release, *Clin. Transl. Sci.* 3 (2010) 158-169.
99. Matsumoto, Y., Funahashi, J., Mori, K., Hayashi, K., Yano, H. The noncompetitive antagonism of histamine H1 receptors expressed in chinese hamster ovary cells by olopatadine hydrochloride: Its potency and molecular mechanism, *Pharmacology* 81 (2008) 266-274.
100. Edwards, A. M., The discovery of cromolyn sodium and its effect on research and practice in allergy and immunology, *J. Allergy Clin. Immunol.* 115 (2005) 885-888.
101. Cairns, H., Cox, D., Gould, K. J., Ingall, A. H., Suschitzky, J. L., New antiallergic pyrano[3,2-g]quinoline-2,8-dicarboxylic acids with potential for the topical treatment of asthma, *J. Med. Chem.* 28 (1985) 1832-1842.
102. Sinniah, A., Yazid, S., Flower, R. J., The anti-allergic cromones: Past, present, and future, *Front. Pharmacol.* 8 (2017) 827.

103. Yazid, S., Sinniah, A., Solito, E., Calder, V., Flower, R. J., Anti-allergic cromones inhibit histamine and eicosanoid release from activated human and murine mast cells by releasing annexin A1, *PLOS ONE* 8 (2013) e58963.
104. Ciriaco, M., Ventrice, P., Russo, G., Scicchitano, M., Mazzitello, G., Scicchitano, F., Russo, E., Corticosteroid-related central nervous system, side effects, *J. Pharmacol. Pharmather.* 4 (2013) S94-S98.
105. Bergmann, K.-C., Ring, J. (eds): History of allergy. *Chem. Immunol. Allergy. Basel*, Karger 100 (2014) 311-316.
106. Karatzanis, A., Chatzidakis, A., Milioni, A., Vlaminc, S., Kawauchi, H., Velegarakis, S., Prokopakis, E., Contemporary use of corticosteroids in rhinology, *Curr. Allergy Asthma Rep.* 17 (2017) 11.
107. Bisgaard, H., Hermansen, M. N., Loland, L., Halkjaer, L. B., Buchvald, F., Intermittent inhaled corticosteroids in infants with episodic wheezing, *N. Engl. J. Med.* 354 (2006) 1998-2005.
108. Barnes, P. J., Inhaled corticosteroids, *Pharmaceuticals* 3 (2010) 514-540.
109. Wolkowitz, O. M., Prospective controlled studies of the behavioral and biological effects of exogenous corticosteroids, *Psychoneuroendocrinol.* 19 (1994) 233-255.
110. Landolina, N., Levi-Schaffer, F., Monoclonal antibodies: The new magic bullets for allergy: IUPHAR Review 17, *Brit. J. Pharmacol.* 173 (2016) 793-803.
111. Busse, W. W., Katial, R., Gossage, D., Sari, S., Wang, B., Kolbeck, R., Coyle, A. J., Koike, M., Spitalny, G. L., Kiener, P. A., Geba, G. P., Molfino, N. A., Safety profile, pharmacokinetics, and biologic activity of MEDI-563, an anti-IL-5 receptor alpha antibody, in a phase I study of subjects with mild asthma, *J. Allergy Clin. Immunol.* 125 (2010) 1237-1244.
112. Chung, K. F., Targeting the interleukin pathway in the treatment of asthma, *Lancet* 386 (2015) 1086-1096.
113. Djukanović, R., Wilson, S. J., Kraft, M., Jarjour, N. N., Steel, M., Chung, K. F., Bao, W., Fowler-Taylor, A., Matthews, J., Busse, W. W., Holgate, S. T., Fahy, J. V., Effects of treatment with anti-immunoglobulin E antibody omalizumab on airway inflammation in allergic asthma, *Am. J. Resp. Crit. Care* 170 (2004) 583-593.
114. Maurer, M., Giménez-Arnau, A. M., Sussman, G., Metz, M., Baker, D. R., Bauer, A., Bernstein, J. A., Brehler, R., Chu, C.-Y., Chung, W.-H., Danilycheva, I., Grattan, C., Hébert, J., Katelaris, C., Makris, M., Meshkova, R., Savic, S., Sinclair, R., Sitz, K., Staubach, P., Wedi, B., Löffler, J., Barve, A., Kobayashi, K., Hua, E., Severin, T., Janocha, R., Ligelizumab for chronic spontaneous urticaria, *N. Engl. J. Med.* 381 (2019) 1321-1332.
115. Wedi, B., Ligelizumab for the treatment of chronic spontaneous urticaria, *Expert Opin. Biol. Ther.* 2020.
116. Harris, J. M., Maciuga, R., Bradley, M. S., Cabanski, C. R., Scheerens, H., Lim, J., Cai, F., Kishnani, M., Liao, X. C., Samineni, D., Zhu, R., Cochran, C., Soong, W., Diaz, J. D., Perin, P., Tsukayama, M., Dimov, D., Agache, I., Kelsen, S. G., A randomized trial of the efficacy and safety of quilizumab in adults with inadequately controlled allergic asthma, *Resp. Res.* 17 (2016) 29.
117. Gauvreau, G. M., Harris, J. M., Boulet, L.-P., Scheerens, H., Fitzgerald, J. M., Putnam, W. S., Cockcroft, D. W., Davis, B. E., Leigh, R., Zheng, Y., Dahlén, B., Wang, Y., Maciuga, R., Mayers, I., Liao, X. C., Wu, L. C., Matthews, J. G., O'Byrne, P. M., Targeting membrane-expressed IgE B

References

- cell receptor with an antibody to the M1 prime epitope reduces IgE production, *Sci. Transl. Med.* 243 (2014) 85.
118. Harris, J. M., Maciucia, R., Bradley, M. S., Cabanski, C. R., Scheerens, H., Lim, J., Cai, F., Kishnani, M., Liao, X. C., Samineni, D., Zhu, R., Cochran, C., Soong, W., Diaz, J. D., Perin, P., Tsukayama, M., Dimov, D., Agache, I., Kelsen, S. G., A randomized trial of the efficacy and safety of quilizumab in adults with inadequately controlled allergic asthma, *Respir. Res.* 17 (2016) 29.
 119. Bagnasco, D., Ferrando, M., Varricchi, G., Passalacqua, G., Canonica, G. W., A Critical evaluation of anti-IL-13 and anti-IL-4 strategies in severe asthma, *Int. Arch. Allergy Immunol.* 170 (2016) 122-131.
 120. Schmidt-Weber, C. B., Anti-IL-4 as a new strategy in allergy, *Chem. Immunol. Allergy*, 96 (2012) 120-125.
 121. PDL BioPharma, Inc., Pilot study in patients with symptomatic steroid-naive asthma (accessed October 19, 2020). Available from: <http://clinicaltrials.gov/ct2/show/NCT00024544>.
 122. Maes, T., Joos, G. F., Brusselle, G. G., Targeting interleukin-4 in asthma: Lost in translation?, *Am. J. Respir. Cell Mol. Biol.* 47 (2012) 261-270.
 123. Sanderson, C. J., Interleukin-5, eosinophils, and disease. *Blood* 79 (1992) 3101-3109.
 124. Inman, M. D., Bone marrow events in animal models of allergic inflammation and hyperresponsiveness, *J. Allergy Clin. Immunol.* 106 (2000) S235-S241.
 125. Kazani, S., Israel, E., Update in asthma, *Am. J. Respir. Crit. Care Med.* 186 (2012) 35-40.
 126. Garcia, G., Taillé, C., Laveneziana, P., Bourdin, A., Chanez, P., Humbert, M., Anti-interleukin-5 therapy in severe asthma, *Eur. Respir. Rev.* 22 (2013) 251-257.
 127. Walsh, G. M., Mepolizumab and eosinophil-mediated disease, *Curr. Med. Chem.* 16 (2009) 4774-4778.
 128. Garrett, J. K., Jameson, S. C., Thomson, B., Collins, M. H., Wagoner, L. E., Freese, D. K., Beck, L. A., Boyce, J. A., Filipovich, A. H., Villanueva, J. M., Sutton, S. A., Assa'ad, A. H., Rothenberg, M. E., Anti-interleukin-5 (mepolizumab) therapy for hypereosinophilic syndromes, *J. Allergy Clin. Immunol.* 113 (2004) 115-119.
 129. Walsh, G. M., Reslizumab, a humanized anti-IL-5 mAb for the treatment of eosinophil mediated inflammatory conditions, *Curr. Opin. Mol. Ther.* 11 (2009) 329-336.
 130. Brightling, C. E., Saha, S., Hollins, F., Interleukin-13: prospects for new treatments, *Clin. Exp. Allergy* 40 (2009) 42-29.
 131. Eli Lilly and Company, Long-term safety and efficacy study of lebrikizumab (LY3650150) in participants with moderate-to-severe atopic dermatitis (accessed October 19, 2020). Available from: <https://clinicaltrials.gov/ct2/show/NCT04392154>.
 132. Corren, J., Lemanske, R. F., Hanania, N. A., Korenblat, P. E., Parsey, M. V., Arron, J. R., Harris, J. M., Scheerens, H., Wu, L. C., Su, Z., Mosesova, S., Eisner, M. D., Bohlen, S. P., Matthews, J. G., Lebrikizumab treatment in adults with asthma, *N. Engl. J. Med.* 365 (2011) 1088-98.
 133. Scheerens, H., Arron, J. R., Zheng, Y., Putnam, W. S., Erickson, R. W., Choy, D. F., Harris, J. M., Lee, J., Jarjour, N. N., Matthews, J. G., The effects of lebrikizumab in patients with mild asthma following whole lung allergen challenge, *Clin. Exp. Allergy* 44 (2014) 38-46.
 134. Hanania, N. A., Noonan, M., Corren, J., Korenblat, P., Zheng, Y., Fischer, S. K., Cheu, M., Putnam, W. S., Murray, E., Scheerens, H., Holweg, C. T. J., Maciucia, R., Gray, S., Doyle, R.,

- McClintock, D., Olsson, J., Matthews, J. G., Yen, K., Lebrikizumab in moderate-to-severe asthma: pooled data from two randomized placebo-controlled studies, *Thorax* 70 (2015) 748-756.
135. LEO Pharma, Tralokinumab in combination with topical corticosteroids for moderate to severe atopic dermatitis - ECZTRA 3 (ECZema TRAlokinumab Trial no. 3) (accessed October 19, 2020). Available from: <https://clinicaltrials.gov/ct2/show/NCT03363854>.
136. Piper, E., Brightling, C. E., Niven, R., Oh, C., Faggioni, R., Poon, K., She, D., Kell, C., May, R. D., Geba, G. P., Molfino, N. A., A phase II placebo-controlled study of tralokinumab in moderate-to-severe asthma, *Eur. Respir. J.* 41 (2013) 330-38.
137. Brightling, C. E., Chanez, P., Leigh, R., O'Byrne, P. M., Korn, S., She, D., May, R. D., Streicher, K., Ranade, K., Piper, E., Efficacy and safety of tralokinumab in patients with severe uncontrolled asthma: a randomised, double-blind, placebo-controlled, phase 2b trial, *Lancet Respir. Med.* 3 (2015) 692-701.
138. Wenzel, S., Ford, L., Pearlman, D., Spector, S., Sher, L., Skobieranda, F., Wang, L., Kirkesseli, S., Rocklin, R., Bock, B., Hamilton, J., Ming, J. E., Radin, A., Stahl, N., Yancopoulos, G. D., Graham, N., Pirozzi, G., Dupilumab in persistent asthma with elevated eosinophil levels, *N. Engl. J. Med.* 368 (2013) 2455-2466.
139. Nair, P., Wenzel, S., Rabe, K. F., Bourdin, A., Lugogo, N. L., Kuna, P., Barker, P., Sproule, S., Ponnarambil, S., Goldman, M., Oral glucocorticoid-sparing effect of benralizumab in severe asthma, *N. Engl. J. Med.* 376 (2017) 2448-2458.
140. O'Connell, M., The burden of atopy and asthma in children, *Allergy* 59 (2004) 7-11.
141. Muzalyova, A., Brunner, J. O., Traidl-Hoffmann, C., Pollen allergy and health behavior: patients trivializing their disease, *Aerobiologia* 35 (2019), 327-341.
142. Holgate, S. T., Polosa, R., Treatment strategies for allergy and asthma, *Nat Rev. Immunol.* 8 (2008) 218-230.
143. Schiavoni, G., D'Amato, G., Afferni, C., The dangerous liaison between pollens and pollution in respiratory allergy, *Ann. Allergy Asthma Immunol.* 118 (2017) 269-275.
144. Bellanti, J. A., Settignano, R. A., Genetics, epigenetics, and allergic disease: A gun loaded by genetics and a trigger pulled by epigenetics, *Allergy Asthma Proc.* 40 (2019) 73-75.
145. Ono, S. J., Molecular Genetics of Allergic Diseases, *Annu. Rev. Immunol.* 18 (2000) 347-366.
146. Marsh, D. G., Meyers, D. A., Bias, W. B., The epidemiology and genetics of atopic allergy, *New. Engl. J. Med.* 305 (1981) 1551-1559.
147. Barrios, C., Brawang, P., Berney, M., Brandt, C., Lambert, P. H., Siegrist, C. A., Neonatal and early life immune responses to various forms of vaccine antigens qualitatively differ from adult responses: Predominance of a Th2-biased pattern which persists after adult boosting, *Eur. J. Immunol.* 26 (1996) 1489-1496.
148. Prescott, S. L., Macaubas, C., Holt, B. J., Smallacombe, T. B., Loh, R., Sly, P. D., Holt, P. G., Transplacental priming of the human immune system to environmental allergens: Universal skewing of initial T cell responses toward the Th2 cytokine profile, *J. Immunol.* 160 (1998) 4730-4737.
149. Prescott, S. L., Macaubas, C., Smallacombe, T., Holt, B. J., Sly, P. D., Loh, R., Holt, P. G., Reciprocal age-related patterns of allergen-specific T-cell immunity in normal vs. atopic infants, *Clin. Exp. Allergy* 28, (1998) 39-44.
150. Strachan, D. P., Hay fever, hygiene, and household size, *BMJ* 299 (1989) 1259-1260.

References

151. Scudellari, M., Cleaning up the hygiene hypothesis, *PNAS* 114 (2017) 1433-1436.
152. Rook, G. A. W., Hygiene hypothesis and autoimmune diseases, *Clin. Rev. Allergy Immunol.* 42 (2012) 5-15.
153. Hanski, I., von Hertzen, L., Fyhrquist, N., Koskinen, K., Torppa, K., Laatikainen, T., Karisola, P., Auvinen, P., Paulin, L., Mäkelä, M. J., Vartiainen, E., Kosunen, T. U., Alenius, H., Haahtela, T., Environmental biodiversity, human microbiota, and allergy are interrelated, *PNAS* 109 (2012) 8334-8339.
154. The International Study of Asthma and Allergies in Childhood Steering Committee, Worldwide variation in prevalence of symptoms of asthma, allergic rhinoconjunctivitis, and atopic eczema: ISAAC, *Lancet* 351 (1998) 1225-1232.
155. Yemaneberhan, H., Bekele, Z., Venn, A., Lewis, S., Parry, E., Britton, J., Prevalence of wheeze and asthma and relation to atopy in urban and rural Ethiopia, *Lancet* 350 (1997) 85-90.
156. Riedler, J., Eder, W., Oberfeld, G. & Schreuer, M. Austrian children living on a farm have less hay fever, asthma and allergic sensitization. *Clin. Exp. Allergy* 30 (2000) 194-200.
157. Majkowska-Wojciechowska, B., Pelka, J., Korzon, L., Kozłowska, A., Kaczała, M., Jarzebska, M., Gwardys, T., Kowalski, M. L., Prevalence of allergy, patterns of allergic sensitization and allergy risk factors in rural and urban children, *Allergy* 62 (2007) 1044-1050.
158. Heinrich, J., Hoelscher, B., Frye, C., Meyer, I., Wjst, M., Wichmann, H.-E., Trends in prevalence of atopic diseases and allergic sensitization in children in East Germany, *Eur. Respir. J.* 19 (2002) 1040-1046.
159. Liu, A. H., Revisiting the hygiene hypothesis for allergy and asthma, *J. Allergy Clin. Immunol* 136 (2015) 860-865.
160. Yazdanbakhsh, M., Kremsner, P.G., van Ree, R., Allergy, parasites, and the hygiene hypothesis, *Science* 296 (2002) 490-494.
161. Briggs, N., Weatherhead, J., Sastry, K. J., Hotez, P. J., The hygiene hypothesis and its inconvenient truths about helminth infections, *PLOS Neglect. Trop. D.* 10 (2016).
162. Santiago, H. C., Nutman, T. B., Human helminths and allergic disease: The hygiene hypothesis and beyond, *Am. J. Trop. Med. Hyg.* 95 (2016) 746-753.
163. Smits, H. H., Hammad, H., van Nimwegen, M., Soullie, T., Willart, M. A., Lievers, E., Kadouch, J., Kool, M., Kos-van Oosterhoud, J., Deelder, A. M., Lambrecht, B. N., Yazdanbakhsh, M., Protective effect of *Schistosoma mansoni* infection on allergic airway inflammation depends on the intensity and chronicity of the infection, *J. Allergy Clin. Immunol.* 120 (2007) 932-940.
164. Flohr, C., Quinnell, R. J., Britton, J., Do helminth parasites protect against atopy and allergic disease?, *Clin. Exp. Allergy* 39 (2008) 20-32.
165. Stene, L.C., Nafstad, P., Relation between occurrence of type 1 diabetes and asthma, *Lancet* 357 (2001) 607-608.
166. Liu, A. H., Murphy, J. R., Hygiene hypothesis: Fact or fiction?, *J. Allergy Clin. Immunol.* 111 (2003) 471-478
167. van Tilburg Bernardes, E., Arietta, M.-C., Hygiene hypothesis in asthma development: Is hygiene to blame?, *Arch. Med. Res.* 48 (2017) 717-726.
168. Bach, J.-F., The hygiene hypothesis in autoimmunity: the role of pathogens and commensals, *Nat. Rev. Immunol.* 18 (2018) 105-120.

169. Bloomfield, S. F., Rook, G. A. W., Scott, E. A., Shanahan, F., Stanwell-Smith, R., Turner, P., Time to abandon the hygiene hypothesis: new perspectives on allergic disease, the human microbiome, infectious disease prevention and the role of targeted hygiene, *Perspect. Public Heal.* 136 (2016) 213-224.
170. Salminen, S., Endo, A., Isolauri, E., Scalabrin, D., Early gut colonization with lactobacilli and staphylococcus in infants: The hygiene hypothesis extended, *JPNG* 62 (2016) 80-86.
171. Schwarz, H. P., Dorner, F., Karl Landsteiner and his major contributions to haematology, *Brit. J. Haematol.* 121 (2003) 556-565.
172. Landsteiner, K., Jacobs, J., Studies on the sensitization of animals with simple chemical compounds, *J. Exp. Med.* 61 (1935) 643-656.
173. Weltzien, H. U., Moulon, C., Martin, S., Padovan, E., Hartmann, U., Kohler, J., T cell immune responses to haptens. Structural models for allergic and autoimmune reactions, *Toxicology* 107 (1996) 141-151.
174. Pichler, W. J., Hausmann, O., Classification of drug hypersensitivity into allergic, p-i, and pseudo-allergic forms, *Int. Arch. Allergy Immunol.* 171 (2016) 166-179.
175. Shreder K., Synthetic haptens as probes of antibody response and immunorecognition. *Methods* 20 (2000) 372-379.
176. Divkovic, M., Pease, C. K., Gerberick, G. F., Basketter, D. A., Hapten-protein binding: from theory to practical application in the *in vitro* prediction of skin sensitization, *Contact Dermatitis* 53 (2005) 189-200.
177. Gräfvvert, E., Shao, L. P., Karlberg A.-T., Nilsson, U., Nilsson, J. L. G., Contact allergy to resin acid hydroperoxide. Hapten binding via free radicals and epoxides, *Chem. Res. Toxicol.* 7 (1994) 260-266.
178. Saint Mezard, P., Rosieres, A., Krasteva, M., Berard, F., Dubois, B., Kaiserlian, D., Nicolas, J.-F., Allergy contact dermatitis, *Eur. J. Dermatol.* 14 (2004) 284-95.
179. Saint-Mezard, P., Krasteva, M., Chavagnac, C., Bosset, S., Akiba, H., Kehren, J., Kanitakis, J., Kaiserlian, D., Nicolas, J. F., Berard, F., Afferent and efferent phases of allergic contact dermatitis (ACD) can be induced after a single skin contact with haptens: Evidence using a mouse model of primary ACD, *J. Invest. Dermatol.* 120 (2003) 641-647.
180. Divkovic, M., Pease, C. K., Gerberick, G. F., Basketter, D. A., Hapten-protein binding: from theory to practical application in the *in vitro* prediction of skin sensitization, *Contact Dermatitis* 53 (2005) 189-200.
181. Rustemeyer, T., van Hoogstraten I. M. W., von Blomberg, B. M. E., Scheper, R. J., (2012) Mechanisms of Allergic Contact Dermatitis. In: Rustemeyer, T., Elsner, P., John, S. M., Maibach, H.I. (eds), *Kanerva's Occupational Dermatology*. Springer, Berlin, Heidelberg.
182. Roujeau, J.-C., Immune Mechanisms in Drug Allergy, *Allergol. Int.* 55 (2006) 27-33.
183. Bircher, A. J., (2020) Drug Allergens. In: John, S. M., Johansen, J.D., Rustemeyer, T., Elsner, P., Maibach, H. I. (eds.), *Kanerva's Occupational Dermatology*. Springer Nature Switzerland AG.
184. Ball, T., Vrtala, S., Sperr, W. R., Valent, P., Susani, M., Kraft, D., Valenta, R., Isolation of an immunodominant IgE hapten from an epitope expression cDNA library, *J. Biol. Chem.* 269 (1994) 28323-28328.

References

185. Rattray, N. J., Botham, P. A., Hext, P. M., Woodcock, D. R., Fielding, I., Dearman, R. J., Kimber, I., Induction of respiratory hypersensitivity to diphenylmethane-4,4'-diisocyanate in guinea pigs. Influence of route of exposure, *Toxicology* 88 (1994) 15-30.
186. Dudeck, A., Dudeck, J., Scholten, J., Petzold, A., Surianarayanan, S., Köhler, A., Peschke, K., Vöhringer, D., Waskow, C., Krieg, T., Müller, W., Waisman, A., Hartmann, K., Gunzer, M., Roers, A., Mast cells are key promoters of contact allergy that mediate the adjuvant effects of haptens, *Immunity* 34 (2011), 973-984.
187. Girolomoni, G., Gisondi, P., Ottaviani, C., Cavani, A., Immunoregulation of allergic contact dermatitis, *J. Dermatol.* 31 (1004) 264-270.
188. McFadden, J. P., White, J. M. L., Basketter, D. A., Kimber, I., Does hapten exposure predispose to atopic disease? The hapten-atopy hypothesis, *Trends Immunol.* 30 (2009) 67-74.s
189. Matzinger, P., The danger model: A renewed sense of self, *Science* 296 (2002) 301-305.
190. Matzinger, P., Essay 1: The danger model in its historical context, *Scand. J. Immunol.* 54 (2001) 4-9.
191. Matzinger, P., Tolerance, danger, and the extended family, *Annu. Rev. Immunol.* 12 (1994) 991-1045.
192. Smith, H. R., Basketter, D. A., MacFadden, J. P., Irritant dermatitis, irritancy and its role in allergic contact dermatitis, *Clin. Exp. Dermatol.* 27 (2002) 138-146.
193. McFadden, J. P., Basketter, D. A., Contact allergy, irritancy and 'danger', *Contact Dermatitis* 42 (2000) 123-127.
194. McFadden, J. P., Puangpet, P., Basketter, D. A., Dearman, R. J., Kimber, I., Why does allergic contact dermatitis exist?, *Brit. J. Dermatol.* 168 (2013) 692-699.
195. Gruchalla, R. S., Drug metabolism, danger signals, and drug-induced hypersensitivity, *J. Allerg Clin. Immunol.* 108 (2001) 475-488.
196. Noble, A., Do we have memory of danger as well as antigen?, *Trends Immunol.* 30 (2009), 150-156.
197. Willart, M. A. M., Hammad, H., Alarming dendritic cells for allergic sensitization, *59* (2010) 95-103.
198. Mascarenhas, J. P., Molecular mechanisms of pollen tube growth and differentiation, *Plant Cell* 5 (1993), 1303-1314.
199. Bedinger, P., The remarkable biology of pollen, *Plant Cell* 4 (1992) 879-887.
200. Radauer, C., Breiteneder, H., Pollen allergens are restricted to few protein families and show distinct patterns of species distribution, *J. Allergy Clin. Immunol.* 117 (2006) 141-147.
201. Marowa, P., Ding, A., Kong, Y., Expansins: roles in plant growth and potential applications in crop improvement, *Plant Cell Rep.* 35 (2016) 949-965.
202. Rodríguez del Río, O. Díaz-Perales, A., Sánchez-García, S., Escudero, C., Ibáñez, M. D., Méndez-Brea, P., Barber, D., Proflin, a change in the paradigm, *J. Investig. Allergol. Clin. Immunol.* 28 (2018) 1-12.
203. Roth-Walter, F., Gomez-Casado, C., Pacios, L. F., Mothes-Luksch, N., Roth, G. A., Singer, J., Diaz-Perales, A., Jensen-Jarolim, E., Bet v 1 from birch pollen is a lipocalin-like protein acting as allergen only when devoid of iron by promoting Th2 lymphocytes, *J. Biol. Chem.* 289 (2014) 17416-17421.

204. Bufe, A., Spangfort, M. D., Kahlert, H., Schlaak, M., Becker, W.-M., The major birch pollen allergen, Bet v 1, shows ribonuclease activity, *Planta* 199 (1996) 413-415.
205. Songnuan, W., Wind-pollination and the roles of pollen allergenic proteins, *Asian Pac. J. Allergy Immunol* 31 (2013) 261-270.
206. Pummer, B. G., Bauer, H., Bernardi, J., Chazallon, B., Facq, S., Lendl, B., Whitmore, K., Grothe, H., Chemistry and morphology of dried-up pollen suspension residues, *J. Raman Spectrosc.* 44 (2013) 1654-1658.
207. Johri, B. M., Vasil, I. K., Physiology of pollen, *Bot. Rev.* 27 (1961) 326-368.
208. Schulte, F., Lingott, J., Panne, U., Kneipp, J., Chemical characterization and classification of pollen, *Anal. Chem.* 80 (2008) 9551-9556.
209. Mueller, M. J., Radically novel prostaglandins in animals and plants: the isoprostanes, *Chem. Biol.* 5 (1998) 323-333.
210. Parchmann, S., Mueller, M. J., Evidence for the formation of dinor isoprostanes E₁ from α -linolenic acid in plants, *J. Biol. Chem.* 273 (1998) 32650-32655.
211. Thoma, I., Loeffler, C., Sinha, A. K., Gupta, M., Krischke, M., Staffen, B., Roitsch, T., Mueller, M. J., Cyclopentenone isoprostanes induced by reactive oxygen species trigger defense gene activation and phytoalexin accumulation in plants, *Plant J.* 34 (2003) 363-365.
212. Mueller, M. J., Archetype signals in plants: The phytoprostanes, *Curr. Opin. Plant Biol.* 7 (2004) 441-448.
213. Gilles, S., Mariani, V., Bryce, M., Mueller, M. J., Ring, J., Behrendt, H., Jakob, T., Traidl-Hoffmann, C., Pollen allergens do not come alone: pollen associated lipid mediators (PALMS) shift the human immune system towards a Th2-dominated response, *All. Asth. Clin. Immunol.* 5 (2009) 3.
214. Hoehne, J. H., Reed, C. E., Where is the allergic reaction in ragweed asthma?, *J. Allergy Clin. Immunol* 48 (1971) 36-39.
215. Wilson, A. F., Novey, H. S., Berke, R. A., Surprenant, E. L., Deposition of inhaled pollen and pollen extract in human airways, *N. Engl. J. Med.* 228 (1973) 1056-1058.
216. D'Amato, G., Cecchi, L., Bonini, S., Nunes, C., Amnesi-Maesano, I., Behrendt, H., Liccardi, G., Popov, T., van Cauwenberge, P., Allergenic pollen and pollen allergy in Europe, *Allergy* 62 (2007) 976-990.
217. Behrendt, H., Kasche, A., Ebner von Eschenbach, C., Risse, U., Huss-Marp, J., Ring, J., Secretion of proinflammatory eicosanoid-like substances precedes allergen release from pollen grains in the initiation of allergic sensitization, *Int. Arch. Allergy Immunol.* 124 (2001) 121-125.
218. Plötz, S. G., Traidl-Hoffmann, C., Feussner, I., Kasche, A., Feser, A., Ring, J., Jakob, T., Behrendt, H., Chemotaxis and activation of human peripheral blood eosinophils induced by pollen-associated lipid mediators, *J. Allergy Clin. Immunol.* 113 (2004) 1152-1160.
219. Traidl-Hoffmann, C., Kasche, A., Jakob, T., Huger, M., Plötz, S., Feussner, I., Ring, J., Behrendt, H., Lipid mediators from pollen act as chemoattractants and activators of polymorphonuclear granulocytes, *J. Allergy Clin. Immunol.* 109 (2002) 831-838.
220. Allakhverdi, Z., Bouguermouh, S., Rubio, M., Delespesse, G., Adjuvant activity of pollen grains, *Allergy* 60 (2005) 1157-1164.
221. Bundy, F. P., Bassett, W. A., Weathers, M. S., Hemley, R. J., Mao, H. K., Goncharov, A. F., The pressure-temperature phase and transformation diagram for carbon; updated through 1994, *Carbon* 34 (1996) 141-153.

References

222. Pearson, R. G., Hard and Soft Acids and Bases, HSAB, Part I, *J. Chem. Educ.* 45 (1968) 581-587.
223. Pearson, R. G., Hard and Soft Acids and Bases, HSAB, Part II, *J. Chem. Educ.* 45 (1968) 643-647.
224. LoPachin, R. M., Gavin, T., DeCaprio, A., Barber, D. S., Application of the hard and soft, acids and bases (HSAB) theory to toxicant-target interactions, *Chem. Res. Toxicol.* 25 (2012) 239-251.
225. Gersch, M., Kreuzer, J., Sieber, S. A., Electrophilic natural products and their biological targets, *Nat. Prod. Rep.* 29 (2012) 659-682.
226. Soglia, J. R., Contillo, L. G., Kalgutkar, A. S., Zhao, S., Hop, C. E. C. A., Boyd, J. G., Cole, M. J., A Semiquantitative method for the determination of reactive metabolite conjugate levels in vitro utilizing liquid chromatography-tandem mass spectrometry and novel quaternary ammonium glutathione analogues, *Chem. Res. Toxicol.* 19 (2006) 480-490.
227. Liebler, D. C., Protein damage by reactive electrophiles: Targets and consequences, *Chem. Res. Toxicol.* 21 (2008) 117-128.
228. Stone, M. J., Williams, D. H., On the evolution of functional secondary metabolites (natural products), *Mol. Microbiol.* 6 (1992), 29-34.
229. Ho, T. T., Tran, Q. T. N., Chai, C. L. L., The polypharmacology of natural products, *Future Med. Chem.* 11 (2018) 1361-1368.
230. Newman, D. J., Cragg, G. M., Natural products as sources of new drugs over the nearly four decades from 01/1981 to 09/2019, *J. Nat. Prod.* 83 (2020) 770-803.
231. Miller, E. C., Miller, J. A., Searches for ultimate chemical carcinogens and their reactions with cellular macromolecules, *Cancer* 47 (1981) 2327-2345.
232. Benigni, R., Bossa, C., Mechanisms of chemical carcinogenicity and mutagenicity: a review with implications for predictive toxicology, *Chem. Rev.* 111 (2011) 2507-2536.
233. LoPachin, R. M., Gavin, T., Reactions of electrophiles with nucleophilic thiolate sites: Relevance to pathophysiological mechanisms and remediation, *Free Radical Res.* 50 (2016) 195-205.
234. Cavins, J. F., Friedman, M., Specific modification of protein sulfhydryl groups with α,β -unsaturated compounds, *J. Biol. Chem.* 243 (1968) 3357-3360.
235. Holmström, K. M., Finkel, T., Cellular mechanisms and physiological consequences of redox-dependent signalling, *Nat. Rev. Mol. Cell Biol.* 15 (2014) 411-421.
236. Klomsiri, C., Karplus, P. A., Poole, L. B., Cysteine-based redox switches in enzymes, *Antioxid. Redox Signal.* 14 (2011) 1065-1077.
237. Parvez, A., Long, M. J. C., Poganik, J. R., Aye, Y., Redox signaling by reactive electrophiles and oxidants, *Chem. Rev.* 118 (2018) 8798-8888.
238. Miseta, A., Csutora, P., Relationship between the occurrence of cysteine in proteins and the complexity of organisms, *Mol. Biol. Evol.* 17 (2000) 1232-1239.
239. Go, A.-M., Chandler, J. D., Jones, D. P., The cysteine proteome, *Free Radical Bio. Med.* 84 (2015) 227-245.
240. Khan, S., Vihinen, M., Spectrum of disease-causing mutations in protein secondary structures, *BMC Struct. Biol.* 7 (2007) 56.
241. Vitkup, D., Sander, C., Church, G. M., The amino-acid mutational spectrum of human genetic disease, *Genome Biol.* 4 (2003) R72.

242. Gehring, M., Laufer, S. A., Emerging and re-emerging warheads for targeted covalent inhibitors: Applications in medicinal chemistry and chemical biology, *J. Med. Chem.* 62 (2019) 5673-5724.
243. Singh, J., Petter, R. C., Baillie, T. A., Whitty, A., The resurgence of covalent drugs, *Nat. Rev. Drug Discov.* 10 (2011) 307-317.
244. Long, M. J. C., Aye, Y., Privileged electrophile sensors: a resource for covalent drug development, *Cell Chem. Biol.* 24 (2017) 787-800.
245. Macpherson, L. J., Dubin, A. E., Evans, M. J., Marr, F., Schultz, P. G., Cravatt, B. F., Patapoutian, A., Noxious compounds activate TRPA1 ion channels through covalent modification of cysteines, *Nature* 445 (2007) 541-545.
246. Ghosh, A. K., Samanta, I., Mondal, A., Liu, W. R., Covalent inhibition in drug discovery, *ChemMedChem* 14 (2019) 889-906.
247. Pucheault, M., Natural products: chemical instruments to apprehend biological symphony, *Org. Biomol. Chem.* 6 (2008) 424-432.
248. Ghantous, A., Gali-Muhtasib, H., Cuorela, H., Saliba, N. A., Darwiche, N., What made sesquiterpene lactones reach cancer clinical trials?, *Drug Discov. Today* 15 (2010) 668-678.
249. Neelakantan, S., Nasim, S., Guzman, M. L., Jordan, C. T., Crooks, P. A., Aminoparthenolides as novel anti-leukemic agents: discovery of the NF- κ B inhibitor, DMAPT (LC-1), *Bioorg. Med. Chem. Lett.* 19 (2009) 4346-4349.
250. Freund, R. R. A., Gobrecht, P., Fischer, D., Arndt, H.-D., Advances in chemistry and bioactivity of parthenolide, *Nat. Prod. Rep.* 37 (2020) 542-565.
251. Wymann, M. P., Bulgarelli-Leva, G., Zvelebil, M. J., Pirola, L., Vanhaesebroeck, B., Waterfield, M. D., Panayotou, G., Wortmannin inactivates phosphoinositide 3-kinase by covalent modification of Lys-802, a residue involved in the phosphate transfer reaction, *Mol. Cell Biol.* 16 (1996) 1722-1733.
252. Wipf, P., Halter, R. J., Chemistry and biology of wortmannin, *Org. Biomol. Chem.* 3 (2005) 2053-2061.
253. Ui, M., Okada, T., Hazeki, K., Hazeki, O., Wortmannin as a unique probe for an intracellular signalling protein, phosphoinositide 3-kinase, *Trends Biochem. Sci.* 20 (1995) 303-307.
254. Walker, E. H., Pacold, M. E., Perisic, O., Stephens, L., Hawkins, P. T., Wymann, M. P., Williams, R. L., Structural determinants of phosphoinositide 3-kinase inhibition by wortmannin, LY294002, quercetin, myricetin, and staurosporine, *Mol. Cell* 6 (2000) 909-919.
255. Wang, Y., Kuramitsu, Y., Baron, B., Kitagawa, T., Tokuda, K., Akada, J., Maehara, S.-I., Maehara, Y., Nakamura, K., PI3K inhibitor LY294002, as opposed to wortmannin, enhances AKT phosphorylation in gemcitabine-resistant pancreatic cancer cells, *Int. J. Oncol.* 50 (2017) 606-612.
256. Harada, S., Tsubotani, S., Hida, T., Ono, H., Okazaki, H., Structure of lactivicin, an antibiotic having a new nucleus and similar biological activities to β -lactam antibiotics, *Tetrahedron Lett.* 27 (1986) 6229-6232.
257. Brown, T., Charlier, P., Herman, R., Schofield, C. J., Sauvage, E., Structural basis for the interaction of lactivicins with serine β -lactamases, *J. Med. Chem.* 53 (2010) 5890-5894.
258. Calvopiña, K., Umland, K.-D., Rydzik, A. M., Hinchliffe, P., Brem, J., Spencer, J., Schofield, C. J., Avison, M. B., Sideromimic modification of lactivicin dramatically increases potency against

References

- extensively drug-resistant *Stenotrophomonas maltophilia* clinical isolates, *Antimicrob. Agents Ch.* 60 (2016) 4170-4175.
259. Wall, S. B., Smith, M. R., Ricart, K., Zhou, F., Vayalil, P. K., Oh, J.-Y., Landar, A., Detection of electrophile-sensitive proteins, *BBA-Gen. Subjects* 1840 (2014) 913-922.
260. Carlsson, H., Törnqvist, M., An adductomic approach to identify electrophiles *in vivo*, *Basic Clin. Pharmacol.* 121 (2017) 44-54.
261. Domon, B., Aebersold, R., Mass spectrometry and protein analysis, *Science* 312 (2006) 212-217.
262. Preston, G. W., Phillips, D. H., Protein adductomics: Analytical developments and applications in human biomonitoring, *Toxics* 7 (2019) 29.
263. Rappaport, S. M., Li, H., Grigoryan, H., Funk, W. E., Williams, E. R., Adductomics: characterizing exposures to reactive electrophiles, *Toxicol. Lett.* 213 (2012) 83-90.
264. Törnqvist, M., Kautiainen, A., Adducted proteins for identification of endogenous electrophiles, *Environ. Health Persp.* 99 (1992) 39-44.
265. von Stedingk, H., Rydberg, P., Törnqvist, M., A new modified Edman procedure for analysis of *N*-terminal valine adducts in hemoglobin by LC-MS/MS, *J. Chromatogr. B Analyt. Technol. Biomed. Life Sci.* 878 (2010) 2483-2490.
266. Carlsson, H., von Stedingk, H., Nilsson, U., Törnqvist, M., LC-MS/MS screening strategy for unknown adducts to *N*-terminal valine in hemoglobin applied to smokers and nonsmokers, *Chem. Res. Toxicol.* 27 (2014) 2062-2070.
267. Evans, D. C., Watt, A. P., Nicoll-Griffith, D. A., Baillie, T. A., Drug-protein adducts: in industry perspective on minimizing potential for drug bioactivation in drug discovery and development, *Chem. Res. Toxicol.* 17 (2004) 3-16.
268. Chauret, N., Nicoll-Griffith, D., Friesen, R., Li, C., Trimble, L., Dube, D., Fortin, R., Girard, Y., Yergey, J., Microsomal metabolism of the 5-lipoxygenase inhibitors L-746,530 and L-739,010 to reactive intermediates that covalently bind to protein: the role of the 6,8-dioxabicyclo[3.2.1]octanyl moiety, *Drug Metab. Dispos.* 23 (1995) 1325-1334.
269. Zhang, K. E., Naue, J. A., Arison, B., Vyas, K. P., Microsomal metabolism of the 5-lipoxygenase inhibitor L-739,010: evidence for furan bioactivation, *Chem. Res. Toxicol.* 9 (1996) 547-554.
270. Argoti, D., Liang, L., Conteh, A., Chen, L., Bershas, D., Yu, C.-P., Vouros, P., Yang, E., Cyanide trapping of iminium reactive intermediates followed by detection and structure identification using liquid chromatography-tandem mass spectrometry (LC-MS/MS), *Chem. Res. Toxicol.* 18 (2005) 1537-1544.
271. Castro-Perez, J., Plumb, R., Liang, L., Yang, E., A high-throughput liquid chromatography/tandem mass spectrometry method for screening glutathione conjugates using exact mass neutral loss acquisition, *Rapid Commun. Mass Spectrom.* 19 (2005) 798-804.
272. Gan, J., Harper, T. W., Hsueh, M. M., Qu, Q., Humphreys, W. G., Dansyl glutathione as a trapping agent for the quantitative estimation and identification of reactive metabolites, *Chem. Res. Toxicol.* 18 (2005) 896-903.
273. Nikolic, D., Fan, P. W., Bolton, J. L., van Breemen, R. B., Screening for xenobiotic electrophilic metabolites using pulsed ultrafiltration-mass spectrometry, *Comb. Chem. High T. Scr.* 2 (1999) 165-175.
274. Mulliner, D., Wondrousch, D., Schüürmann, G., Predicting Michael-acceptor reactivity and toxicity through quantum chemical transition-state calculations, *Org. Biomol. Chem.* 9 (2011) 8400-8412.

275. Caprioglio, D., Minassi, A., Avonto, C., Tagliatalata-Scafati, O., Appendino, G., Thiol-trapping natural products under the lens of cysteamine assay: friends, foes, or simply alternatively reversible ligands?, *Phytochem. Rev.*, (2020).
276. Castro-Falcón, G., Hahn, D., Reimer, D., Hughes, C. C., Thiol probes to detect electrophilic natural products based on their mechanism of action, *ACS Chem. Biol.* 11 (2016) 2328-2336.
277. Cox, C. L., Tietz, J. I., Sokolowski, K., Melby, J. O., Doroghazi, J. R., Mitchell, D. A., Nucleophilic 1,4-additions for natural product discovery, *ACS Chem. Biol.* 9 (2014) 2014-2022.
278. Miles, C. O., Sandvik, M., Nonga, H. E., Rundberget, T., Wilkins, A. L., Rise, D., Ballot, A., Thiol derivatization for LC-MS identification of microcystins in complex matrices, *Environ. Sci. Technol.* 46 (2012) 8937-8944.
279. Marfey, P., Determination of D-amino acids. II. Use of a bifunctional reagent, 1,5-difluoro-2,4-dinitrobenzene, *Carlsberg Res. Commun.* 49 (1984) 591-596.
280. Rudolf, G. C., Kock, M. F., Mandl, F. A. M., Sieber, S. A., Subclass-specific labeling of protein-reactive natural products with customized nucleophilic probes, *Chem. Eur. J.* 21 (2015) 3701-3707.
281. Jeon, H., Lim, C., Lee, J. M., Kim, S., Chemical assay-guided natural product isolation via solid-supported chemodosimetric fluorescent probe, *Chem. Sci.* 6 (2015) 2806-2811.
282. Avonto, C., Tagliatalata-Scafati, O., Pollastro, F., Minassi, A., Di Marzo, V., De Petrocellis, L., Appendino, G., An NMR spectroscopic method to identify and classify thiol-trapping agents: revival of Michael acceptors for drug discovery?, *Angew. Chem.* 123 (3011) 487-491.
283. Wagner, M., Kunz, H., Fluorinating cleavage of solid phase linkers for combinatorial synthesis, *Angew. Chem. Int. Ed.* 41 (2002) 317-321.
284. Božičević, A., De Mieri, M., Nassenstein, C., Wiegand, S., Hamburger, M., Secondary metabolites in allergic plant pollen samples modulate afferent neurons and murine tracheal rings, *J. Nat. Prod.* 80 (2017), 2953-2961.
285. Woodward, R. G., Structure and the absorption spectra of α,β -unsaturated ketones, *J. Am. Chem. Soc.* 63 (1941) 1123-1126.
286. Salapovic, H., Geier, J., Reznicek, G., Quantification of sesquiterpene lactones in Asteraceae plant extracts: evaluation of their allergenic potential, *Sci. Pharm.* 2013, 81, 807-818.
287. Sangster, A. W., Stuart, K. L., Ultraviolet spectra of alkaloids, *Chem. Rev.* 65 (1965) 59-130
288. Meister, A., Anderson, M. E., Glutathione, *Ann. Rev. Biochem.* 52 (1983) 711-60.
289. Chasseaud, L. F., The Role of Glutathione and Glutathione S-Transferases in the Metabolism of Chemical Carcinogens and Other Electrophilic Agents, *Adv. Cancer Res.* 29 (1979) 175-274.
290. Soglia, J. R., Contillo, L. G., Kalgutkar, A. S., Zhao, S., Hop, C. E. C. A., Boyd, J. G., Cole, M. J., A Semiquantitative Method for the Determination of Reactive Metabolite Conjugate Levels in Vitro Utilizing Liquid Chromatography-Tandem Mass Spectrometry and Novel Quaternary Ammonium Glutathione Analogues, *Chem. Res. Toxicol.* 19 (2006) 480-490.
291. Brink, A., Pähler, A., Funk, C., Schuler, F., Schadt, S., Minimizing the risk of chemically reactive metabolite formation of new drug candidates: implications for preclinical drug design, *Drug Discov. Today* 22 (2016) 751-756.
292. Schadt, S., Simon, A., Kustermann, S., Boess, F., McGinnis, C., Brink, A., Lieven, R., Fowler, S., Youdim, K., Ullah, M., Marschmann, M., Zihlmann, C., Siegrist, Y. M., Cascais, A. C., Di Lenarda, E. Durr, E., Schaub, N., Ang, X., Starke, V., Singer, T., Alvarez-Sanchez, R., Roth, A. B., Schuler,

References

- F., Funk, C., Minimizing DILI risk in drug discovery – A screening tool for drug candidates, *Toxicol. In Vitro* 30 (2015) 429-437.
293. Thompson, R. A., Isin, E. M., Ogese, M. O., Mettetal, J. T., Williams, D. P., Reactive Metabolites: Current and Emerging Risk and Hazard Assessments, *Chem. Res. Toxicol.* 29 (2016) 505-533.
294. Huang, K., Huang, L. van Breemen, R. B., Detection of reactive metabolites using isotope-labeled glutathione trapping and simultaneous neutral loss and precursor ion scanning with ultra-high-pressure liquid chromatography triple quadrupole mass spectrometry, *Anal. Chem.* 87 (2015) 3646-3654.
295. Ma, S., Subramanian, R., Detecting and characterizing reactive metabolites by liquid chromatography/tandem mass spectrometry, *Mass Spectrom.* 41 (2006) 1121-1139.
296. Young, C. L., Britton, Z. T., Robinson, A. S., Recombinant protein expression and purification: a comprehensive review of affinity tags and microbial applications, *Biotechnol. J.* 7 (2012) 620-634.
297. Weber, P. C., Ohlendorf, D. H., Wendoloski, J. J., Salemme, F. R., Structural origins of high-affinity biotin binding to streptavidin, *Science*, 243 (1989) 85-88.
298. Guesdon, J. L., Ternynck, T., Avrameas, S., The use of avidin-biotin interaction in immunoenzymatic techniques, *J. Histochem. Cytochem.* 27 (1979) 1131-1139.
299. Mehlenbacher, M. R., Bou-Abdallah, F., Liu, X. X., Melman, A., Calorimetric studies of ternary complexes of Ni(II) and Cu(II) nitrilotriacetic acid and N-acetyloligohistidines, *Inorg. Chim. Acta* 437 (2015) 152-158.
300. Amblard, M., Fehrentz, J.-A., Martinez, J., Subra, G., Methods and protocols of modern solid phase peptide synthesis, *Mol. Biotechnol.* 33 (2006) 239-254.
301. Castañeda-Acosta, J., Fischer, N. H., Biomimetic transformations of parthenolide, *J. Nat. Prod.* 56 (1993) 90-98.
302. Bollhagen, R., Schmiedberger, M., Barlos, K., Frell, E., A new reagent for the cleavage of fully protected peptides synthesized on 2-chlorotriyl chloride resin, *J. Chem. Soc.. Chem. Commun.* (1994) 2559-2560.
303. Hellmuth, C., Koletzko, B., Peissner, W., Aqueous normal phase chromatography improves quantification and qualification of homocysteine, cysteine and methionine by liquid chromatography-tandem mass spectrometry, *J. Chromatogr. B* 879 (2011) 83-89.
304. Ortmayr, K., Schwaiger, M., Hann, S., Koellensperger, G., An integrated metabolomics workflow for the quantification of sulfur pathway intermediates employing thiol protection with *N*-ethyl maleimide and hydrophilic interaction liquid chromatography tandem mass spectrometry, *Analyst* 140 (2015) 7687-7695.
305. Dogan, C. E., Cebi, N., Develioglu, A., Olgun, E. O., Sagdic, O., Detection of cystine and cysteine in wheat flour using a robust LC-MS/MS method, *J. Cereal Sci.* 84 (2018) 49-54.
306. Freund, R.R. A., Gobrecht, P., Fischer, D., Arndt, H.-D., Advances in chemistry and bioactivity of parthenolide, *Nat. Prod. Rep.* 37 (2020) 541-565.
307. Avonto, C., Tagliatalata-Scafati, O., Pollastro, F., Minassi, A., Di Marzo, V., De Petrocellis, L., Appendino, G., An NMR spectroscopic method to identify and classify thiol-trapping agents: revival of Michael acceptors for drug discovery?, *Angew. Chem. Int. Ed.* 50 (2011) 467-471.
308. Mabry, T. J., Miller, H. E., Kagan, H. B., Renold, W., The structure of psilostachyin, a new sesquiterpene dilactone from *Ambrosia psilostachya*, *Tetrahedron* 22 (1966) 1139-1146.

309. Koshino, H., Yoshihara, T., Okuno, M., Sakamura, S., Tajimi, A., Shimanuki, T., Gamaholides A, B, and gamahorin, noval antifungal compounds from Stromata of *Epichloe typhina* on *Phleum pratense*, Biosci. Biotech. Biochem. 56 (1992) 1096-1099.
310. Pokhilo, N. D., Denisenko, V. A., Makhankov, V. V., Uvarova, N. I., Triterpenoids of the leaves of *Betula pendula* from different growth sites, Chem. Nat. Compd. 22 (1986) 166-171.
311. Pinelli, P., Ieri, F., Vignolini, P., Bacci, L., Baronti, S., Romani, A., Extraction and HPLC analysis of phenolic compounds in leaves, stalks and textile fibers of *Urtica dioica* L., J. Agric. Food Chem. 56 (2008) 9127-9132.
312. Amaral, J. S., Ferreres, F., Andrade, P. B., Valentão, P., Pinheiro, C., Santos, A., Seabra, R., Phenolic profile of hazelnut (*Corylus avellana* L.) leaves cultivars grown in Portugal, Nat. Prod. Res. 19 (2005) 157-163.
313. Masullo, M., Cerulli, A., Olas, B., Pizza, C., Piacente, S., Giffonins A-I, antioxidant cyclized diarylheptanoids from the leaves of the hazelnut tree (*Corylus avellana*), source of the Italian PGI product "Nocciola di Giddoni", J. Nat. Prod. 78 (2015) 17-25.